Diabetic foot ulcer early detection

BY

Mohammad Abo Homyd

Muath Awad

Ahmad Karajeh

Supervisor
Eng. Fida'a Al - Ja'afrah

Palestine Polytechnic University
College of Engineering
Department of Electrical Engineering

اهداء

الحمد لله رب العالمين الذي تتم بنعمته الصالحات ... والصلاة والسلام على رسولنا الكريم معلمنا ومعلم الأمة ...

باسمنا نحن محمد أبوحميد وأحمد كرجة ومعاذ عوض نهدي هذا العمل ونجاحه لكل الأشخاص الذين وقفو الى جانبنا ودعمونا خلال مسيرتنا التعليمية ولجامعتنا الحبيبة

ونوجه شكرنا الخاص الى رئيس الجامعة الدكتور عماد الخطيب والدكتور أمجد برهم المحترمين.

كما ونوجه شكرنا الخاص الى معلمينا المهندسة فداء جعافرة والمهندس علي عمرو والدكتور عبد الله عرمان والى الأساتذة الأفاضل الأستاذ محمد القيسي والأستاذ معتز جواعدة والأستاذ شحدة زاهدة والأستاذ بهاء أبو قرندل الذين دعمونا خلال مسيرتنا التعليمة وكانوا ذو الفضل الأكبر في إنجاح هذا المشروع ...

وشكرنا الخاص لصديقنا الذي كان شعلة الأمل بداخلنا والأخ الحبيب الذي نفتقد الأخ إياد غيث ...
وشكرنا الخاص للصديق والأخ عكرمة درامنة ...
وشكرنا الخاص للأهل والأصدقاء على وقوفهم الى جانبنا ودعمنا على طول مسيرتنا التعليمية ...
شكراً لكم جميعاً لكم منا كل المحبة والاحترام ...

اهداء محمد أبوحميد

لك يا من رسمت الطريق بلون الورد وتركت همك مصبوبا بألمي مداويا وزعت الأمل رغم يأسي يا أعذب الناس في قلبي... لك يا أغلى أب (عبد الله) ...

لك يا جنة الرحمن وعشقي منذ الأزمان وريحانة الحب في كل مكان وزهرة مدت بأوراقها لي بكل حنان ونور القلب بكل مكان... لك يا أجمل أم (رتيبة) ...

لك يا من بتعبك كنت سندي وهمي قبل همك كان يا من رسمت بعرقك وجهدك روح السلام وبكلامك كنت أحيا بأمان يا من كنت بجانبي كغصن الرمان ... لك يا أغلى أخ (أحمد) ...

لك يا من كنتي أنشودة السلام وجنتي بالدنيا وروح الأمل حين يغيب وأضيع بين دروب الظلام كنتي الشمعة التي أمسك بها لأضيء طريقي ... لك يا أجمل أخت (أحلام) (زينب) ...

لكم يا من كنتم نبض وجداني وشعلة النجاح بداخلي التي لا تنطفئ والقمر الذي يضيء دروب النصر... لكم يا أجمل عم وعمة (إسحاق) (مها) ...

لكم يا من كبرنا معاً وكبرت أحلامنا وآمالنا وذكرياتنا تحيا في العقل كأنها نقشٌ جميل ... لكم أصدقائي لكم يا أخوتي (علاء النجار) (رشاد العمور) (محمد أبو فنار) (أحمد فنشه) (عبيدة النجار) (حمزة النجار) (علي النجار) (أحمد أبو فنار) (معاذ عوض) (أحمد كرجة) (عامر أبو فارة) (عبد الرحمن قشقيش) (عكرمة درامنة) (أنس القوقا) (محمود نجاجرة) (خالد أبوحميد) (منذر رشيد) لكم كل التحية أخوتي ...

لكم يا من كنتم السند والخلان ... لكم أقربائي يا عز السند وخلان (جميل أبوحميد) (علي أبوحميد) (سامي أبوحميد) (تيسير أبوحميد) (محمد أبوحميد) (موسى أبوحميد) (عيسى أبوحميد) (يوسف أبوحميد)

(حنان أبوحميد) (حسن أبوحميد) (نجاح أبوحميد) (فاطمة أبوحميد) (جميلة أبوحميد) ...
لكم يا من كنتم قدوتي وأهلي يا من بهم كنت أستظل ومنهم أتعلم يا من كنتم سبباً يسره الله لي يا أروع من تعلمت من أفكارهم وبنيت أولى أهداف حياتي ... لكم أساتذتي (المهندسة فداء جعافرة) (المهندس علي عمرو) (المهندس عبد الله عرمان) (المهندس بهاء أبو قرندل) (المهندس شحدة زاهدة) (المهندس محمد القيسي) (المهندس معتز جواعدة) (الدكتور أيمن وزوز) (الدكتور أمجد برهم)
لك يا من كنتي كالعود الرنان بأجمل الألحان وحبة المسك بكلامك الداعم في كل ثوان وعنبر الجمال بصبرك عليَ حين أغيب وجورية الأغصان في وجه يأسي ... لك يا أجمل من وجدت الى جانبي (بنان) ...
لكم يا من كنتم ببالي كالجرس الرنان في قلبي وعقلي تدقون ناقوس الحزن كلما مرت ببالي ذكرياتكم الجميلة لكم يا من فارقتموني بأجسادكم وبقيت روحكم بداخلي وتركتم بقلبي الألم على فراقكم وكم تمنيتكم الى جانبي ... لكم يا أغلى من فقد قلبي عمي (محمد جبر أبوحميد) جدتي (مريم أبوحميد) وصديقي (اياد غيث) ... لكم كل المحبة والوفاء ... شكراً لكم جميعاً يا أغلى ما أملك ...

اهداء معاذ عوض

اليك أبي ... يا من يقف التكريم حائراً عاجزاً عن تكريمك ...
اليك أمي ... يا من تعجز الكلمات عن ذكر بعضك ...
اليك أخي ... يا معنى الوفاء في كل اللحظات ...
اليك أختي ... يا عطر الحب في كل الورود ...
اليك صديقي ... يا رجل المواقف في كل زمان ...
اليك معلمي ... يا رسماً حفر في الأذهان بأجمل الألوان ...
اليك ... ومن غيرك يأبى الا وعلى ذكراك توجع كل الأذهان والوجدان أخي اياد غيث سلامٌ لاسمك الرنان ...
اليك ... يا بلسم الحب في كل وجدان ...
اليكم جميعا مني كل الحب والريحان لكم أهديكم هذا الإنجاز ومن غيركم لا يصان ... ستبقون معنى الوفاء يا أجمل الناس بقلبي ...

اهداء أحمد كرجة

إلى الرحمة المرسلة هدى للعالمين ... إلى سيد الخليقة وإمام المرسلين ... إلى نور وضياء الحق وخاتم النبيين.
إلى الرسول عليه أفضل الصلاة وأتم التسليم

إلى من تتضاءل ينابيع الأرض أمام نبع حنانها، إلى من كانت سبب وجودي لتنحني الدنيا أمام عظمة صبرها، ويسكن دفء الشمس في أعماق قلبها، وينطفئ نور القمر أمام نور وجهها إلى ملاذ روحي وملاذي الحنون.

أمي

إلى من كان لي المثل والقدوة، إلى من علمني أن الحياة جد وعمل وكفاح، إلى الصخرة التي تكسرت عليها كل مصاعبي، إلى من أمدني بكل ما عنده لأكمل طريقه وأحقق طموحه، إليك يا أغلى إنسان أول حصاد السنين ....

أبي

في عيونهم كنت أقرأ أقسى آيات الكفاح والتحدي والثبور....
وفي حكمتهم لمست معنى أن يصل المرء إلى معالي الأمور....
وفي حزمهم عرفت ماذا يعني أن تكون الشمس مقبرة النسور....
إليهم جميعا أولئك الذين نذروا حياتهم قرباناً محاولين شق طريق البسمة من سطح الوجه حتى أعماق الصدور....

إخوتي

في بحر عنوان الاغتراب اجتمعنا ....
وتحت سقف الصداقة والمحبة عشنا أروع أيام حياتنا ....
وحول راية العلم .... سوياً في الدرب سرنا ....
في الحقيقة لا أعرف ما أصبحوا بالنسبة لي .... أهم الأصدقاء أم هم الإخوان ....

أصدقائي

إلى كل من علمني حرفاً .... إلى كل صاحب يد بيضاء علي ....
إلى من يحبني .... إلى من أحب ....

الملخص

مرض السكري من الامراض المزمنة التي تواجه الانسان ومع مرور الزمن ربما يصاحبه مضاعفات ناتجة عن المرض، وهو مرض قرحة القدم السكرية وهو مرض خطير قد يؤدي الى بتر القدم في حال لم يعالج في بداياته، وهذا المرض ينتج بسبب ضعف سريان الدم او اعتلال في الاعصاب الطرفية وهؤلاء المرضى يحتاجون الى عناية خاصة بأقدامهم.
لذا قمنا بجمع المعلومات والأفكار حول مرض قرحة القدم السكرية لإفادة هؤلاء المرضى، فكانت الفكرة الأساسية أن نقوم بتصميم أداة تقوم على الكشف المبكر لمرض قرحة القدم السكرية وذلك من خلال طريقتين: الاولى الإشارة الكهربائية لعضلة القدم حيث ان مرض السكري او القدم السكرية يؤثر بشكل واضح على هذه الإشارة الناتجة من حيث الشكل أو قيمة الجهد الناتج.وقد تم استنتاج أن الإشارة الكهربائية للعضلة تتأثر مع التقدم بالعمر وتتأثر بازدياد الوزن ومدة الإصابة بمرض السكري، وأن قيمة الجهد الناتجة تتأثر فكانت في حالة قرحة القدم السكرية بالنسبة للأشخاص السليمين تتراوح ما بين (19.2-0.99)، وفي حالة المصابين بمرض السكري بالنسبة للأشخاص السليمين تتراوح ما بين (64.1-30.7).

أما الثانية وهي عن طريق وضع مجسات في اماكن محددة داخل ضبانة ويقوم المريض بالضغط على هذه الضبانة عن طريق الوقوف عليها فقط فتقوم المجسات باستشعار الضغط الناتج من القدم على الضبانة ومن خلال قيمة الضغط الناتجة يتم معرفة إذا كان المريض مصاب بمرض القدم السكرية ام لا.
وقد تم استنتاج أن الضغوط في المناطق الأربعة يمكن ترتيبها على النحو التالي: أن الضغط في منطقة الكعب يكون أعلى من باقي المناطق ومن ثم منطقة الأصبع الكبير ومن ثم منطقة الوسادة ومن ثم منطقة القدم الجانبية.
وأن المناطق الأكثر عرضة للإصابة بمرض قرحة القدم السكرية هي منطقة الأصبع الكبير ومنطقة الوسادة.

Abstract

Diabetes is one of the chronic diseases that a person faces with the passage of time, it may be accompany by complications resulting from the disease, which is a

Content	Page

diabetic foot ulcer disease and it is a serious disease that may lead to amputation of the foot if it was not treated at its beginning. In addition, these patients need special care for their feet.

Therefore, we collected information and ideas about diabetic ulcer disease to benefit these patients. Therefore, the basic idea was to design a tool based on early detection of diabetic foot ulcer disease through two methods: The first is the electrical signal of the foot muscle where diabetes or diabetic foot ulcer affects. This resulting signal is in terms of the shape or value of the output voltage.
After that, it was concluded that the electrical signal of the muscle is affected with age and is affected by the increase in weight and the duration of diabetes, and that the value of the resulting effort is affected and was in the case of diabetic foot ulcers. In the case of foot ulcers in the ratio between (19.2-0.99), and in the case of diabetes for healthy people, it occurs ratio between (64.1-30.7).The shape of the signal changes and appears differently apparently when displayed, whether it is the signal of a diabetic foot ulcer patient, a diabetic patient, or a healthy person.

The second is by placing sensors in specific places inside the insole and the patient presses this insole by standing on it only. The sensors sense the pressure from the foot on the insole and through the resulting pressure value it is known if the patient has diabetic foot ulcer or not.
It has been concluded that the pressure in the four areas can be arranged as follows: that the pressure in the heel area is higher than the rest of the areas and then the big toe area and then the pad area and then the side foot area.
The area’s most prone to developing diabetic ulcer disease are the big toe and the pad area.

Table of Content:-

List of figures:-

List of tables:

Chapter One:

Introduction

1.1 Overview :

Our project aims to design a device that helps in the early detection of diabetic foot ulcer disease, which is considered a serious disease in patients with diabetes, which may lead to amputation of the foot.

Where the device will early detection of the disease in two ways:
The first is where a set of sensors are placed in the foot in specific places that measure the pressure caused by the foot and through these pressures the disease is detected.
Second: it is by taking the EMG signal for the foot and then find the signal produced from the foot by the specific electrodes placed in the foot and then displayed on the screen and know the status of the foot.

1.2 Project Motivation:

Diabetes is one of the most common chronic diseases worldwide. the International Federation of Diabetes (IFA) President Petra Wilson confirmed that diabetes rates have risen significantly around the world, which requires urgent intervention to reduce its brutality, adding that the number of diabetics in the world has reached about 415 million people in 2015 , as the number of people with diabetes in the statistics of the Ministry of Health for 2017 in the West Bank 6313 are distributed by sex on 2792 males at a rate of 213 per 100,000 population and 3521 females at 279.6 per 100,000 population.
There is a close relationship between amputation and diabetes, where global statistics talk about the procedure of amputation every 30 seconds somewhere in the world, and that 6_8 of every 1000 patients with diabetes may lose the lower limb due to carelessness in the foot care, and there is a clear relationship between The incidence of coronary atherosclerosis and peripheral disease and the length of the duration of diabetes, the patient with the disease for more than 10 years more susceptible to atherosclerosis than the injury or injury for 5 years, where the incidence of atherosclerosis more than 45% in patients with diabetes for More than 20 years old, the infection has been discovered Diabetic foot disease caused by complications of diabetes, and this disease leads to amputation of the foot because of symptoms such as gangrene in the foot, and for diabetic foot ulcer disease, the rate of infection is more than six times in patients with diabetes for 20 years or more, compared to those who did not And the risk of recurrence of diabetes mellitus is up to 60% of these patients.

١.3 Project objective:

- ✓ Early detection of the disease of foot ulcer diabetes.
- ✓ Design and implementation of medical tools can detect early the disease of foot ulcers.
- ✓ Design the EMG circuit resulting from the foot to know the relationship between normal person, the patient of diabetic disease and patient of foot ulcer diabetes.

-

١.4 Literature Review:

The development of miniature, lightweight, and energy efficient circuit solutions for healthcare sensor applications is an increasingly important research focus given the rapid technological advances in healthcare monitoring equipment, micro fabrication processes and wireless communication. One area that has attracted considerable attention by researchers in

biomedical and sport related applications is the analysis of foot plantar pressure distributions to reveal the interface pressure between the foot plantar surface and the shoe sole. Typical applications are footwear design [1], and diagnosing disease [2], based on this researches it is clear that technique capable of accurately and efficiently measuring foot pressure are crucial to further developments.

1.5 Time Plan:

The Table 1.1 shows the activities that done in the project, and the time of each one.

Table 1.1: Activities planning.

Weeks / Activities	1	2	3	4	5	6	7	8	9	10	11	12	13	14	15	16
Obtaining Required components	■	■	■	■												
System Design					■	■	■	■								
Recording analysis and conclusion									■	■	■	■	■			
Results analysis and conclusion														■	■	■
Documentation				■	■	■	■	■	■	■	■	■	■	■		

1.6 Project Cost:

The following table shows the cost of electronic parts that required to implementation of our project.

Table 1.2: Project cost.

Component	Cost JD
Operational amplifiers Resistors , Potentiometers Connectors.	١٥٠ JD
8-Flexi-force sensor	٦٤٠JD
LCD display, Arduino.	٩٠JD
LM7805CT,LM7905CT	٢٠ JD
Outer cover “case”	١٠٠ JD
Total	١٠٠٠ JD

Chapter Two:

Foot Anatomy

2.1 Foot Installation

The man and the foot are the source of the movement of the human person, the "loco motor system", and the presence of any defect in its anatomical structure or its functions that leads to the so-called motor disability and the human's failure to exercise the movement in completely or in part.

2.1.1 Foot definition:-

The foot is an intricate part of the body, consisting of 26 bones, 33 joints, 107 ligaments, and ٢٠ muscles. Where the bones and joints in the feet experience wear and tear, so conditions that cause damage to the foot can directly affect its health.

2.1.2 Foot bones and anatomy:-

The human foot consists of 26 bones. These bones fall into three groups: the tarsal bones, metatarsal bones, and phalanges.

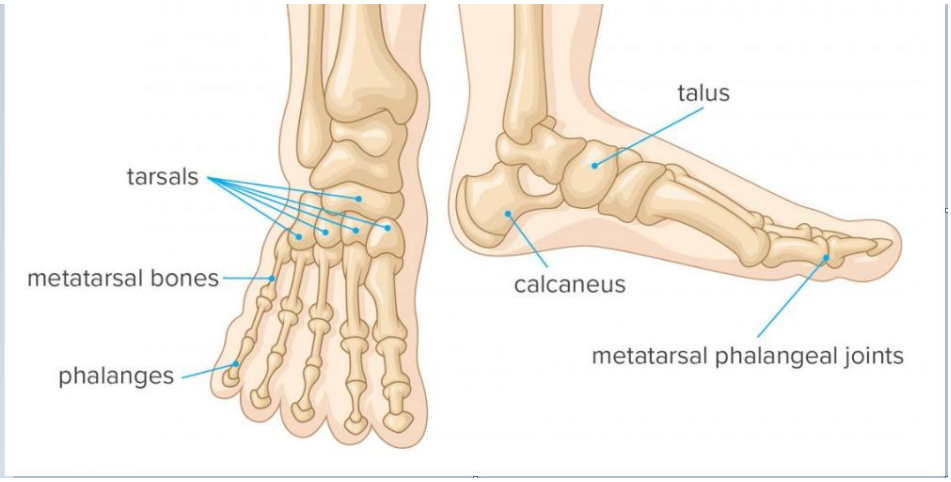

Fig.2.1: Foot bones and anatomy

2.1.3 Muscles:-

Twenty muscles give the foot its shape, support and the ability to move. The main muscles of the foot are:

- The tibilias posterior, which supports the foot's arch.
- The tibilias anterior, which allows the foot to move upward.
- The tibilias peroneal, which controls movement on the outside of the ankle.
- The extensors, which help raise the toes, making it possible to take a step.
- The flexors, which help stabilize the toes.

2.1.4 Tarsal bones:-

The tarsal bones are a group of seven bones that make up the rear section of the foot

* Tarsal bones include-

- The talus or anklebone: The talus is the bone at the top of the foot. It connects with the tibia and fibula bones of the lower leg.
- The calcaneus or heel bone: The calcaneus is largest of the tarsal bones. It sits below the talus and plays an essential role in supporting body weight.
- The tarsals: These five bones form the arch of the midfoot. They are the medial, intermediate, and lateral cuneiforms, the cuboid, and the navicular.

* Phalanges:-

The phalanges are the bones in the toes. The second to fifth toes each contain three phalanges, From the back of the foot to the front, doctors call them the proximal, middle, and distal phalanges, the big toe or hallux contains only two phalanges, which are proximal and distal, the metatarsal phalangeal joints are the joints between the metatarsals and the proximal phalanx of each toe. These joints form the ball of the foot, the first metatarsal phalangeal joint sits in line with the big toe. It is a common area for foot pain and other problems.

2.1.5 Joints:-

Joints in the feet are form wherever two or more of these bones meet. Except for the big toe, each of the toes has three joints, which include:
Metatarsophalangeal joint (MCP) – the joint at the base of the toe
Proximal interphalangeal joint (PIP) – the joint in the middle of the toe
Distal phalangeal joint (DP) – the joint closest to the tip of the toe.

2.1.6 Tendons and Ligaments:-

Many tendons attach the muscles to the bones and ligaments that hold the bones together to maintain the foot's arch.
The main tendon of the foot is the Achilles tendon, which runs from the calf muscle to the heel. The Achilles tendon makes it possible to run, jump, climb stairs and stand on your toes.
The main ligaments of the foot are:

- Plantar fascia – the longest ligament of the foot. The ligament, which runs along the sole of the foot, from the heel to the toes, forms the arch. By stretching and contracting, the plantar fascia helps us balance and gives the foot strength for walking.
- Plantar calcaneonavicular ligament – a ligament of the sole of the foot that connects the calcaneus and navicular and supports the head of the talus.
- calcaneocuboid ligament – the ligament that connects the calcaneus and the tarsal bones and helps the plantar fascia support the arch of the foot.[1]

٢. 2 Diabetes: -

2.2.1 Introduction:-

Diabetes and diabetes is one of the most common chronic diseases worldwide. The International Federation of Diabetes (IFA) President Petra Wilson confirmed that diabetes rates have risen significantly around the world, which requires urgent intervention to reduce its brutality, adding that the number of diabetics in the world has reached about 415 million people in 2015, as the number of people with diabetes in the statistics of the Ministry of Health for 2017 in the West Bank 6313 distributed by sex on 2792 male rate of incidence of 213 per 100,000 population, and 3521 females at 279.6 per 100,000 population, It is divided into two types: the first type is autoimmune disease The immune system attacks and destroys beta cells responsible for the production of insulin in the pancreas. The second type is the most common type of diabetes among people, accounting for between 90 and 95 percent of all patients with diabetes. Diabetes, usually, by age, obesity, heredity and history of the medical family with the disease, personal medical record (cases of gestational diabetes, for example). [2]

2.2.2 Diabetes definition:-

Diabetes is the condition in which the body does not properly process food for use as energy. Most of the food we eat is turned into glucose, or sugar, for our bodies to use for energy. The pancreas, an organ that lies near the stomach, makes a hormone called insulin to help glucose get into the cells of our bodies. When you have diabetes, your body either does not make enough insulin or cannot use its own insulin as well as it should. This causes sugars to build up in your blood. This is why many people refer to diabetes as "sugar." Diabetes can cause serious health complications including heart disease, blindness, kidney failure, and lower-extremity amputations. Diabetes is the seventh leading cause of death in the United States.

*Type 1 diabetes:-

Previously called insulin-dependent diabetes mellitus (IDDM) or juvenile onset diabetes, may account for 5 percent to 10 percent of all diagnosed cases of diabetes. Risk factors less well defined for Type 1 diabetes than for Type 2 diabetes, but autoimmune, genetic, and environmental factors are involved in the development of this type of diabetes.

Type 1 Diabetes Symptoms:-

The initial symptoms of type 1 diabetes often occur suddenly and are very serious. As insulin production decreases, glucose accumulates in the bloodstream instead of being transported into the body's cells, which need it for energy. To generate this missing energy, the body breaks down fat tissue and releases fatty acids. These fatty acids are then metabolized into toxic chemicals called ketones, which increase the blood's acidity to dangerous levels (a state called ketoacidosis).

The initial symptoms of diabetic ketoacidosis include excessive thirst and urination, dehydration, weight loss, nausea, vomiting, fatigue, dry or flushed skin, rapid breathing, abdominal pain, and mental confusion.

*Type 2 diabetes:-

Previously called non-insulin-dependent diabetes mellitus (NIDDM) or adult-onset diabetes. Type 2 diabetes may account for about 90 percent to 95 percent of all diagnosed cases of diabetes. Risk factors for Type 2 diabetes include older age, obesity, and family history of diabetes, prior history of gestational diabetes, impaired glucose tolerance, physical inactivity, and race/ethnicity [3]

Type 2 Diabetes Symptoms:-

Type 2 diabetes develops gradually over many years and the initial symptoms may be almost unnoticeable. In fact, many people find out that they have type 2 diabetes when a routine laboratory test shows high blood glucose levels. As glucose levels continue to increase, most people develop the classic initial symptoms:

Increased frequency of urination, increased thirst and fluid intake and, in later stages, weight loss despite increased hunger and food intake fortunately, these symptoms go away once blood glucose levels brought under control.

Other common symptoms of type 2 diabetes include blurred vision (due to changing levels of glucose in the eye), weakness and fatigue, recurrent vaginal yeast infections, and infections of the skin and gums. These symptoms are temporary, do not indicate any permanent damage, and can be eliminated by controlling blood glucose levels.

In some people, complications of diabetes such as peripheral neuropathy (nerve damage in the hands or feet) or coronary heart disease are the first indication of diabetes. These complications can controlled but cannot cured once they develop.

Another possible initial symptom of diabetes is hyperosmolar nonketotic syndrome. It occurs when the stress of an injury or major illness, such as a stroke, heart attack, or severe infection, causes extremely high blood glucose levels (above 1,000 mg/dL). Although insulin levels are adequate to avert excessive ketone production (as occurs in ketoacidosis), the insulin levels are not high enough to prevent high blood glucose and hyperosmolarity, a condition in which the blood has high concentrations of sodium, glucose, and other molecules that draw water from cells into the bloodstream.[4]

Table 2.1: Amit Jain's classification of diabetic foot complications.

Type of complications	lesions
Type1 diabetic foot complication (infective)	We get gangrene abscess necrotizing fasciitis etc.
Type2 diabetic foot complication (non-infective)	Neuropathic/trophic ulcers , hammer toe claw toes diabetic bullae charcot foot dry gangrene etc.

2.3 Foot ulcer:-

Ulceration of the foot in diabetes is common and disabling and frequently leads to amputation of the leg. Mortality is high and healed ulcers often recur. The pathogenesis of foot ulceration is complex, clinical presentation variable, and management requires early expert assessment. Interventions should directed at infection, peripheral ischemia, and abnormal pressure loading caused by peripheral neuropathy and limited joint mobility. Despite treatment, ulcers readily become chronic wounds. Diabetic foot ulcers have neglected in health-care research and planning, and clinical practice based more on opinion than scientific fact. Furthermore, the pathological processes poorly understood and poorly taught and communication between the many specialties involved is disjointed and insensitive to the needs of patients [5]

2.3.1 Definition Diabetic Foot Ulcer:-

Is as a foot affected by ulceration that associated with neuropathy and/or peripheral arterial disease of the lower limb in a patient with diabetes the classical triad of DFU is neuropathy, ischemia, and infection. Impaired metabolic mechanisms in DM increased the risk of infection and poor wound healing. It happens due to series of mechanisms which include decreased cell and growth factor response, diminished peripheral blood flow and decreased local angiogenesis. So, the feet influenced by damage to peripheral nerves, the peripheral vascular disease, ulcerations, deformities, and gangrene. [6][7]

2.3.2 Foot infection:-

Infection in a diabetic foot is a limb threatening condition because the consequences of deep infection in a diabetic foot are more disastrous than elsewhere mainly because of certain anatomical peculiarities. The foot has several compartments, which are inter-communicating and the infection can spread from one into another, and lack of pain allows the patient to continue ambulation further facilitating the spread. The foot also has soft tissues, which cannot resist infection, like plantar Apo neurosis, tendons, muscle sheaths, and fascia. A combination of neuropathy, ischemia, and hyperglycemia worsens the situation by reducing the defense mechanism.

2.3.3 Osteomyelitis:-

Osteomyelitis generally results from a contiguous spread of deep soft tissue infection through the cortex to the bone marrow. A majority of deep, longstanding foot infections are associated with osteomyelitis. Diagnosing osteomyelitis in a patient with diabetic foot is often difficult. Major problems include differentiating soft tissue infection from bone infection and infections from non-infectious disorders (Charcot Foot). Plain radiography usually shows focal osteopenia, cortical erosions or periosteal reaction in the early stage and sequestration in the late stage. A simple clinical test is probing to the bone. A sterile metal probe is inserted into the ulcer if it penetrates to the bone it almost confirms the diagnosis of osteomyelitis. Chronic discharging sinus and sausage-like appearance of the toe are the clinical markers of osteomyelitis. Definitive diagnosis requires obtaining a bone biopsy for microbial culture and histopathology. [8]

2.3.4 Classification:-

Diabetic foot is classify into two major types.

- The Neuropathic Foot where neuropathy dominates
- The Neuroischemic Foot, where occlusive vascular disease is the main factor, although neuropathy is present.

Neuropathy leads to fissures, bullae, neuropathic (Charcot) joint, neuropathic edema, and digital necrosis. Ischemia leads to pain at rest, ulceration on foot margins, digital necrosis, and gangrene. Differentiating between these entities is essential because their complications are different and they require different therapeutic strategies.
The University of Texas Wound Classification System is the most acceptable classification.

Table2.2: Wound classification system:-

Stages	**Description**
Stage A	No infection present
Stage B	Infection present
Stage C	Ischemia present
Stage D	Infection and ischemia present
Grading	**----------**
Grade 0	Epithelialized wound
Grade 1	Superficial wound
Grade 2	Wound penetrates to tendon or capsule
Grade 3	Wound penetrates to bone or joint

2.3.5 The risk of major amputation of diabetic:-

This figures show that (Figure 2.2-2.4):-

- Patient with non-healing ulcer of 5 months over forefoot that got infected showing abscess and gangrene. This is Amit Jain’s type 3 diabetic foot complication.

Fig.2.2: The risk of major amputation of diabetic (state1)

- The above patient subjected initially to Tran's metatarsal amputation. As per Amit Jain's scoring, his score was ulcer 2 + gangrene 2 + pus 4 + cellulitis 6 + gas up to midfoot 2 = 16, which renders the patient to high risk for major amputation.

Fig.2.3: The risk of major amputation of diabetic (state2)

Fig.2.4: The risk of major amputation of diabetic (state3)

In Fig (2.2-2.4): patient who actually ended up in major amputation with infected stump postoperatively [9]:

2.4 Electromyography (EMG):-

Surface electromyography (SEMG) is the non–invasive recording of electrical muscle activity that used to diagnose neuromuscular disorders, among other applications.
Muscle fibers are activated by motor neurons and the resulting electrical signals produced by the muscle. Most SEMG signals have a frequency content ranging from zero to 500 Hz, with dominant [19].

2.٥ Electromyography (EMG) Physiology:-

Muscle contraction and relaxation controlled by the central nervous system. The nervous system sends a signal through a motor neuron to a grouping of muscle cells, called fibers. That grouping of muscle cells, and the motor neuron that innervates them, is a motor unit
— A basic building block of the neuromuscular system, the smallest functional part of muscle tissue. The signal of the motor neuron causes a chemical reaction that changes the membrane potential of muscle fibers. If the threshold potential reached a motor unit action potential (MUAP) occurs, causing the electrical activation to spread along the entire surface of the muscle fiber at a rate of approximately 3–5 m/s.

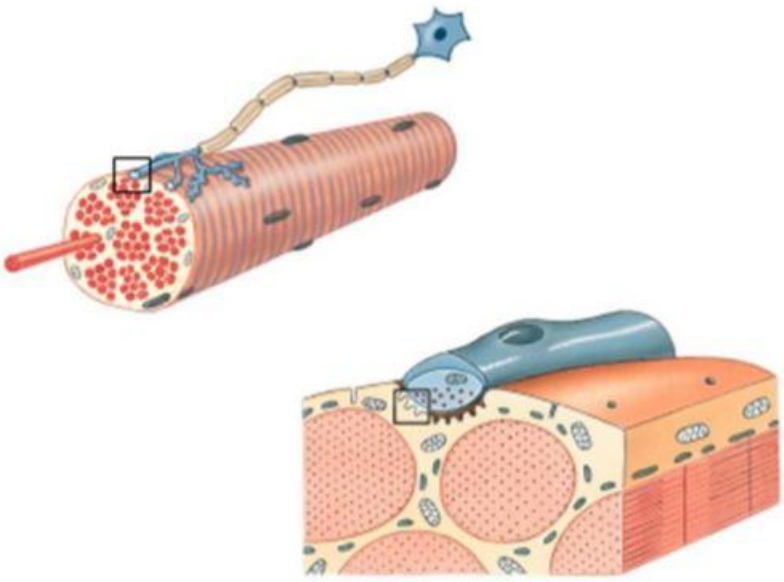

Fig.2.5: is an image of a motor neuron connected to a group of muscle fibers.

Chapter Three:

Theoretical Background

3.1 Introduction

The development of miniature, lightweight, and energy efficient circuit solutions for healthcare sensor applications is an increasingly important research focus given the rapid technological advances in healthcare monitoring equipment, micro fabrication processes and wireless communication. One area that has attracted considerable attention by researchers in biomedical and sport related applications is the analysis of foot plantar pressure distributions to reveal the interface pressure between the foot plantar surface and the shoe sole. Typical applications are footwear design [10], sports performance analysis and injury prevention [11], improvement in balance control [12], and diagnosing disease [13]. More recently innovative applications have also been made to human identification [14], biometric [15], monitoring posture allocation [16] and rehabilitation support systems [17–19]. Based on this research it is clear that techniques capable of accurately and efficiently measuring foot pressure are crucial to further developments. The plantar pressure systems available on the market or in research laboratories vary in sensor configuration to meet different application requirements. Typically, the configuration is one of three types: pressure distribution platforms, imaging technologies with sophisticated image processing software and in-shoe systems. In designing plantar pressure measurement devices the key requirements are spatial resolution, sampling frequency, accuracy, sensitivity and calibration [20].

In-shoe foot plantar sensors have paved the way to better efficiency, flexibility, mobility and reduced cost measurement systems. For the system to be mobile and wearable for monitoring activities of daily life.

This review will first summarize the existing methods for measuring foot plantar pressure and the advantages and disadvantages of a range of commercial pressure sensors used in published research.

3.2 Needs for Plantar Pressure Measurement:-

Feet provide the primary surface of interaction with the environment during locomotion. Thus, it is important to diagnose foot problems at an early stage for injury prevention, risk management and general wellbeing.

With regard to applications involving disease diagnosis, many researchers have focused on foot ulceration problems due to diabetes that can result in excessive foot plantar pressures in specific areas under the foot. Diabetes is now considered an epidemic and, according to some reports, the number of affected patients is expected to increase from 171 million in 2000 to 366 million in 2030 [21]. Improvement in balance is considered important both in sports and biomedical applications. Notable applications in sport are soccer balance training [22] and forefoot loading during running [23]. With respect to healthcare, pressure distributions can be relate to gait instability in the elderly and other balance impaired individuals and foot plantar pressure information can used for improving balance in the elderly.

3.3 Foot Plantar Pressure Measurement Environments

There are varieties of plantar pressure measurement systems but in general, they can be classify into one of two types: platform systems and in-shoe systems.

1. Platform Systems:-

Platform systems are construct from a flat, rigid array of pressure sensing elements arranged in a matrix configuration and embedded in the floor to allow normal gait. Platform systems can used for both static and dynamic studies but are generally restricted to research laboratories. One advantage is that a platform is easy to use because it is stationary and flat but has the disadvantage that the patient requires familiarization to ensure natural gait. Furthermore, it is important for the foot to contact the center of the sensing area for an accurate reading [24]. Limitations include space, indoor measurement, and patient's ability to make contact with the platform, Figures 1 and 2 show a platform-based sensor [25, 26].

Figure 3.1. A platform-based foot plantar pressure sensor (static)

Figure 3.2. A platform based foot plantar pressure sensor (dynamic)

2. Insole Systems:-

In-shoe sensors are flexible and embedded in the shoe such that measurements reflect the interface between the foot and the shoe. The system is flexible making it portable, which allows a wider variety of studies with different gait tasks, footwear designs, and terrains [24].

Figure 3. 3. An in-shoe based foot plantar pressure sensor (uniform)

Figure 3.4. An in-shoe based foot plantar pressure sensor

They are highly recommended [20, 24] for studying orthotics and footwear, design but there is the possibility of the sensor slipping. Sensors should be suitably secure to prevent slippage and ensure reliable results. A further limitation is that the spatial resolution of the data is low compare to platform systems due to fewer sensors [20, 24]. Figures 3 and 4 illustrate in-shoe based systems [25, 27].

3.4 Requirement of Foot Plantar Sensors:-

In taking any biomechanical measurements, devices must be optimize for the specific application to ensure that readings are accurate. Detailed analysis must be thoroughly undertaken prior to any measurements and for foot plantar system two main considerations must met the target implementation requirements and the sensor requirements.

1. Target Implementation Requirements:-

Real-time measurement of natural gait parameters requires that sensors should be mobile, untethered, can be placed in the shoe sole, and can sample effectively in the target environment. The main requirements of such sensors are as follows:

(1) Very Mobile: To make a sensor mobile, it must be light and of small overall size [28, 29], the suggested shoe mounted device should be 300 g or less.

(2) Limited Cabling: A foot plantar system should have limited wiring, wireless is ideal. This is to ensure comfortable, safe and natural gait [29].

(3) Shoe and Sensor Placement: To be located in the shoe sole the sensor must be thin, flexible [30] and light [28]. It is report that a shoe attachment of mass 300 g or less does not affect gait significantly [28]. Shu et al. [31] mentioned that the sole of foot can be divided into 15 areas: heel (area 1–3), midfoot (area 4–5), metatarsal (area 6–10), and toe (area 11–15), as

illustrated in Figure 5. These areas support most of the body weight and are adjust by the body's balance; therefore, ideally the 15 sensors are necessary to cover most of the body weight changes based on the Figure 5 anatomy.

(4) Low Cost: The sensor must be affordable for general application [29] to benefit from inexpensive, mass-produced electronics components combined with novel sensor solutions.
(5) Low Power Consumption: It should exhibit low power consumption such that energy from a small battery is sufficient for collecting and recording the required data.

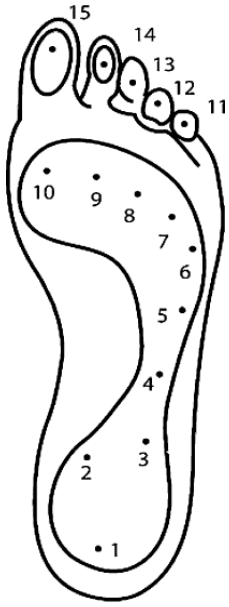

Figure 3.5. Foot anatomical areas

2. Plantar Pressure Sensor Requirements:-

The key specifications for sensor performance include linearity, hysteresis, sensing size, and pressure range and temperature sensitivity [28, 30, and 32]. Brief discussion of these is important as a basis for the selection of a sensor for specific applications.

(1) Hysteresis: Hysteresis can be determined by observing the output signal when the sensor is loaded and unloaded. When the applied pressure is increase by loading or decreased by unloading, two different, responses are observe (Figures 6 and 7).

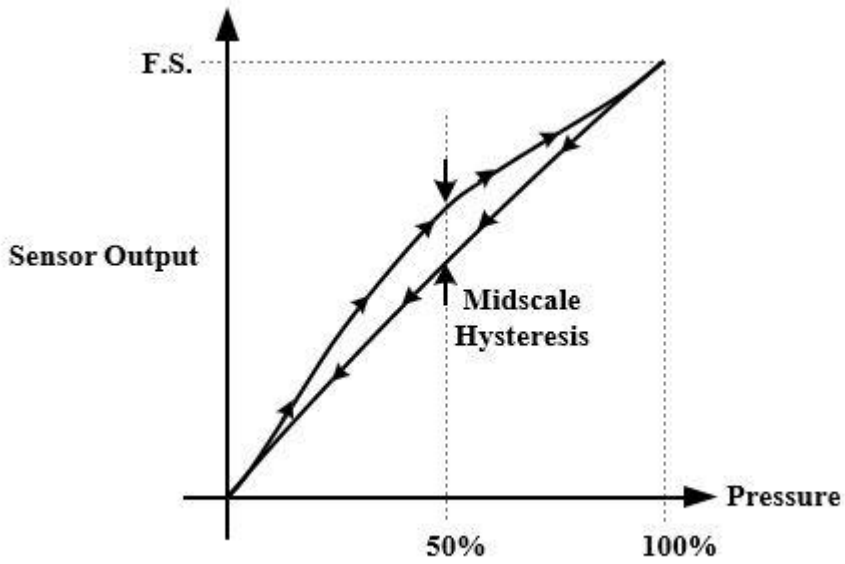

Figure 3.6. Hysteresis caused by loading and unloading a pressure sensor usually measured at the 50% pressure range.

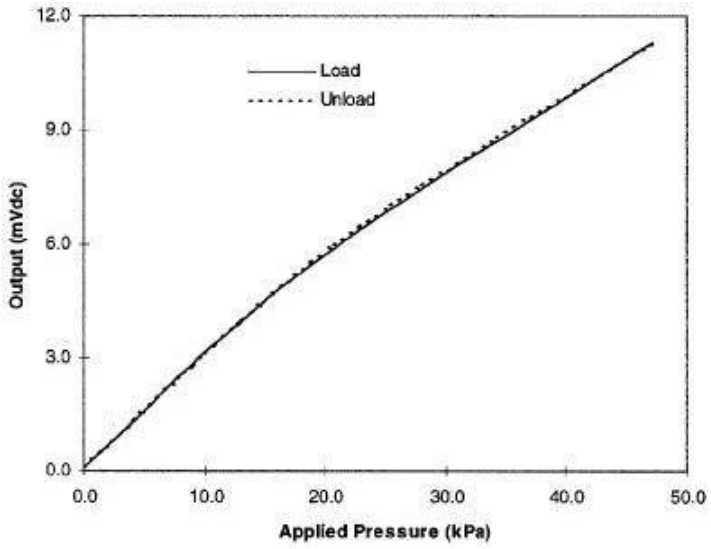

Figure 3.7. Negligible hysteresis of MEMS-based pressure sensor

(2)Linearity: The response of the sensor to the applied pressure, when plotted, will show the linearity figure of merit, i.e., how straight the plotted line is. Linearity indicates how simple or complicated the signal processing circuitry will be, a linear response requires very simple signal processing circuitry and vice versa, a linear pressure sensor is, therefore, preferred.

(3)Temperature Sensitivity: Sensors may produce different pressure readings as the ambient temperature changes. This may be due to the materials that are part of the sensor body as they respond differently to temperature change. A sensor with low temperature sensitivity in the 20 °C to 37 °C range is preferred [30].

(4)Pressure Range: The pressure range is the key specification for a pressure sensor. As different applications require different operating pressures, application-specific sensor development is normally adoptee in the design. Maximum pressure is the upper limit that the pressure sensor can measure and vice versa. It is also important to note that burst pressure is the maximum pressure that the sensor can withstand before breakage as opposed to maximum pressure. Foot plantar pressure values of up to 1,900 kPa are typically report in the literature but an extreme pressure of up to three MPa has been document by Urry [32]. One of the foot plantar pressure sensor designs considers 3 MPa as burst pressure value, for comparison when a healthy person of 75 kg body mass is standing on only one forefoot, if pressure is evenly distributed, the interfacial pressure for every 31.2 mm^2 foot plantar area approximates 2.3 MPa [33].

(5)Sensing Area of the Sensor: Size and placement of the sensor are also critical, as shown in Figure 8. As a large sensor may underestimate the peak pressure and it is suggested that a minimum sensor of 5 mm × 5 mm should be used, whereas sensors smaller than this must be designed as array sensors.

(6)Operating Frequency: It recommended [32] that to measure foot plantar pressure precisely for running activities the sensors must be capable of sampling at 200 Hz. This frequency is generally consider sufficient for sampling most everyday gait activities.

(7)Creep and Repeatability: Creep is the deformation of material under elevated temperature and static stress. It directly relates to the time dependent permanent deformation of materials when subjected to a constant load or stress [34], as in Figure 9. Low creep sensors are one of the key requirements in foot pressure measurement. Repeatability refers to the ability to produce reliable result even after long period of time [30]. High cyclic loads may cause deformation or fatigue [34]. Repeatability problems can be eliminate if the sensor exhibits no creep or deformation over repetitive or high cyclic loads.

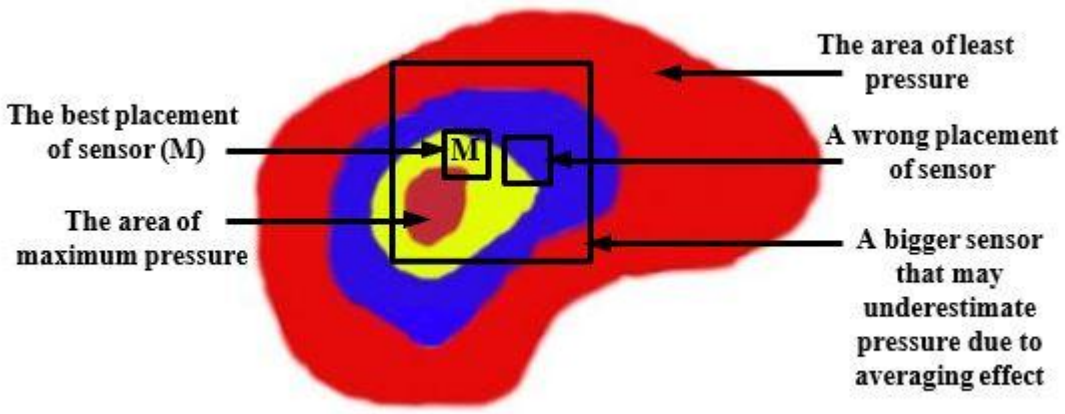

Figure 3.8. Effect of sensor sizing and placement.

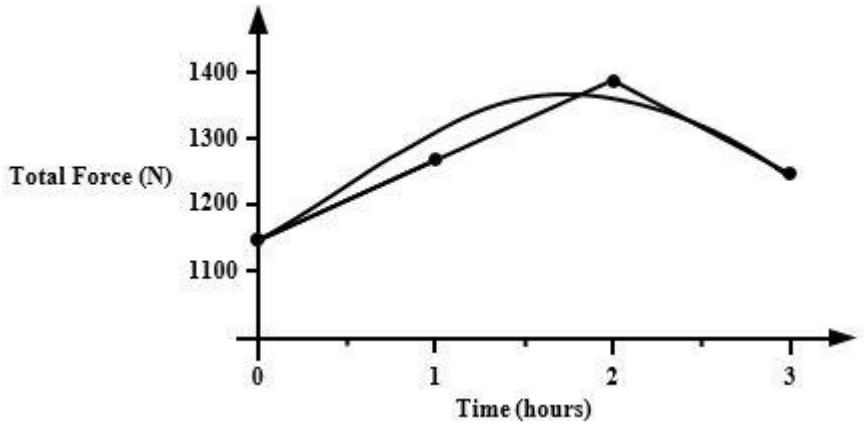

Figure 3.9. Example of erroneous readings due to sensor creep of Insole. The curve is the error reading by the sensor and plotted line is the correct pressure values.

3.5 Commercial Foot Plantar Pressure Measurement Sensors:-

There are several pressure sensors available on the market. Such sensor technologies utilize capacitive sensors, resistive sensors, piezoelectric sensors and piezoresistive sensors. These sensors provide electrical signal output (either voltage or current) that is proportional to the measured pressure. The required key specifications for a pressure sensor in terms of sensor performance include linearity, hysteresis, and temperature sensitivity, sensing size and pressure range. The most common pressure sensors are capacitive sensors, resistive sensors, piezoelectric sensor and piezoresistive sensor.

1. Capacitive Sensors:-

The sensor consists of two conductive electrically charged plates separated by a dielectric elastic layer. Once a pressure is applied the dielectric elastic layer bends, which shortens the distance between the two plates resulting in a voltage change proportional to the applied pressure [20, 32]. Figure 10 shows the capacitive sensor construction.

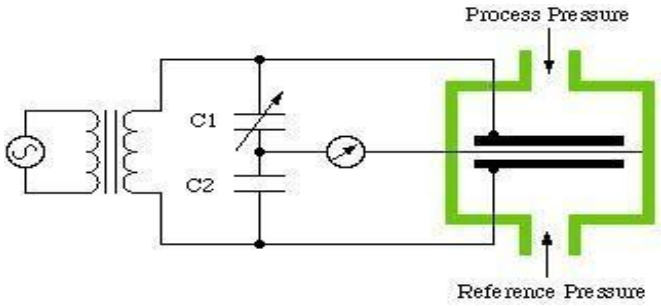

Figure 3.10. Capacitive pressure sensor construction

2. Resistive Sensors:-

Force-Sensing Resistor (FSR) is a good example of the resistive sensor. When pressure is apply, the sensor measures the resistance of conductive foam between two electrodes. The current through the resistive sensor increases as the conductive layer changes (*i.e.*, decreases resistance) under pressure. FSRs are made of a conductive polymer that changes resistance with force, applying force causes conductive particles to touch increasing the current through the sensors [20, 32]. Figure 11 shows the resistive sensor construction.

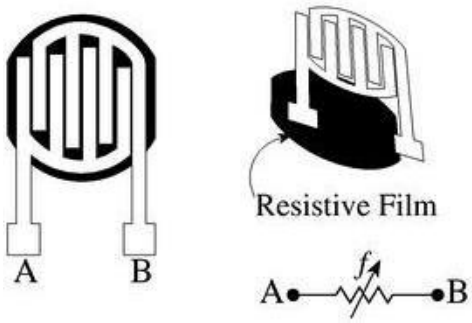

Figure 3.11. Resistive pressure sensor construction

3. Piezoelectric Sensors:-

The sensor produces an electric field (voltage) in response to pressure. Piezoelectric devices have high impedance and therefore susceptible to excessive electrical interference that leads to an unacceptable signal-to-noise ratio.

The most suitable material for clinically oriented body pressure measurement is polyvinylidene fluoride (PVDF) because it is flexible, thin and deformable [20, 32]. Figure 12 shows the piezoelectric sensor construction.

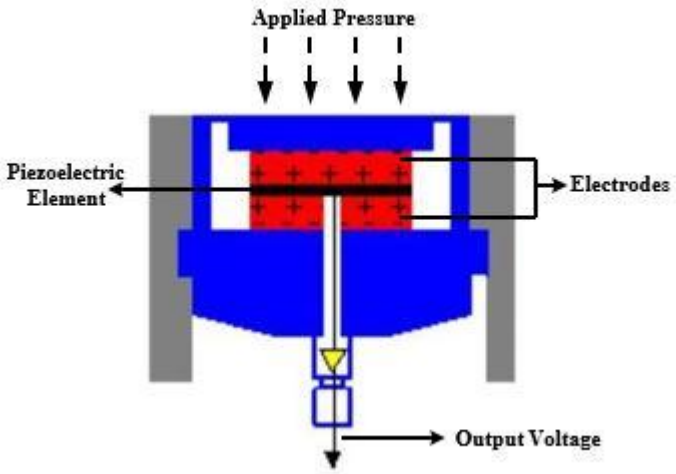

Figure 3.12. Piezoelectric pressure sensor construction

4. Piezoresistive Sensors:-

This sensor is made of semiconductor material. In Piezoresistive material, the bulk resistivity is influence by the force or pressure applied, when the sensor is unloaded resistivity is high and when force is apply resistance decreases [20]. Figure 13 shows the piezoresistive sensor construction. When there is pressure on the piezoelectric element (quartz crystal), it produces electric charges from its surface. These charges create voltage proportional to the applied force.

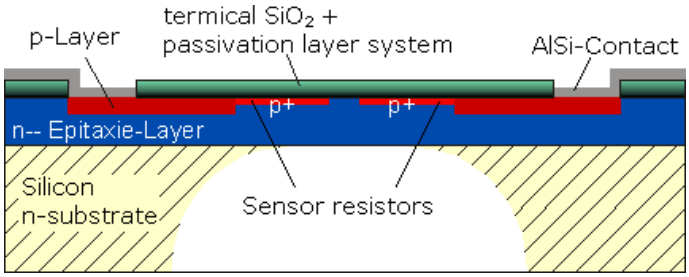

Figure 3.13. Piezoresistive pressure sensor construction

The requirements of the pressure sensor for the specific application are low hysteresis, linearity of output, and pressure range [28, 30, and 32]. A recommended pressure range for gait analysis (walking) is approximately 1,000 kPa [32] but for sports, the pressure range should be larger due to the nature of the movements. There are a number of commercially available foot-pressure sensors on the market but they generally do not fulfil the requirements of many biomechanical applications due to specification and performance limitations. The limitations include but not limited to, the specified hysteresis [30], pressure span and physical sensor dimensions [35].

Comparison with traditional foot plantar pressure sensors such as capacitive sensors, resistive sensors, piezoelectric sensors and piezoresistive sensors the MEMS pressure sensors have many advantages. For example, easy communication with electrical elements in semiconductor chips, small size, lower power consumption, low cost, increased reliability and higher precision. To provide a better alternative developments of a specifically designed miniature foot pressure sensor based on MEMS technology have been explore. In response to the needs of such sensors, successfully designed, fabricated and tested a miniature foot pressure sensor based on MEMS technology that can be insert in the insole of a shoe [36]. As significant performance enhancements have been, achieve, for example, the sensor is small, has high-pressure range measurement capability, and excellent linearity both at low and high pressures and possesses negligible hysteresis.

Currently available in-shoe pressure sensor parameters are compare to Wahab *et al.* [36] in Table 1. Sensors from Vista Medical, Novel and Tekscan show some performance limitations as they are made of sheets of polymer or elastomer leading to issues such as repeatability, hysteresis, creep and non-linearity of the sensor output [30]. In addition to the above limitations, some sensors (e.g., Parotic) have limited pressure range and relatively large dimensions. Figure 14 demonstrates the linearity of the MEMS based pressure sensor and the fabricated sensor as displayed in Figure 15.

Table 3.1. Commercially available in-shoe pressure sensors compared to Wahab *et al.* sensor[31].

	Vista Medical [44]	**Tekscan [26]**	**Novel [24]**	**Parotec [45]**	**Textile Sensor [30]**	**Wahab *et al.* [43]**
Sensor Size	2 mm thick	0.15 mm thick	1.9 mm thick	~4 cm^2 (hydrocell)	Not Specified	2 mm thick
Number of Sensor	128 (in shoe)	960 (insole)	99 (insole)	24 (insole)	6 (insole)	15 (insole)
Range (kPa)	260	1,034	1,200	625	800	3,000
Frequency (Hz)	Not Specified	500	Not Specified	250	100	200
Hysteresis	Not Specified	24%	<7%	0.05% at 20 Ncm^{-2}	Not Specified	Negligible

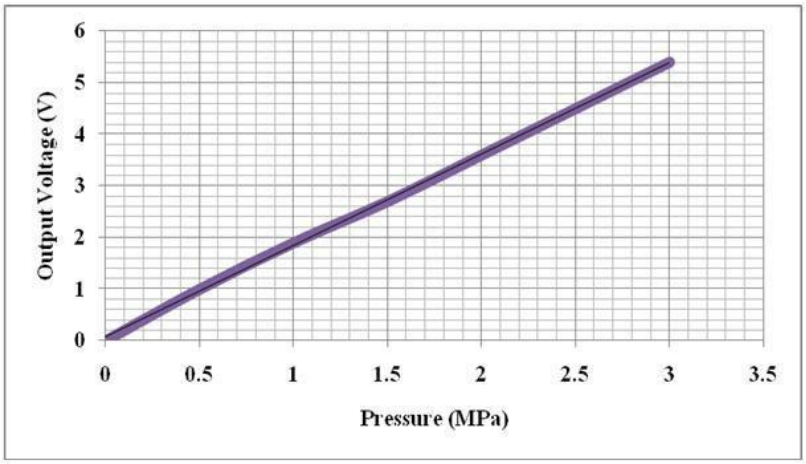

Figure 3.14. Graph demonstrating linear output voltage vs. pressure relationship [33].

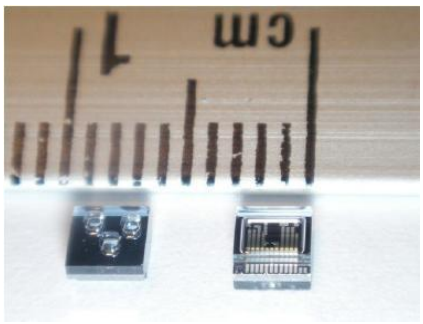

Figure 3.15. Picture of fabricated sensors [32].

3.6 Recent Trends in Foot Plantar Pressure Measurement:-

Trends in biomedical monitoring are toward using real-time and *in-situ* measurement of normal daily life parameters to keep pace with a fast-changing and demanding scientific environment. Gait analysis researchers are focusing on designing systems for uninterrupted measurement of real life parameters, which is important in understanding the effect of daily activities on health. The ideal system to achieve this would be mobile, un-tethered, placed in the shoe sole and able to measure effectively in the targeted environment.
As early as the 1990s, Zhu *et al.* [37] developed a system for measuring the pressure distribution beneath the foot using seven force-sensitive resistors (FSR) and they used it to differentiate pressure between walking and shuffling [38]. In 1995, Hausdorff *et al.* [39] built a footswitch system capable of detecting temporal gait parameters using two FSR sensors. Later, in 1997, Cleveland Medical Devices Inc. [40] created an in-shoe wireless system, which could measure time of foot contact, the weight on each foot and the Centre of pressure (COP) of each foot. The system used a set of thick-film force sensors and since then there has been further development of in-shoe pressure sensor systems. In this paper, the focus is on the current development of the system.

3.6.1 Wired Systems Application:-

Over the past two years, there has been increasing interest in developing in-shoe foot plantar pressure systems and recently there have been applications to plantar pressure using both wired and wireless systems. In 2011, a paper employed dynamic plantar pressure for human

identification using a Flexi Force (Tekscan, USA) in-sole pressure sensor [14]. They compared the pressure at different positions of key points then identified and classified them using a support vector machine (SVM) running on a PC. The system uses wire to transfer data from the sensor to a data acquisition card on a PC (Figure 16) and it is reporter that the system has 96% identification accuracy.

Yamakawa *et al.* [15] also proposed their own biometric identification in-shoe system based on both feet pressure change and reported that the system could recognize over 90% of the test subjects. The system used F-scan (Nitta Corp, Japan) as the pressure sensor (see Figure 17). Another innovative application is an in-shoe system to measure triaxial stress in high-heeled shoes [41]. The paper investigated the distribution of contact pressure and sheer stress simultaneously in high-heeled shoes utilizing five in-shoe triaxial force transducers commercialized by Anhui June Sport, China.

Figure 3.16. Identification based on dynamic plantar pressure in-shoe system

Figure 3.17. Biometric identification based on foot pressure pattern changes

Shear stresses can cause blisters, callosities and trophic ulcers. The size of transducer is 17 mm × 18 mm × 10 mm and has 870-kPa full-scale pressure range. In the system the transducer in mounted under the hallux, the first, second and fourth metatarsal heads as well as the heel as shown in Figure 18. As can be seen from the figure, peak sheer stress occurs at the second metatarsal; this type of information can be useful for future high-heeled shoe design.

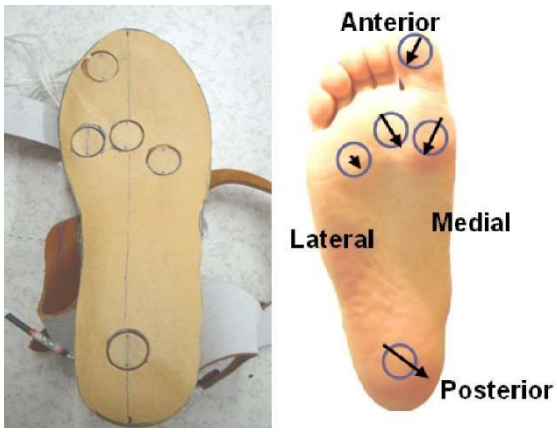

Figure 3.18. Mounted transducer in high-heeled shoe

Work undertaken by Healy *et al.* [42] claimed that their in-shoe system has a better repeatability compared to other commercially available systems. The sensor is practically similar to F-Scan (Tekscan, USA) which uses resistive force sensor.
The system is name "WalkinSense" and consists of a data acquisition and processing unit and eight individual sensors. It appears that only the sensor part is their own development, the rest of the system is similar to F-Scan (Tekscan, USA) hardware and software. The location of the sensors is illustrate in Figure 19, whilst the WalkinSense® System shown in Figure 20.

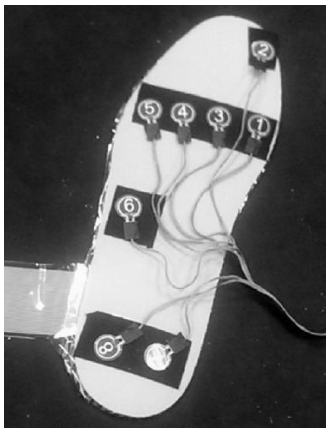

Figure 3.19. WalkinSense sensor placement

Figure 3.20. WalkinSense system

All of the works described above [14, 15, 41, and 42] have a common feature that is wire to the processing unit or PC. All of them have certain benefits but for a wired system, the major limitation is application in everyday monitoring. The wired system may encumber the test subject causing trip hazards or even a fall, and it can affect the normal gait patterns. Therefore, it is recommend making the system mobile for everyday usage, and the system must adapt to a wireless system. Research presented in [41, 42] developed their own transducers but seems to have limited number of sensor placement. As mentioned in section IV, pressure recording from 15 locations is regard as ideal for gait analysis. Papers [14, 15] on the other hand used off-the-shelf sensors.

3.6.2 General Wireless Systems Application:-

As mentioned earlier, there is a need for a system that can provide a wireless, real-time and reliable result to measure foot plantar pressure. There have been quite a few works undertaken in both research and commercial platforms that focused on developing a more mobile method of measuring foot pressure. Shoe based systems have been increasing, in terms of the number of

publications and commercial products, due to shrinking in size of sensors, processing unit communication device and data storage. Further, the obvious reason for its usefulness is that such a system could measure the pressure distribution directly beneath the foot.
The work undertaken by Bamberg et al. 2008 [28] from Massachusetts Institute of Technology (MIT), had been mentioned in a large number of the papers that were reviewed. The main reason why
Bamberg et al. have received so much attention in the literature is that they had come up with arguably the most complete wireless in-shoe system for gait analysis to date. They called it Gait Shoe. In their system, the sensors included three orthogonal accelerometers, three orthogonal gyroscopes, four force sensors, two bidirectional bend sensors, two dynamic pressure sensors and electric field height sensors. The devices were capable of detecting heel-strike, estimating foot orientation and position and toe-off. The microcontroller (Silicon Laboratories), RF Monolithic (as the transceiver), antenna and power supply were also attached to the shoes. Figure 21 displays the Gait Shoe with all the hardware mounted on the shoes.
In 2009, Benocci et al. [43] from University of Bologna, Italy developed a wireless system for gait and posture analysis. The wearable system utilized 24 hydrocells (by Paromed) to measure the plantar pressure and inertial measurement unit (IMU) in each shoe insole. The IMU integrated a 3-axes accelerometer and a digital 3-axes gyroscope. To control the system, Texas Instrument MPS430 microcontroller was implement and Bluetooth acted as the transceiver. The collected data from the sensor allowed the user to recognize walking phases such as swing and stance, step and stride duration, double support and single duration.

Figure 3.21. Shoe-integrated wireless sensor system, Gait Shoe, showing all the hardware components.

Figure 3.22. A wireless systems for gait and posture analysis based on pressure insoles and inertial measurement units.

Ming Young Biomedical Corp., Taiwan published a state-of-the-art digital textile sensor for measuring gait analysis [44]. Four dome shaped sensors were kite on each sock. The dome shape sensors were able to record spatio-temporal plantar pressure patterns, which used to calculate the Centre of pressure (COP) excursions. Five-clip type sensors were sew to the pant to record lower

limb movement. The system was report to measure the duration of stride cycles and left/right steps, cadence, walking speed, and COP. The microcontroller (Texas Instrument MPS430) and Bluetooth were attached to the wearer's belt. Figure 23 portrays the digital textile sensors in action.

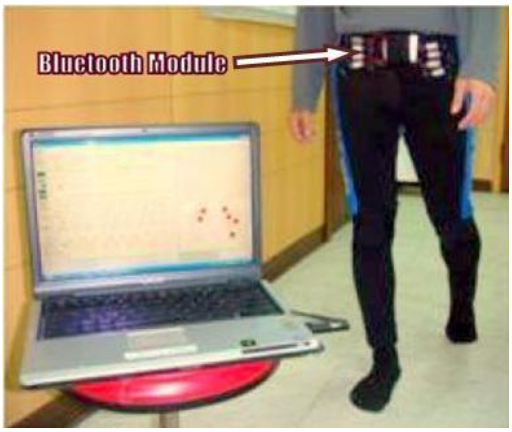

Figure 3.23. Wireless gait analysis system by digital textile sensors.

Shu *et al.* [31] developed an in-shoe plantar pressure measurement and analysis system based on fabric pressure sensing array in collaboration with Hong Kong Research Institute of Textiles and Apparel Ltd. The sensors used were te-xtile fabric sensor array, which is soft, light and has high-pressure sensitivity. The sensors connected with a soft polymeric board through conductive yarns and integrated into the insole.
Sensors were attach to six locations in the insole, as shown in Figure 24. The microcontroller PIC18F452 and the Bluetooth module attached to the ankle of the patient. The system could Interface with desktop, laptop and smart phone and was able to calculate parameters such as mean pressure, peak pressure, COP and shift speed of COP. The results were present for both static and dynamic measurement conditions. Figure 25 shows the in-shoe plantar pressure measurement and analysis system based on fabric pressure sensing array.

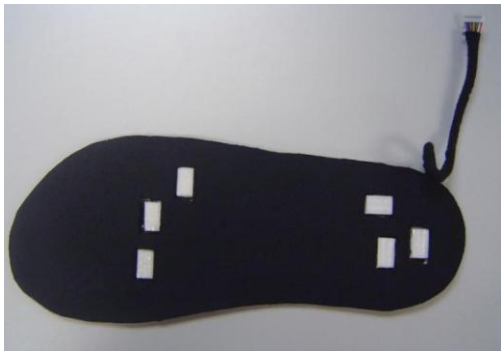

Figure 3.24. Fabric pressure sensing array indicating sensor placement

Figure 3.25. In-shoe plantar pressure measurement and analysis system based on fabric pressure sensing array

The developments of wearable wireless sensor system for measuring foot plantar pressure have been encouraging. There is no doubt about their application potentials, especially the biomechanics communities. Nearly all use off-the-shelf sensors, microprocessors and wireless transmitters, so the product is bulky and not comfortable to wear by the patients. The digital textile sensors by Chang-Ming et al. [44] are small and flexible but it is wire to a Bluetooth based transmitter device at the belt. Both Benocci et al. [43] and Lin Shu et al. [31] used Bluetooth modules to attach to the ankle. Even more uncomfortable would be the system proposed by Bamberg et al. [28] where the whole sensor and wireless communication tools are attach to the top of the shoe. Although Bamberg et al. has developed the in-shoe gait analysis system but the system is not wearable for daily activities monitoring.

3.6.3 Major Application Areas:-

***3.1. Rehabilitation Applications:-**

Wireless foot plantar systems have been apply to a number of areas including rehabilitations, sports and daily life gait monitoring. For example, Crosbie and Nicol ;indicated that as part of rehabilitation procedure of patients with spinal cord injury and diabetes, it is quite useful to measure the efforts exerted by lower limbs such as plantar surface pressure/force distributions and the contact sensation with the ground. This information is essential in providing better rehabilitation strategies. Recent publications on wireless systems for rehabilitation applications include work by Neaga et al. [17] for monitoring the progressive loading of lower limb in post-traumatic rehabilitation, by Wada et al. [18] for rehabilitation support system and by Edgar et al. [19] on wearable shoe for rehabilitation of stroke patients. Neaga et al. used F-Scan® (Tekscan, USA) for the sensor, microcontroller based data acquisition and RF transceiver for wireless communication. The system indicates to the user excessive loading of the lower limb through LED indicators. Figure 26 presents the prototype shoe and the prototype hub. Wada et al. developed their system named "Gait Guide". The system used sensors units (gyro sensor, acceleration sensor, ultrasonic sensor and pressure sensor), a wireless module, an electronic tag to collect data from the shoe and display gait information. The "Gait Guide" could collect the gait information in the form of step length, step width and pressure. The gait information can used to design a specific rehabilitation program for a particular patient. The "Gait Guide" prototype is display in Figure 27. Edgar *et al.* [19] indicated that their system could classify patient's recovery from stroke posture. They claim that the system had 99% accuracy in the classification. The system applied a microcontroller (Texas Instrument, USA), a Bluetooth

module (Roving Network, USA), accelerometer sensor and in-sole pressure sensor. Figure 28 shows components of the developed prototype.

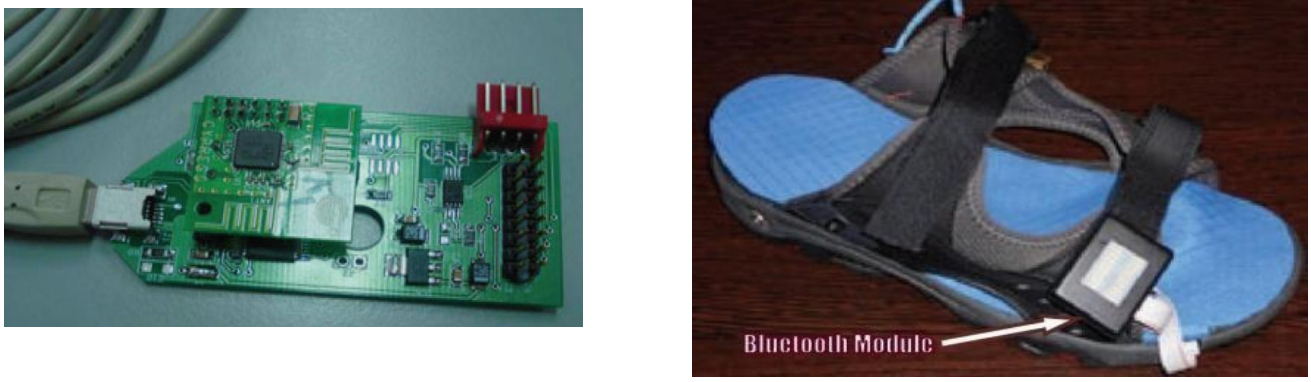

Figure 3.26. Neaga *et al.* microcontroller board and shoe prototype

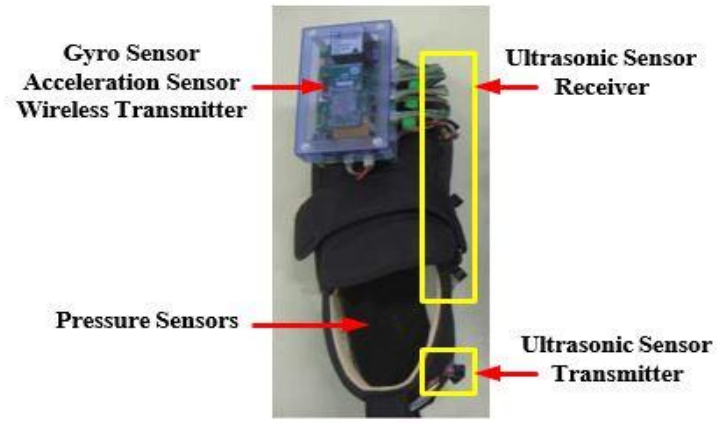

Figure 3.27. "Gait Guide" shoe prototype

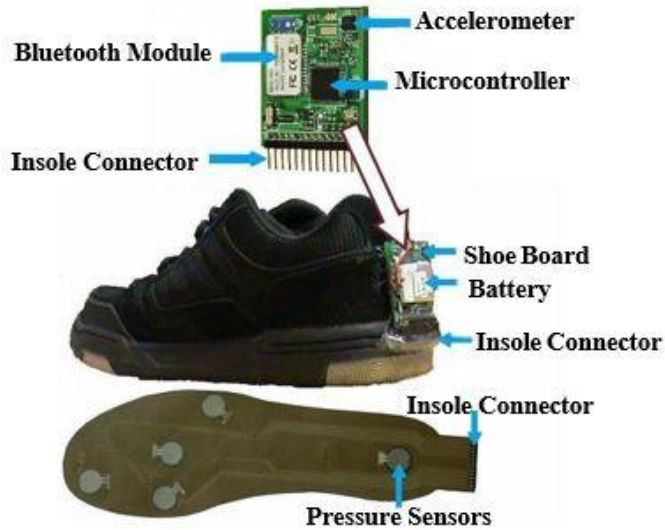

Figure 3.28. Edgar *et al.* shoe prototype**.**

These published researches [17–19] are all wireless, and all are design to assist patients with mobility problems. Figures 26–28, however, indicate that these bulky electronics may not be suitable for monitoring recovery in post-traumatic patients. Another point worth noting is that

these three systems used commercial foot plantar pressure sensors, and the limitations of commercial sensors have been highlight.

4 Sport Applications:-

Another application that relies on a wireless system is sport application. Noteworthy mentions are research by Salpavaara et al. [45] and Holleczek et al. [46]. These two papers employed innovative new sensors for their application using custom made laminated capacitive sensor matrix and textile pressure sensors respectively. Salpavaara et al. system can be utilize to monitor the timing and movement of the legs of the athlete during throwing, jumping and running in various sports events. The obtained data can used for improving sports coaching. They opt for javelin throwing for their case study. In their case study they conclude that the timing of the steps, support and release phase has a great importance in the performance and the pace of steps should increase towards the end of the throw event. In their system, they employ a capacitance-to-digital converter (Analog Device, USA), microcontroller (Atmel, USA) and a Zigbee-compliant radio. Figure 29 shows the five sensors placement. Holleczek et al. developed "SnowPro", a wearable sport trainer, capable of supporting snowboarders in improving their skill. The system is able to analyze the dynamics of the weight distribution inside the boots. This type of information is essential for identifying the wrong weight shifting techniques, which usually lead to painful crashes in snowboarding sport. The system gives feedback to the user in real-time or after the activity about user performance and support user during learning process. This system utilizes three integrated textile pressure sensors, six capacitance-to-digital converters and a Bluetooth module. Figure 30 displays the final design by Holleczek et al. [46].

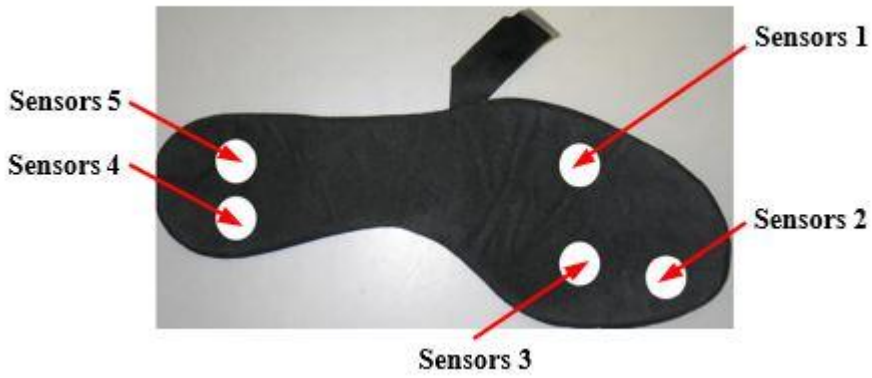

Figure 3.29. The five sensors placement of Salpavaara *et al.* designed system

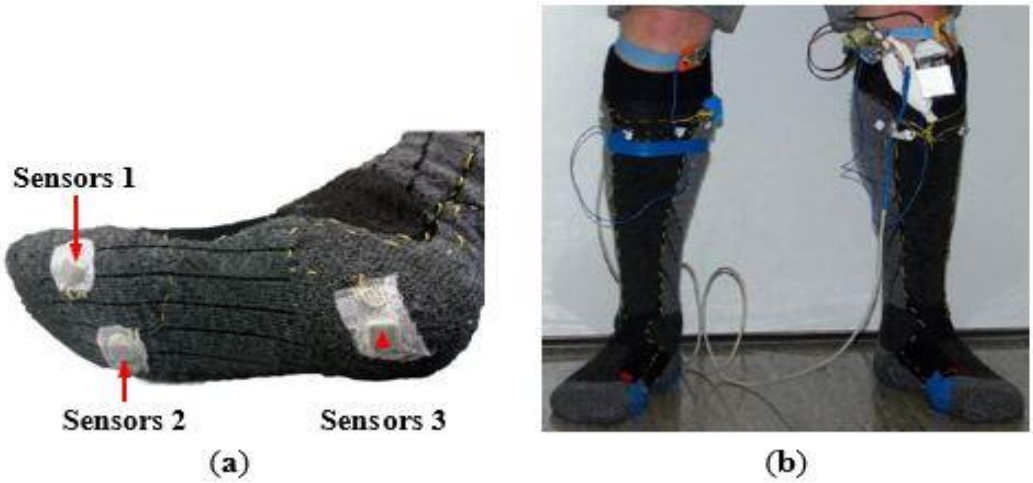

Figure 3.30. The three sensors placement of Holleczek *et al.* sensor sock designed. (**a**) Three sensors placement; and (**b**) wearable system

The obvious deficiency in the system is the number of sensors used. Salpavaara *et al.* [45] used five and Holleczek *et al.* [46] used only three. For many sport biomechanics applications, this number may not be adequate. Besides that, for sport applications the system should not obstruct the athlete's movement. From Figure 30(b) it is apparent that it is not very practical. This is because both systems utilized off-the-shelf equipment that is usually very bulky.

***4.1. Other Wireless Systems Application:-**

Other wireless in-shoe foot plantar pressure system that can be highlighted are those proposed by Saito *et al.* [47] and De Rossi *et al.* [48] which employ unique pressure sensors to measure plantar pressure during daily human activity. Saito *et al.* device consists of a shoe insole with seven pressure-sensitive conductive rubber (PSCR) sensors (Yokohama Image System, Japan), 10-bit analog-to-digital converter and a RF wireless transmission unit. Each (PSCR) sensor is about 15 mm × 10 mm × 0.8 mm. In addition, can measure pressure in the range 25–250 kPa. The seven sensors are place at heel, lateral midfoot, great toe, head of the first metatarsal, Centre midfoot and Centre forefoot as portrayed in Figure 31. Figure 31 also displays the complete shoe with the power source, wireless transmitter and pressure measurement unit.

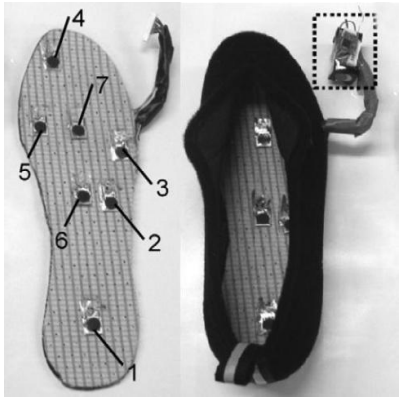

Figure 3.31. The seven sensors placement and the complete shoe. The box inlet is the power source, wireless transmitter and pressure measurement unit

Saito *et al.* [47] system has several benefit over the other system, namely they did not adopt a processing/microcontroller unit attached to the shoe ensuring the electronic circuitry is keep small, and their processing unit is at the receiving end of the system. This benefit also makes the power consumption lower compared to other systems, thus the system is capable of monitoring

up to 20 hours with changing power source. On the contrary, the sensor has limited pressure range; the maximum the transducer could sense is 250 kPa. A typical obese person can generate more than 500 kPa average peak pressure for both men and women [49] and for sport application for instance during triple jump it is reported that the maximum pressure can reach around 750 kPa to 1 MPa depends on the athletes [50].
De Rossi *et al.* [48] employed 64 silicone-covered opto-electronic pressure sensors array, four 16-channel 14-bit analog-to-digital converters, a microcontroller and a Bluetooth module. The sensors have 12 mm × 12 mm × 5.5 mm dimension, maximum loading of 500 kPa without damaging the sensor. Figure 32 shows the dimensions of the sensor. The transduction principle of the sensors is demonstrate in Figure 33. When a load is apply to the top face, the cover causes a deformation, and lowers silicone „curtain" which obstructs the light path from the LED to the photodiode. Therefore, lower the light from the LED receiving at the photodiode producing lower voltage at the output of the photodiode. Thus, it is inversely proportional the relationship between input force and output voltage. The sensors also show no significant static hysteresis. Figure 34 plots the force *vs*. output voltage characterization. Figure 35 depicts the complete insole pressure system and the system fitted inside a shoe.

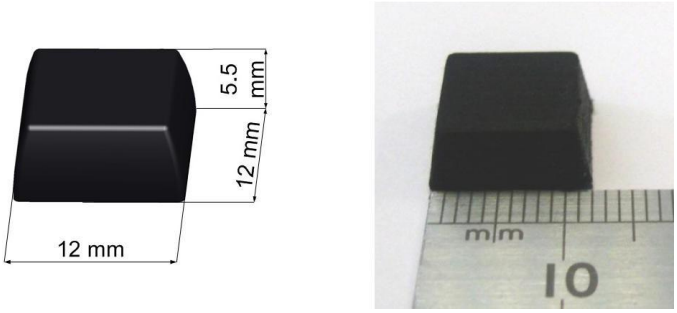

Figure 3.32. De Rossi *et al.* sensor dimension.

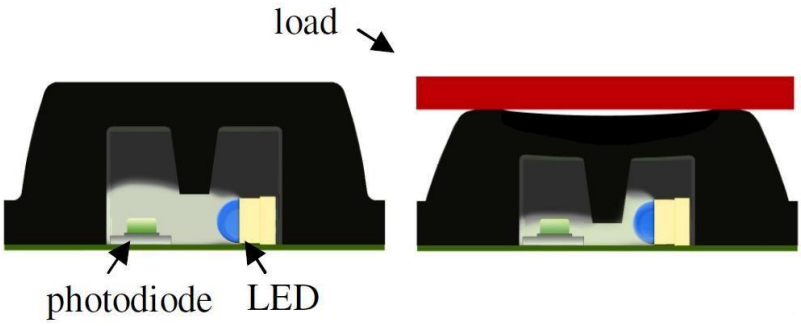

Figure 3.33. Working principle of De Rossi *et al.* sensor.

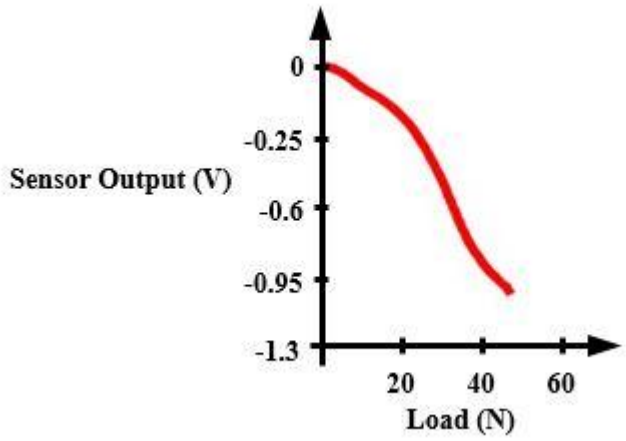

Figure 3.34. De Rossi *et al.* sensor characterization: Force *vs*. Output Voltage.

Figure 3.35. De Rossi *et al.* insole sensor system and the system fitted inside a shoe.

Based on the information in reference [48] the sensor design by De Rossi et al. has a number of advantages. The advantages are the number of sensor placement nearly covers the whole surface of the foot, the bulky electronics board is well hide in the medial arch of the foot and the sensor has no significant hysteresis. On the flipside, the sensors has a bad linearity at low and high pressure which will require a more complex signal processing to ascertain a more accurate representation of the pressure. Another downside is that the sensor has limited life expectancy, the sensor will damage if a pressure exceeding one MPa is force on it. The housing for the electronic board is make out of thin PCB, which the authors mention that it is comfortable to wear.

From the review, there is one common limitation in most of these systems, which is the wireless transmitter/transceiver. If only the wireless transmitter/transceiver could be integrate and minimized the size, it could be insert inside the insole of the shoe with the entire sensor. This would make the shoe more wearable for daily life activities, and help with diagnosing foot problems.

3.7 Proposed Wireless DAQ Foot Plantar Pressure System:-

Based on the reviewed current in-shoe foot plantar systems, it seems there are some limitations that could be improve. One area of the improvement could be development in the wireless data acquisition (DAQ) for the in-shoe foot plantar pressure sensor system. So we propose to design and implement miniaturized insole, low power and wearable wireless system using customized MEMS sensors for measuring foot plantar pressure and interface it with wireless DAQ unit that can be also slotted in the in-sole of the shoe. The research work requires a systematic understanding of different types of wireless systems on chip, the requirement of MEMS pressure sensor for measuring foot plantar pressure and realistic scenarios for their implementation and the application. The MEMS pressure sensors have several advantages compared to others such as small in size, high-pressure range, linear and high reliability. The specific aim of the research is to design a wireless foot plantar pressure measurement system. The transmitter must be compatible with the MEMS sensor, meet the requirement of measuring foot plantar pressure analysis and wearable for in-shoe applications. The receiver should be suitable for interfacing with data logger, desktop or laptop for further data analysis. Figure 36 shows the block diagram of the proposed system.

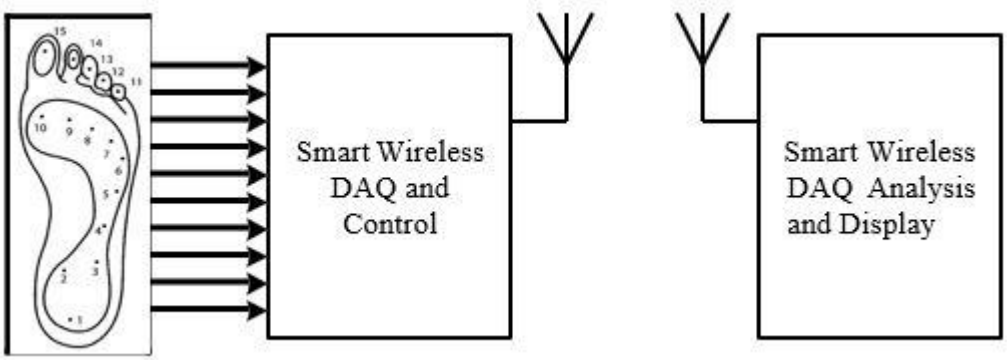

Figure 3.36. Block diagram of the proposed system

A wireless DAQ-IC that can be insert in the insole of a shoe has been design and simulated [51]. The system architecture shown in Figure 37. In this design, the first task was to transmit data from only a single MEMS sensor. The layout design of the IC is display in Figure 38. The total chip size of the design including pads is about one mm^2.

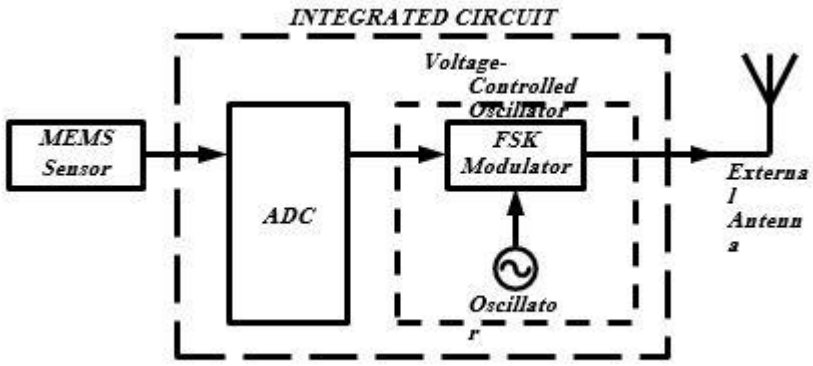

Figure 3.37. Block diagram of system design

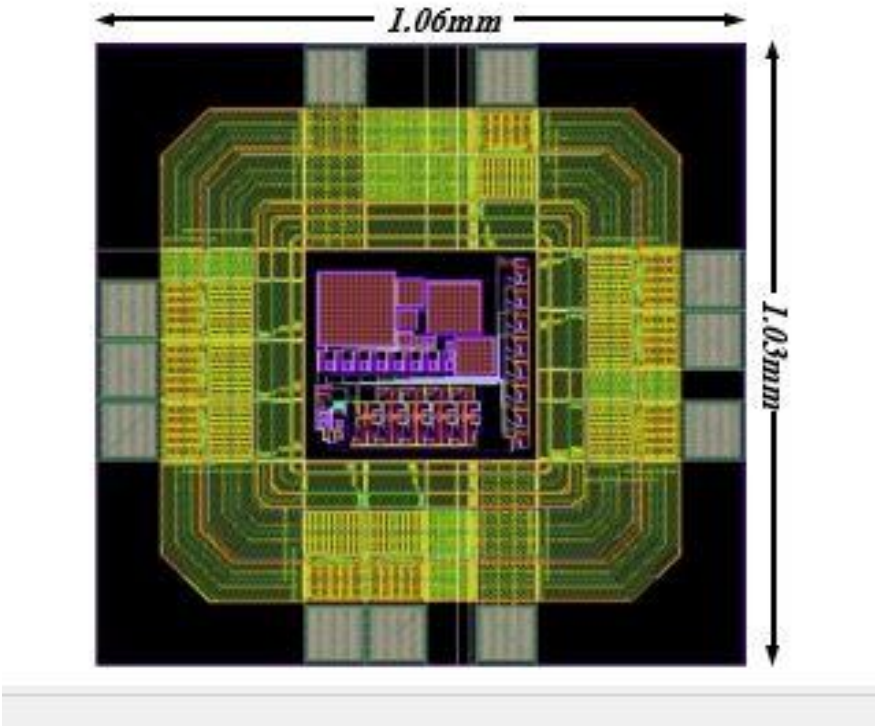

Figure 3.38. The layout design with padding

For further improvement of the system, we added more features based on our earlier design. First, including an analog multiplexer (MUX) to ensure the single DAC chip can cater for all 15 sensors based on our initial block diagram. Second, after the inclusion of the MUX a controlling unit add to the design (Figure 39) to control the whole system design making it a smart system and finally, we integrated an on-chip antenna thus creating the whole wireless DAQ system in a single chip with only the addition of the power supply. The new proposed design is depict in Figure 39.

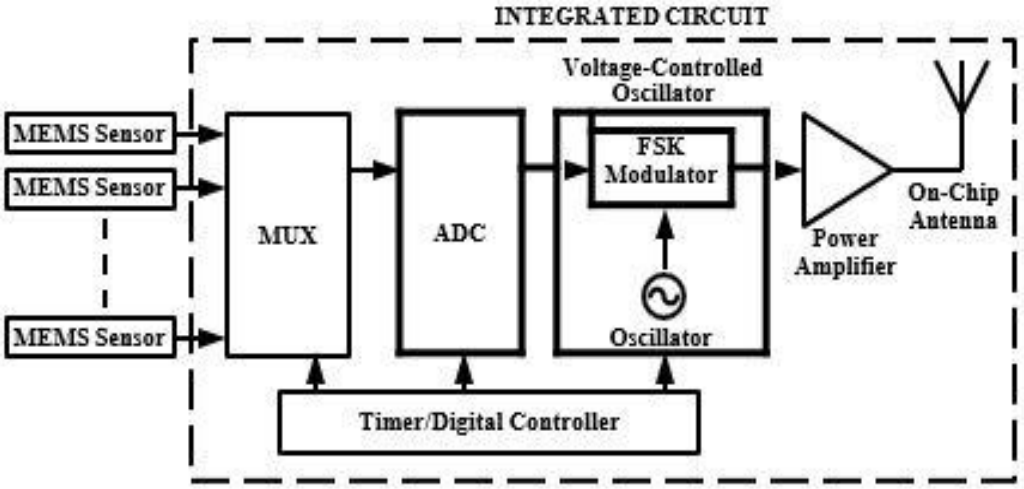

Figure 3.39. The new proposed system design block diagram.

3.8 Techniques for testing diabetic foot disease:

1. **Sphygmomanometer test:-**

This is the first test in the diagnosis of diabetic foot ulcer. Sphygmomanometer is the instrument used in the blood pressure measurement. It is composed of an inflatable cuff to restrict blood flow, and a mercury or mechanical manometer to measure the pressure. It is always use in conjunction with a means to determine at what pressure blood flow is just starting, and at what pressure it is unimpeded. Manual sphygmomanometers are uses in conjunction with a stethoscope. The systolic pressure and diastolic pressure can be measure using this device. Here we are taking only the systolic pressure. The systolic pressure of both right and left hand is measured and then the pressure in the foot ankle measured. The variation in the pressure is a prior indicator of abnormalities in foot.

Figure 3.40. Sphygmomanometer

2. Monofilament Test:-

In this simple yet sensitive evaluation, the monofilament, which is a piece of plastic fiber resembling fishing line, is touched against various parts of the sole of your foot, and your ability to feel it at varying pressure is assessed. It is sometimes call the 10-gram monofilament test because the fiber is calibrate to bend to 10 grams of pressure. Your doctor may also use a tuning fork on the bottoms of your feet to see if you can sense the vibration. Nerve conduction studies or velocity tests, which use electrodes to stimulate nerves and then measure the resulting impulses, are a less frequently used, sophisticated method of diagnosing some neuropathies. Electromyography (EMG), which uses thin needles inserted into the muscles to measure electrical impulses, may also be prescribe. These latter two tests can be painful, and may not be order unless there is some question about the diagnosis. Therefore, monofilament test is an effective indicator of diabetic foot ulcer.

Figure 3.41. Monofilament Test

3. Doppler test:-

Doppler test is perform to check whether there is a blood blow in foot region. In this technique, a gel is make to spread on the foot area. Then the device is make to move on that area and the blow flow recognize by a sound and the region with no blood flow will not produce that sound.

Figure 3.42. Doppler Test

The above tests done normally to diabetics to check whether they had prone to diabetic foot ulcer. In our project, we are introducing a new technique for the early detection of diabetic foot ulcer using pressure sensors.

4. Sensitometer Vibration Pressure Threshold:-

Vibration Pressure Threshold technique is used to measure the sense of vibration in foot. Here in this technique a vibration given to the above-mentioned six areas of foot. The threshold value is the vibration in which the patient can feel. This is an indication of sensational loss in foot.

Figure 3.43. Sensitometer Vibration Pressure Threshold

Chapter Four:

Design and Implementation

4.1 Design Principles:

This project aims to design a circuit, which can measure forces in a specific area in foot to detect diabetic foot ulcer. This can be achieved by using specific type of force sensor called "Flexi-Force"- A401", and A502. In addition, there is a system to measure EMG signal.

According to foot surface area, 8 sensors needed for acquiring the pressure from foot surface that are responsible for generating it.

The Flexi-Force sensors separate to four sections:

1- Heel sensor: we use Flexi-Force sensor A502.
2- Toe sensor: we use Flexi-Force sensor A401.
3- Pad sensors: that separate to 3 areas: MT1, MT2&MT3 that all of them we will used Flexi-Force sensor A401.
4- Side foot sensors: that separate to 3 areas: T1, T2&T3 that all of them we will used Flexi-Force sensor A401.

We will put the 8 sensors in insole (shown in figure 4.1) and the places of the sensors position distribution are shown in the Figure 4.2.

Figure 4.1: insole

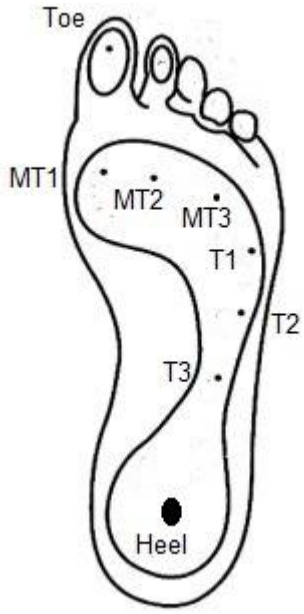

Figure 4.2: sensors positions in insole

4.2 Force Sensor Specifications:

Flexi-Force act as a force-sensing resistor in electrical circuit that if there is no load on the sensor the resistance it will be very high and the resistance decreases when applied force on the sensor.

Flexi-Force sensor constructed from two layers substrate such as polyester Filmso it is safe. On each layer, a conductive material (silver) applied, followed by a layer of pressure sensitive area. The active sensing areas defined by the silver circle on top of the pressure sensitive area. Silver

extends from the sensing area to the connectors at the other end of the sensor, forming the conductive leads.
"Flexi-Force" – A401: this sensor has chosen because it with a large sensing area: **25.4 mm (1 in.)** and measurement ranges of 0-1 lb and 0-7,000 lb are achievable with the A401 sensor by utilizing the recommended circuitry. It shown in figure 4.3. The force range can extended by reducing the drive voltage, VT (the input voltage to the sensor), or the resistance value of the feedback resistor, RF. Conversely, the sensitivity can increased for measurement of lower forces by increasing VT or RF. **See to appendix A.**
"Flexi-Force" – A502: this sensor has chosen because it with a large sensing area: 50.8 mm x 50.8 mm (2 in. x 2 in.). It shown in figure 4.4. This sensor can measure up to 44,448 N (10,000 lb). **See to appendix B.**
We can notes the difference between the two sensors in figure 4.3 and 4.4, also the shape of "Flexi-Force" – A502 is more suitable for the heel than the "Flexi-Force" – A401 because it larger and fit with heel.

Figure 4.3: Flexi – Force A401.

Figure 4.4: Flexi – Force A502

4.3 Diabetic foot ulcer pressure block diagram:

Form Flexi – Force sensors we will get values which will pass through Procedures to get a real value that can be useful for detect diabitic foot ulcer .

4.3.1 Heel pressure:

In the figure ٤.٥ below, it shows the design stages of the tool that takes the result of pressing the heel area:

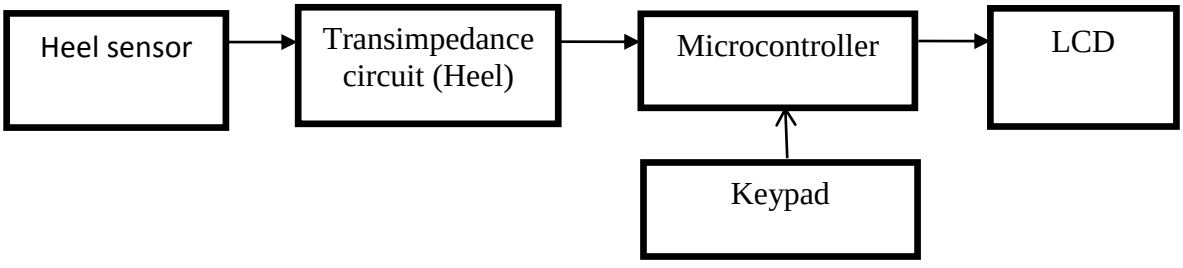

Figure 4.5 : Heel pressure block digram.

Heel Trans-impedance circuit:
It is a circuit that convert the change of resistance (according to Heel force) to change in voltage. The following circuit describe how to mesuare Heel force by using Flexi – Force sensor A502 as shown in Figure 4.6
We will use op-Amp from type AD822 because that is a dual precision, low power FET input op amp that can operate from a single supply of +3.0 V to 36 V, or dual supplies of ±1.5 V to ±18 V. Furthermore, The AD822 is an Output Swings Rail to Rail, The AD822 Input Impedance=0.5-10^{13} Ω, CMRR=80dB.

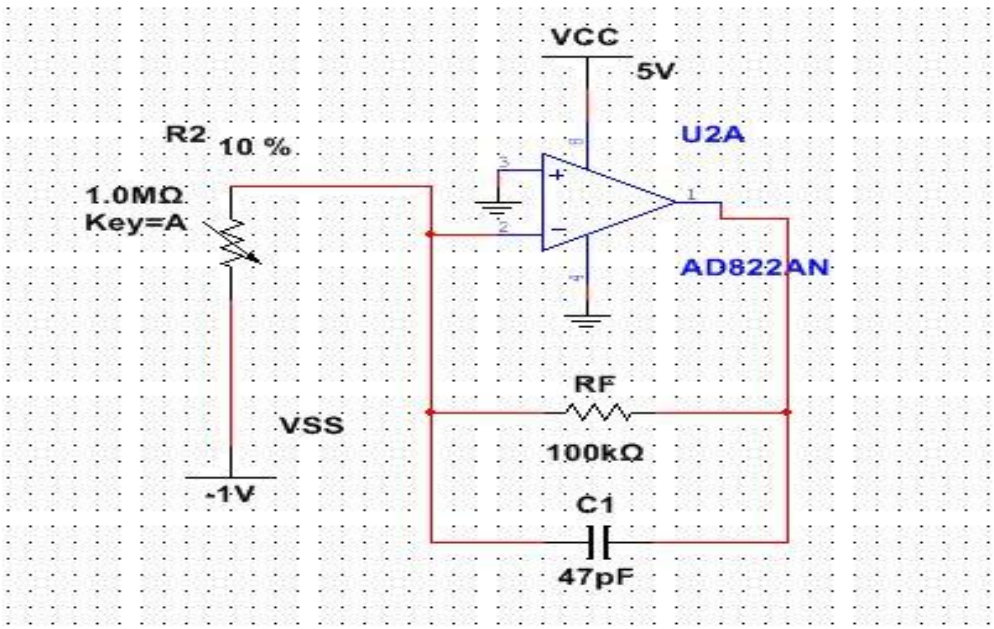

Figure 4.6: Schematic Diagram Heel Sensor Transimpedance.

According to Appendix B, the recommended value of input value of the sensor is -1 volt because we use an inverting amplifier and the recommended value of the R_F is 100K Ohm.
The potentiometer it represents the Flexi force A502 sensor.
There is a changing in the output voltage value so we use a capacitor and its value recommended from the datasheet for the sensor.

Pressure values:
We insert the Figure 4.7 (from Appendix A) in Getdata program to find values that we insert it in Excel program to get the equation that describe the relation between resistance and force :
Force = $295.13R^{-0.85}$ ……. (4.1)
Refer to Appendix B to see the values.

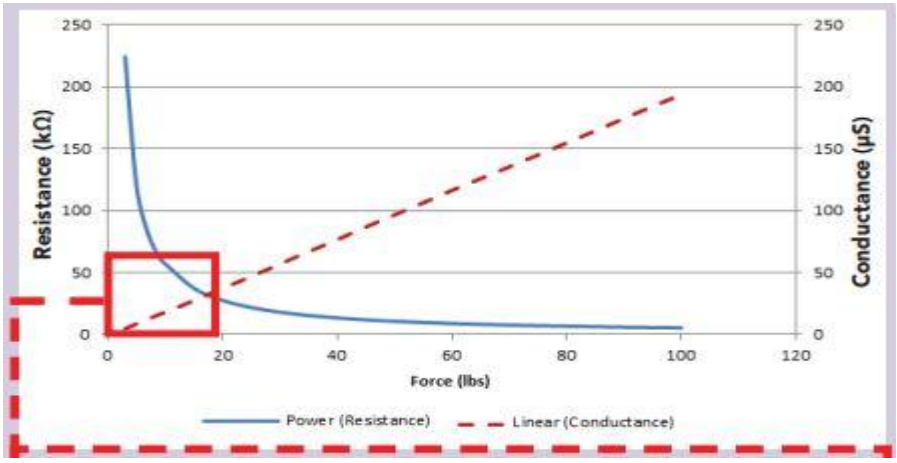

Figure 4.7: Resistance – Force Relation.

Then we convert the relation from force and resistance to force and output voltage as shown:

$V_{out} = V_{in} * (R_F/R_s)$

$= 1 * (100K\Omega / 224.576K\Omega) = 0.445284volt$ Rs: test value

See appendix B to more results.

Where Vin =1v, R_F =100kΩ and for R_s values refer to appendix B

We choose the value of V_{in} & R_F based on the recommendation of the data sheet**. See appendix B.**

After we got the values using Microsoft Excel draw the curve that describe the relation between force (shown in Fig. 4.8) and voltage and represent it by equation.

$F = 0.0238V^3 - 1.2217V^2 + 20.199V + 0.7896$ …….. (4.2)

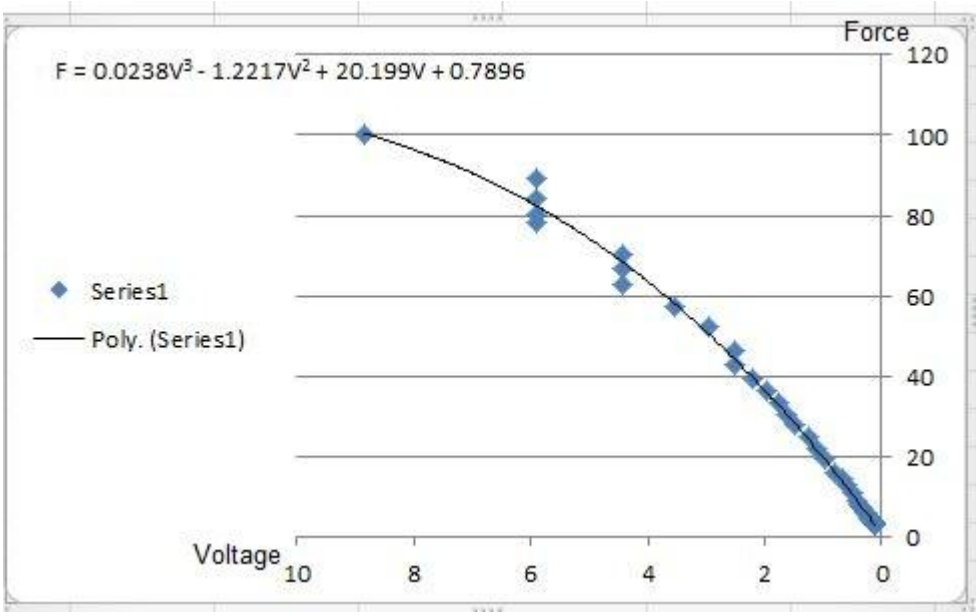

Figure 4.8: Relation between Force and Voltage.

Convert from force and voltage to a pressure and voltage:

Convert from lb to newton

$F = (0.0238V^3 - 1.2217V^2 + 20.199V + 0.7896)*4.448$

$F = (0.105V^3 - 5.43V^2 + 89.85V + 3.51)$ …… (4.3)

Form datasheet Sensing area (A) = $(50.8 * 10^{-3})^2$

$= 2.58*10^{-3}$ m2

Pressure = F/A where F: force

By divide equation (4.3) on $2.02 * 10^{-3}$ $m^{2,}$ we got the equation that represents pressure:

Pressure = $40.7V^3 – 2104.7V^2 + 34825.6V + 1360.5$ N/m^2

Pressure = $(0.040.7V^3 - 2.1047V^2 + 34.8256V + 1.3605)$ K Pa …….. (4.4)

4.3.2 Toe pressure:

In the figure ٤.9 below, it shows the design stages of the tool that takes the result of pressing the Toe area:

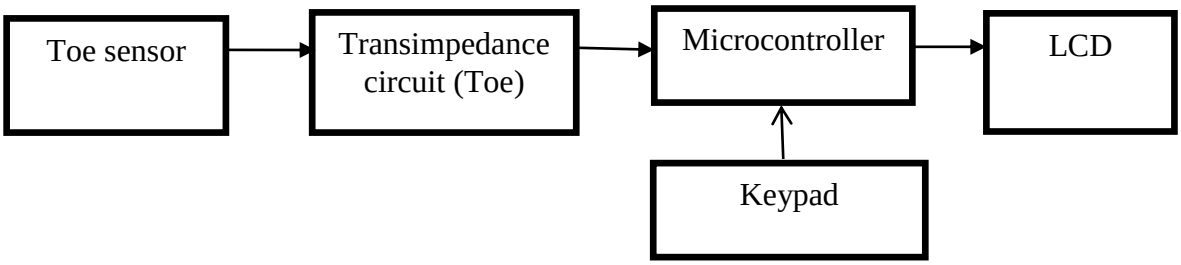

Figure 4.9 : Toe pressure block digram.

Toe Trans-impedance circuit:

The following circuit describe how to mesuare Toe force by using Flexi – Force sensor A401 as shown in figure 4.10.

We will use Amplifier from type AD822 for the same reasons in Heel Transimpedance circuit and we will use it for all of the sensors circuits.

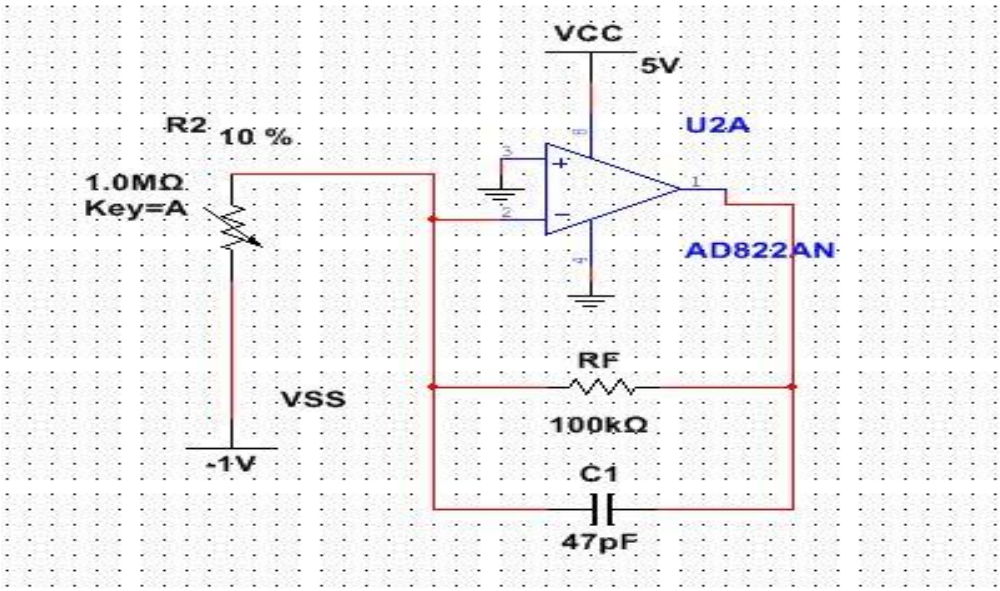

Figure 4.10: Schematic Diagram Toe Sensor Transimpedance.

According to Appendix A the recommended value of input value of the sensor is -1 volt and the recommended value of the R_F is 100K Ohm.

The capacitor and its value recommended from the datasheet for the sensor.

Pressure values:

We insert the Fig. 4.11 (from Appendix A) in Getdata program to find values that we insert it in Excel program to the equation that describe the relation between voltage and force. Refer to Appendix A to see the values

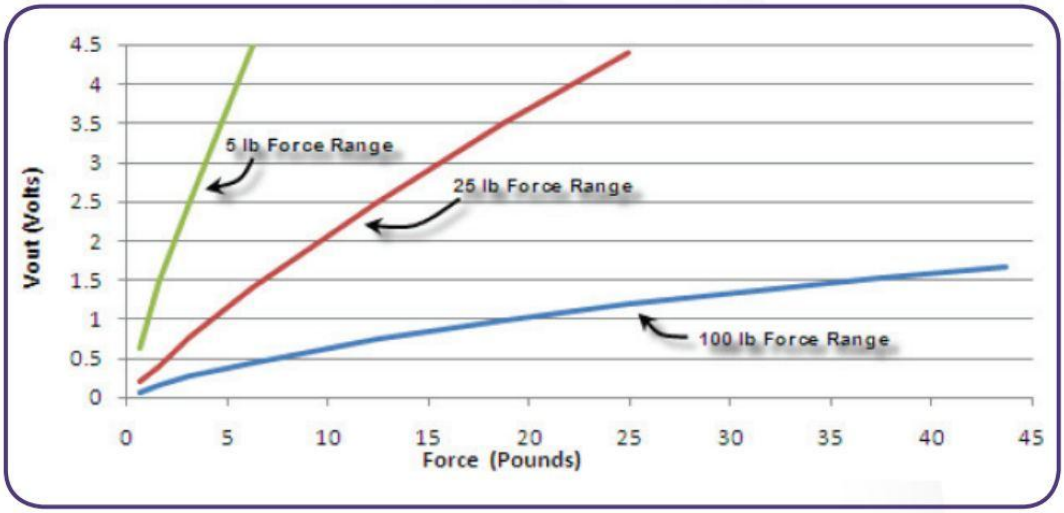

Figure 4.11: Voltage – Force Relation.

After we take the values using Microsoft Excel draw the curve that describe the relation between force and voltage (shown in Fig. 4.12) then we can reach to the equation that represent the relation between the force and voltage as shown.

Force = $-7.4525V^5 + 32.942V^4 - 51.167V^3 + 42.825V^2 + 1.4868V + 0.5156$... (4.5)

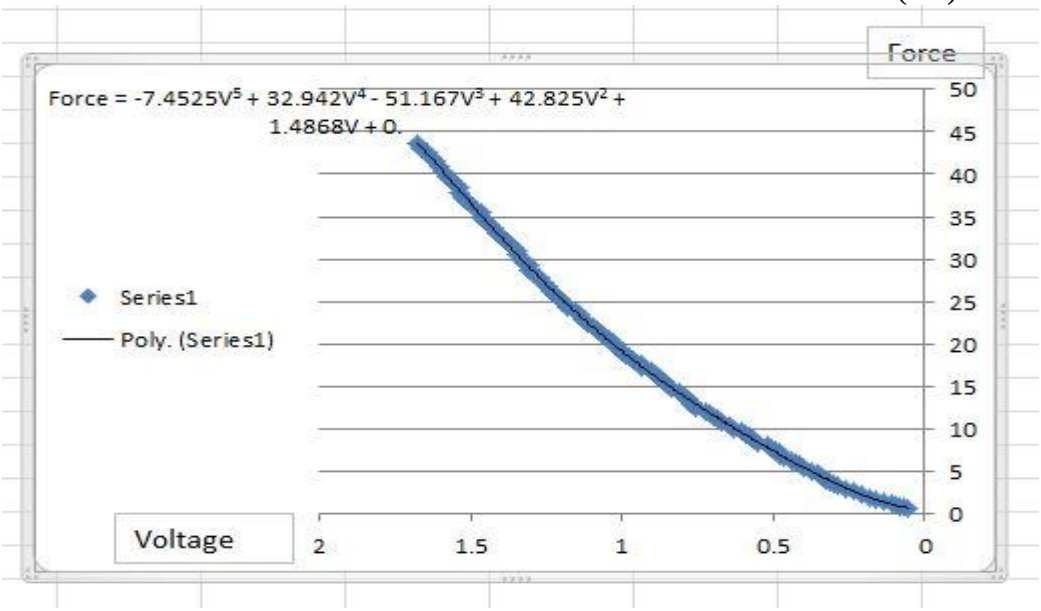

Figure 4.12: Relation between Force and Voltage.

Convert from force and voltage to a pressure and voltage:

Convert from lb. to newton

Force = $(-7.4525V^5 + 32.942V^4 - 51.167V^3 + 42.825V^2 + 1.4868V + 0.5156)*4.448$

Force = $(-33.2V^5 + 146.5\ V^4 - 227.6V^3 + 190.5\ V^2 + 6.61V + 2.3)$ ……. (4.6)

Sensing area (A) = πr^2

$= \pi\ (25.4*10^{-3})^2 = 2.02 * 10^{-3}$ m2

Pressure = F/A where F: force & A: area of sensor

By divide equation (4.6) on g we got this equation that represents pressure:

Pressure= $-16435.6V^5 + 72524.7V^4 - 112673.3V^3 + 94307V^2 + 3272.3V + 1138.6$ N/m^2

$= (-16.4356V^5 + 72.5247V^4 - 112.6733V^3 + 94.307V^2 + 3.272V + 1.1386)$ K Pa... (4.7)

4.3.3 Pad pressure:

In the figure ٤.13 below, it shows the design stages of the tool that takes the result of pressing the Pad area:

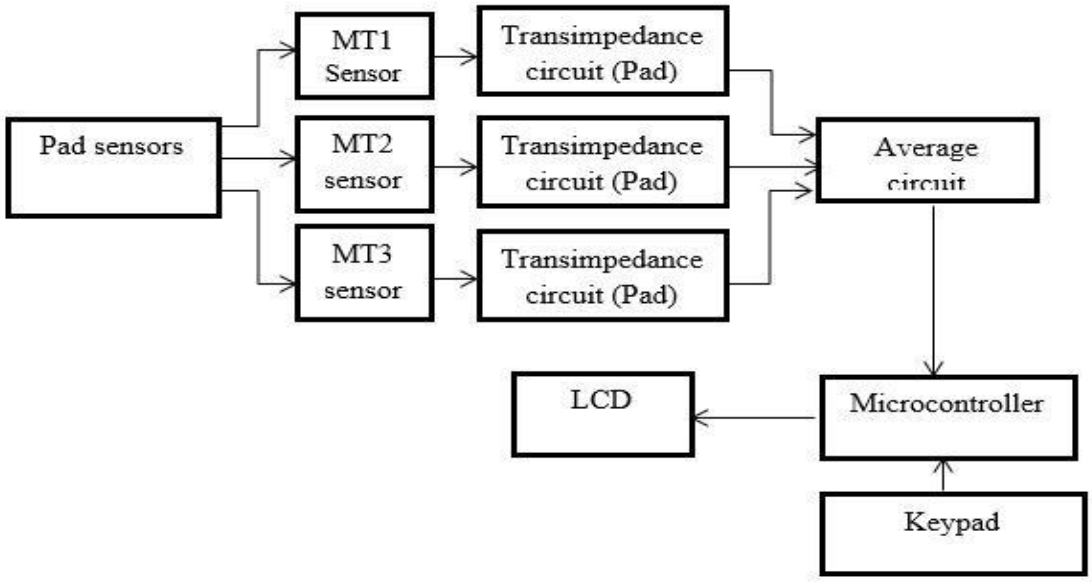

Figure 4.13 : Pad pressure block digram.

The following circuits describe how to mesuare Pad force by using Flexi – Force sensor A401 as shown in figures 4.14 and there is no difernce between the three circuit except the name (MT1,MT2&MT3).

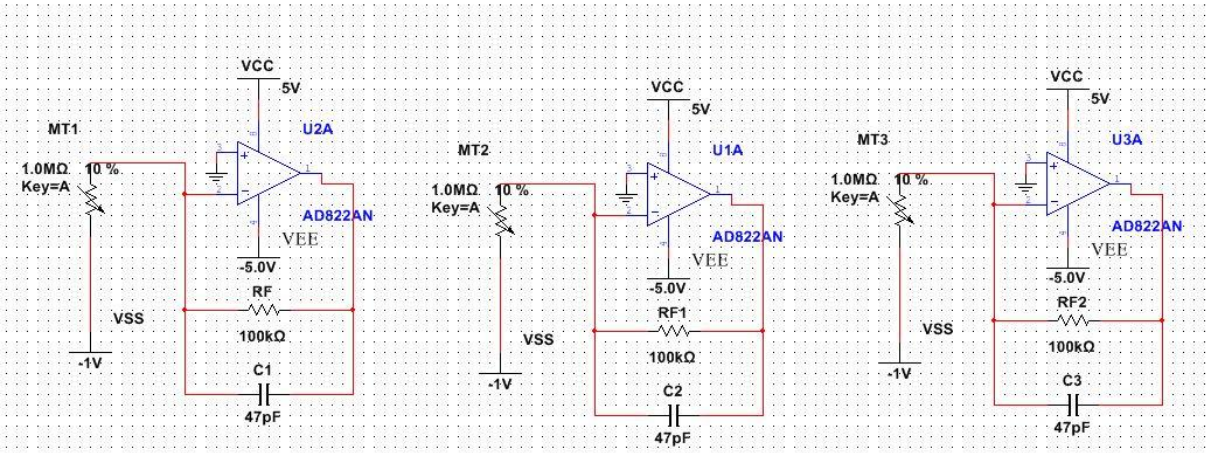

Figure 4.14: Pad sensors schematic diagram

According to Appendix A, the recommended value of input value of the sensor is 1 volt and the recommended value of the R_F is 100K Ohm. The capacitor and its value recommended from the datasheet for the sensor.

Average circuit:

The **averaging Amplifier** is another type of operational amplifier circuit configuration that used to combine the voltages present on two or more inputs into a single output voltage. Figure 4.15 shown the average circuit that use to combine voltages that out form Pad sensors Transimpedance circuit.

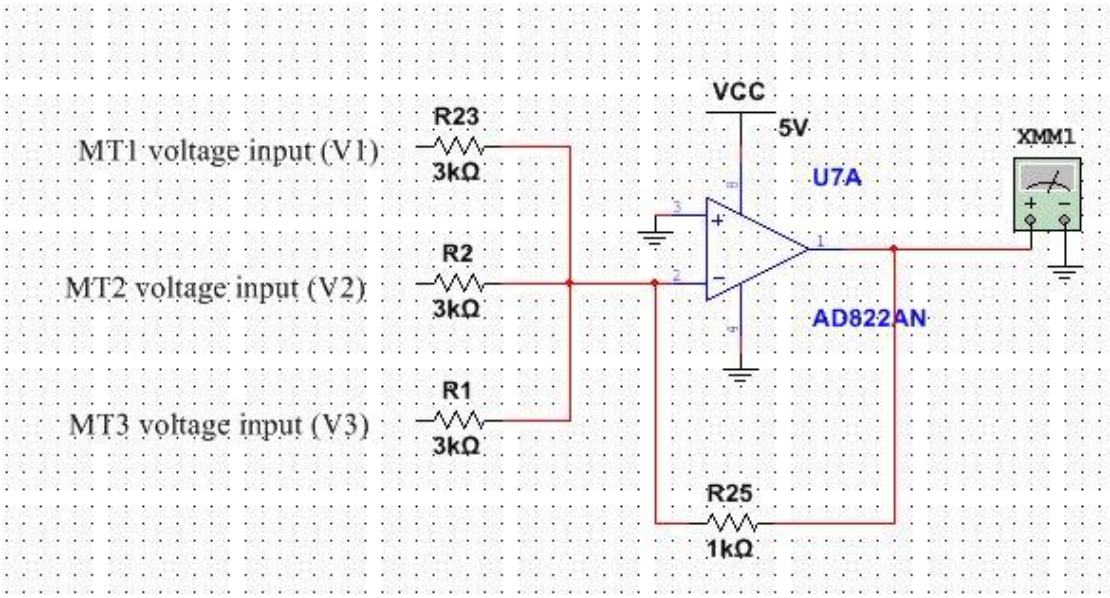

Figure 4.15: Pad sensors average circuit schematic diagram.

We use a single amplifier because the output is always positive, because the output voltage from (MT1,MT2,& MT3) circuit negative.
All the resisitance is the same value for take the avarege of the inputs with gain equal 1/3 .

$V_{sum} = V_1 [-R_{25} / R1] + V_2 [-R_{25} / R_2] + V_3 [-R_{25} / R_{23}]$ …… (4.8)

But V_1 & V_2 & V_3 negative so :

$V_{sum} = V_1 [R_{25} / R1] + V_2 [R_{25} / R_2] + V_3 [R_{25} / R_3]$

$= (V_1 + V_2 + V_3) / 3$

$= (1/3) * (V_1 + V_2 + V_3)$ …… (4.9)

4.3.4 Side foot pressure:

In the figure ٤.16 below, it shows the design stages of the tool that takes the result of pressing the side foot area:

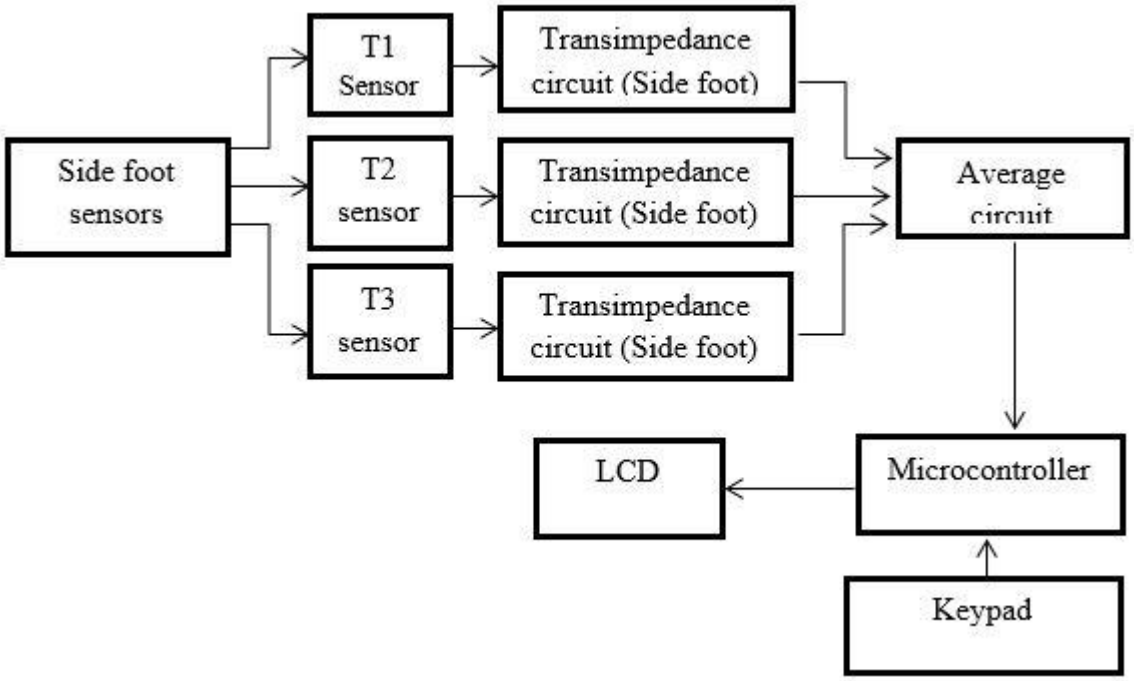

Figure 4.16: block diagram Side foot pressure.

The following circuits describe how to mesuare Side foot force by using Flexi – Force sensor A401 as shown in figures 4.17.

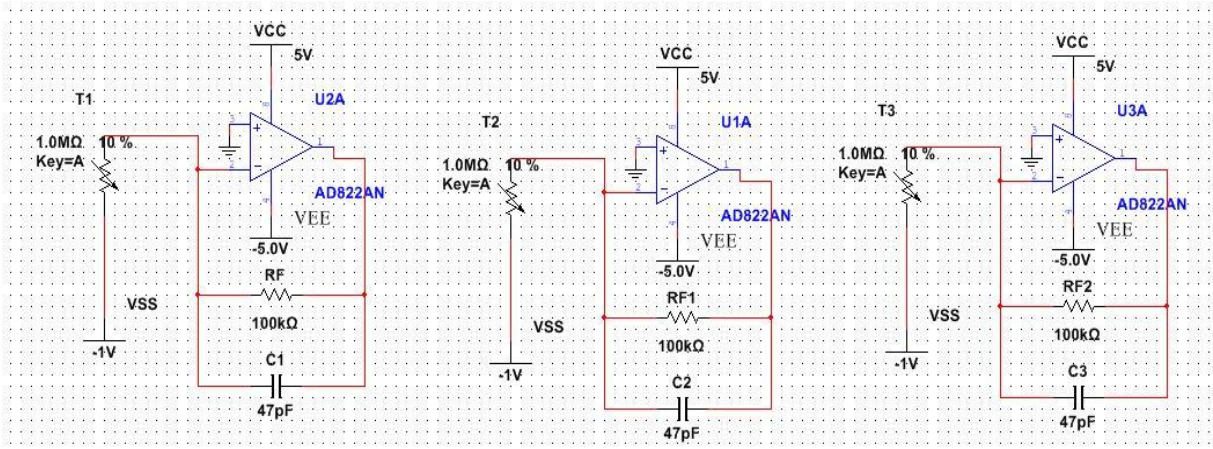

Figure 4.17: Side foot sensors schematic diagram

Average circuit:

The figure 4.18 shown the average circuit that use to combine voltages that out form Side foot sensors transimpedance circuit and it is the same of Pad average circuit.

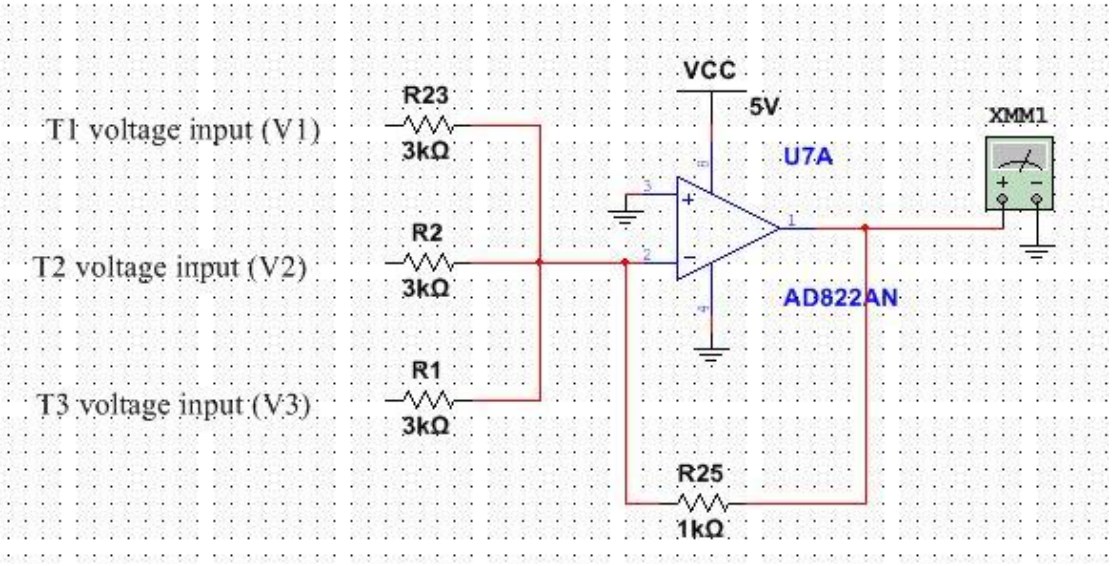

Figure 4.18: Side foot sensors average circuit schematic diagram

4.4 Electromyography (EMG):-

This section aims to design EMG circuit that can be captured EMG signal from foot muscles. According to what has been studies in previous studies and research, the diabetes foot disease leads to weakness of the signal resulting from the foot and hence we started the idea of taking the foot signal and used in the detection of the disease.
The following block diagram related to EMG foot muscle, that describe the basic component needed to detective of EMG signal.

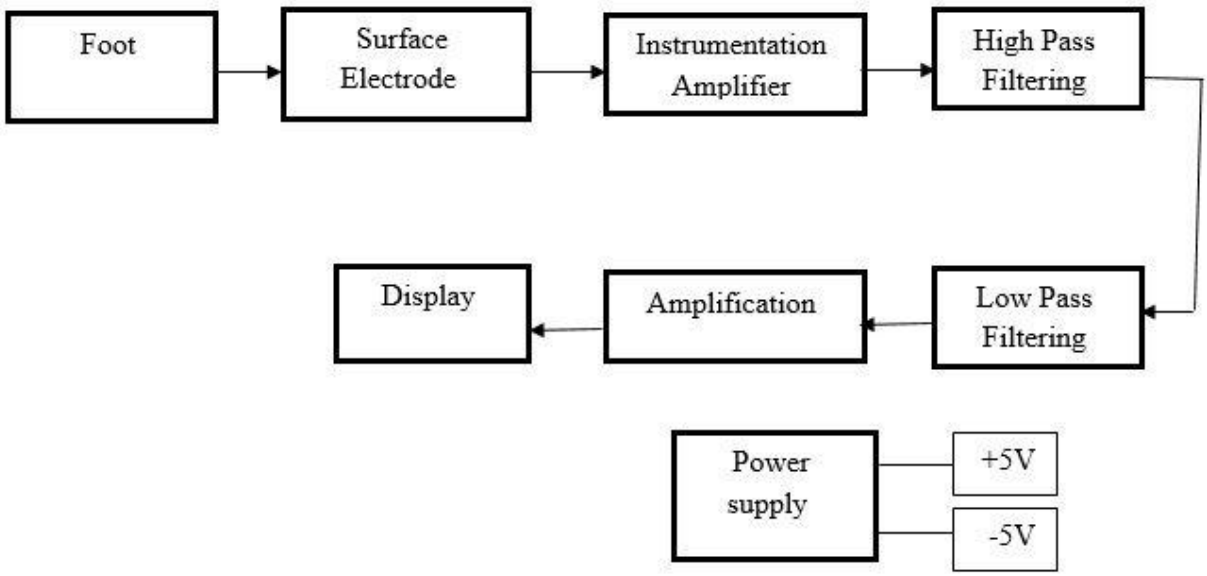

Figure 4.19: Block Diagram of EMG

This section provides a description of the existing electrode; it depicts the composition of each functional block in the circuit. The electrode–amplifier and its signal conditioning circuit are comprised of five main blocks: electrode, Instrumentation amplifier, high pass filter, low pass filter and selectable gain amplifier.

4.4.1 Surface Electrode:-

Surface electrodes will be use Ag-AgCl type; a type of Ag/AgCl electrodes based on a hydrophobic ionic liquid has been propose. The electrode consists of an Ag/AgCl electrode immersed in or coated with an AgCl-saturated ionic liquid.

Figure 4.20: Ag-AgCl Electrode

In the figure 4.21 below, the equivalent circuit of electrode (Ag-AgCl) as shown:

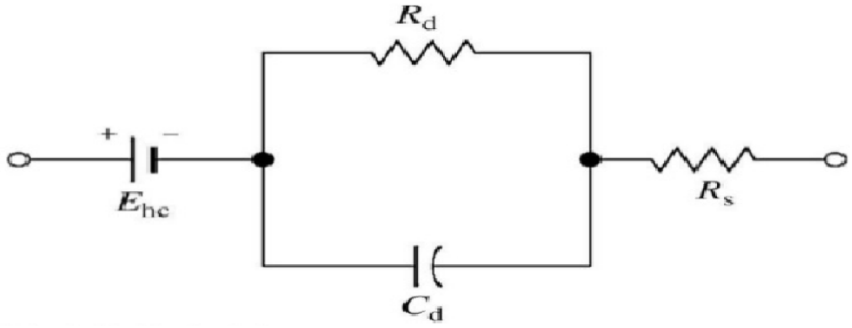

Figure 4.21: equivalent circuit of electrode for Ag-AgCl

4.4.2 Instrumentation Amplifier:-

However, because of a large DC offset potential of as EMG signal (200–300 mV), the instrumentation amplifier of the electrode–amplifier cannot have a large DC gain.

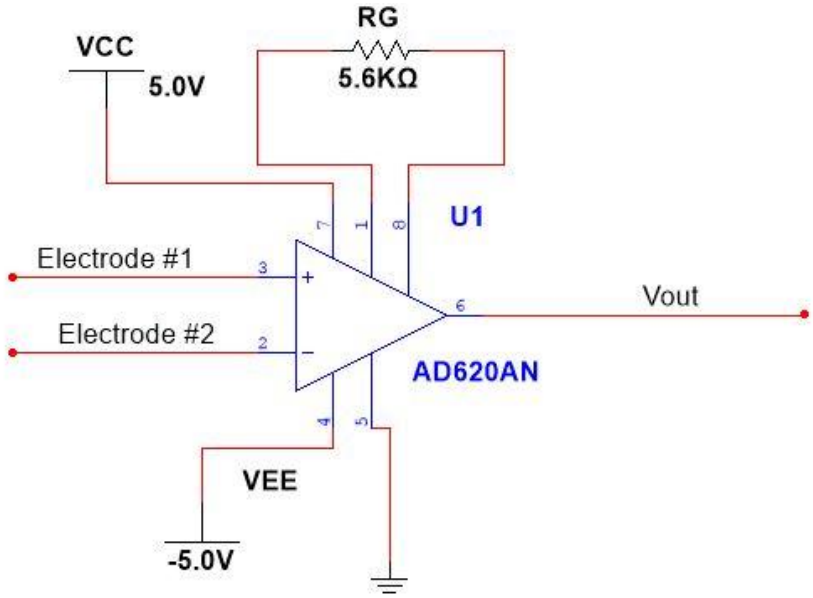

Figure 4.22: Instrumentation Amplifier circuit (AD620)

The AD620 will be use because it has a lower cost and because when the instrumentation amplifier circuit is build it takes more space and less accuracy when built manually.

The AD620 is a low cost, high accuracy instrumentation amplifier that requires only one external resistor to set gains of 1 to 10,000. Furthermore, the low noise, low input bias current and low power of the AD620 make it well suited for medical applications, such as ECG and noninvasive blood pressure monitors. Furthermore, The AD620 is an Input Impedance =2 to 10 GΩ, Common-Mode Rejection Ratio DC to 60 Hz with 1 kΩ Source Imbalance VCM = 0V to ± 10 V, Gain=10 → CMRR=110dB.

$$RG = \frac{49.9K\Omega}{Gain - 1} \dots\dots\dots\dots\dots\dots\dots (4.10)$$

$$RG = \frac{49.9K\Omega}{10 - 1}$$

$$RG = 5.6K\Omega$$

$$Vout = (Velectrode\ \#1 - Velectrode\ \#2) * Gain \dots\dots\dots\dots\dots\dots\dots (4.11)$$

4.4.3 Band Pass Filter (BPF):

The surface electrode put in foot muscle, they captured different signals, but we need the EMG foot signal, so we need Band Pass Filter that pass the frequency range from (7Hz to 542Hz)[19] only.

We used op-amp from type AD822 is chosen because that is a dual precision, low power FET input op amp that can operate from a single supply of +3.0 V to 36 V, or dual supplies of ±1.5 V to ±18 V. Furthermore, The AD822 is an Output Swings Rail to Rail, The AD822 is an Input Impedance=0.5-10^{13} Ω, CMRR=80dB.

1) High Pass Filter:

A high-pass filter –sallen key- (HPF) is an electronic filter that passes signals with a frequency higher than a certain cutoff frequency and attenuates signals with frequencies lower than the cutoff frequency. The amount of attenuation for each frequency depends on the filter design.

The Gain of HPF is equal 1.56 and the critical frequency (Fc) equal 7Hz [19].

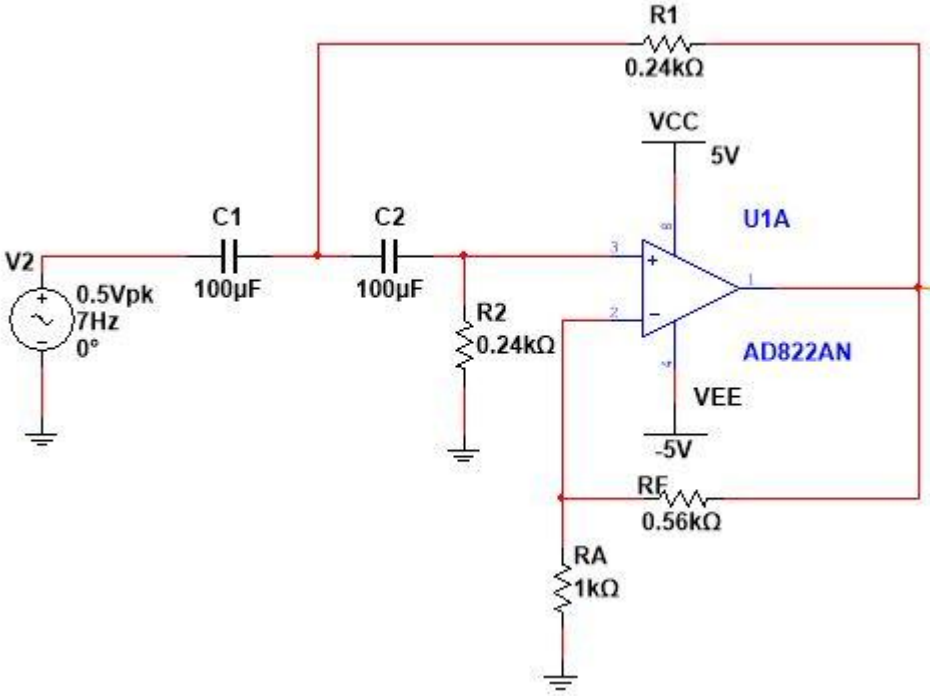

Figure 4.23: HPF circuit

$$Gain\ HPF = 1 + \frac{RF}{RA} \dots\dots\dots\dots\dots\dots\dots\dots\dots (4.12)$$

$$Let\ RA = 1k\Omega\ \ from\ standerd\ resistance\ table$$

$$0.56 = \frac{RF}{1k\Omega}$$

$$RF = 0.56k\Omega\ \ from\ standerd\ resistance\ table$$

To calculate the critical frequency (7Hz) for HPF as follow:-

Consider that C1=C2=C, R1=R2=R so let

$$C = 100\mu F\ \ from\ standerd\ capacitance\ \ table$$

$$Fc = \frac{1}{2\pi RC} \dots\dots\dots\dots\dots\dots\dots\dots\dots (4.13)$$

$$7 * R * 2 * 3.14 * 100 * (10^{-6}) = 1$$

$$R = 0.227k\Omega \approx 0.24k\Omega\ from\ standerd\ resistance\ table$$

After we design the HPF circuit, we simulate it by using mulitisim software and the table (4.1) shows the characteristics of HPF at critical frequency equal (7Hz) , and gain (1.56) where the input signal equal(1Vp-p).

Table (4.1): characteristic of HPF

Freq (H_z)	Vout (Vp-p)	Gain
1k	1.57	1.57
900	1.57	1.57
700	1.56	1.56
500	1.56	1.56
300	1.56	1.56
100	1.56	1.56
70	1.55	1.55
50	1.55	1.55
30	1.54	1.54
10	1.45	1.45
8	1.26	1.26
7	1.15	1.15
5	0.777	0.777
3	0.3	0.3
1	0.0353	0.0353

$$\text{Vout (Fc HPF)} = \text{Vin} * \text{Gain} * 0.707$$
$$\text{Vout (7 H}_z\text{)} = 1\text{Vp-p} * 1.56 * 0.707$$
$$= 1.1\ \text{Vp-p}$$

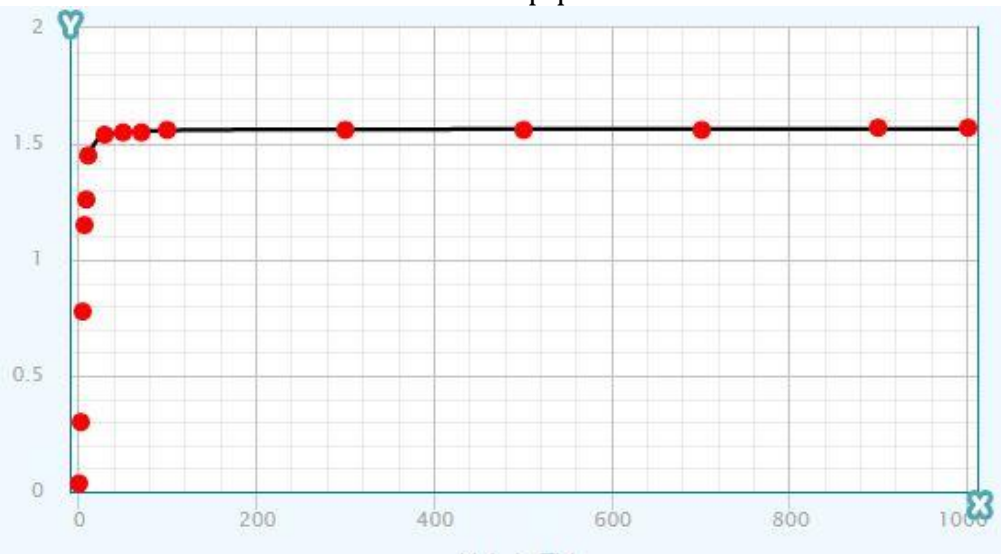

Figure 4.24: Curve of HPF result from simulate

2) Low Pass Filter:-

A low-pass filter –sallen key- (LPF) is a filter that passes signals with a frequency lower than a selected cutoff frequency and attenuates signals with frequencies higher than the cutoff frequency.

The Gain of LPF is equal 1.56 and the critical frequency (Fc) equal 542 H_z [19].

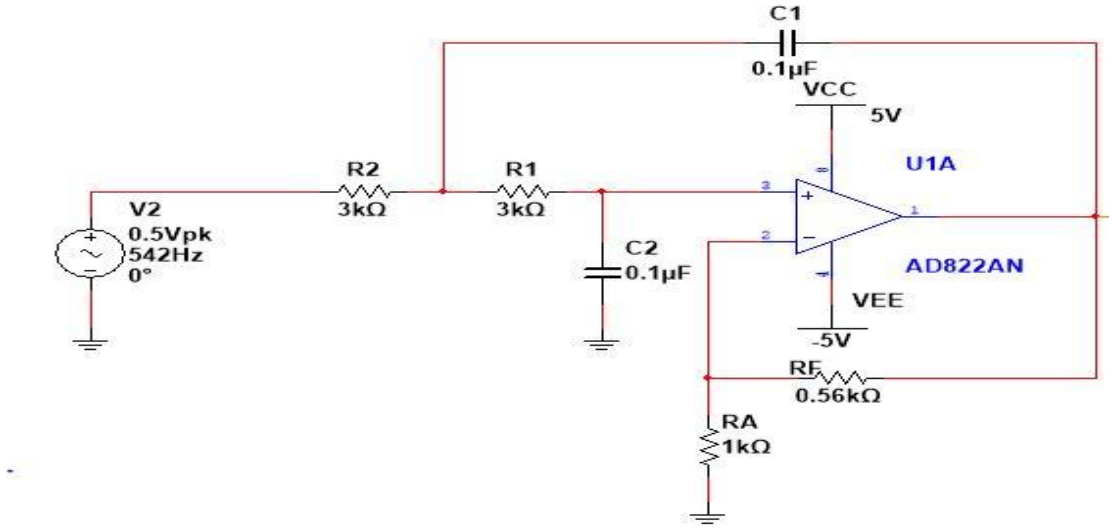

Figure 4.25: LPF circuit

$$Gain\ LPF = 1 + \frac{RF}{RA} \dots\dots\dots\dots\dots\dots\dots\dots (4.14)$$

$$Let\ RA = 1k\Omega\ \ from\ standerd\ resistance\ table$$

$$0.56 = \frac{RF}{1k\Omega}$$

$$RF = 0.56k\Omega\ \ from\ standerd\ resistance\ table$$

To calculate the critical frequency (542Hz) for LPF as follow:-

Consider that C1=C2=C, R1=R2=R so let

$$C = 0.1\mu F\ \ from\ standerd\ capacitance\ table$$

$$Fc = \frac{1}{2\pi RC} \dots\dots\dots\dots\dots\dots\dots\dots (4.15)$$

$$542 * 2 * 3.14 * 0.1 * (10^{-6}) * R = 1$$

$$R = 2.94k\Omega \approx 3\text{k}\Omega\ from\ standerd\ resistance\ table$$

After we design the LPF circuit, we simulate it by using mulitisim software and the table (4.2) shows the characteristics of LPF at critical frequency equal (542Hz) , and gain (1.56) where the input signal equal(1Vp-p).

Table (4.2): characteristic of LPF

Freq (Hz)	Vout (Vp-p)	Gain
5	1.56	1.56
10	1.56	1.56
50	1.55	1.55
100	1.55	1.55
400	1.3	1.3
500	1.13	1.13
542	1.05	1.05
600	0.932	0.932
700	0.749	0.749
800	0.606	0.606
900	0.483	0.483
1K	0.4	0.4

Vout (Fc LPF) = Vin * Gain * 0.707
Vout (542 $H_{z)}$ = 1Vp-p * 1.56 * 0.707
= 1.1 Vp-p

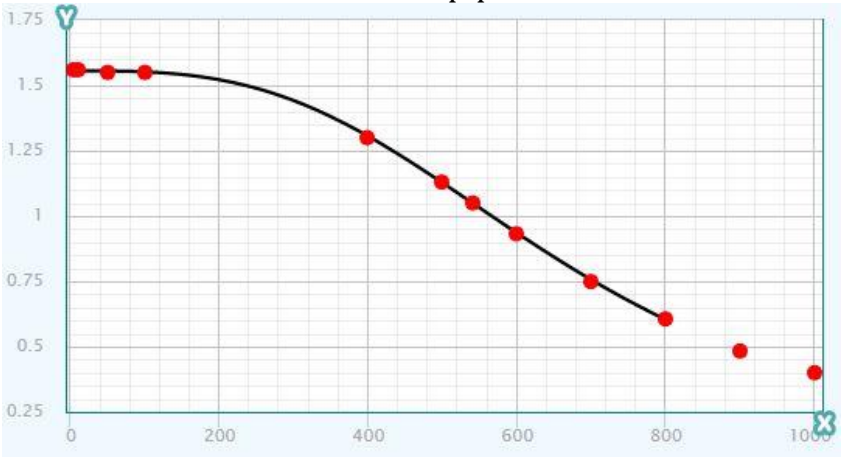

Figure 4.26: Curve of LPF result from simulate

4.4.4 Amplification:

The amount of amplification provided by an amplifier measured by its gain: the ratio of output voltage, current, or power to input. The signal generated by process HPF will be amplification of The Gain Amplification is approximately equal 44.
Total gain equal 1000.

$$\text{Gain Amplification} = 1 + \frac{R2}{R1} \dots\dots\dots\dots\dots\dots\dots\dots\dots\dots (4.16)$$

$$\text{Let R1} = 10k\Omega \ \ from\ standerd\ resistance\ table$$

$$44 - 1 = \frac{R2}{10k\Omega}$$

$$R2 = 430K\Omega \ \ from\ standerd\ resistance\ table$$

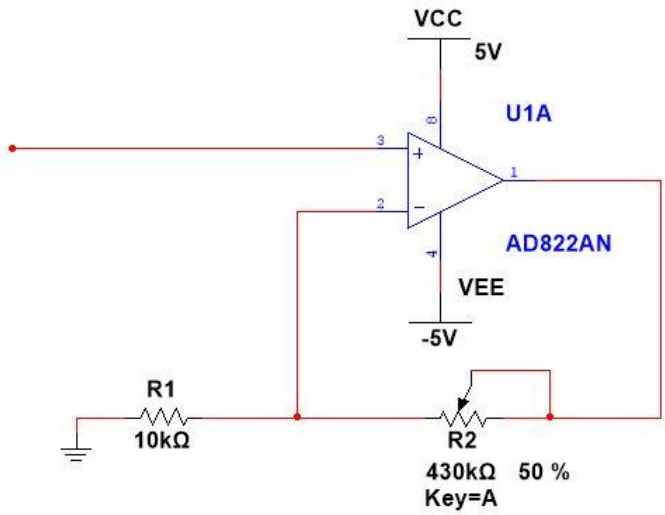

Figure 4.27: Amplification circuit.

4.5 Microcontroller:-

We use Arduino (Mega), in entering the values of the resulting voltages from each region, whether they are (Heel, Pad, Side foot, big toe), and then compensating them in the equations for each region and then obtaining the result (pressure in units Kilo Pascal) from Through (LCD).

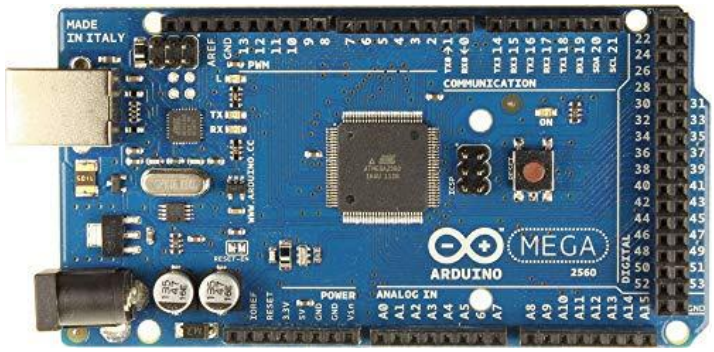

Figure 4.28: Arduino Mega.

4.6 Keypad:-

Keypad was use until the area was choose to show its result on the (LCD), Number 1 has programmed to show the result of pressing the area of the big toe. Number 2 to show the result pressing the area Pad. Number 3 to show the result of the pressure on the side foot area. Number 4 to show pressure from the heel area.

Figure 4.29: Keypad.

4.7 Liquid Crystal Display (LCD):-

The display will use to show the results according to the desired region selection.

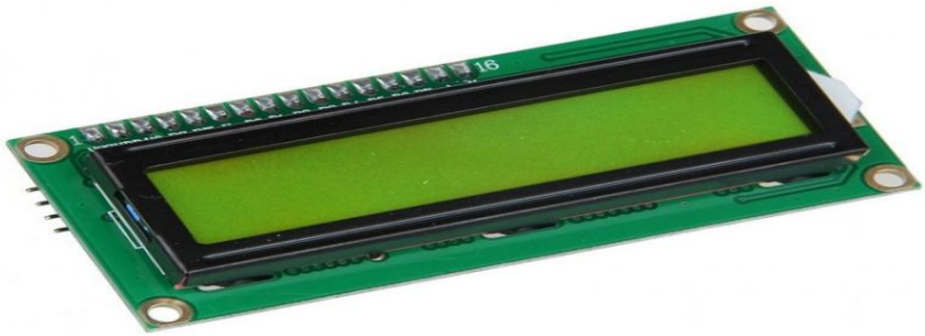

Figure 4.30: Liquid Crystal Display.

4.8 Power supply:

The EMG and the foot pressure circuit supplying through power supply and the following figure shows the value of the voltage that was use to feed the designed electrical circuits:

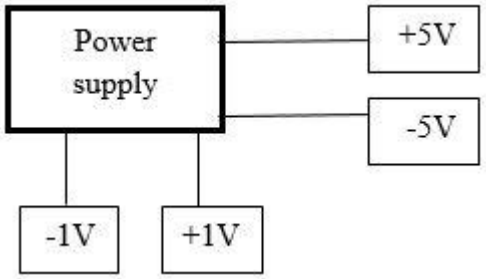

Figure 4.٣1: Block Diagram of power supply

We will use battery (9V), after that we will get different voltages (+5V,-5V, 1V& -1V)
By using (LM7805), (LM7905) & (voltage divider) respectively.

First +5 volt power supply:
We will use LM7805 to get output equal +5V and figure 4.30 shown the circuit to convert form 9-volt battery to 5 volt.

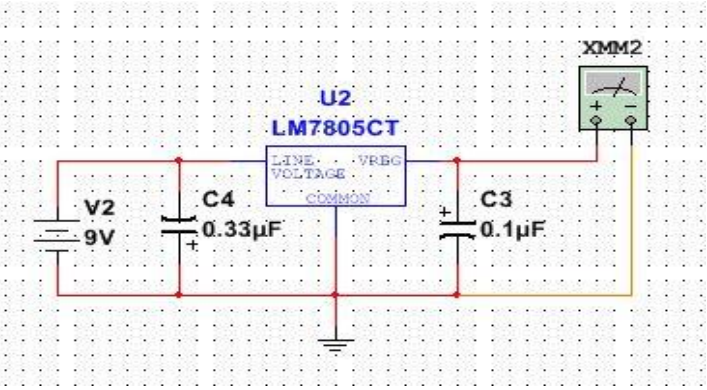

Figure 4.٣2: 5 volt power supply circuit.

According the datasheet in appendix D we choose the capacitor values.

Second -5 volt power supply:

We will use LM7905 to get output equal +5V and figure 4.31 shown the circuit to convert form 9 volt battery to -5 volt.

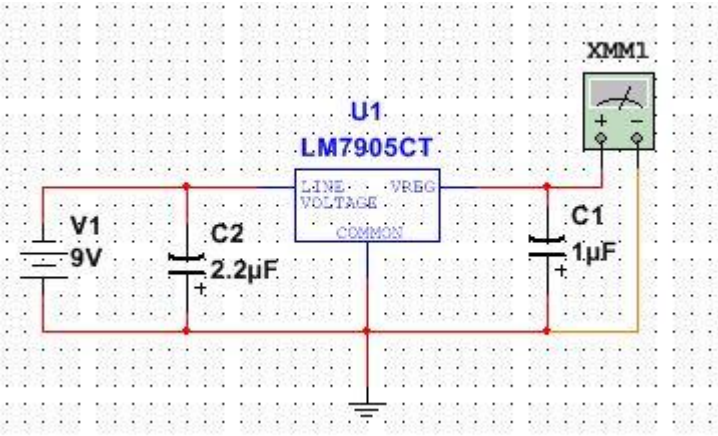

Figure 4.٣3: -5 volt power supply circuit.

According the datasheet in appendix D we choose the capacitor values.

Third +1 volt power supply:

To get a 1volt form 9 volt we will use the voltage divider as shown in figure 4.32

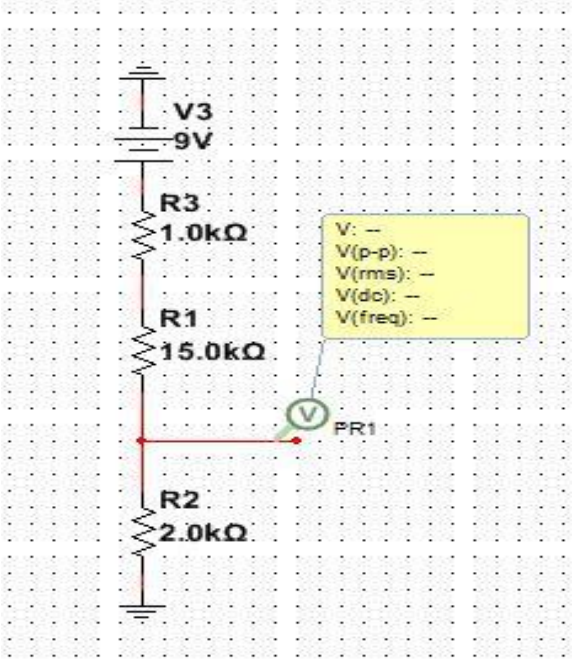

Figure 4.34: +1 volt power supply circuit.

$V_{out} = V_{in} * R2 / (R2 + R)$ if R=R1+R2

let R2 = 2kΩ (standard value)

1 = 9 * 2K / (2k + R)

R = 16kΩ

However, R not a standard value so we use two resistance with a standard value:

R1=15KΩ and R3= 1KΩ

Fourth -1 volt power supply:

To get a -1volt form 9 volt we will use the voltage divider as shown in figure 4.33

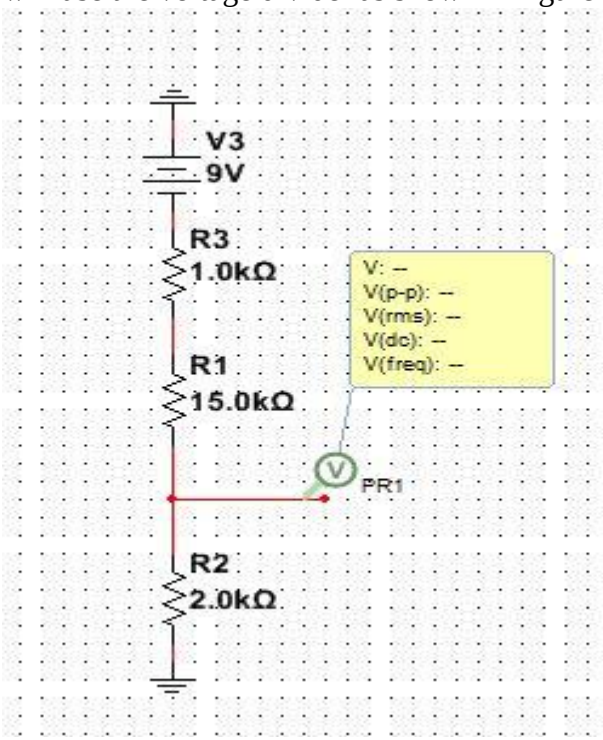

Figure 4.35: -1 volt power supply circuit.

$V_{out} = V_{in} * R2 / (R2 + R)$ if R=R1+R2

Let R2 = 2kΩ (standard value)

-1 = -9 * 2K / (2k + R)

R = 16kΩ

However, R not a standard value so we use two resistance with a standard value:

R1=15KΩ and R3= 1

Chapter Five:

Result Simulation

Heel pressure:

The following circuit describe how to measure pressure in the Heel area as shown in figure 5.1

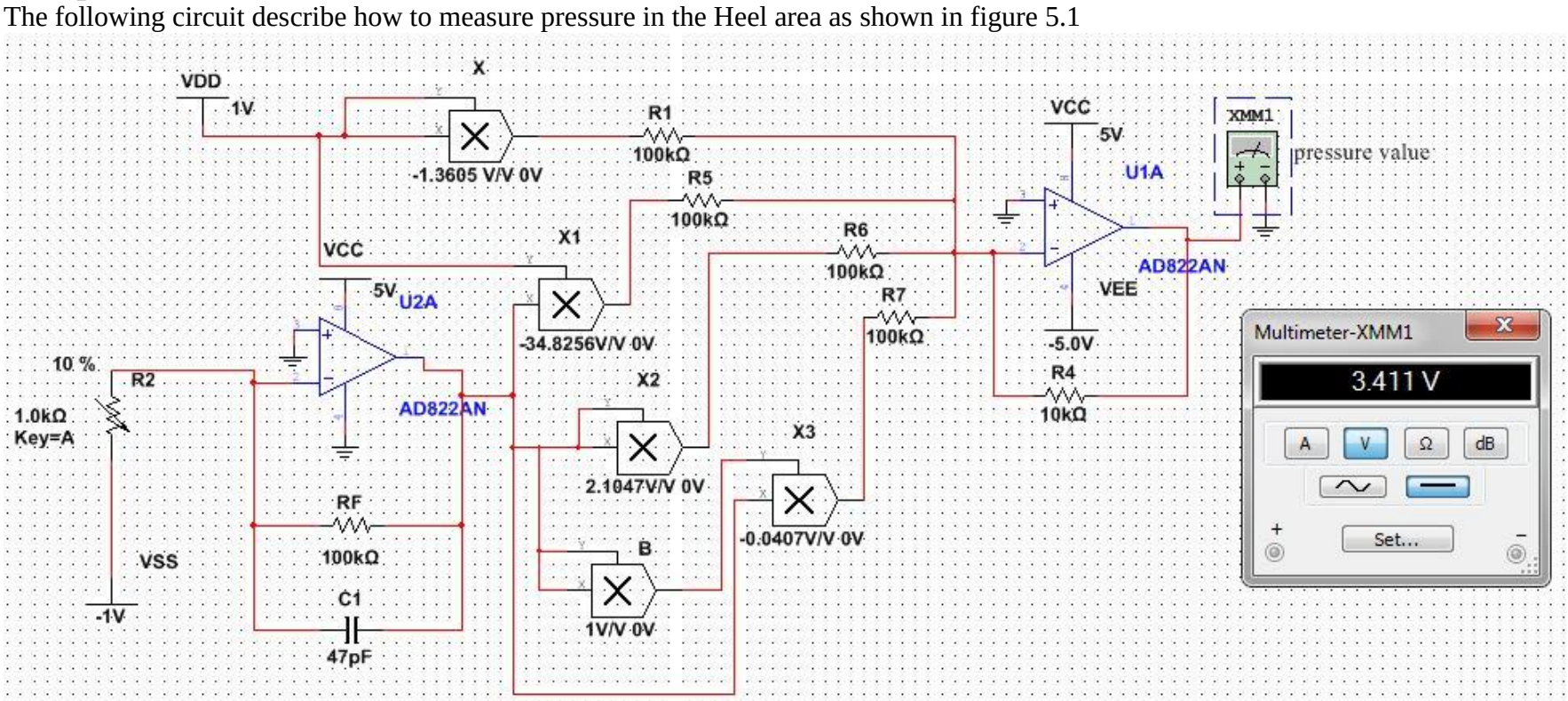

Figure 5.1: General Schematic Diagram of Heel pressure.

The output of the circuit it represent the Heel pressure that equal (3.411 * 10) KPa (because the gain is 0.1 of the summation circuit)

Toe pressure:

The following circuit describe how to measure pressure in the Toe area as shown in figure 5.2

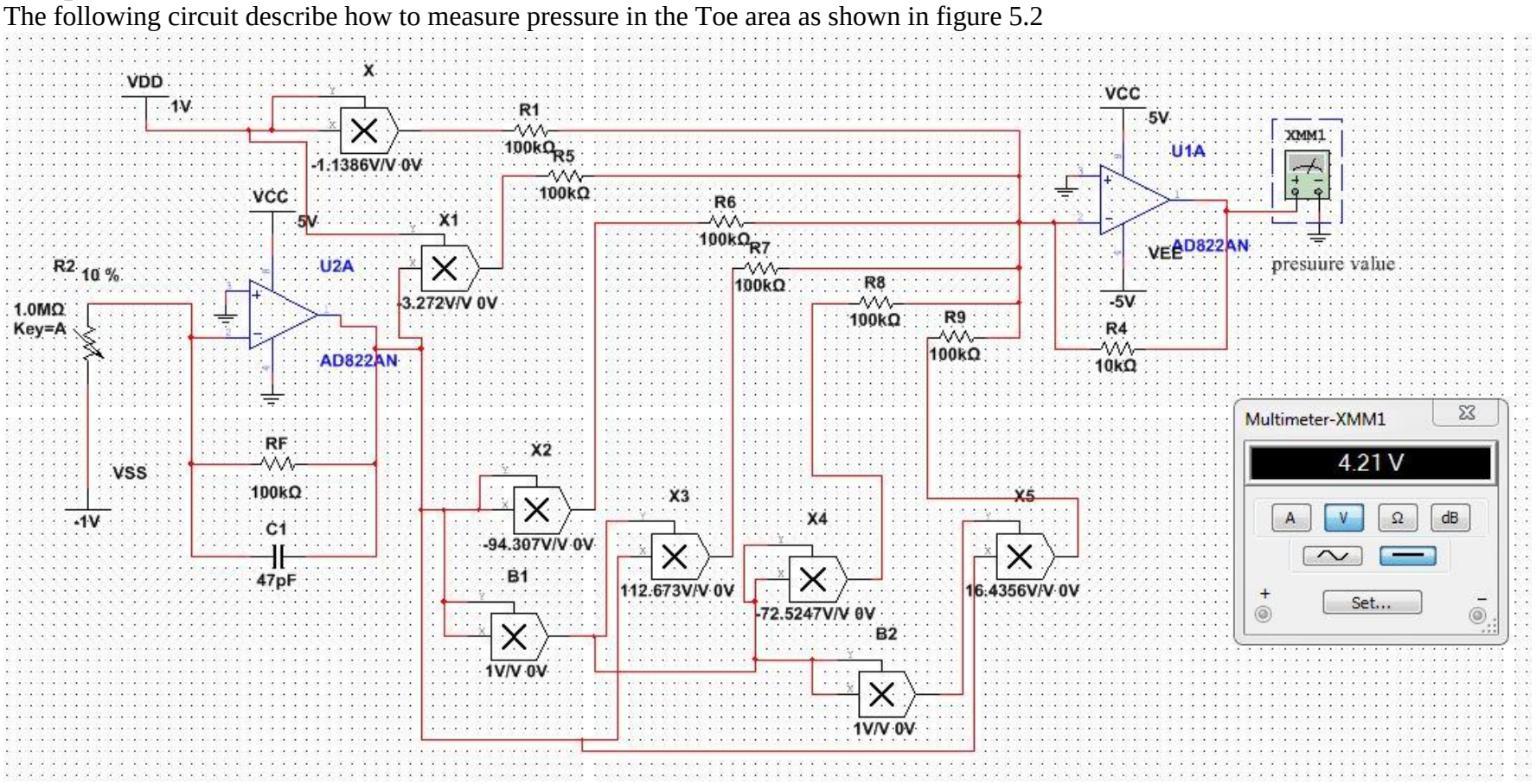

Figure 5.2: General Schematic Diagram of Toe pressure.

The output of the circuit it represent the Heel pressure that equal (4.21 * 10) KPa (because the gain is 0.1 of the summation circuit)

Chapter Six:

Result and Analyses

6.1 Introduction:

The project was design and the values and signals obtained from 30 cases were taken, whether they had diabetic ulcer disease, diabetes, or healthy people from both diseases.

In the attached pictures, the stages of implementing the project in terms of installing electronic parts on the PCB board, preparing the insole, and placing the fittings on the insole:

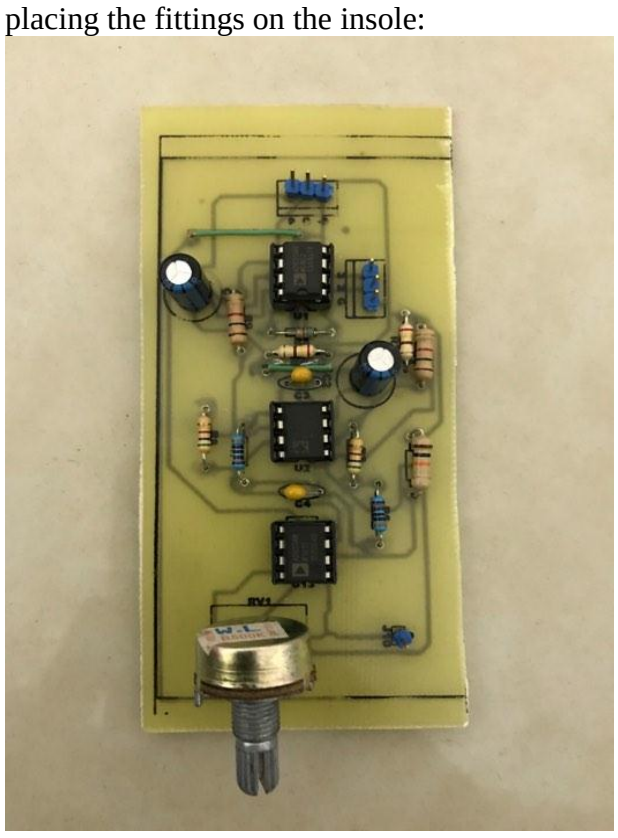

Figure 6.1: PCB of EMG.

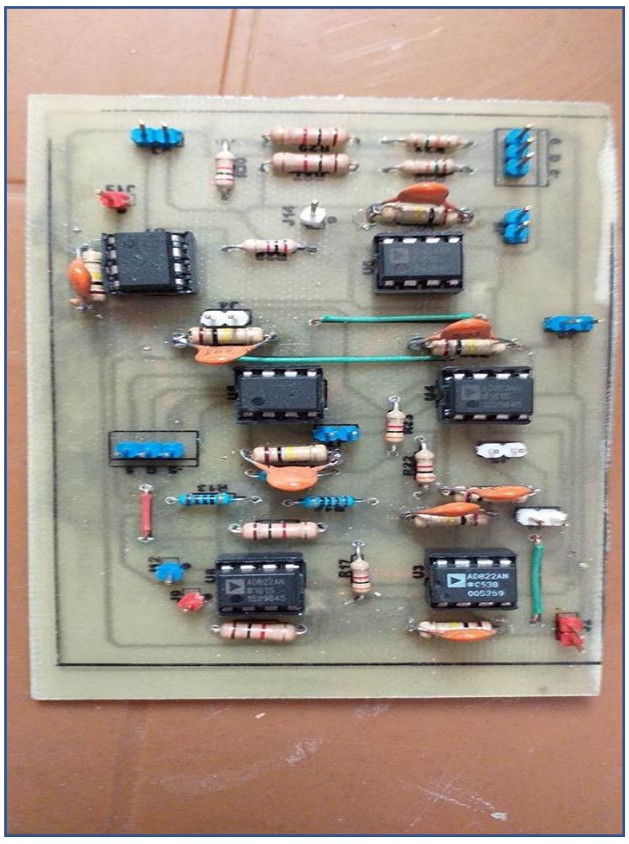

Figure 6.2: PCB of pressure circuit

Figure 6.3: insole

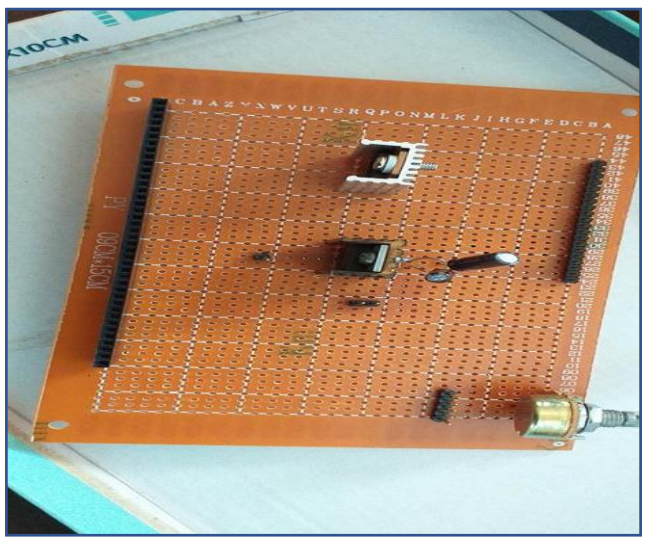

Figure 6.4: power supply

Here are some pictures of some patients with diabetic ulcer disease:

Figure 6.٥: Patient with diabetic foot ulcers in the Big Toe.

Figure 6.٦: Patient with diabetic foot ulcers in the pad

6.2 Result for EMG signal:

In the following table, the special data that was taken from 30 cases in which EMG signal was taken from them whether they have diabetic ulcer disease or have diabetes or healthy people from both diseases are included.
Whereas, the cases of (P1 - P10) have diabetes ulcers, the cases (P11 - P20) have diabetes, and the cases of (P21 - P30) are healthy people from both diseases, with ages ranging from (40 - 85 years).

Table 6.1: result of EMG signal, (---): he does not have.

Patient	M/F	Wight (Kg)	Age (year)	Length (cm)	Size shoe (cm)	Genetics cause disease	Duration of the disease	foot Infected with the disease	Place of injury	EMG signal-Voltage (P_K-P_K)	Caused
P1	F	84	64	163	39	NO	15 year	Left	Big toe	١٥٤mV	Neuropathy
P2	M	85	69	167	42	YES	18 year	right	heel	114mV	Neuropathy
P3	M	97	52	178	42	YES	17 year	Left	pad	162mV	Amputation in the little finger
P4	F	95	70	163	40	NO	19 year	right	Pad	97mV	Neuropathy (very week)
P5	F	75	69	175	41	NO	20 year	Two	All foot	L 270mV R 260mV	Neuropathy
P6	F	90	71	150	39	NO	21 year	right	Heel	39mV	Neuropathy (very week)
P7	M	79	50	150	45	NO	29 year	right	Big toe	40mV	Neuropathy (very week)
P8	F	85	55	158	39	NO	22 year	Left	Pad	236mV	Neuropathy
P9	F	100	60	165	41	NO	20 year	Left	Pad Big toe	270mV	Neuropathy
P10	F	٨٥	٦٤	١٦٥	٣٩	YES	15 year	right	Big toe	230mV	Neuropathy
P11	M	95	51	190	45	YES	10 year	---	---	16mV	Neuropathy (very week)
P12	M	80	57	160	42	YES	2 year	---	---	0.82V	---
P13	F	100	84	167	42	NO	15 year	---	---	260mV	Neuropathy (very week)
P14	F	88	44	156	40	YES	1 year	---	---	1.2V	---
P15	F	102	72	160	39	YES	12 year	---	---	672mV	---
P16	F	100	60	170	41	YES	1 year	---	---	0.92V	---
P17	F	92	56	160	40	YES	6 year	---	---	534mV	---
P18	F	70	60	160	39	YES	1 year	---	---	280mV	Neuropathy
P19	F	80	47	157	40	YES	3 year	---	---	597mV	---
P20	F	93	51	150	39	YES	1 year	---	---	130mV	Neuropathy (very week)
P21	M	110	56	180	46	YES	---	---	---	1.31V	---
P22	F	76	52	160	38	YES	---	---	---	1.57V	---
P23	F	105	59	160	38	YES	---	---	---	1.11V	---
P24	M	73	40	156	40	YES	---	---	---	1.45V	---
P25	M	97	60	180	43	YES	---	---	---	600mV	Neuropathy

P26	M	100	40	178	45	NO	---	---	---	1.6V	---
P27	F	79	50	173	40	NO	---	---	---	1.36V	---
P28	F	65	45	160	37	NO	---	---	---	1.27V	---
P29	M	85	55	165	42	YES	---	---	---	1.34V	---
P30	M	100	47	176	41	NO	---	---	---	1.53V	---

6.3 Analyses for EMG:

1) The electrical signal of the muscle is affected with age, as it is affected by weight and the duration of diabetes. There are some abnormal conditions, such as the presence of muscle or nerve weakness due to diseases of the nerves or because of other conditions such as accidents with traffic accidents.
2) In the case of diabetic foot ulcers, the value of the resulting voltage ranges between (10 mV - 300 mV) as shown in the table above.
3) In the case of diabetes, the value of the resulting voltage ranges between (310 mV - 1 V) as shown in the table above.
4) In the case of healthy people from both diseases, the value of the resulting voltage ranges between (1.01 V - 1.56 V) as shown in the table above.

Based on previous studies [٥٢] and compared to the results obtained, the results that were found in that study in the form of the resulting EMG signal:

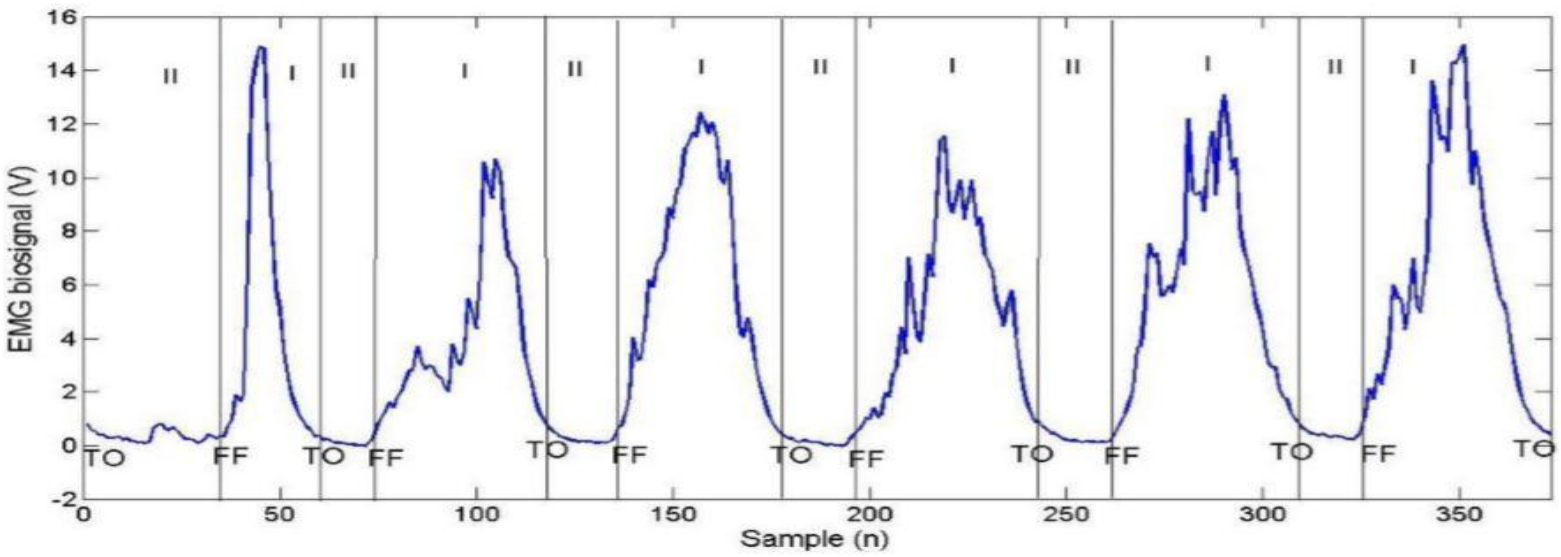

Figure 6.٧: Gait classification based on EMG bio signal. The gait is classified into two: stance phase (I) and swing phase (II).

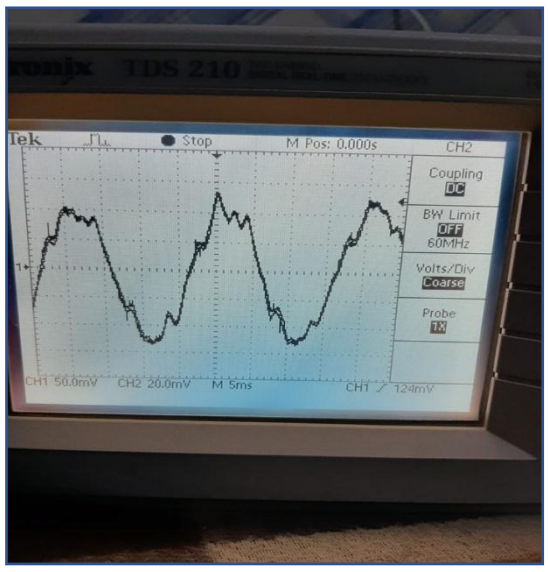

Figure 6.٨: EMG for normal person

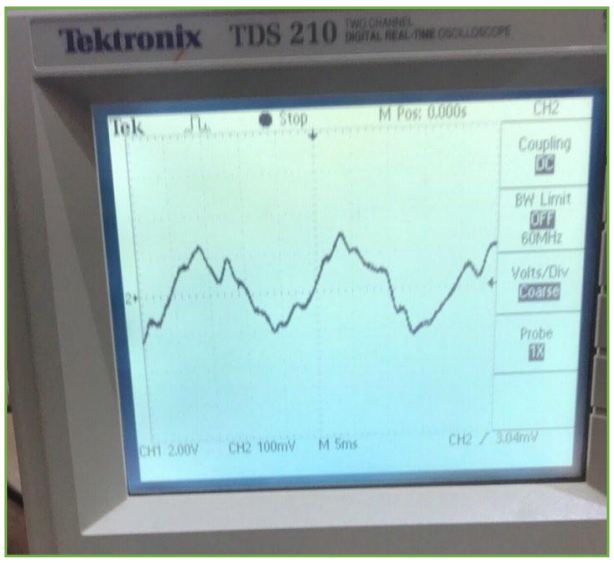

Figure 6.٩: EMG for diabetic patient

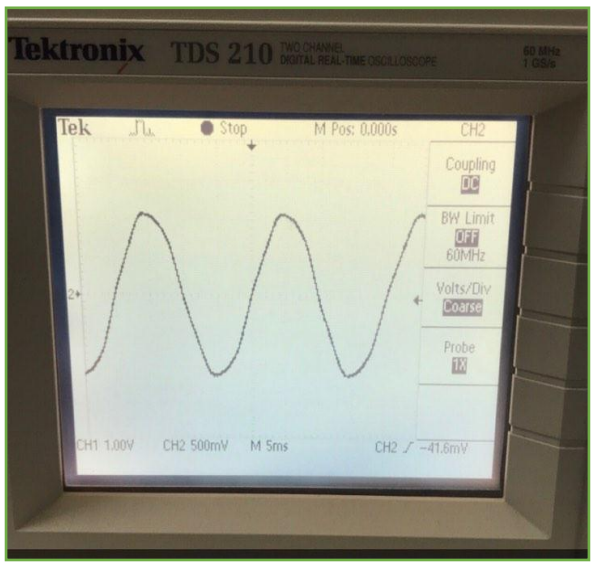

Figure 6.١٠: EMG for ulcer patient

6.4 Result for pressure sensors:

In the following table, the special data that was taken from 30 cases in which work was taken to take the pressure values resulting from them whether they had diabetes ulcers or diabetic or healthy people from both diseases were included.
As the cases from (P1 - P8) suffer from diabetic foot ulcers, the cases from (P9 - P15) have diabetes, and the cases from (P16 - P25) are healthy people from both diseases, with ages ranging from (40 - 72 years old).

Table 6.2: result for pressure sensor for age (40 -72 year).

Patient	M/F	Wight (Kg)	Age (year)	Length (cm)	Size shoe (cm)	Pressure (KPa)				Caused
						Big Toe	Pad	Side Foot	Heel	
P1	F	84	64	163	39	107.4	179.15	32.13	114.8	The injury was in the big Toe area and the Pad area, and the big Toe area was stiff.
P2	M	85	69	167	42	110	81.66	22.7	124.7	The injury was in the big Toe area and skin is very stiff.
P3	F	95	70	163	42	119.6	99.5	93.13	71.5	The injury was in the big Toe area and Heel area and skin is very stiff in big toe (He has flat foot).
P4	F	90	71	150	39	63.53	41.65	33.45	120.72	She had a swelling in the big Toe and Pad make the tissue more soft than the normal
P5	M	79	50	180	45	85.64	84.43	31.34	95.46	He can't walk normally because had a surgery in big toe and his spine after an accident happened to him
P6	F	85	55	158	39	27.5	89.5	54.04	124.3	There is a swelling in the Pad
P7	F	100	60	165	41	106.3	60.61	50.24	85.3	The injury was in the big Toe area and Heel area and skin is very stiff in big toe (He has flat foot).
P8	F	85	60	165	39	113.98	109.25	74.35	123.6	The injury was in the big Toe area and the Pad area, and the big Toe area was stiff.
P9	M	80	57	160	42	91.11	99.5	33.4	119.19	He suffers from a problem in the heel area and pad area (inflammation).
P10	F	90	44	156	40	76.48	66.12	35.62	125.92	He performed an operation on the area of the big toe
P11	F	80	47	157	40	98.97	57.26	39.83	127.9	---
P12	F	93	51	150	39	95.92	70.88	37.88	124.02	---
P13	F	78	60	160	39	94.11	84.34	33.9	108.18	He swollen in the heel area
P14	M	100	60	165	42	108.04	67.72	66.5	116.19	He suffers from a problem in the heel area and big toe area (inflammation).
P15	M	89	47	174	40	88.42	82.53	74.22	127.3	---
P16	F	105	59	160	38	99.4	98.5	79.9	127.96	---
P17	M	85	42	169	42	87.87	85.15	43.78	127.9	---
P18	F	87	52	160	38	93.44	52.02	38.5	127.73	---
P19	M	85	55	165	42	74.53	81.66	42.25	127.4	---
P20	F	84	46	173	37	97.32	89.53	49.91	122.46	---
P21	M	89	54	185	40	69.53	79.92	35.9	126.81	---
P22	F	79	50	173	40	71.59	82.53	31.06	127.68	---
P23	M	97	60	176	43	92.57	70.56	44.62	127.9	---
P24	M	92	63	165	42	96.91	63.74	42.65	127.69	---
P25	F	65	45	160	37	93.87	85.62	42.52	127.83	---

In the following table, special data were taken from 10 cases in which work was perform to take the resulting pressure values for healthy people from both diseases, with ages ranging from (19 - 24 years).

Table 6.٣: result for pressure sensor for age (19 - 24 year).

Patient	M/F	Wight (Kg)	Age (year)	Length (cm)	Size shoe (cm)	Pressure (KPa)			
						Big Toe	Pad	Side Foot	Heel
P١	M	66	19	173	42	79.35	65.43	32.39	127.96
P٢	M	56	19	184	43	76.05	52.42	33.35	125.71
P٣	M	113	19	184	45	98.67	87.12	48.91	127.96
P٤	M	60	19	185	44	72.41	55.53	33.27	126.8
P٥	M	80	20	170	42	96.00	71.39	68.25	118.32
P٦	M	90	20	178	43	79.55	76.94	57.75	126.49
P٧	M	78	23	180	42	84.47	66.94	47.59	127.96
P٨	M	105	24	169	41	94.55	76.91	55.36	127.96
P٩	M	75	24	178	43	74.09	57.26	32.39	127.27
P١٠	M	74	23	178	42	70.04	58.77	32.39	127.96

6.5 Analyses for pressure sensors:

1) If we take the average of the Heel pressure values of normal cases equal 126.78KPa and its approximately equal the most read repeated in the pressure reading (127.96Kpa).
2) The highest pressure read in the heel area and the minimum pressure in the side foot area.
3) If the pressure of side foot area higher than the pressure in any area in foot the mean there abnormal condition.
4) A person may be consider uninfected in the heel area if the result of pressure is between (120 KPa - 128 KPa).
5) The lowest area prone to developing diabetic ulcer disease is the side foot because the pressure on it is less.
6) The most susceptible areas for diabetic foot ulcers are (Big Toe & Pad)[53].
7) The resulting pressure value increases in the affected areas further, so that people with diabetic foot ulcers have a higher-pressure result than diabetes patients and healthy people, and diabetes patients have a higher-pressure result than healthy people do.
8) Pressures can be arrange in the four regions as follows:
* The pressure in the heel area is higher than the rest of the areas.
* The pressure in the big toe area is higher than the pressure in the Pad area and the pressure in the side foot.
* The pressure in the Pad area is higher than the pressure in the side foot.
* The pressure in the side foot area is the lowest.
Based on previous studies [53] and compared to the results obtained, the results that were found in that study in the value of the resulting pressure sensor:

Table ٦.٤: Comparison of dynamic foot pressure in various study [53], DM: Diabetics mellitus, P0: big toe, P1: pad, P2: side foot.

Study groups	Dynamic foot pressure points	Number of participants	Dynamic foot pressures (K pascal) Mean±SD
Normal	P0	30	87.82±26.29
	P1	30	76.63±25.83
	P2	29	66.55±26.51
DM	P0	30	105.32±23.56
	P1	30	91.52±25.13
	P2	30	76.98±25.73
DM with neuropathy	P0	19	105.32±23.56
	P1	19	91.52±25.13
	P2	19	76.98±25.73
Foot ulcer	P0	31	92.7±33.253
	P1	31	76.31±35.363
	P2	31	80.25±34.124
Total	P0	110	95.42±28.919
	P1	110	81.07±29.823
	P2	109	75.45±29.57

6.6 Calibration:

Work was done on calibrating sensors and filters before starting to work on them and extracting results. The work was done through four parts:

1) Calibration for (A401) sensor:

The A401 was calibrated by placing different weights on the sensor and calculating the resulting resistance, Then the weight was converted from (g) to (pound) and then to (Force). Through the resistance value, the resulting voltages were calculated.

Table 6.٥: For big toe & Side foot & pad sensors (A401):

Wight(g)	Wight(Pound)	Force(N)	Resister(Ω)	Volt(v)
100	0.220	0.981	3.46M	٢٨.٩m
150	0.331	1.471	2.34M	42.74m
170	0.375	1.667	1.98M	50.5m
180	0.397	1.765	1.83M	54.64m
185	0.408	1.814	1.8M	55.6m
200	0.441	1.961	1.86M	53.76m
220	0.485	2.157	1.61M	62.11m
240	0.529	2.354	1.6M	62.5m
260	0.573	2.549	1.42M	70.42m
280	0.617	2.746	1.31M	76.34m
300	0.661	2.942	1.28M	78.13m
320	0.705	3.138	1.21M	82.64m
340	0.749	3.334	1.09M	91.74m
360	0.794	3.530	1.06M	94.34m
380	0.838	3.727	1.03M	97.1m
400	0.882	3.923	0.96M	104.2m
420	0.926	4.119	0.92M	108.7m
440	0.970	4.315	0.9M	111.11m
460	1.014	4.511	0.88M	113.64m
480	1.058	4.707	0.86M	116.3m
500	1.102	4.903	0.86M	116.3m
520	1.146	5.099	0.81M	123.46m
540	1.191	5.296	0.77M	129.87m
560	1.235	5.492	0.76M	131.58m
580	1.279	5.688	0.73M	136.9m
600	1.323	5.884	0.74M	135.14m

$$Vout = Vref * \frac{-Rf}{Rs} \dots\dots\dots\dots\dots\dots\dots\dots\dots\dots\dots\dots\dots\dots\dots (6.1)$$

Where the, Vref = -1 volt, Rf = 100 KΩ
However, we need to display the value as a force according to the following equation:
F = 3828.2*V4 - 881.59*V3 + 167.24*V2 + 25.55*V + 0.1059 …… (6.2)
Area (A) = □ r2
A = 2.02*10-3 m2
Pressure $= \frac{F}{A}$
Where F: force & A: area of sensor
Pressure = (١٨٩٥١٤٨.٥*V4 - 436430.67*V3 + 82792.08*V2 + 12648.52*V + 52.426) N/m^2
Pressure = (1895.1485*V4 – 436.43067*V3 + 82.79208*V2 + 12.64852*V + 0.052426) KPa … (6.3)

2) Calibration for (A502) sensor:

The A502 was calibrated by placing different weights on the sensor and calculating the resulting resistance, Then the weight was converted from (g) to (pound) and then to (Force). Through the resistance value, the resulting voltages were calculated.

Table 6.٦: For Heel sensor (A502):

Wight(g)	Wight(Pound)	Force(N)	Resister(Ω)	Volt(v)
100	0.220	0.981	٤.٤٤M	٢٢.٥m
150	0.331	1.471	3.1M	32.3m
170	0.375	1.667	2.4M	41.7m
180	0.397	1.765	2.26M	44.3m
185	0.408	1.814	2.12M	47.16m
200	0.441	1.961	2.1M	47.2m
220	0.485	2.157	1.99M	50.3m
240	0.529	2.354	1.65M	60.6m
260	0.573	2.549	1.62M	61.7m
280	0.617	2.746	1.52M	65.8m
300	0.661	2.942	1.39M	71.9m
320	0.705	3.138	1.32M	75.8m
340	0.749	3.334	1.28M	78.1m
360	0.794	3.530	1.23M	81.3m
380	0.838	3.727	1.11M	90.1m
400	0.882	3.923	1.1M	90.9m

420	0.926	4.119	0.99M	101.1m
440	0.970	4.315	0.96M	104.2m
460	1.014	4.511	0.94M	106.4m
480	1.058	4.707	0.93M	107.5m
500	1.102	4.903	0.87M	114.9m
520	1.146	5.099	0.85M	117.6m
540	1.191	5.296	0.82M	121.9m
560	1.235	5.492	0.78M	128.2m
580	1.279	5.688	0.77M	129.9m
600	1.323	5.884	0.62M	161.3m

$$Vout = Vref * \frac{-Rf}{Rs} \ldots\ldots\ldots\ldots\ldots\ldots\ldots\ldots\ldots\ldots (6.1)$$

Where the, V_{ref} = -1 volt, R_f = 100 KΩ
However, we need to display the value as a force according to the following equation:

$F = -0.000003*V^3 + 0.0006*V^2 - 0.0016*V + 0.8615$ …… (6.4)
$A= (50.8*10^{-3})^2$
$= 2.58*10^{-3}\ m^2$
Pressure $= \frac{F}{A}$
Where F: force & A: area of sensor
Pressure $= (-0.00116*V^3 + 0.233*V^2 + 0.6202*V + 333.9)\ N/m^2$
Pressure $= (-0.00000116*V^3 + 0.000233*V^2 + 0.0006202*V + 0.3339)$ KPa ….. (6.5)

3) calibration of High Pass Filter (HPF):

The High Pass Filter was calibrate by installing the pieces on the breadboard and then taking the resulting voltage value.

Table 6.٧: calibration of HPF

Freq (H_Z)	Vout (Vp-p)
1k	1.53
900	1.53
700	1.5
500	1.5
300	1.49
100	1.47
70	1.43
50	1.4
30	1.39
10	1.36
8	1.3
7	1.21
5	0.8
3	0.2
1	0.04

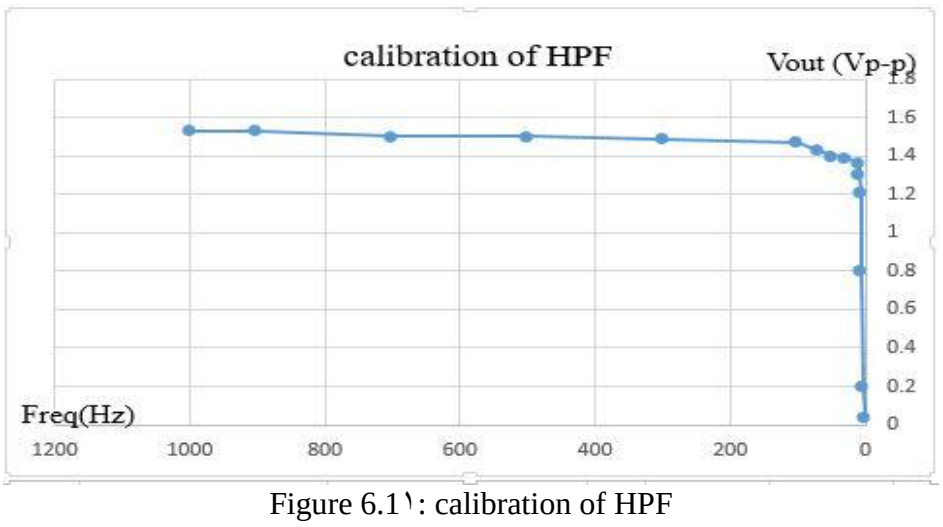

Figure 6.1١: calibration of HPF

4) calibration of Low Pass Filter (LPF):

The Low Pass Filter was calibrate by installing the pieces on the breadboard and then taking the resulting voltage value.

Table 6.٨: calibration of LPF

Freq (Hz)	Vout (Vp-p)
1	1.54
5	1.54
10	1.54
50	1.52
100	1.5
400	1.32
500	1.2
542	1.07
600	0.82
700	0.73
800	0.65
900	0.52
1K	0.4

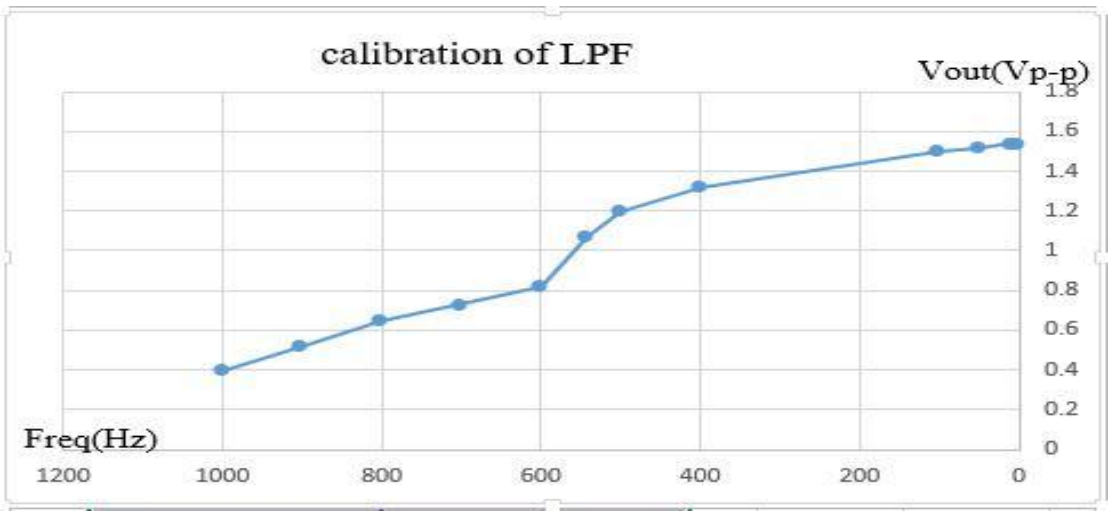

Figure 6.1٢: calibration of LPF

Chapter Seven:

Future Work and Challenges

7.1 Future Work:

The project was implemented using wires, while new technology technologies can be used to send information via Wi Fi or via Bluetooth, and a greater number of cases can be taken in order to establish a relationship between variables such as the effect of weight and age and length on the amount of pressure. and the impact of the duration of a disease Diabetes in the value of the resulting effort in order to find a stable relationship that can be adopted in the impact of these variables.as well as building gender-specific relationships, whether male or female, and the extent of that impact on pressure, as well as in building relationships for uninfected persons flat foot.

7.2 Challenges:

During the project implementation the system, some challenge was faced, such as:

- Some of the system components are expensive like flexi-force sensors.
- Not all of the required component for the project are available in the Palestinian market.

Appendix A

Appendix B

Appendix C

Appendix D

Appendix E

Appendix F

Appendix G

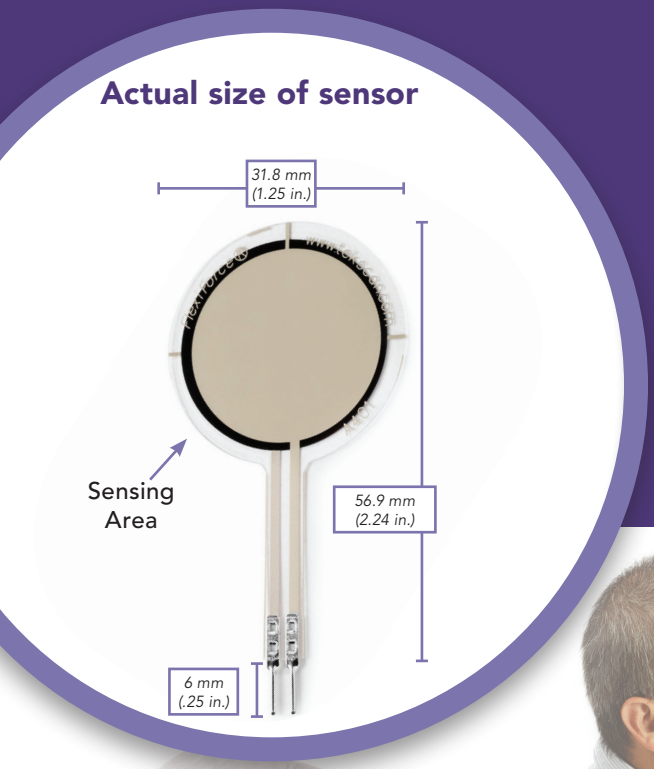

FlexiForce™

Standard Model A401

The FlexiForce A401 is our standard piezoresistive force sensor with the largest sensing area. It is available off-the-shelf for easy proof of concept and is also available in large volumes for design-in applications. The A401 can be used with our test & measurement, prototyping, and embedding electronics, including the OEM Development Kit, FlexiForce Quickstart Board, and the ELF™ System*. You can also use your own electronics, or multimeter.

Physical Properties

Thickness	0.203 mm (0.008 in.)
Length	56.9 mm (2.24 in.)**
Width	31.8 mm (1.25 in.)
Sensing Area	25.4 mm (1 in.) diameter
Connector	2-pin Male Square Pin
Substrate	Polyester
Pin Spacing	2.54 mm (0.1 in.)

Benefits

- Thin and flexible
- Easy to use
- Convenient and affordable

✓ROHS COMPLIANT

** Sensor will require an adapter/extender to connect to the ELF System. Contact your Tekscan representative for assistance.*

***Length does not include pins. Please add approximately 6 mm (0.25 in.) for pin length for a total length of approximately 32 mm (1.25 in).*

ISO 9001 Compliant & 13485 Registered

Tekscan™

Standard Force Ranges
as Tested with Circuit Shown

111 N (0 - 25 lb) †

† This sensor can measure up to 31,138 N (7,000 lb). The force range can be extended by reducing the drive voltage, VT, or the resistance value of the feedback resistor, RF. Conversely, the sensitivity can be increased for measurement of lower forces by increasing VT or RF.

Sensor output is a function of many variables, including interface materials. Therefore, Tekscan recommends the user calibrate each sensor for the application. The graph below-right is an illustration of how a sensor can be used to measure varying force ranges by changing the feedback resistor (the graph below-right should not be used as a calibration chart).

Recommended Circuit

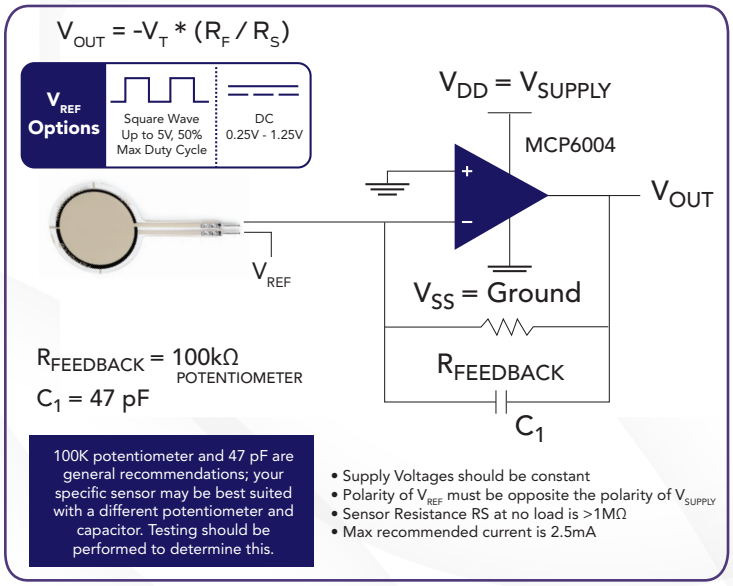

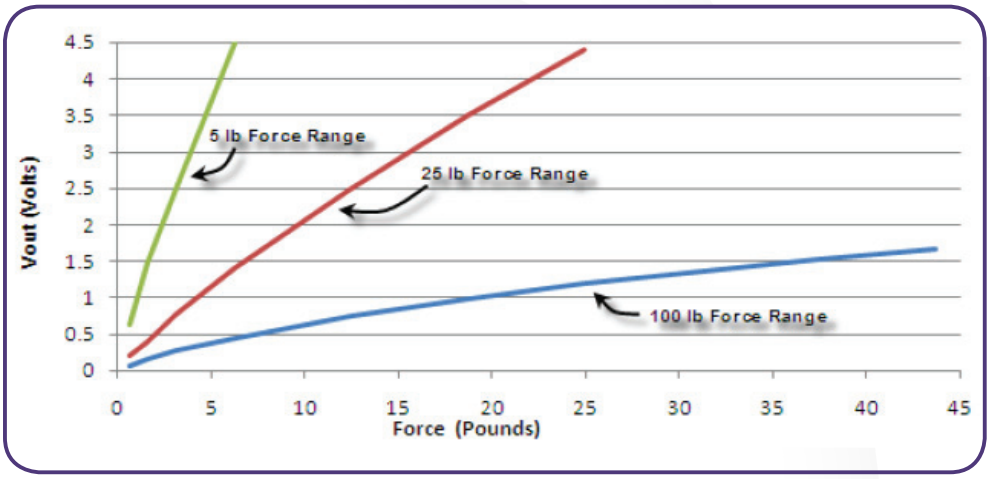

	Typical Performance	Evaluation Conditions
Linearity (Error)	< ±3% of full scale	Line drawn from 0 to 50% load
Repeatability	< ±2.5%	Conditioned sensor, 80% of full force applied
Hysteresis	< 4.5% of full scale	Conditioned sensor, 80% of full force applied
Drift	< 5% per logarithmic time scale	Constant load of 111 N (25 lb)
Response Time	< 5µsec	Impact load, output recorded on oscilloscope
Operating Temperature	-40°C - 60°C (-40°F - 140°F)	Convection and conduction heat sources
Acceptance Criteria	±40% sensor-to-sensor variation	

*

***All data above was collected utilizing an Op Amp Circuit.** If your application cannot allow an Op Amp Circuit, visit www.tekscan.com/flexiforce-integration-guides, or contact a FlexiForce Applications Engineer.

Force reading change per degree of temperature change = 0.36%/°C (±0.2%/°F).

Relation between force and voltage:

Voltage	Force
0.054878	0.640569
0.068598	0.800712
0.082317	0.907473
0.096037	1.06762
0.109756	1.22776
0.137195	1.44128
0.164634	1.70819
0.178354	1.97509
0.205793	2.29537
0.233232	2.61566
0.260671	2.93594
0.28811	3.25623
0.301829	3.52313
0.315549	3.79004
0.329268	4.05694
0.342988	4.37722
0.356707	4.69751
0.370427	5.01779
0.397866	5.39146
0.411585	5.76512
0.425305	6.03203
0.439024	6.29893
0.466463	6.61922
0.480183	6.9395
0.480183	7.20641
0.493902	7.47331
0.507622	7.79359
0.521341	8.0605
0.54878	8.38078
0.5625	8.75445
0.57622	9.07473
0.589939	9.39502
0.603659	9.7153
0.631098	10.0356
0.644817	10.3559
0.672256	10.7295
0.685976	11.1566

0.699695	11.5302
0.713415	11.7972
0.727134	12.1174
0.754573	12.4377
0.768293	12.8114
0.768293	13.1851
0.782012	13.5053
0.795732	13.879
0.809451	14.2527
0.83689	14.7331
0.85061	15.2135
0.864329	15.6406
0.878049	16.0676
0.891768	16.4947
0.905488	16.9217
0.932927	17.2954
0.932927	17.669
0.960366	18.0427
0.974085	18.4164
0.987805	18.79
1.00152	19.1103
1.01524	19.5374
1.02896	20.0712
1.04268	20.4982
1.0564	20.8185
1.07012	21.2456
1.08384	21.6726
1.09756	22.0996
1.11128	22.5267
1.125	22.9537
1.13872	23.4342
1.15244	23.8612
1.17988	24.395
1.1936	24.8754
1.20732	25.3025
1.22104	25.7829
1.23476	26.2633
1.24848	26.7972
1.2622	27.2242
1.27591	27.758
1.28963	28.3452
1.30335	28.7722
1.30335	29.2527
1.31707	29.573
1.33079	30
1.34451	30.4804
1.34451	30.9609
1.35823	31.3879
1.37195	31.7616
1.38567	32.1886
1.39939	32.669
1.41311	33.0961
1.42683	33.5765

1.44055	34.0569
1.45427	34.5374
1.46799	34.9644
1.46799	35.4448
1.48171	36.032
1.50915	36.6726
1.52287	37.2598
1.53659	37.7936
1.53659	38.3808
1.5503	38.8612
1.56402	39.2883
1.57774	39.7687
1.59146	40.3559
1.60518	40.9431
1.6189	41.5302
1.63262	42.0641
1.64634	42.5979
1.66006	43.0783
1.67378	43.6655

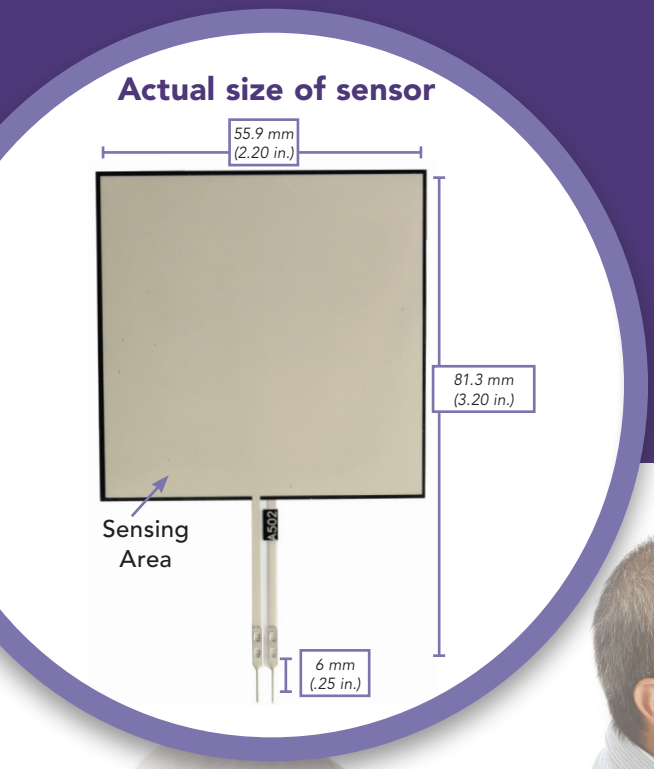

FlexiForce™

Standard Model A502

The FlexiForce™ A502 is a square sensor, with a sensing area measuring 50.8 mm x 50.8 mm (2 in. x 2 in.). This sensor is available off-the-shelf for easy proof of concept. The A502 can be used with our test & measurement, prototyping, and embedding electronics, including the OEM Development Kit, FlexiForce Quickstart Board, and the ELF™ System*. You can also use your own electronics, or multimeter.

Physical Properties

Thickness	0.203 mm (0.008 in.)
Length	81.3 mm (3.20 in.)**
Width	55.9 mm (2.20 in.)
Sensing Area	50.8 mm x 50.8 mm (2 in. x 2 in.)
Connector	2-pin Male Square Pin
Substrate	Polyester
Pin Spacing	2.54 mm (0.1 in.)

Benefits

- Thin and flexible
- Low-power
- Ideal for prototyping and integration
- Easy to use

✓ROHS COMPLIANT

* *Sensor will require an adapter/extender to connect to the ELF System. Contact your Tekscan representative for assistance.*

** *Length does not include pins. Please add approximately 6 mm (0.25 in.) for pin length for a total length of approximately 87 mm (3.4 in).*

ISO 9001 Compliant & 13485 Registered

Tekscan™

Typical Performance

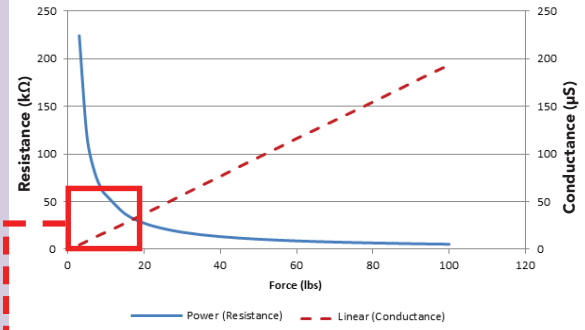

Superior performance and range compared to other sensors of its kind

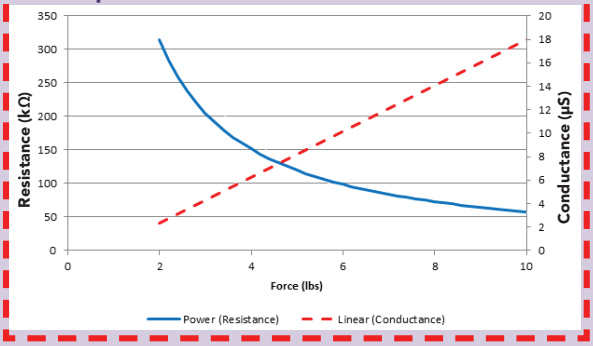

Voltage (V)	Force (lbs)	Resistance (kΩ)	Conductance (µS)
0.5	20	34.36	29.11
0.5	40	17.14	58.33
0.5	60	11.57	86.41
0.5	80	8.71	114.76
0.5	100	6.97	143.54

- Sensor acceptance criteria ±40% of nominal
- Sensor resistance measured 20 seconds after applied load
- Sensor loaded through a polycarbonate puck equal to 68% (2.72 in^2) of total active area
- Sensor was not attached to any drive circuitry

Standard Force Ranges
as Tested with Circuit Shown

222 N (0 - 50 lb) †

† This sensor can measure up to 44,448 N (10,000 lb). In order to measure higher forces, apply a lower drive voltage (-0.5 V, -0.25 V, etc.) and reduce the resistance of the feedback resistor (1kΩ min.) To measure lower forces, apply a higher drive voltage and increase the resistance of the feedback resistor.

Sensor output is a function of many variables, including interface materials. Therefore, Tekscan recommends the user calibrate each sensor for the application.

Recommended Circuit

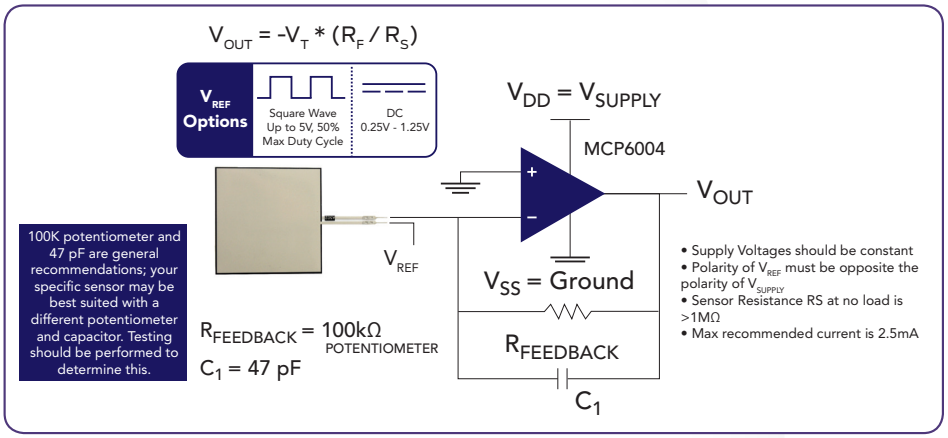

	Typical Performance	Evaluation Conditions *
Linearity (Error)	< ±3% of full scale	Line drawn from 0 to 50% load
Repeatability	< ±2.5%	Conditioned sensor, 80% of full force applied
Hysteresis	< 4.5% of full scale	Conditioned sensor, 80% of full force applied
Drift	< 5% per logarithmic time scale	Constant load of 111 N (25 lb)
Response Time	< 5µsec	Impact load, output recorded on oscilloscope
Operating Temperature	-40°C - 60°C (-40°F - 140°F)	Convection and conduction heat sources

All data above was collected utilizing an Op Amp Circuit. If your application cannot allow an Op Amp Circuit, visit www.tekscan.com/flexiforce-integration-guides, or contact a FlexiForce Applications Engineer.

Force reading change per degree of temperature change = 0.36%/°C (±0.2%/°F).

Relation of voltage and force table

Rs	Voltage	Force
224.576	0.445284	3.12419
216.102	0.462744	3.1123
207.627	0.481633	3.10041
196.328	0.509352	3.43542
186.441	0.536363	3.42155
176.554	0.566399	3.75855
166.667	0.599999	3.74467
158.192	0.632143	4.08366
148.305	0.674286	4.06978
137.006	0.729895	4.4048
129.944	0.769562	4.39489
120.056	0.832945	4.73189
110.169	0.907696	5.06889
97.4576	1.026087	5.7528
88.9831	1.123809	6.09178
80.5085	1.242105	6.78164
72.0339	1.388235	7.4715
64.9718	1.539129	8.16335
57.9096	1.726829	9.20607
49.435	2.022858	10.9486
40.9605	2.441376	13.0419
36.7232	2.723074	14.4395
31.0734	3.218187	16.1859
25.4237	3.933338	19.3359
22.5989	4.424994	22.139
19.774	5.057146	24.942
16.9492	5.899983	27.7451
15.5367	6.436373	30.1992
14.1243	7.079997	33.3551
12.7119	7.866645	36.1602
11.2994	8.850027	39.3161
9.88701	10.11428	42.8229
9.88701	10.11428	46.3316
8.47458	11.79999	52.2946
7.06215	14.15999	57.5558
5.64972	17.69999	62.8169
5.64972	17.69999	67.0275
5.64972	17.69999	70.5362

4.23729	23.59999	78.2535
4.23729	23.59999	80.3588
4.23729	23.59999	84.2185
4.23729	23.59999	89.4816
2.82486	35.39998	100.006

www.robotshop.com

La robotique à votre service! - Robotics at your service!

ARDUINO

Arduino Mega 2560 Datasheet

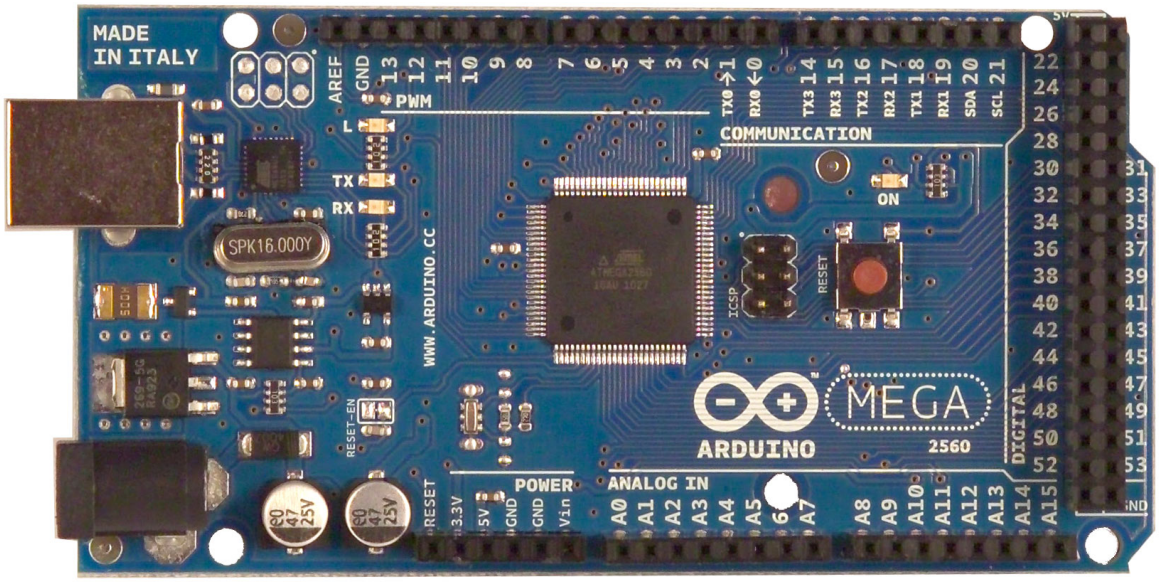

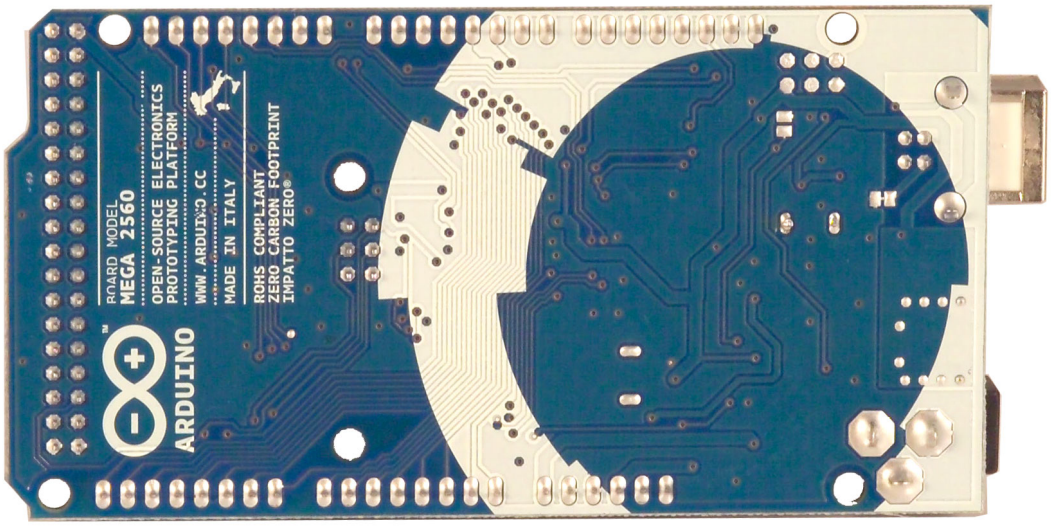

Overview

The Arduino Mega 2560 is a microcontroller board based on the ATmega2560 (datasheet). It has 54 digital input/output pins (of which 14 can be used as PWM outputs), 16 analog inputs, 4 UARTs (hardware serial ports), a 16 MHz crystal oscillator, a USB connection, a power jack, an ICSP header, and a reset button. It contains everything needed to support the microcontroller; simply connect it to a computer with a USB cable or power it with a AC-to-DC adapter or battery to get started. The Mega is compatible with most shields designed for the Arduino Duemilanove or Diecimila.

Schematic & Reference Design

EAGLE files: arduino-mega2560-reference-design.zip

Schematic: [arduino-mega2560-schematic.pdf]

Summary

Microcontroller	ATmega2560
Operating Voltage	5V
Input Voltage (recommended)	7-12V
Input Voltage (limits)	6-20V
Digital I/O Pins	54 (of which 14 provide PWM output)
Analog Input Pins	16
DC Current per I/O Pin	40 mA
DC Current for 3.3V Pin	50 mA
Flash Memory	256 KB of which 8 KB used by bootloader
SRAM	8 KB
EEPROM	4 KB
Clock Speed	16 MHz

Power

The Arduino Mega can be powered via the USB connection or with an external power supply. The power source is selected automatically.

External (non-USB) power can come either from an AC-to-DC adapter (wall-wart) or battery. The adapter can be connected by plugging a 2.1mm center-positive plug into the board's power jack. Leads from a battery can be inserted in the Gnd and Vin pin headers of the POWER connector.

The board can operate on an external supply of 6 to 20 volts. If supplied with less than 7V, however, the 5V pin may supply less than five volts and the board may be unstable. If using more than 12V, the voltage regulator may overheat and damage the board. The recommended range is 7 to 12 volts.

The Mega2560 differs from all preceding boards in that it does not use the FTDI USB-to-serial driver chip. Instead, it features the Atmega8U2 programmed as a USB-to-serial converter.

The power pins are as follows:

- **VIN.** The input voltage to the Arduino board when it's using an external power source (as opposed to 5 volts from the USB connection or other regulated power source). You can supply voltage through this pin, or, if supplying voltage via the power jack, access it through this pin.
- **5V.** The regulated power supply used to power the microcontroller and other components on the board. This can come either from VIN via an on-board regulator, or be supplied by USB or another regulated 5V supply.
- **3V3.** A 3.3 volt supply generated by the on-board regulator. Maximum current draw is 50 mA.
- **GND.** Ground pins.

Memory

The ATmega2560 has 256 KB of flash memory for storing code (of which 8 KB is used for the bootloader), 8 KB of SRAM and 4 KB of EEPROM (which can be read and written with the EEPROM library).

Input and Output

Each of the 54 digital pins on the Mega can be used as an input or output, using pinMode() , digitalWrite(), and digitalRead() functions. They operate at 5 volts. Each pin can provide or receive a maximum of 40 mA and has an internal pull-up resistor (disconnected by default) of 20-50 kOhms. In addition, some pins have specialized functions:

- **Serial: 0 (RX) and 1 (TX); Serial 1: 19 (RX) and 18 (TX); Serial 2: 17 (RX) and 16 (TX); Serial 3: 15 (RX) and 14 (TX).** Used to receive (RX) and transmit (TX) TTL serial data. Pins 0 and 1 are also connected to the corresponding pins of the ATmega8U2 USB-to-TTL Serial chip.
- **External Interrupts: 2 (interrupt 0), 3 (interrupt 1), 18 (interrupt 5), 19 (interrupt 4), 20 (interrupt 3), and 21 (interrupt 2).** These pins can be configured to trigger an interrupt on a low value, a rising or falling edge, or a change in value. See the attachInterrupt() function for details.
- **PWM: 0 to 13.** Provide 8-bit PWM output with the analogWrite() function.
- **SPI: 50 (MISO), 51 (MOSI), 52 (SCK), 53 (SS).** These pins support SPI communication using the SPI library. The SPI pins are also broken out on the ICSP header, which is physically compatible with the Uno, Duemilanove and Diecimila.
- **LED: 13.** There is a built-in LED connected to digital pin 13. When the pin is HIGH

value, the LED is on, when the pin is LOW, it's off.
- **I2C: 20 (SDA) and 21 (SCL).** Support I2C (TWI) communication using the Wire library (documentation on the Wiring website). Note that these pins are not in the same location as the I2C pins on the Duemilanove or Diecimila.

The Mega2560 has 16 analog inputs, each of which provide 10 bits of resolution (i.e. 1024 different values). By default they measure from ground to 5 volts, though is it possible to change the upper end of their range using the AREF pin and analogReference() function.

There are a couple of other pins on the board:

- **AREF.** Reference voltage for the analog inputs. Used with analogReference().
- **Reset.** Bring this line LOW to reset the microcontroller. Typically used to add a reset button to shields which block the one on the board.

Communication

The Arduino Mega2560 has a number of facilities for communicating with a computer, another Arduino, or other microcontrollers. The ATmega2560 provides four hardware UARTs for TTL (5V) serial communication. An ATmega8U2 on the board channels one of these over USB and provides a virtual com port to software on the computer (Windows machines will need a .inf file, but OSX and Linux machines will recognize the board as a COM port automatically. The Arduino software includes a serial monitor which allows simple textual data to be sent to and from the board. The RX and TX LEDs on the board will flash when data is being transmitted via the ATmega8U2 chip and USB connection to the computer (but not for serial communication on pins 0 and 1).
A SoftwareSerial library allows for serial communication on any of the Mega2560's digital pins.
The ATmega2560 also supports I2C (TWI) and SPI communication. The Arduino software includes a Wire library to simplify use of the I2C bus; see the documentation on the Wiring website for details. For SPI communication, use the SPI library.

Programming

The Arduino Mega can be programmed with the Arduino software (download). For details, see the reference and tutorials.
The ATmega2560 on the Arduino Mega comes preburned with a bootloader that allows you to upload new code to it without the use of an external hardware programmer. It

communicates using the original STK500 protocol (reference, C header files).
You can also bypass the bootloader and program the microcontroller through the ICSP (In-Circuit Serial Programming) header; see these instructions for details.

Automatic (Software) Reset

Rather then requiring a physical press of the reset button before an upload, the Arduino Mega2560 is designed in a way that allows it to be reset by software running on a connected computer. One of the hardware flow control lines (DTR) of the ATmega8U2 is connected to the reset line of the ATmega2560 via a 100 nanofarad capacitor. When this line is asserted (taken low), the reset line drops long enough to reset the chip. The Arduino software uses this capability to allow you to upload code by simply pressing the upload button in the Arduino environment. This means that the bootloader can have a shorter timeout, as the lowering of DTR can be well-coordinated with the start of the upload.
This setup has other implications. When the Mega2560 is connected to either a computer running Mac OS X or Linux, it resets each time a connection is made to it from software (via USB). For the following half-second or so, the bootloader is running on the Mega2560. While it is programmed to ignore malformed data (i.e. anything besides an upload of new code), it will intercept the first few bytes of data sent to the board after a connection is opened. If a sketch running on the board receives one-time configuration or other data when it first starts, make sure that the software with which it communicates waits a second after opening the connection and before sending this data.
The Mega2560 contains a trace that can be cut to disable the auto-reset. The pads on either side of the trace can be soldered together to re-enable it. It's labeled "RESET-EN". You may also be able to disable the auto-reset by connecting a 110 ohm resistor from 5V to the reset line; see this forum thread for details.

USB Overcurrent Protection

The Arduino Mega2560 has a resettable polyfuse that protects your computer's USB ports from shorts and overcurrent. Although most computers provide their own internal protection, the fuse provides an extra layer of protection. If more than 500 mA is applied to the USB port, the fuse will automatically break the connection until the short or overload is removed.

Physical Characteristics and Shield Compatibility

The maximum length and width of the Mega2560 PCB are 4 and 2.1 inches respectively, with the USB connector and power jack extending beyond the former dimension. Three screw holes allow the board to be attached to a surface or case. Note that the distance between digital pins 7 and 8 is 160 mil (0.16"), not an even multiple of the 100 mil spacing of the other pins.

The Mega2560 is designed to be compatible with most shields designed for the Uno, Diecimila or Duemilanove. Digital pins 0 to 13 (and the adjacent AREF and GND pins), analog inputs 0 to 5, the power header, and ICSP header are all in equivalent locations. Further the main UART (serial port) is located on the same pins (0 and 1), as are external interrupts 0 and 1 (pins 2 and 3 respectively). SPI is available through the ICSP header on both the Mega2560 and Duemilanove / Diecimila. *Please note that I^2C is not located on the same pins on the Mega (20 and 21) as the Duemilanove / Diecimila (analog inputs 4 and 5).*

SLVS056J – MAY 1976 – REVISED MAY 2003

- **3-Terminal Regulators**
- **Output Current up to 1.5 A**
- **Internal Thermal-Overload Protection**
- **High Power-Dissipation Capability**
- **Internal Short-Circuit Current Limiting**
- **Output Transistor Safe-Area Compensation**

KC (TO-220) PACKAGE
(TOP VIEW)

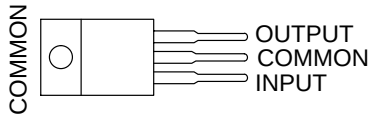

KCS (TO-220) PACKAGE
(TOP VIEW)

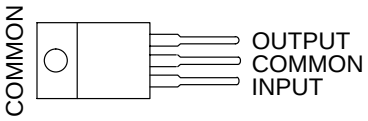

KTE PACKAGE
(TOP VIEW)

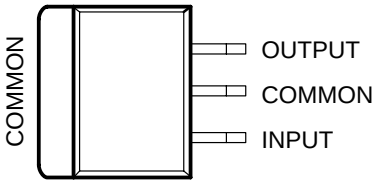

description/ordering information

This series of fixed-voltage integrated-circuit voltage regulators is designed for a wide range of applications. These applications include on-card regulation for elimination of noise and distribution problems associated with single-point regulation. Each of these regulators can deliver up to 1.5 A of output current. The internal current-limiting and thermal-shutdown features of these regulators essentially make them immune to overload. In addition to use as fixed-voltage regulators, these devices can be used with external components to obtain adjustable output voltages and currents, and also can be used as the power-pass element in precision regulators.

ORDERING INFORMATION

T_J	$V_{O(NOM)}$ (V)	PACKAGE†		ORDERABLE PART NUMBER	TOP-SIDE MARKING
0°C to 125°C	5	POWER-FLEX (KTE)	Reel of 2000	μA7805CKTER	μA7805C
		TO-220 (KC)	Tube of 50	μA7805CKC	μA7805C
		TO-220, short shoulder (KCS)	Tube of 20	μA7805CKCS	
	8	POWER-FLEX (KTE)	Reel of 2000	μA7808CKTER	μA7808C
		TO-220 (KC)	Tube of 50	μA7808CKC	μA7808C
		TO-220, short shoulder (KCS)	Tube of 20	μA7808CKCS	
	10	POWER-FLEX (KTE)	Reel of 2000	μA7810CKTER	μA7810C
		TO-220 (KC)	Tube of 50	μA7810CKC	μA7810C
	12	POWER-FLEX (KTE)	Reel of 2000	μA7812CKTER	μA7812C
		TO-220 (KC)	Tube of 50	μA7812CKC	μA7812C
		TO-220, short shoulder (KCS)	Tube of 20	μA7812CKCS	
	15	POWER-FLEX (KTE)	Reel of 2000	μA7815CKTER	μA7815C
		TO-220 (KC)	Tube of 50	μA7815CKC	μA7815C
		TO-220, short shoulder (KCS)	Tube of 20	μA7815CKCS	
	24	POWER-FLEX (KTE)	Reel of 2000	μA7824CKTER	μA7824C
		TO-220 (KC)	Tube of 50	μA7824CKC	μA7824C

† Package drawings, standard packing quantities, thermal data, symbolization, and PCB design guidelines are available at www.ti.com/sc/package.

schematic

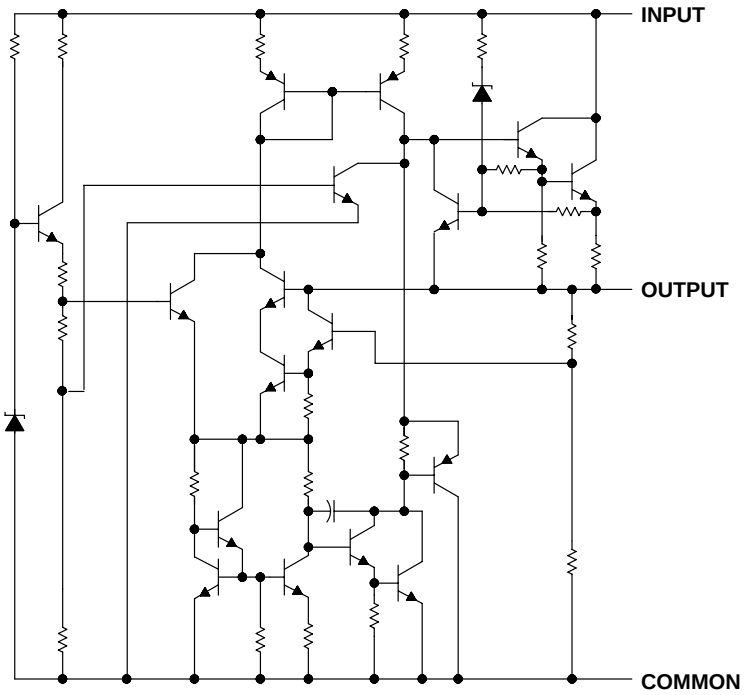

absolute maximum ratings over virtual junction temperature range (unless otherwise noted)†

Input voltage, V_I: μA7824C . . . . . 40 V
All others . . . . . 35 V
Operating virtual junction temperature, T_J . . . . . 150°C
Lead temperature 1,6 mm (1/16 inch) from case for 10 seconds . . . . . 260°C
Storage temperature range, T_{stg} . . . . . –65°C to 150°C

† Stresses beyond those listed under “absolute maximum ratings” may cause permanent damage to the device. These are stress ratings only, and functional operation of the device at these or any other conditions beyond those indicated under “recommended operating conditions” is not implied. Exposure to absolute-maximum-rated conditions for extended periods may affect device reliability.

package thermal data (see Note 1)

PACKAGE	BOARD	θ_{JC}	θ_{JA}
POWER-FLEX (KTE)	High K, JESD 51-5	3°C/W	23°C/W
TO-220 (KC/KCS)	High K, JESD 51-5	3°C/W	19°C/W

NOTE 1: Maximum power dissipation is a function of $T_J(max)$, θ_{JA}, and T_A. The maximum allowable power dissipation at any allowable ambient temperature is $P_D = (T_J(max) – T_A)/\theta_{JA}$. Operating at the absolute maximum T_J of 150°C can affect reliability.

recommended operating conditions

			MIN	MAX	UNIT
V_I	Input voltage	μA7805C	7	25	V
		μA7808C	10.5	25	
		μA7810C	12.5	28	
		μA7812C	14.5	30	
		μA7815C	17.5	30	
		μA7824C	27	38	
I_O	Output current			1.5	A
T_J	Operating virtual junction temperature	μA7800C series	0	125	°C

electrical characteristics at specified virtual junction temperature, V_I = 10 V, I_O = 500 mA (unless otherwise noted)

PARAMETER	TEST CONDITIONS	T_J†	μA7805C			UNIT
			MIN	TYP	MAX	
Output voltage	I_O = 5 mA to 1 A, V_I = 7 V to 20 V, $P_D \le$ 15 W	25°C	4.8	5	5.2	V
		0°C to 125°C	4.75		5.25	
Input voltage regulation	V_I = 7 V to 25 V	25°C		3	100	mV
	V_I = 8 V to 12 V			1	50	
Ripple rejection	V_I = 8 V to 18 V, f = 120 Hz	0°C to 125°C	62	78		dB
Output voltage regulation	I_O = 5 mA to 1.5 A	25°C		15	100	mV
	I_O = 250 mA to 750 mA			5	50	
Output resistance	f = 1 kHz	0°C to 125°C		0.017		Ω
Temperature coefficient of output voltage	I_O = 5 mA	0°C to 125°C		–1.1		mV/°C
Output noise voltage	f = 10 Hz to 100 kHz	25°C		40		μV
Dropout voltage	I_O = 1 A	25°C		2		V
Bias current		25°C		4.2	8	mA
Bias current change	V_I = 7 V to 25 V	0°C to 125°C			1.3	mA
	I_O = 5 mA to 1 A				0.5	
Short-circuit output current		25°C		750		mA
Peak output current		25°C		2.2		A

† Pulse-testing techniques maintain the junction temperature as close to the ambient temperature as possible. Thermal effects must be taken into account separately. All characteristics are measured with a 0.33-μF capacitor across the input and a 0.1-μF capacitor across the output.

electrical characteristics at specified virtual junction temperature, V_I = 14 V, I_O = 500 mA (unless otherwise noted)

PARAMETER	TEST CONDITIONS	T_J†	μA7808C			UNIT
			MIN	TYP	MAX	
Output voltage	I_O = 5 mA to 1 A, V_I = 10.5 V to 23 V, $P_D \le 15$ W	25°C	7.7	8	8.3	V
		0°C to 125°C	7.6		8.4	
Input voltage regulation	V_I = 10.5 V to 25 V	25°C		6	160	mV
	V_I = 11 V to 17 V			2	80	
Ripple rejection	V_I = 11.5 V to 21.5 V, f = 120 Hz	0°C to 125°C	55	72		dB
Output voltage regulation	I_O = 5 mA to 1.5 A	25°C		12	160	mV
	I_O = 250 mA to 750 mA			4	80	
Output resistance	f = 1 kHz	0°C to 125°C		0.016		Ω
Temperature coefficient of output voltage	I_O = 5 mA	0°C to 125°C		–0.8		mV/°C
Output noise voltage	f = 10 Hz to 100 kHz	25°C		52		μV
Dropout voltage	I_O = 1 A	25°C		2		V
Bias current		25°C		4.3	8	mA
Bias current change	V_I = 10.5 V to 25 V	0°C to 125°C			1	mA
	I_O = 5 mA to 1 A				0.5	
Short-circuit output current		25°C		450		mA
Peak output current		25°C		2.2		A

† Pulse-testing techniques maintain the junction temperature as close to the ambient temperature as possible. Thermal effects must be taken into account separately. All characteristics are measured with a 0.33-μF capacitor across the input and a 0.1-μF capacitor across the output.

electrical characteristics at specified virtual junction temperature, V_I = 17 V, I_O = 500 mA (unless otherwise noted)

PARAMETER	TEST CONDITIONS	T_J†	μA7810C			UNIT
			MIN	TYP	MAX	
Output voltage	I_O = 5 mA to 1 A, V_I = 12.5 V to 25 V, $P_D \le 15$ W	25°C	9.6	10	10.4	V
		0°C to 125°C	9.5	10	10.5	
Input voltage regulation	V_I = 12.5 V to 28 V	25°C		7	200	mV
	V_I = 14 V to 20 V			2	100	
Ripple rejection	V_I = 13 V to 23 V, f = 120 Hz	0°C to 125°C	55	71		dB
Output voltage regulation	I_O = 5 mA to 1.5 A	25°C		12	200	mV
	I_O = 250 mA to 750 mA			4	100	
Output resistance	f = 1 kHz	0°C to 125°C		0.018		Ω
Temperature coefficient of output voltage	I_O = 5 mA	0°C to 125°C		–1		mV/°C
Output noise voltage	f = 10 Hz to 100 kHz	25°C		70		μV
Dropout voltage	I_O = 1 A	25°C		2		V
Bias current		25°C		4.3	8	mA
Bias current change	V_I = 12.5 V to 28 V	0°C to 125°C			1	mA
	I_O = 5 mA to 1 A				0.5	
Short-circuit output current		25°C		400		mA
Peak output current		25°C		2.2		A

† Pulse-testing techniques maintain the junction temperature as close to the ambient temperature as possible. Thermal effects must be taken into account separately. All characteristics are measured with a 0.33-μF capacitor across the input and a 0.1-μF capacitor across the output.

electrical characteristics at specified virtual junction temperature, V_I = 19 V, I_O = 500 mA (unless otherwise noted)

PARAMETER	TEST CONDITIONS	T_J†	μA7812C			UNIT
			MIN	TYP	MAX	
Output voltage	I_O = 5 mA to 1 A, V_I = 14.5 V to 27 V, $P_D \le 15$ W	25°C	11.5	12	12.5	V
		0°C to 125°C	11.4		12.6	
Input voltage regulation	V_I = 14.5 V to 30 V	25°C		10	240	mV
	V_I = 16 V to 22 V			3	120	
Ripple rejection	V_I = 15 V to 25 V, f = 120 Hz	0°C to 125°C	55	71		dB
Output voltage regulation	I_O = 5 mA to 1.5 A	25°C		12	240	mV
	I_O = 250 mA to 750 mA			4	120	
Output resistance	f = 1 kHz	0°C to 125°C		0.018		Ω
Temperature coefficient of output voltage	I_O = 5 mA	0°C to 125°C		–1		mV/°C
Output noise voltage	f = 10 Hz to 100 kHz	25°C		75		μV
Dropout voltage	I_O = 1 A	25°C		2		V
Bias current		25°C		4.3	8	mA
Bias current change	V_I = 14.5 V to 30 V	0°C to 125°C			1	mA
	I_O = 5 mA to 1 A				0.5	
Short-circuit output current		25°C		350		mA
Peak output current		25°C		2.2		A

† Pulse-testing techniques maintain the junction temperature as close to the ambient temperature as possible. Thermal effects must be taken into account separately. All characteristics are measured with a 0.33-μF capacitor across the input and a 0.1-μF capacitor across the output.

electrical characteristics at specified virtual junction temperature, V_I = 23 V, I_O = 500 mA (unless otherwise noted)

PARAMETER	TEST CONDITIONS	T_J†	μA7815C			UNIT
			MIN	TYP	MAX	
Output voltage	I_O = 5 mA to 1 A, V_I = 17.5 V to 30 V, $P_D \le 15$ W	25°C	14.4	15	15.6	V
		0°C to 125°C	14.25		15.75	
Input voltage regulation	V_I = 17.5 V to 30 V	25°C		11	300	mV
	V_I = 20 V to 26 V			3	150	
Ripple rejection	V_I = 18.5 V to 28.5 V, f = 120 Hz	0°C to 125°C	54	70		dB
Output voltage regulation	I_O = 5 mA to 1.5 A	25°C		12	300	mV
	I_O = 250 mA to 750 mA			4	150	
Output resistance	f = 1 kHz	0°C to 125°C		0.019		Ω
Temperature coefficient of output voltage	I_O = 5 mA	0°C to 125°C		–1		mV/°C
Output noise voltage	f = 10 Hz to 100 kHz	25°C		90		μV
Dropout voltage	I_O = 1 A	25°C		2		V
Bias current		25°C		4.4	8	mA
Bias current change	V_I = 17.5 V to 30 V	0°C to 125°C			1	mA
	I_O = 5 mA to 1 A				0.5	
Short-circuit output current		25°C		230		mA
Peak output current		25°C		2.1		A

† Pulse-testing techniques maintain the junction temperature as close to the ambient temperature as possible. Thermal effects must be taken into account separately. All characteristics are measured with a 0.33-μF capacitor across the input and a 0.1-μF capacitor across the output.

electrical characteristics at specified virtual junction temperature, V_I = 33 V, I_O = 500 mA (unless otherwise noted)

PARAMETER	TEST CONDITIONS	T_J†	μA7824C			UNIT
			MIN	TYP	MAX	
Output voltage	I_O = 5 mA to 1 A, V_I = 27 V to 38 V, $P_D \le 15$ W	25°C	23	24	25	V
		0°C to 125°C	22.8		25.2	
Input voltage regulation	V_I = 27 V to 38 V	25°C		18	480	mV
	V_I = 30 V to 36 V			6	240	
Ripple rejection	V_I = 28 V to 38 V, f = 120 Hz	0°C to 125°C	50	66		dB
Output voltage regulation	I_O = 5 mA to 1.5 A	25°C		12	480	mV
	I_O = 250 mA to 750 mA			4	240	
Output resistance	f = 1 kHz	0°C to 125°C		0.028		Ω
Temperature coefficient of output voltage	I_O = 5 mA	0°C to 125°C		–1.5		mV/°C
Output noise voltage	f = 10 Hz to 100 kHz	25°C		170		μV
Dropout voltage	I_O = 1 A	25°C		2		V
Bias current		25°C		4.6	8	mA
Bias current change	V_I = 27 V to 38 V	0°C to 125°C			1	mA
	I_O = 5 mA to 1 A				0.5	
Short-circuit output current		25°C		150		mA
Peak output current		25°C		2.1		A

† Pulse-testing techniques maintain the junction temperature as close to the ambient temperature as possible. Thermal effects must be taken into account separately. All characteristics are measured with a 0.33-μF capacitor across the input and a 0.1-μF capacitor across the output.

APPLICATION INFORMATION

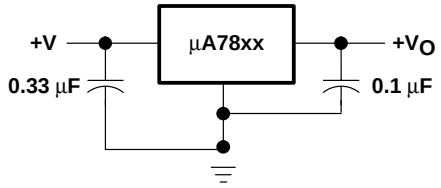

Figure 1. Fixed-Output Regulator

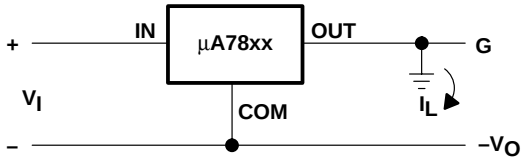

Figure 2. Positive Regulator in Negative Configuration (V_I Must Float)

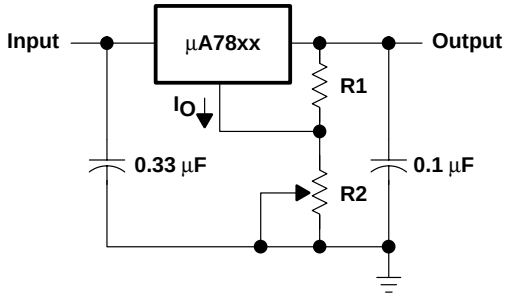

NOTE A: The following formula is used when V_{XX} is the nominal output voltage (output to common) of the fixed regulator:

$$V_O = V_{xx} + \left(\frac{V_{xx}}{R1} + I_Q\right)R2$$

Figure 3. Adjustable-Output Regulator

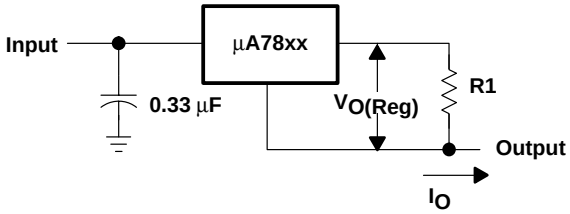

$I_O = (V_O/R1) + I_O$ Bias Current

Figure 4. Current Regulator

APPLICATION INFORMATION

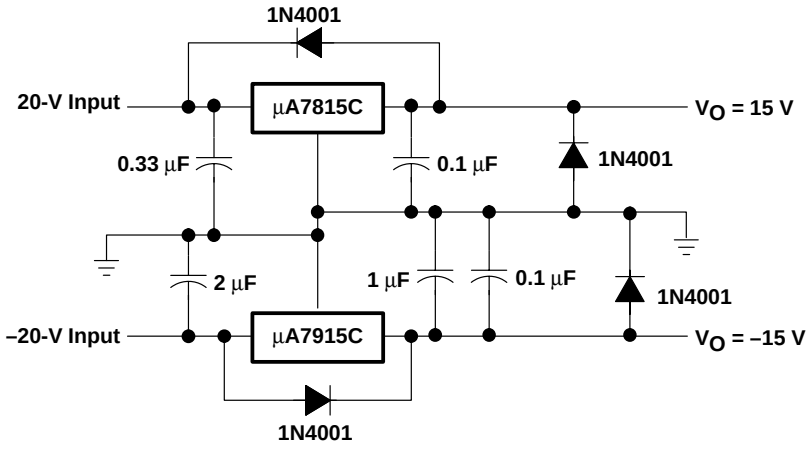

Figure 5. Regulated Dual Supply

operation with a load common to a voltage of opposite polarity

In many cases, a regulator powers a load that is not connected to ground but, instead, is connected to a voltage source of opposite polarity (e.g., operational amplifiers, level-shifting circuits, etc.). In these cases, a clamp diode should be connected to the regulator output as shown in Figure 6. This protects the regulator from output polarity reversals during startup and short-circuit operation.

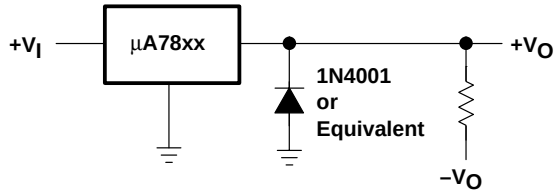

Figure 6. Output Polarity-Reversal-Protection Circuit

reverse-bias protection

Occasionally, the input voltage to the regulator can collapse faster than the output voltage. This can occur, for example, when the input supply is crowbarred during an output overvoltage condition. If the output voltage is greater than approximately 7 V, the emitter-base junction of the series-pass element (internal or external) could break down and be damaged. To prevent this, a diode shunt can be used as shown in Figure 7.

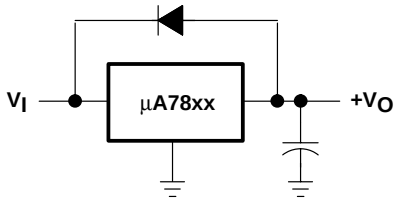

Figure 7. Reverse-Bias-Protection Circuit

MPFM001E – OCTOBER 1994 – REVISED JANUARY 2001

KTE (R-PSFM-G3) **PowerFLEX™ PLASTIC FLANGE-MOUNT**

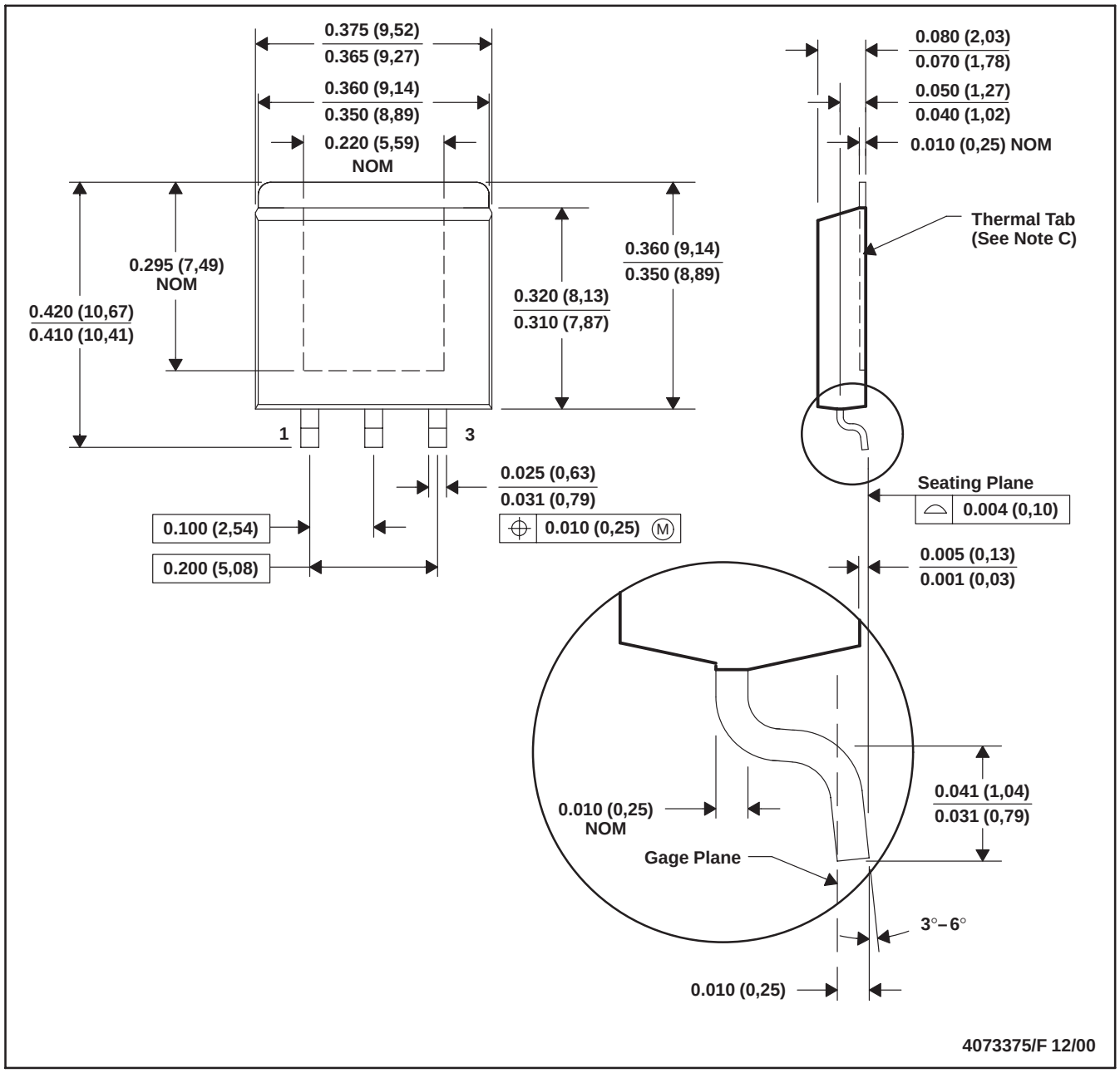

NOTES: A. All linear dimensions are in inches (millimeters).
B. This drawing is subject to change without notice.
C. The center lead is in electrical contact with the thermal tab.
D. Dimensions do not include mold protrusions, not to exceed 0.006 (0,15).
E. Falls within JEDEC MO-169

PowerFLEX is a trademark of Texas Instruments.

KCS (R–PSFM–T3) PLASTIC FLANGE–MOUNT PACKAGE

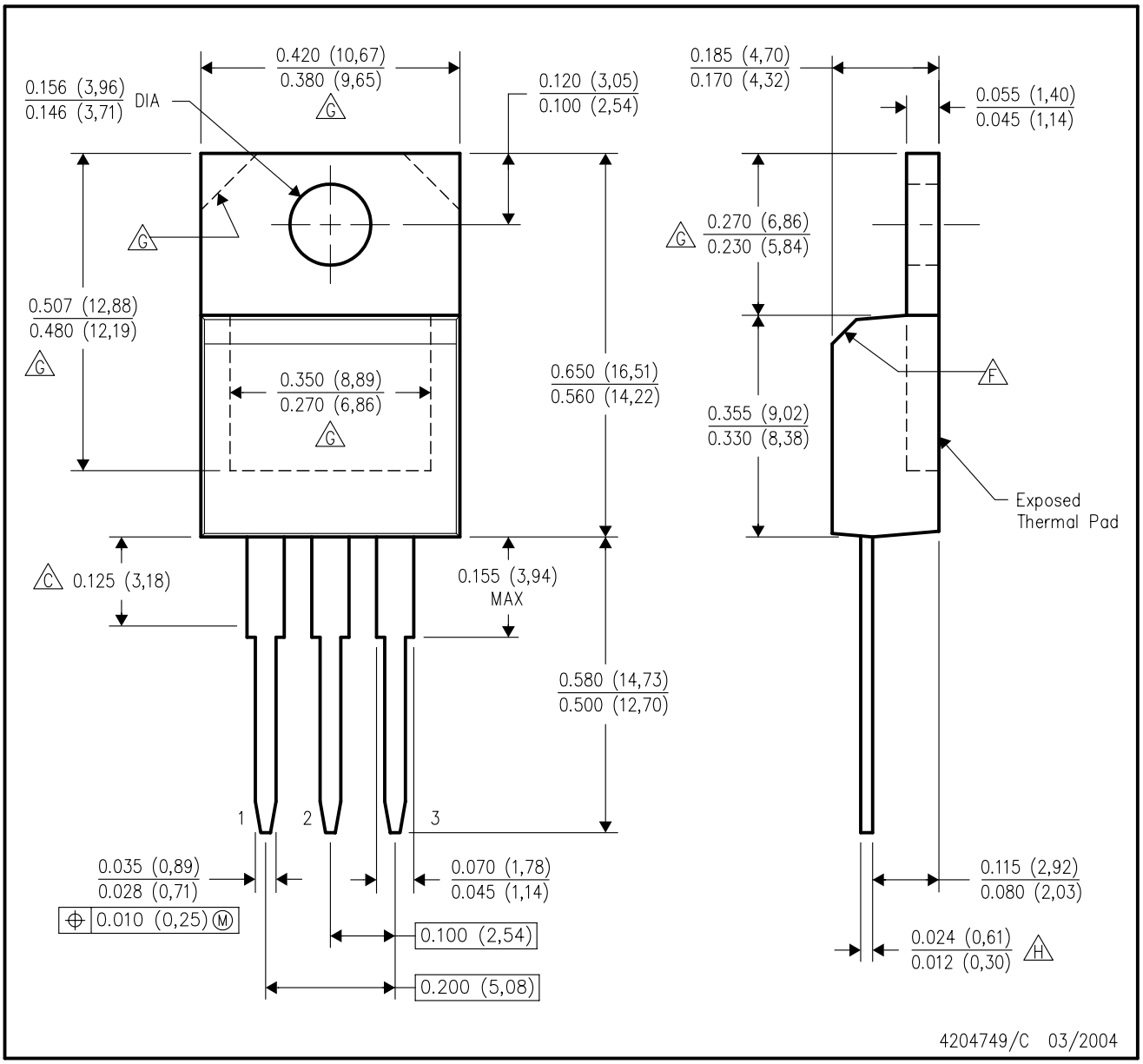

NOTES:
A. All linear dimensions are in inches (millimeters).
B. This drawing is subject to change without notice.
C. Lead dimensions are not controlled within this area.
D. All lead dimensions apply before solder dip.
E. The center lead is in electrical contact with the mounting tab.
F. The chamfer is optional.
G. Thermal pad contour optional within these dimensions.
H. Falls within JEDEC TO–220 variation AB, except minimum lead thickness.

KC (R–PSFM–T3) PLASTIC FLANGE–MOUNT PACKAGE

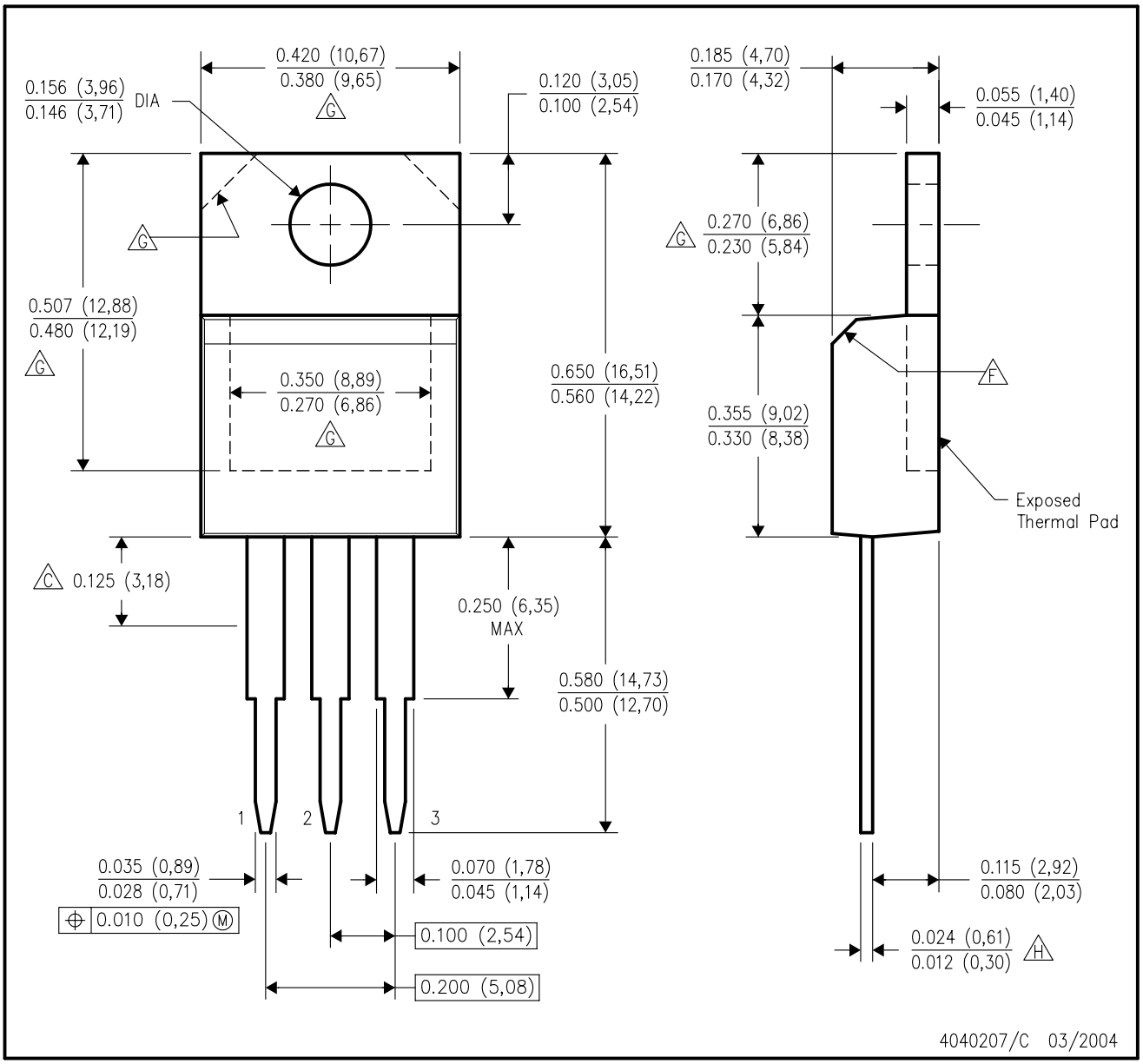

NOTES:
- A. All linear dimensions are in inches (millimeters).
- B. This drawing is subject to change without notice.
- C. Lead dimensions are not controlled within this area.
- D. All lead dimensions apply before solder dip.
- E. The center lead is in electrical contact with the mounting tab.
- F. The chamfer is optional.
- G. Thermal pad contour optional within these dimensions.
- H. Falls within JEDEC TO–220 variation AB, except minimum lead thickness.

IMPORTANT NOTICE

Texas Instruments Incorporated and its subsidiaries (TI) reserve the right to make corrections, modifications, enhancements, improvements, and other changes to its products and services at any time and to discontinue any product or service without notice. Customers should obtain the latest relevant information before placing orders and should verify that such information is current and complete. All products are sold subject to TI's terms and conditions of sale supplied at the time of order acknowledgment.

TI warrants performance of its hardware products to the specifications applicable at the time of sale in accordance with TI's standard warranty. Testing and other quality control techniques are used to the extent TI deems necessary to support this warranty. Except where mandated by government requirements, testing of all parameters of each product is not necessarily performed.

TI assumes no liability for applications assistance or customer product design. Customers are responsible for their products and applications using TI components. To minimize the risks associated with customer products and applications, customers should provide adequate design and operating safeguards.

TI does not warrant or represent that any license, either express or implied, is granted under any TI patent right, copyright, mask work right, or other TI intellectual property right relating to any combination, machine, or process in which TI products or services are used. Information published by TI regarding third-party products or services does not constitute a license from TI to use such products or services or a warranty or endorsement thereof. Use of such information may require a license from a third party under the patents or other intellectual property of the third party, or a license from TI under the patents or other intellectual property of TI.

Reproduction of information in TI data books or data sheets is permissible only if reproduction is without alteration and is accompanied by all associated warranties, conditions, limitations, and notices. Reproduction of this information with alteration is an unfair and deceptive business practice. TI is not responsible or liable for such altered documentation.

Resale of TI products or services with statements different from or beyond the parameters stated by TI for that product or service voids all express and any implied warranties for the associated TI product or service and is an unfair and deceptive business practice. TI is not responsible or liable for any such statements.

Following are URLs where you can obtain information on other Texas Instruments products and application solutions:

Products		**Applications**	
Amplifiers	amplifier.ti.com	Audio	www.ti.com/audio
Data Converters	dataconverter.ti.com	Automotive	www.ti.com/automotive
DSP	dsp.ti.com	Broadband	www.ti.com/broadband
Interface	interface.ti.com	Digital Control	www.ti.com/digitalcontrol
Logic	logic.ti.com	Military	www.ti.com/military
Power Mgmt	power.ti.com	Optical Networking	www.ti.com/opticalnetwork
Microcontrollers	microcontroller.ti.com	Security	www.ti.com/security
		Telephony	www.ti.com/telephony
		Video & Imaging	www.ti.com/video
		Wireless	www.ti.com/wireless

Mailing Address: Texas Instruments
Post Office Box 655303 Dallas, Texas 75265

National Semiconductor

November 1994

LM79XX Series 3-Terminal Negative Regulators

General Description

The LM79XX series of 3-terminal regulators is available with fixed output voltages of −5V, −8V, −12V, and −15V. These devices need only one external component—a compensation capacitor at the output. The LM79XX series is packaged in the TO-220 power package and is capable of supplying 1.5A of output current.

These regulators employ internal current limiting safe area protection and thermal shutdown for protection against virtually all overload conditions.

Low ground pin current of the LM79XX series allows output voltage to be easily boosted above the preset value with a resistor divider. The low quiescent current drain of these devices with a specified maximum change with line and load ensures good regulation in the voltage boosted mode.

For applications requiring other voltages, see LM137 data sheet.

Features

- Thermal, short circuit and safe area protection
- High ripple rejection
- 1.5A output current
- 4% tolerance on preset output voltage

Connection Diagrams

TO-220 Package

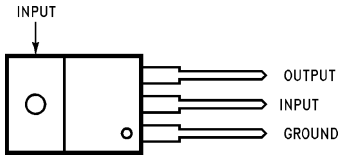

TL/H/7340–14

Front View

Order Number LM7905CT, LM7912CT or LM7915CT
See NS Package Number TO3B

Typical Applications

Fixed Regulator

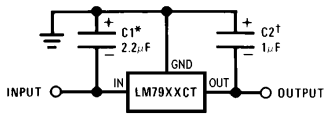

TL/H/7340–3

*Required if regulator is separated from filter capacitor by more than 3″. For value given, capacitor must be solid tantalum. 25 μF aluminum electrolytic may be substituted.

†Required for stability. For value given, capacitor must be solid tantalum. 25 μF aluminum electrolytic may be substituted. Values given may be increased without limit.

For output capacitance in excess of 100 μF, a high current diode from input to output (1N4001, etc.) will protect the regulator from momentary input shorts.

RRD-B30M115/Printed in U. S. A.

Absolute Maximum Ratings (Note 1)

If Military/Aerospace specified devices are required, please contact the National Semiconductor Sales Office/Distributors for availability and specifications.

Input Voltage	
(V_o = −5V)	−25V
(V_o = −12V and −15V)	−35V
Input-Output Differential	
(V_o = −5V)	25V
(V_o = −12V and −15V)	30V
Power Dissipation (Note 2)	Internally Limited
Operating Junction Temperature Range	0°C to +125°C
Storage Temperature Range	−65°C to +150°C
Lead Temperature (Soldering, 10 sec.)	230°C

Electrical Characteristics

Conditions unless otherwise noted: I_{OUT} = 500 mA, C_{IN} = 2.2 μF, C_{OUT} = 1 μF, 0°C ≤ T_J ≤ +125°C, Power Dissipation ≤ 1.5W.

Part Number			LM7905C			Units
Output Voltage			−5V			
Input Voltage (unless otherwise specified)			−10V			
Symbol	**Parameter**	**Conditions**	**Min**	**Typ**	**Max**	
V_O	Output Voltage	T_J = 25°C	−4.8	−5.0	−5.2	V
		5 mA ≤ I_{OUT} ≤ 1A, P ≤ 15W	−4.75		−5.25	V
				(−20 ≤ V_{IN} ≤ −7)		V
ΔV_O	Line Regulation	T_J = 25°C, (Note 3)		8	50	mV
				(−25 ≤ V_{IN} ≤ −7)		V
				2	15	mV
				(−12 ≤ V_{IN} ≤ −8)		V
ΔV_O	Load Regulation	T_J = 25°C, (Note 3)				
		5 mA ≤ I_{OUT} ≤ 1.5A		15	100	mV
		250 mA ≤ I_{OUT} ≤ 750 mA		5	50	mV
I_Q	Quiescent Current	T_J = 25°C		1	2	mA
ΔI_Q	Quiescent Current Change	With Line			0.5	mA
				(−25 ≤ V_{IN} ≤ −7)		V
		With Load, 5 mA ≤ I_{OUT} ≤ 1A			0.5	mA
V_n	Output Noise Voltage	T_A = 25°C, 10 Hz ≤ f ≤ 100 Hz		125		μV
	Ripple Rejection	f = 120 Hz	54	66		dB
				(−18 ≤ V_{IN} ≤ −8)		V
	Dropout Voltage	T_J = 25°C, I_{OUT} = 1A		1.1		V
I_{OMAX}	Peak Output Current	T_J = 25°C		2.2		A
	Average Temperature Coefficient of Output Voltage	I_{OUT} = 5 mA, 0 C ≤ T_J ≤ 100°C		0.4		mV/°C

Typical Applications (Continued)

Variable Output

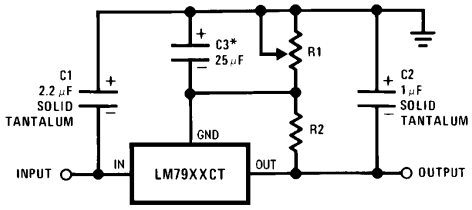

TL/H/7340–2

*Improves transient response and ripple rejection. Do not increase beyond 50 μF.

$$V_{OUT} = V_{SET}\left(\frac{R1 + R2}{R2}\right)$$

Select R2 as follows:

LM7905CT	300Ω
LM7912CT	750Ω
LM7915CT	1k

Electrical Characteristics (Continued) Conditions unless otherwise noted: I_{OUT} = 500 mA, C_{IN} = 2.2 µF, C_{OUT} = 1 µF, 0°C ≤ T_J ≤ +125°C, Power Dissipation = 1.5W.

Part Number			LM7912C			LM7915C			Units
Output Voltage			−12V			−15V			
Input Voltage (unless otherwise specified)			−19V			−23V			
Symbol	Parameter	Conditions	Min	Typ	Max	Min	Typ	Max	
V_O	Output Voltage	T_J = 25°C	−11.5	−12.0	−12.5	−14.4	−15.0	−15.6	V
		5 mA ≤ I_{OUT} ≤ 1A, P ≤ 15W	−11.4		−12.6	−14.25		−15.75	V
			(−27 ≤ V_{IN} ≤ −14.5)			(−30 ≤ V_{IN} ≤ −17.5)			V
ΔV_O	Line Regulation	T_J = 25°C, (Note 3)		5	80		5	100	mV
			(−30 ≤ V_{IN} ≤ −14.5)			(−30 ≤ V_{IN} ≤ −17.5)			V
				3	30		3	50	mV
			(−22 ≤ V_{IN} ≤ −16)			(−26 ≤ V_{IN} ≤ −20)			V
ΔV_O	Load Regulation	T_J = 25°C, (Note 3)							
		5 mA ≤ I_{OUT} ≤ 1.5A		15	200		15	200	mV
		250 mA ≤ I_{OUT} ≤ 750 mA		5	75		5	75	mV
I_Q	Quiescent Current	T_J = 25°C		1.5	3		1.5	3	mA
ΔI_Q	Quiescent Current Change	With Line			0.5			0.5	mA
			(−30 ≤ V_{IN} ≤ −14.5)			(−30 ≤ V_{IN} ≤ −17.5)			V
		With Load, 5 mA ≤ I_{OUT} ≤ 1A			0.5			0.5	mA
V_n	Output Noise Voltage	T_A = 25°C, 10 Hz ≤ f ≤ 100 Hz		300			375		µV
	Ripple Rejection	f = 120 Hz	54	70		54	70		dB
			(−25 ≤ V_{IN} ≤ −15)			(−30 ≤ V_{IN} ≤ −17.5)			V
	Dropout Voltage	T_J = 25°C, I_{OUT} = 1A		1.1			1.1		V
I_{OMAX}	Peak Output Current	T_J = 25°C		2.2			2.2		A
	Average Temperature Coefficient of Output Voltage	I_{OUT} = 5 mA, 0 C ≤ T_J ≤ 100°C		−0.8			−1.0		mV/°C

Note 1: Absolute Maximum Ratings indicate limits beyond which damage to the device may occur. Operating Ratings indicate conditions for which the device is intended to be functional, but do not guarantee Specific Performance limits. For guaranteed specifications and test conditions, see the Electrical Characteristics.

Note 2: Refer to Typical Performance Characteristics and Design Considerations for details.

Note 3: Regulation is measured at a constant junction temperature by pulse testing with a low duty cycle. Changes in output voltage due to heating effects must be taken into account.

Typical Applications (Continued)

Dual Trimmed Supply

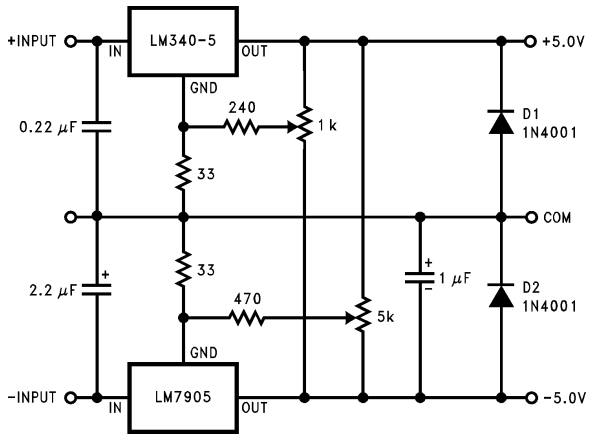

TL/H/7340–4

Design Considerations

The LM79XX fixed voltage regulator series has thermal overload protection from excessive power dissipation, internal short circuit protection which limits the circuit's maximum current, and output transistor safe-area compensation for reducing the output current as the voltage across the pass transistor is increased.

Although the internal power dissipation is limited, the junction temperature must be kept below the maximum specified temperature (125°C) in order to meet data sheet specifications. To calculate the maximum junction temperature or heat sink required, the following thermal resistance values should be used:

Package	Typ θ_{JC} °C/W	Max θ_{JC} °C/W	Typ θ_{JA} °C/W	Max θ_{JA} °C/W
TO-220	3.0	5.0	60	40

$$P_{D\,MAX} = \frac{T_{J\,Max} - T_A}{\theta_{JC} + \theta_{CA}} \text{ or } \frac{T_{J\,Max}\,T_A}{\theta_{JA}}$$

$\theta_{CA} = \theta_{CS} + \theta_{SA}$ (without heat sink)

Solving for T_J:

$T_J = T_A + P_D(\theta_{JC} + \theta_{CA})$ or

$= T_A + P_D\theta_{JA}$ (without heat sink)

Where:

T_J = Junction Temperature

T_A = Ambient Temperature

P_D = Power Dissipation

θ_{JA} = Junction-to-Ambient Thermal Resistance

θ_{JC} = Junction-to-Case Thermal Resistance

θ_{CA} = Case-to-Ambient Thermal Resistance

θ_{CS} = Case-to-Heat Sink Thermal Resistance

θ_{SA} = Heat Sink-to-Ambient Thermal Resistance

Typical Applications (Continued)

Bypass capacitors are necessary for stable operation of the LM79XX series of regulators over the input voltage and output current ranges. Output bypass capacitors will improve the transient response by the regulator.

The bypass capacitors, (2.2 μF on the input, 1.0 μF on the output) should be ceramic or solid tantalum which have good high frequency characteristics. If aluminum electrolytics are used, their values should be 10 μF or larger. The bypass capacitors should be mounted with the shortest leads, and if possible, directly across the regulator terminals.

High Stability 1 Amp Regulator

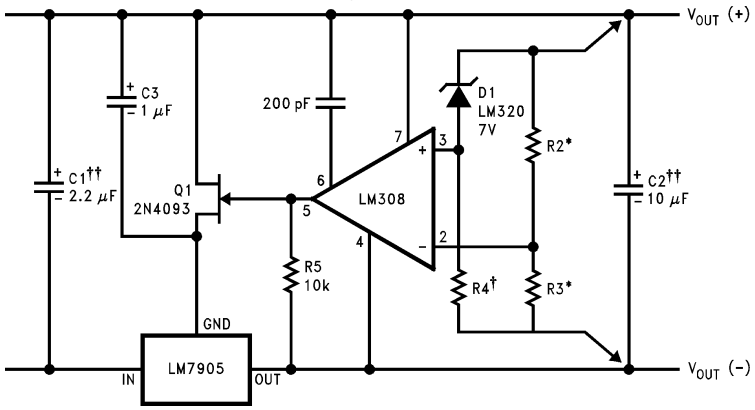

TL/H/7340–5

Load and line regulation < 0.01% temperature stability ≤ 0.2%

†Determine Zener current

††Solid tantalum

*Select resistors to set output voltage. 2 ppm/°C tracking suggested

Typical Applications (Continued)

Current Source

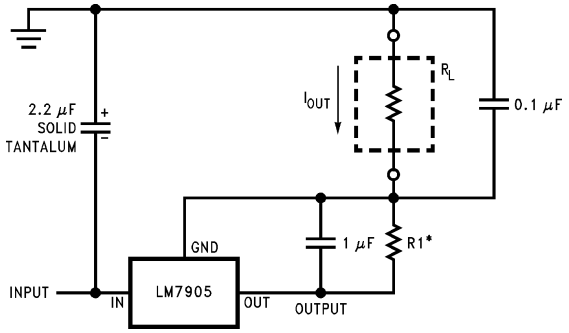

*$I_{OUT} = 1\ mA + \frac{5V}{R1}$

TL/H/7340–7

Light Controller Using Silicon Photo Cell

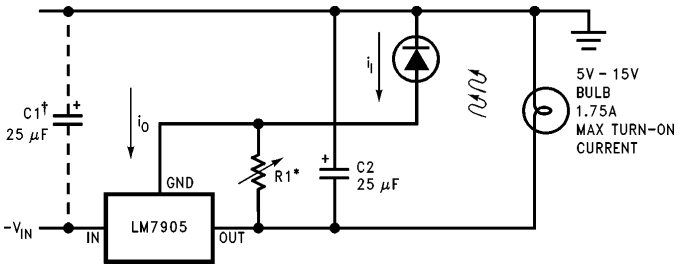

TL/H/7340–8

*Lamp brightness increase until $i_I = i_O$ ($\approx$ 1 mA) + 5V/R1.

†Necessary only if raw supply filter capacitor is more than 2″ from LM7905CT

Typical Applications (Continued)

High-Sensitivity Light Controller

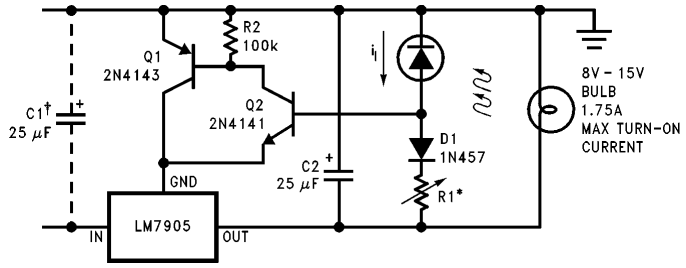

TL/H/7340–9

*Lamp brightness increases until i_I = 5V/R1 (I_I can be set as low as 1 μA)

†Necessary only if raw supply filter capacitor is more than 2″ from LM7905

±15V, 1 Amp Tracking Regulators

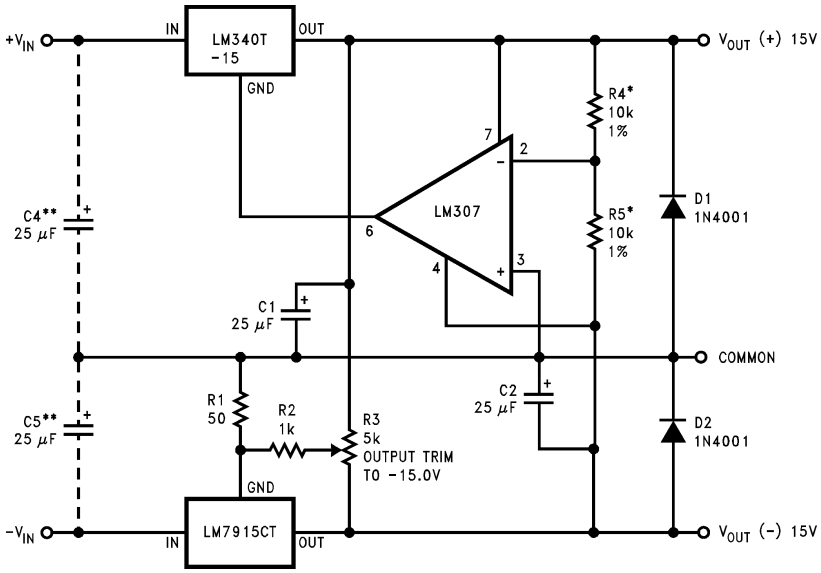

TL/H/7340–1

	(−15)	(+15)
Load Regulation at ΔI_L = 1A	40 mV	2 mV
Output Ripple, C_{IN} = 3000 μF, I_L = 1A	100 μVrms	100 μVrms
Temperature Stability	50 mV	50 mV
Output Noise 10 Hz ≤ f ≤ 10 kHz	150 μVrms	150 μVrms

*Resistor tolerance of R4 and R5 determine matching of (+) and (−) outputs.

**Necessary only if raw supply filter capacitors are more than 3″ from regulators.

Schematic Diagrams

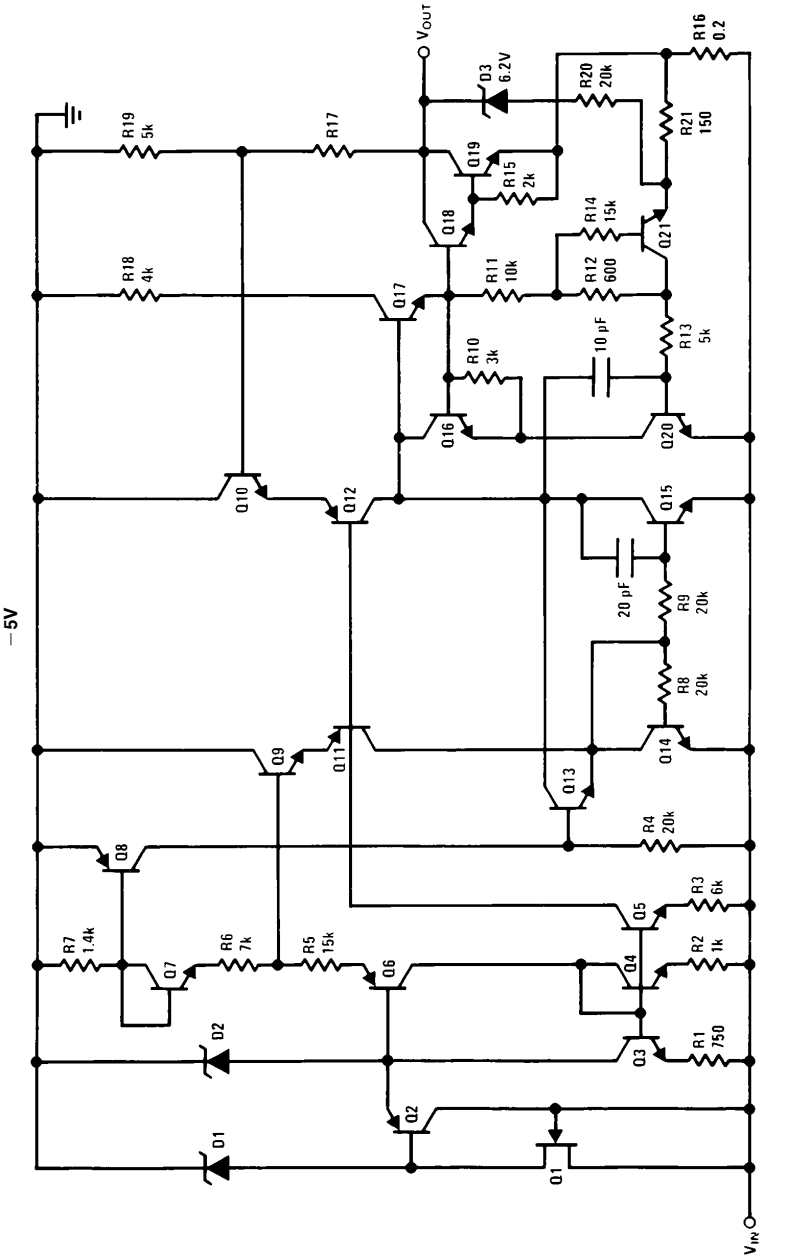

Schematic Diagrams (Continued)

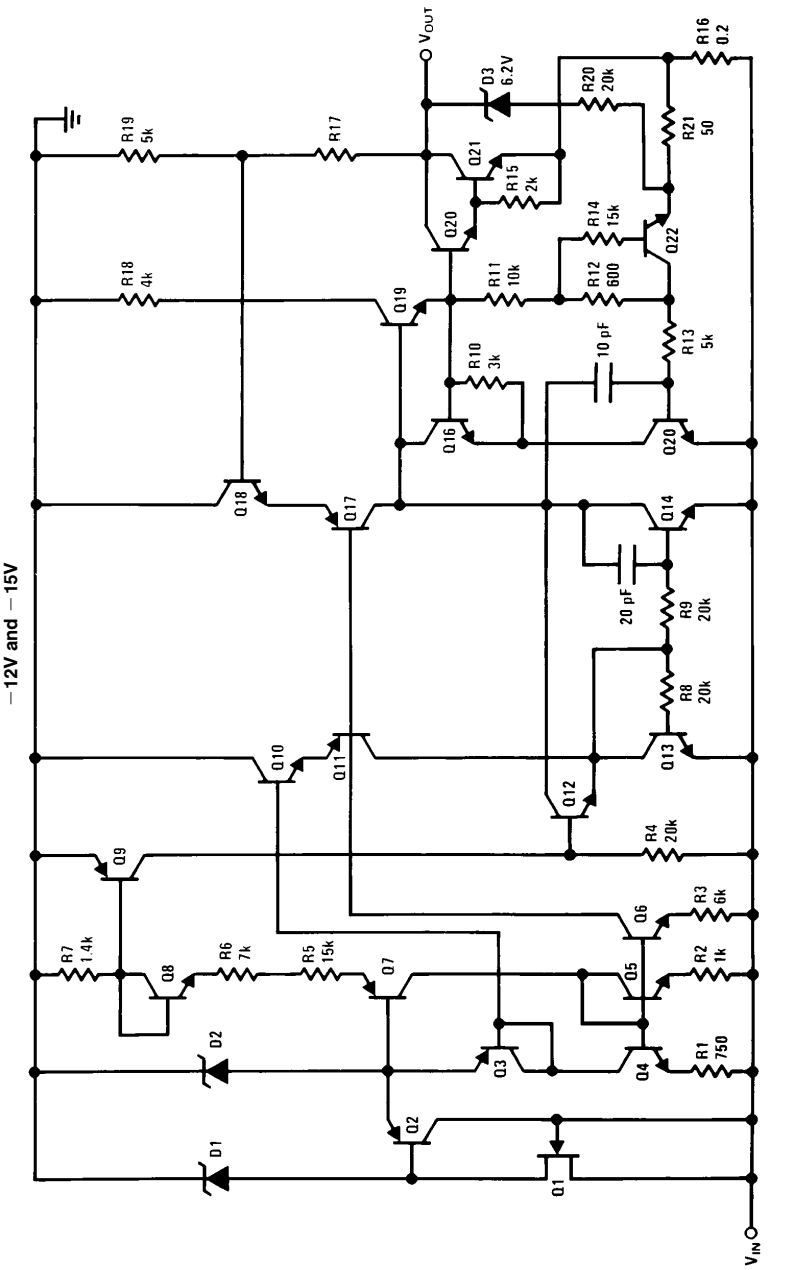

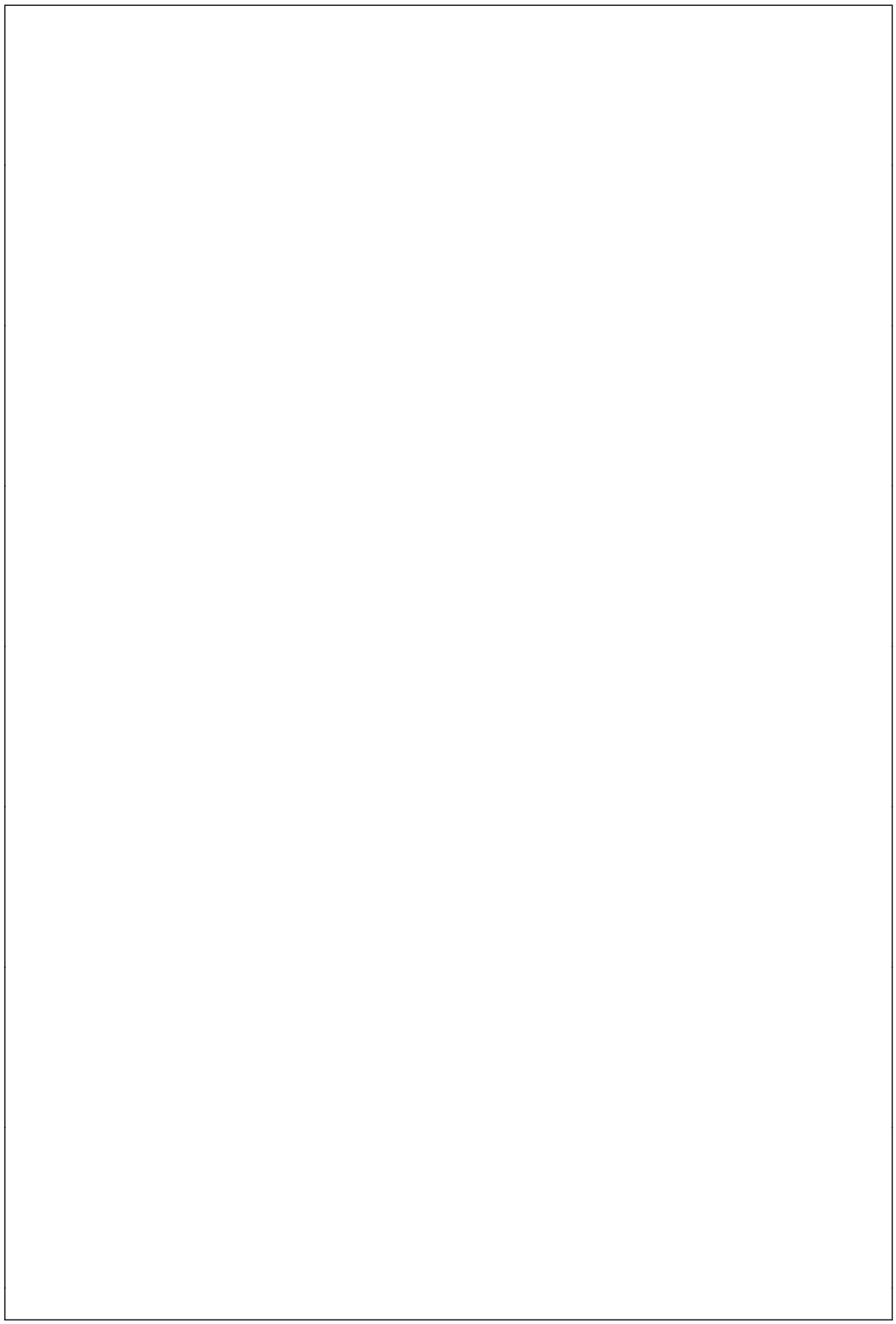

Physical Dimensions inches (millimeters)

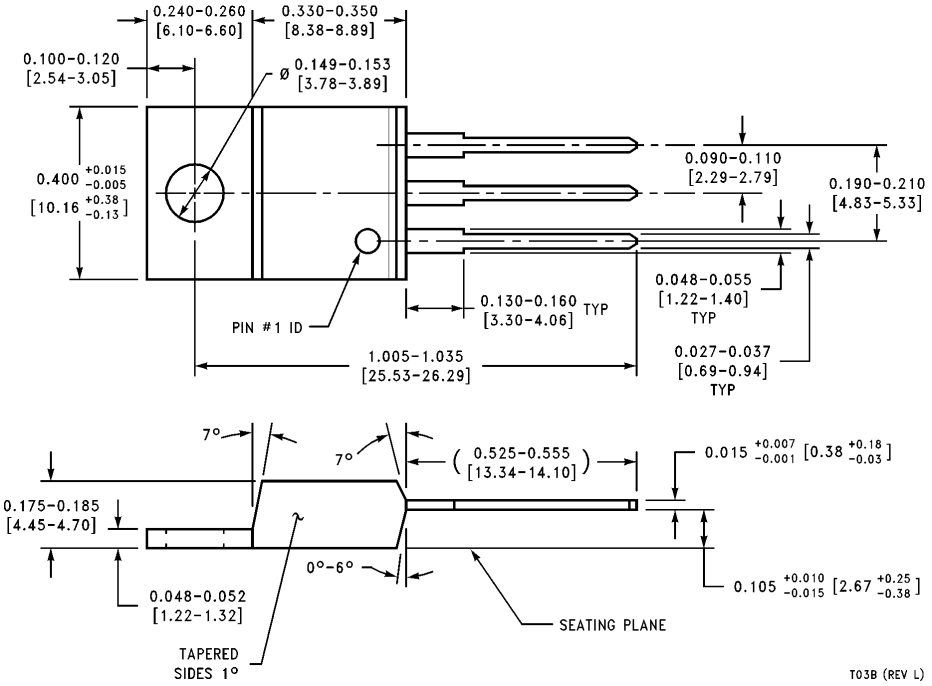

TO-220 Outline Package (T)
Order Number LM7905CT, LM7912CT or LM7915CT
NS Package Number T03B

LIFE SUPPORT POLICY

NATIONAL'S PRODUCTS ARE NOT AUTHORIZED FOR USE AS CRITICAL COMPONENTS IN LIFE SUPPORT DEVICES OR SYSTEMS WITHOUT THE EXPRESS WRITTEN APPROVAL OF THE PRESIDENT OF NATIONAL SEMICONDUCTOR CORPORATION. As used herein:

1. Life support devices or systems are devices or systems which, (a) are intended for surgical implant into the body, or (b) support or sustain life, and whose failure to perform, when properly used in accordance with instructions for use provided in the labeling, can be reasonably expected to result in a significant injury to the user.
2. A critical component is any component of a life support device or system whose failure to perform can be reasonably expected to cause the failure of the life support device or system, or to affect its safety or effectiveness.

National Semiconductor Corporation
1111 West Bardin Road
Arlington, TX 76017
Tel: 1(800) 272-9959
Fax: 1(800) 737-7018

National Semiconductor Europe
Fax: (+49) 0-180-530 85 86
Email: cnjwge@tevm2.nsc.com
Deutsch Tel: (+49) 0-180-530 85 85
English Tel: (+49) 0-180-532 78 32
Français Tel: (+49) 0-180-532 93 58
Italiano Tel: (+49) 0-180-534 16 80

National Semiconductor Hong Kong Ltd.
13th Floor, Straight Block,
Ocean Centre, 5 Canton Rd.
Tsimshatsui, Kowloon
Hong Kong
Tel: (852) 2737-1600
Fax: (852) 2736-9960

National Semiconductor Japan Ltd.
Tel: 81-043-299-2309
Fax: 81-043-299-2408

Single Supply, Rail-to-Rail Low Power FET-Input Op Amp

AD822

FEATURES

TRUE SINGLE SUPPLY OPERATION
- Output Swings Rail to Rail
- Input Voltage Range Extends Below Ground
- Single Supply Capability from +3 V to +36 V
- Dual Supply Capability from ±1.5 V to ±18 V

HIGH LOAD DRIVE
- Capacitive Load Drive of 350 pF, G = 1
- Minimum Output Current of 15 mA

EXCELLENT AC PERFORMANCE FOR LOW POWER
- 800 μA Max Quiescent Current per Amplifier
- Unity Gain Bandwidth: 1.8 MHz
- Slew Rate of 3.0 V/μs

GOOD DC PERFORMANCE
- 800 μV Max Input Offset Voltage
- 2 μV/°C Typ Offset Voltage Drift
- 25 pA Max Input Bias Current

LOW NOISE
- 13 nV/$\sqrt{Hz}$ @ 10 kHz

NO PHASE INVERSION

APPLICATIONS

Battery Powered Precision Instrumentation
Photodiode Preamps
Active Filters
12- to 14-Bit Data Acquisition Systems
Medical Instrumentation
Low Power References and Regulators

CONNECTION DIAGRAM
8-Pin Plastic DIP, Cerdip and SOIC

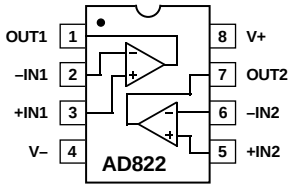

PRODUCT DESCRIPTION

The AD822 is a dual precision, low power FET input op amp that can operate from a single supply of +3.0 V to 36 V, or dual supplies of ±1.5 V to ±18 V. It has true single supply capability with an input voltage range extending below the negative rail, allowing the AD822 to accommodate input signals below ground in the single supply mode. Output voltage swing extends to within 10 mV of each rail providing the maximum output dynamic range.

Offset voltage of 800 μV max, offset voltage drift of 2 μV/°C, input bias currents below 25 pA and low input voltage noise provide dc precision with source impedances up to a Gigaohm. 1.8 MHz unity gain bandwidth, –93 dB THD at 10 kHz and 3 V/μs slew rate are provided with a low supply current of 800 μA per amplifier. The AD822 drives up to 350 pF of direct capacitive load as a follower, and provides a minimum output current of 15 mA. This allows the amplifier to handle a wide range of load conditions. This combination of ac and dc performance, plus the outstanding load drive capability, results in an exceptionally versatile amplifier for the single supply user.

The AD822 is available in four performance grades. The A and B grades are rated over the industrial temperature range of –40°C to +85°C. There is also a 3 volt grade—the AD822A-3V, rated over the industrial temperature range. The mil grade is rated over the military temperature range of –55°C to +125°C and is available processed on standard military drawing.

The AD822 is offered in three varieties of 8-pin package: plastic DIP, hermetic cerdip and surface mount (SOIC) as well as die form.

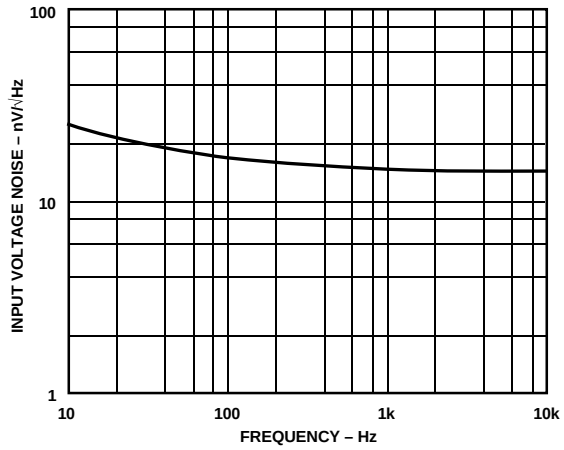

Input Voltage Noise vs. Frequency

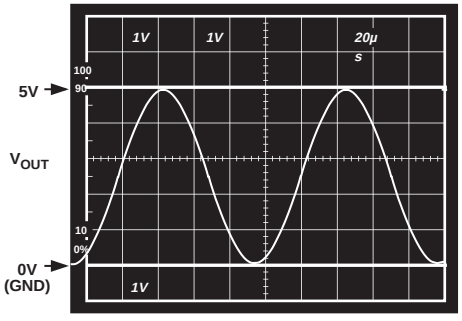

Gain of +2 Amplifier; V_S = +5, 0, V_{IN} = 2.5 V Sine Centered at 1.25 Volts, R_L = 100 kΩ

REV. A

One Technology Way, P.O. Box 9106, Norwood, MA 02062-9106, U.S.A.
Tel: 617/329-4700 **Fax: 617/326-8703**

AD822—SPECIFICATIONS (V_S = 0, 5 volts @ T_A = +25°C, V_{CM} = 0 V, V_{OUT} = 0.2 V unless otherwise noted)

Parameter	Conditions	AD822A Min	AD822A Typ	AD822A Max	AD822B Min	AD822B Typ	AD822B Max	AD822S[1] Min	AD822S[1] Typ	AD822S[1] Max	Units
DC PERFORMANCE											
Initial Offset			0.1	0.8		0.1	0.4		0.1	0.8	mV
Max Offset over Temperature			0.5	1.2		0.5	0.9		0.5		mV
Offset Drift			2			2			2		µV/°C
Input Bias Current	V_{CM} = 0 V to 4 V		2	25		2	10		2	25	pA
at T_{MAX}			0.5	5		0.5	2.5		0.5		nA
Input Offset Current			2	20		2	10		2	20	pA
at T_{MAX}			0.5			0.5			1.5		nA
Open-Loop Gain	V_O = 0.2 V to 4 V										
	R_L = 100 k	500	1000		500	1000		500	1000		V/mV
T_{MIN} to T_{MAX}		400			400						V/mV
	R_L = 10 k	80	150		80	150		80	150		V/mV
T_{MIN} to T_{MAX}		80			80						V/mV
	R_L = 1 k	15	30		15	30		15	30		V/mV
T_{MIN} to T_{MAX}		10			10						V/mV
NOISE/HARMONIC PERFORMANCE											
Input Voltage Noise											
0.1 Hz to 10 Hz			2			2			2		µV p-p
f = 10 Hz			25			25			25		nV/√Hz
f = 100 Hz			21			21			21		nV/√Hz
f = 1 kHz			16			16			16		nV/√Hz
f = 10 kHz			13			13			13		nV/√Hz
Input Current Noise											
0.1 Hz to 10 Hz			18			18			18		fA p-p
f = 1 kHz			0.8			0.8			0.8		fA/√Hz
Harmonic Distortion	R_L = 10 k to 2.5 V										
f = 10 kHz	V_O = 0.25 V to 4.75 V		–93			–93			–93		dB
DYNAMIC PERFORMANCE											
Unity Gain Frequency			1.8			1.8			1.8		MHz
Full Power Response	V_O p-p = 4.5 V		210			210			210		kHz
Slew Rate			3			3			3		V/µs
Settling Time											
to 0.1%	V_O = 0.2 V to 4.5 V		1.4			1.4			1.4		µs
to 0.01%			1.8			1.8			1.8		µs
MATCHING CHARACTERISTICS											
Initial Offset				1.0			0.5			1.6	mV
Max Offset Over Temperature				1.6			1.3				mV
Offset Drift			3			3					µV/°C
Input Bias Current				20			10			20	pA
Crosstalk @ f = 1 kHz	R_L = 5 kΩ		–130			–130			–130		dB
f = 100 kHz			–93			–93			–93		dB
INPUT CHARACTERISTICS											
Common-Mode Voltage Range[2]		–0.2		4	–0.2		4	–0.2		4	V
T_{MIN} to T_{MAX}		–0.2		4	–0.2		4				V
CMRR	V_{CM} = 0 V to +2 V	66	80		69	80		66	80		dB
T_{MIN} to T_{MAX}		66			66						dB
Input Impedance											
Differential			10^{13}‖0.5			10^{13}‖0.5			10^{13}‖0.5		Ω‖pF
Common Mode			10^{13}‖2.8			10^{13}‖2.8			10^{13}‖2.8		Ω‖pF
OUTPUT CHARACTERISTICS											
Output Saturation Voltage[3]											
V_{OL}–V_{EE}	I_{SINK} = 20 µA		5	7		5	7		5	7	mV
T_{MIN} to T_{MAX}				10			10				mV
V_{CC}–V_{OH}	I_{SOURCE} = 20 µA		10	14		10	14		10	14	mV
T_{MIN} to T_{MAX}				20			20				mV
V_{OL}–V_{EE}	I_{SINK} = 2 mA		40	55		40	55		40	55	mV
T_{MIN} to T_{MAX}				80			80				mV
V_{CC}–V_{OH}	I_{SOURCE} = 2 mA		80	110		80	110		80	110	mV
T_{MIN} to T_{MAX}				160			160				mV
V_{OL}–V_{EE}	I_{SINK} = 15 mA		300	500		300	500		300	500	mV
T_{MIN} to T_{MAX}				1000			1000				mV
V_{CC}–V_{OH}	I_{SOURCE} = 15 mA		800	1500		800	1500		800	1500	mV
T_{MIN} to T_{MAX}				1900			1900				mV
Operating Output Current		15			15			15			mA
T_{MIN} to T_{MAX}		12			12						mA
Capacitive Load Drive			350			350			350		pF
POWER SUPPLY											
Quiescent Current T_{MIN} to T_{MAX}			1.24	1.6		1.24	1.6		1.24		mA
Power Supply Rejection	V_S+ = 5 V to 15 V	70	80		66	80		70	80		dB
T_{MIN} to T_{MAX}		70			66						dB

(V_S = ±5 volts @ T_A = +25°C, V_{CM} = 0 V, V_{OUT} = 0 V unless otherwise noted)

Parameter	Conditions	AD822A Min	AD822A Typ	AD822A Max	AD822B Min	AD822B Typ	AD822B Max	AD822S[1] Min	AD822S[1] Typ	AD822S[1] Max	Units
DC PERFORMANCE											
Initial Offset			0.1	0.8		0.1	0.4		0.1		mV
Max Offset over Temperature			0.5	1.5		0.5	1		0.5		mV
Offset Drift			2			2			2		µV/°C
Input Bias Current	V_{CM} = –5 V to 4 V		2	25		2	10		2	25	pA
at T_{MAX}			0.5	5		0.5	2.5		0.5		nA
Input Offset Current			2	20		2	10		2		pA
at T_{MAX}			0.5			0.5			1.5		nA
Open-Loop Gain	V_O = –4 V to 4 V										
	R_L = 100 k	400	1000		400	1000		400	1000		V/mV
T_{MIN} to T_{MAX}		400			400						V/mV
	R_L = 10 k	80	150		80	150		80	150		V/mV
T_{MIN} to T_{MAX}		80			80						V/mV
	R_L = 1 k	20	30		20	30		20	30		V/mV
T_{MIN} to T_{MAX}		10			10						V/mV
NOISE/HARMONIC PERFORMANCE											
Input Voltage Noise											
0.1 Hz to 10 Hz			2			2			2		µV p-p
f = 10 Hz			25			25			25		nV/√Hz
f = 100 Hz			21			21			21		nV/√Hz
f = 1 kHz			16			16			16		nV/√Hz
f = 10 kHz			13			13			13		nV/√Hz
Input Current Noise											
0.1 Hz to 10 Hz			18			18			18		fA p-p
f = 1 kHz			0.8			0.8			0.8		fA/√Hz
Harmonic Distortion	R_L = 10 k										
f = 10 kHz	V_O = ±4.5 V		–93			–93			–93		dB
DYNAMIC PERFORMANCE											
Unity Gain Frequency			1.9			1.9			1.9		MHz
Full Power Response	V_O p-p = 9 V		105			105			105		kHz
Slew Rate			3			3			3		V/µs
Settling Time											
to 0.1%	V_O = 0 V to ±4.5 V		1.4			1.4			1.4		µs
to 0.01%			1.8			1.8			1.8		µs
MATCHING CHARACTERISTICS											
Initial Offset				1.0			0.5			1.6	mV
Max Offset Over Temperature				3			2			2	mV
Offset Drift			3			3					µV/°C
Input Bias Current				25			10			25	pA
Crosstalk @ f = 1 kHz	R_L = 5 kΩ		–130			–130			–130		dB
f = 100 kHz			–93			–93			–93		dB
INPUT CHARACTERISTICS											
Common-Mode Voltage Range[2]		–5.2		4	–5.2		4	–5.2		4	V
T_{MIN} to T_{MAX}		–5.2		4	–5.2		4				V
CMRR	V_{CM} = –5 V to +2 V	66	80		69	80		66	80		dB
T_{MIN} to T_{MAX}		66			66						dB
Input Impedance											
Differential			10^{13}‖0.5			10^{13}‖0.5			10^{13}‖0.5		Ω‖pF
Common Mode			10^{13}‖2.8			10^{13}‖2.8			10^{13}‖2.8		Ω‖pF
OUTPUT CHARACTERISTICS											
Output Saturation Voltage[3]											
V_{OL}–V_{EE}	I_{SINK} = 20 µA		5	7		5	7		5	7	mV
T_{MIN} to T_{MAX}				10			10				mV
V_{CC}–V_{OH}	I_{SOURCE} = 20 µA		10	14		10	14		10	14	mV
T_{MIN} to T_{MAX}				20			20				mV
V_{OL}–V_{EE}	I_{SINK} = 2 mA		40	55		40	55		40	55	mV
T_{MIN} to T_{MAX}				80			80				mV
V_{CC}–V_{OH}	I_{SOURCE} = 2 mA		80	110		80	110		80	110	mV
T_{MIN} to T_{MAX}				160			160				mV
V_{OL}–V_{EE}	I_{SINK} = 15 mA		300	500		300	500		300	500	mV
T_{MIN} to T_{MAX}				1000			1000				mV
V_{CC}–V_{OH}	I_{SOURCE} = 15 mA		800	1500		800	1500		800	1500	mV
T_{MIN} to T_{MAX}				1900			1900				mV
Operating Output Current		15			15			15			mA
T_{MIN} to T_{MAX}		12			12						mA
Capacitive Load Drive			350			350			350		pF
POWER SUPPLY											
Quiescent Current T_{MIN} to T_{MAX}			1.3	1.6		1.3	1.6		1.3		mA
Power Supply Rejection	V_S+ = 5 V to 15 V	70	80		66	80		70	80		dB
T_{MIN} to T_{MAX}		70			66						dB

AD822–SPECIFICATIONS (V_S = ±15 volts @ T_A = +25°C, V_{CM} = 0 V, V_{OUT} = 0 V unless otherwise noted)

Parameter	Conditions	AD822A Min	AD822A Typ	AD822A Max	AD822B Min	AD822B Typ	AD822B Max	AD822S[1] Min	AD822S[1] Typ	AD822S[1] Max	Units
DC PERFORMANCE											
Initial Offset			0.4	2		0.3	1.5		0.4	2.0	mV
Max Offset over Temperature			0.5	3		0.5	2.5		0.5		mV
Offset Drift			2			2			2		µV/°C
Input Bias Current	V_{CM} = 0 V		2	25		2	12		2	25	pA
	V_{CM} = –10 V		40			40			40		pA
at T_{MAX}	V_{CM} = 0 V		0.5	5		0.5	2.5		0.5		nA
Input Offset Current			2	20		2	12		2	20	pA
at T_{MAX}			0.5			0.5			1.5		nA
Open-Loop Gain	V_O = +10 V to –10 V										
	R_L = 100 k	500	2000		500	2000		500	2000		V/mV
T_{MIN} to T_{MAX}		500			500						V/mV
	R_L = 10 k	100	500		100	500		150	400		V/mV
T_{MIN} to T_{MAX}		100			100						V/mV
	R_L = 1 k	30	45		30	45		30	45		V/mV
T_{MIN} to T_{MAX}		20			20						V/mV
NOISE/HARMONIC PERFORMANCE											
Input Voltage Noise											
0.1 Hz to 10 Hz			2			2			2		µV p-p
f = 10 Hz			25			25			25		nV/√Hz
f = 100 Hz			21			21			21		nV/√Hz
f = 1 kHz			16			16			16		nV/√Hz
f = 10 kHz			13			13			13		nV/√Hz
Input Current Noise											
0.1 Hz to 10 Hz			18			18			18		fA p-p
f = 1 kHz			0.8			0.8			0.8		fA/√Hz
Harmonic Distortion	R_L = 10 k										
f = 10 kHz	V_O = ±10 V		–85			–85			–85		dB
DYNAMIC PERFORMANCE											
Unity Gain Frequency			1.9			1.9			1.9		MHz
Full Power Response	V_O p-p = 20 V		45			45			45		kHz
Slew Rate			3			3			3		V/µs
Settling Time											
to 0.1%	V_O = 0 V to ±10 V		4.1			4.1			4.1		µs
to 0.01%			4.5			4.5			4.5		µs
MATCHING CHARACTERISTICS											
Initial Offset				3			2			0.8	mV
Max Offset Over Temperature				4			2.5			1.0	mV
Offset Drift			3			3					µV/°C
Input Bias Current				25			12			25	pA
Crosstalk @ f = 1 kHz	R_L = 5 kΩ		–130			–130			–130		dB
f = 100 kHz			–93			–93			–93		dB
INPUT CHARACTERISTICS											
Common-Mode Voltage Range[2]		–15.2		14	–15.2		14	–15.2		14	V
T_{MIN} to T_{MAX}		–15.2		14	–15.2		14				V
CMRR	V_{CM} = –15 V to 12 V	70	80		74	90		70	90		dB
T_{MIN} to T_{MAX}		70			74						dB
Input Impedance											
Differential			10^{13}‖0.5			10^{13}‖0.5			10^{13}‖0.5		Ω‖pF
Common Mode			10^{13}‖2.8			10^{13}‖2.8			10^{13}‖2.8		Ω‖pF
OUTPUT CHARACTERISTICS											
Output Saturation Voltage[3]											
V_{OL}–V_{EE}	I_{SINK} = 20 µA		5	7		5	7		5	7	mV
T_{MIN} to T_{MAX}				10			10				mV
V_{CC}–V_{OH}	I_{SOURCE} = 20 µA		10	14		10	14		10	14	mV
T_{MIN} to T_{MAX}				20			20				mV
V_{OL}–V_{EE}	I_{SINK} = 2 mA		40	55		40	55		40	55	mV
T_{MIN} to T_{MAX}				80			80				mV
V_{CC}–V_{OH}	I_{SOURCE} = 2 mA		80	110		80	110		80	110	mV
T_{MIN} to T_{MAX}				160			160				mV
V_{OL}–V_{EE}	I_{SINK} = 15 mA		300	500		300	500		300	500	mV
T_{MIN} to T_{MAX}				1000			1000				mV
V_{CC}–V_{OH}	I_{SOURCE} = 15 mA		800	1500		800	1500		800	1500	mV
T_{MIN} to T_{MAX}				1900			1900				mV
Operating Output Current		20			20			20			mA
T_{MIN} to T_{MAX}		15			15						mA
Capacitive Load Drive			350			350			350		pF
POWER SUPPLY											
Quiescent Current T_{MIN} to T_{MAX}			1.4	1.8		1.4	1.8		1.4		mA
Power Supply Rejection	V_S+ = 5 V to 15 V	70	80		70	80		70	80		dB
T_{MIN} to T_{MAX}		70			70						dB

(V_S = 0, 3 volts @ T_A = +25°C, V_{CM} = 0 V, V_{OUT} = 0.2 V unless otherwise noted)

Parameter	Conditions	AD822A-3 V Min	Typ	Max	Units
DC PERFORMANCE					
Initial Offset			0.2	1	mV
Max Offset over Temperature			0.5	1.5	mV
Offset Drift			1		µV/°C
Input Bias Current	V_{CM} = 0 V to +2 V		2	25	pA
at T_{MAX}			0.5	5	nA
Input Offset Current			2	20	pA
at T_{MAX}			0.5		nA
Open-Loop Gain	V_O = 0.2 V to 2 V				
	R_L = 100 k	300	1000		V/mV
T_{MIN} to T_{MAX}		300			V/mV
	R_L = 10 k	60	150		V/mV
T_{MIN} to T_{MAX}		60			V/mV
	R_L = 1 k	10	30		V/mV
T_{MIN} to T_{MAX}		8			V/mV
NOISE/HARMONIC PERFORMANCE					
Input Voltage Noise					
0.1 Hz to 10 Hz			2		µV p-p
f = 10 Hz			25		$nV/\sqrt{Hz}$
f = 100 Hz			21		$nV/\sqrt{Hz}$
f = 1 kHz			16		$nV/\sqrt{Hz}$
f = 10 kHz			13		$nV/\sqrt{Hz}$
Input Current Noise					
0.1 Hz to 10 Hz			18		fA p-p
f = 1 kHz			0.8		$fA/\sqrt{Hz}$
Harmonic Distortion	R_L = 10 k to 1.5 V				
f = 10 kHz	V_O = ±1.25 V		–92		dB
DYNAMIC PERFORMANCE					
Unity Gain Frequency			1.5		MHz
Full Power Response	V_O p-p = 2.5 V		240		kHz
Slew Rate			3		V/µs
Settling Time					
to 0.1%	V_O = 0.2 V to 2.5 V		1		µs
to 0.01%			1.4		µs
MATCHING CHARACTERISTICS					
Initial Offset				1	mV
Max Offset Over Temperature				2	mV
Offset Drift			2		µV/°C
Input Bias Current				10	pA
Crosstalk @ f = 1 kHz	R_L = 5 kΩ		–130		dB
f = 100 kHz			–93		dB
INPUT CHARACTERISTICS					
Common-Mode Voltage Range[2]		–0.2		2	V
T_{MIN} to T_{MAX}		–0.2		2	V
CMRR	V_{CM} = 0 V to +1 V	60	74		dB
T_{MIN} to T_{MAX}		60			dB
Input Impedance					
Differential			10^{13}‖0.5		Ω‖pF
Common Mode			10^{13}‖2.8		Ω‖pF
OUTPUT CHARACTERISTICS					
Output Saturation Voltage[3]					
V_{OL}–V_{EE}	I_{SINK} = 20 µA		5	7	mV
T_{MIN} to T_{MAX}				10	mV
V_{CC}–V_{OH}	I_{SOURCE} = 20 µA		10	14	mV
T_{MIN} to T_{MAX}				20	mV
V_{OL}–V_{EE}	I_{SINK} = 2 mA		40	55	mV
T_{MIN} to T_{MAX}				80	mV
V_{CC}–V_{OH}	I_{SOURCE} = 2 mA		80	110	mV
T_{MIN} to T_{MAX}				160	mV
V_{OL}–V_{EE}	I_{SINK} = 10 mA		200	400	mV
T_{MIN} to T_{MAX}				400	mV
V_{CC}–V_{OH}	I_{SOURCE} = 10 mA		500	1000	mV
T_{MIN} to T_{MAX}				1000	mV
Operating Output Current		15			mA
T_{MIN} to T_{MAX}		12			mA
Capacitive Load Drive			350		pF
POWER SUPPLY					
Quiescent Current T_{MIN} to T_{MAX}			1.24	1.6	mA
Power Supply Rejection	V_S+ = 3 V to 15 V	70	80		dB
T_{MIN} to T_{MAX}		70			dB

AD822–SPECIFICATIONS

NOTES
[1]See standard military drawing for 883B specifications.
[2]This is a functional specification. Amplifier bandwidth decreases when the input common-mode voltage is driven in the range ($+V_S$ – 1 V) to $+V_S$. Common-mode error voltage is typically less than 5 mV with the common-mode voltage set at 1 volt below the positive supply.
[3]V_{OL}–V_{EE} is defined as the difference between the lowest possible output voltage (V_{OL}) and the minus voltage supply rail (V_{EE}). V_{CC}–V_{OH} is defined as the difference between the highest possible output voltage (V_{OH}) and the positive supply voltage (V_{CC}).

Specifications subject to change without notice.

CAUTION

ESD (electrostatic discharge) sensitive device. Electrostatic charges as high as 4000 V readily accumulate on the human body and test equipment and can discharge without detection. Although the AD822 features proprietary ESD protection circuitry, permanent damage may occur on devices subjected to high energy electrostatic discharges. Therefore, proper ESD precautions are recommended to avoid performance degradation or loss of functionality.

ABSOLUTE MAXIMUM RATINGS[1]

Supply Voltage . . . . . ±18 V
Internal Power Dissipation
  Plastic DIP (N) . . . . . Observe Derating Curves
  Cerdip (Q) . . . . . Observe Derating Curves
  SOIC (R) . . . . . Observe Derating Curves
Input Voltage . . . . . ($+V_S$ + 0.2 V) to –(20 V + V_S)
Output Short Circuit Duration . . . . . Indefinite
Differential Input Voltage . . . . . ±30 V
Storage Temperature Range (N) . . . . . –65°C to +125°C
Storage Temperature Range (Q) . . . . . –65°C to +150°C
Storage Temperature Range (R) . . . . . –65°C to +150°C
Operating Temperature Range
  AD822A/B . . . . . –40°C to +85°C
  AD822S . . . . . –55°C to +125°C
Lead Temperature Range (Soldering 60 sec) . . . . . +260°C

NOTES
[1]Stresses above those listed under "Absolute Maximum Ratings" may cause permanent damage to the device. This is a stress rating only and functional operation of the device at these or any other conditions above those indicated in the operational section of this specification is not implied. Exposure to absolute maximum rating conditions for extended periods may affect device reliability.
[2]8-Pin Plastic DIP Package: θ_{JA} = 90°C/Watt
8-Pin Cerdip Package: θ_{JA} = 110°C/Watt
8-Pin SOIC Package: θ_{JA} = 160°C/Watt

MAXIMUM POWER DISSIPATION

The maximum power that can be safely dissipated by the AD822 is limited by the associated rise in junction temperature. For plastic packages, the maximum safe junction temperature is 145°C. For the cerdip packages, the maximum junction temperature is 175°C. If these maximums are exceeded momentarily, proper circuit operation will be restored as soon as the die temperature is reduced. Leaving the device in the "overheated" condition for an extended period can result in device burnout. To ensure proper operation, it is important to observe the derating curves shown in Figure 24.

While the AD822 is internally short circuit protected, this may not be sufficient to guarantee that the maximum junction temperature is not exceeded under all conditions. With power supplies ±12 volts (or less) at an ambient temperature of +25°C or less, if the output node is shorted to a supply rail, then the amplifier will not be destroyed, even if this condition persists for an extended period.

ORDERING GUIDE

Model[1]	Temperature Range	Package Description	Package Option
AD822AN	–40°C to +85°C	8-Pin Plastic Mini-DIP	N-8
AD822BN	–40°C to +85°C	8-Pin Plastic Mini-DIP	N-8
AD822AR	–40°C to +85°C	8-Pin SOIC	R-8
AD822BR	–40°C to +85°C	8-Pin SOIC	R-8
AD822AR-3V	–40°C to +85°C	8-Pin SOIC	R-8
AD822AN-3V	–40°C to +85°C	8-Pin Plastic Mini-DIP	N-8
AD822A Chips	–40°C to +85°C	Die	
Standard Military Drawing[2]	–55°C to +125°C	8-Pin Cerdip	Q-8

NOTES
[1]Spice model is available on ADI Model Disc.
[2]Contact factory for availability.

METALIZATION PHOTOGRAPH

Contact factory for latest dimensions.
Dimensions shown in inches and (mm).

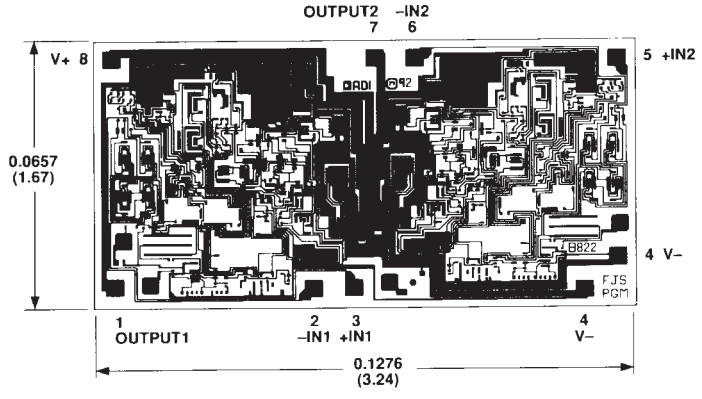

NOTE: BACK OF DIE IS AT $+V_S$ POTENTIAL.

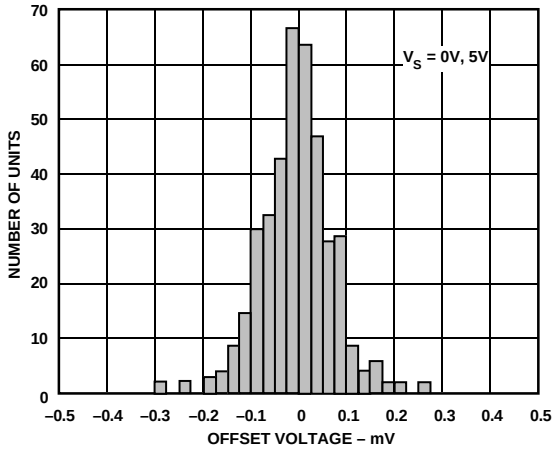

Figure 1. Typical Distribution of Offset Voltage (390 Units)

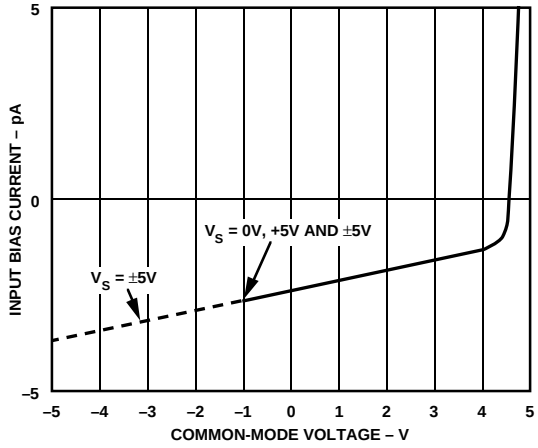

Figure 4. Input Bias Current vs. Common-Mode Voltage; V_S = +5 V, 0 V and V_S = ±5 V

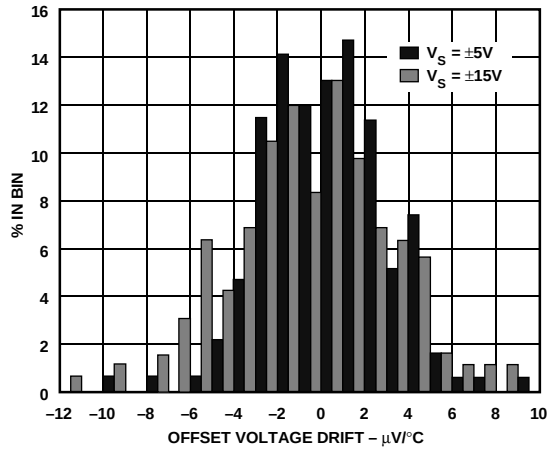

Figure 2. Typical Distribution of Offset Voltage Drift (100 Units)

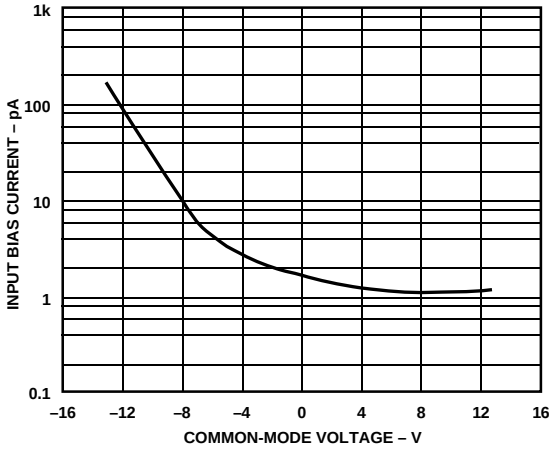

Figure 5. Input Bias Current vs. Common-Mode Voltage; V_S = ±15 V

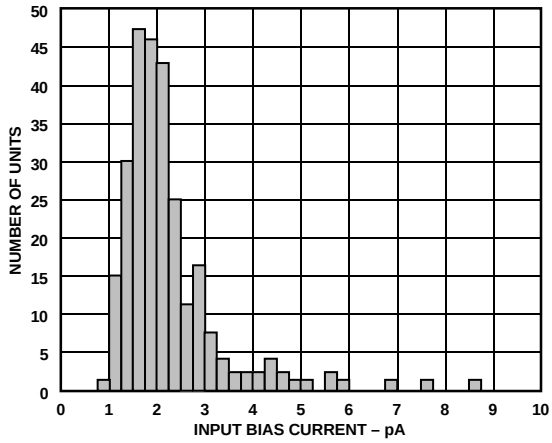

Figure 3. Typical Distribution of Input Bias Current (213 Units)

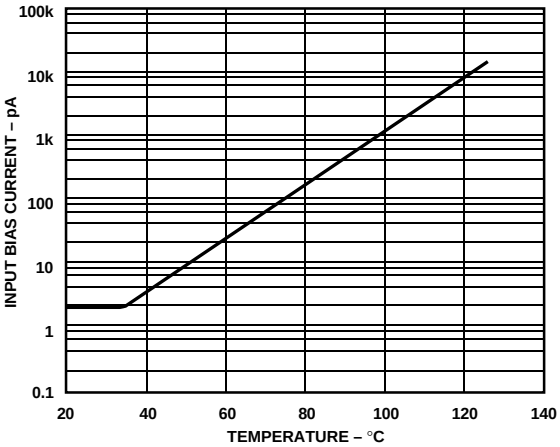

Figure 6. Input Bias Current vs. Temperature; V_S = 5 V, V_{CM} = 0

AD822–Typical Characteristics

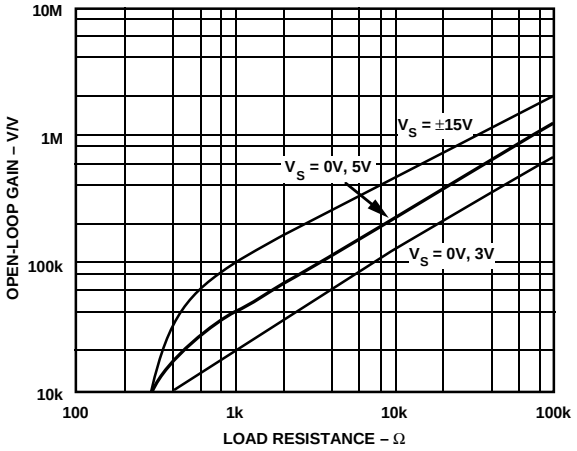

Figure 7. Open-Loop Gain vs. Load Resistance

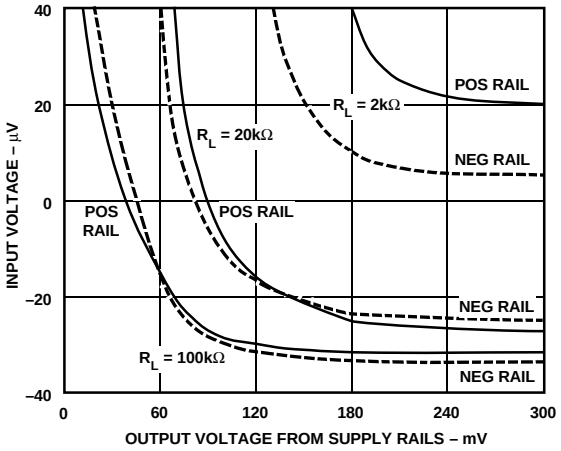

Figure 10. Input Error Voltage with Output Voltage within 300 mV of Either Supply Rail for Various Resistive Loads; V_S = ±5 V

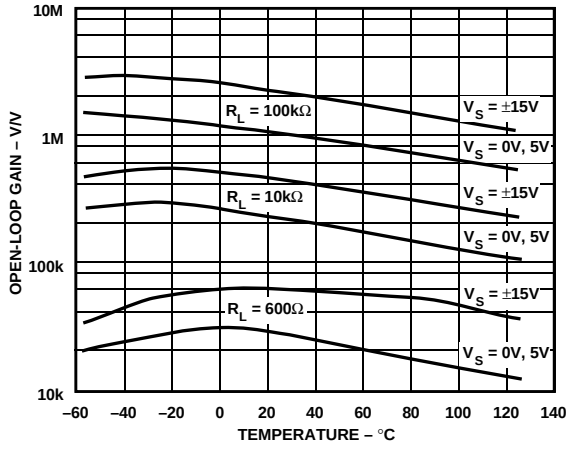

Figure 8. Open-Loop Gain vs. Temperature

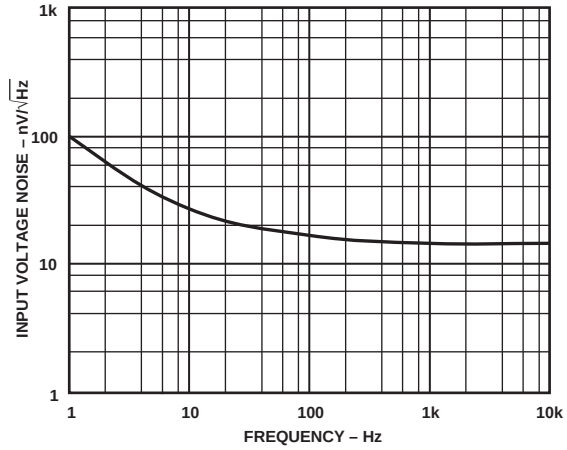

Figure 11. Input Voltage Noise vs. Frequency

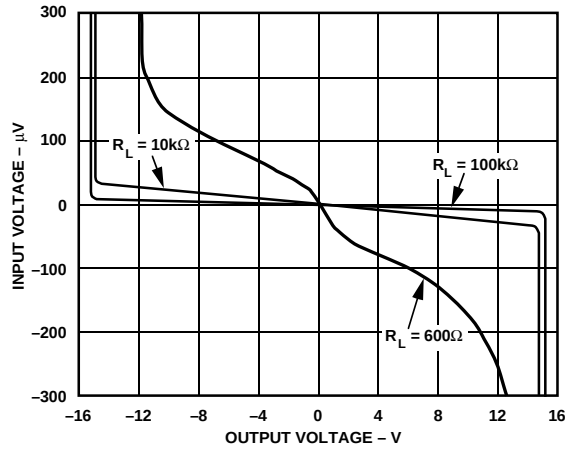

Figure 9. Input Error Voltage vs. Output Voltage for Resistive Loads

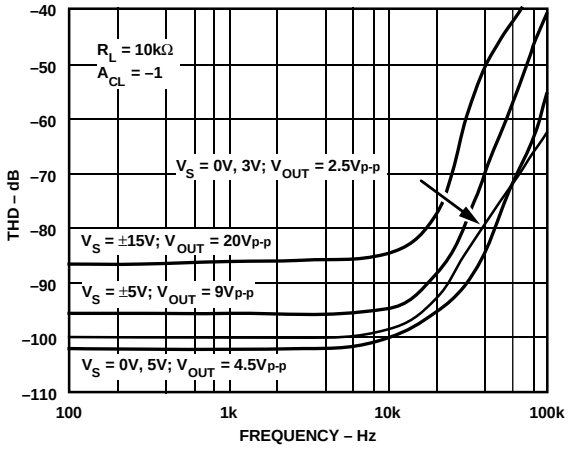

Figure 12. Total Harmonic Distortion vs. Frequency

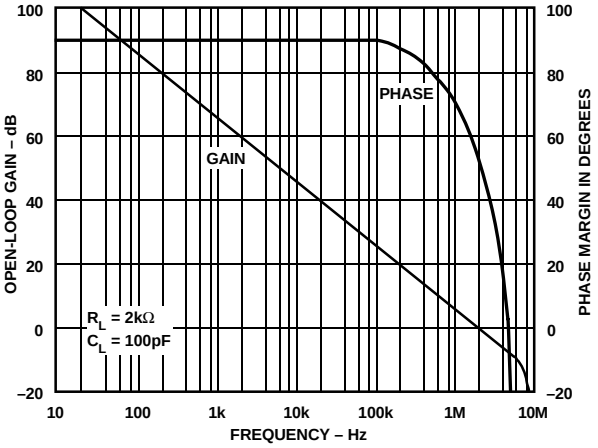

Figure 13. Open-Loop Gain and Phase Margin vs. Frequency

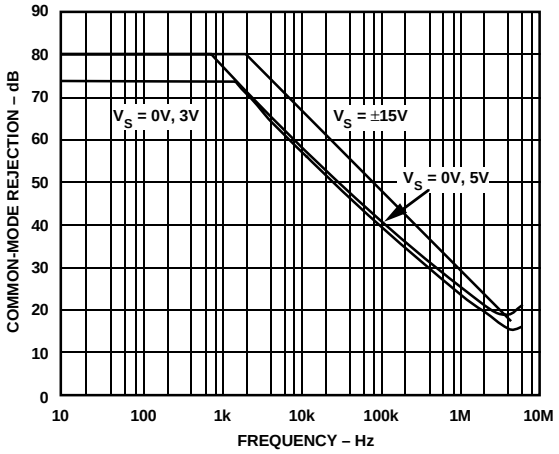

Figure 16. Common-Mode Rejection vs. Frequency

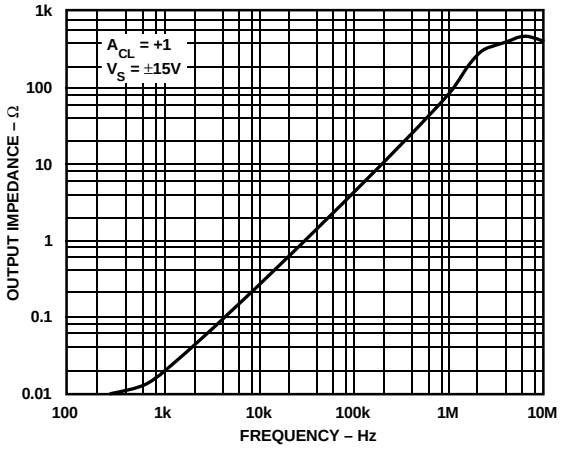

Figure 14. Output Impedance vs. Frequency

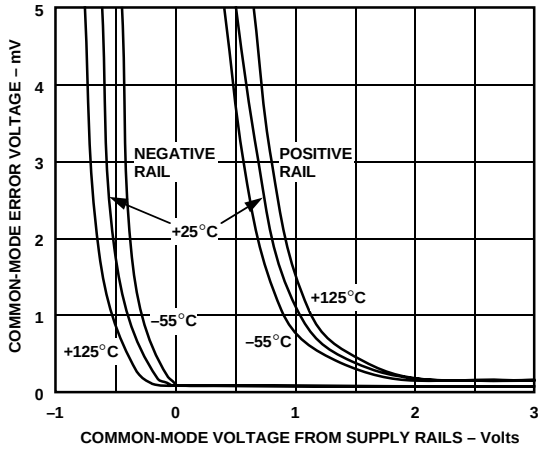

Figure 17. Absolute Common-Mode Error vs. Common-Mode Voltage from Supply Rails ($V_S - V_{CM}$)

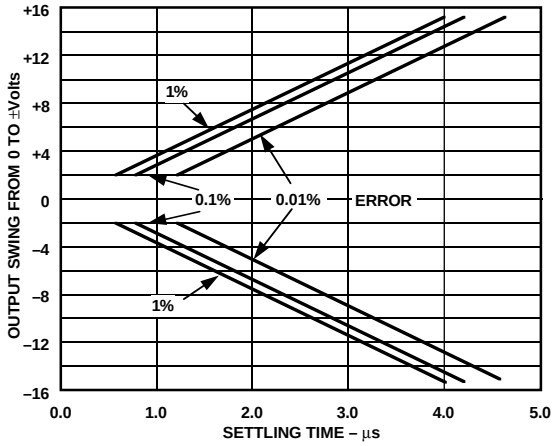

Figure 15. Output Swing and Error vs. Settling Time

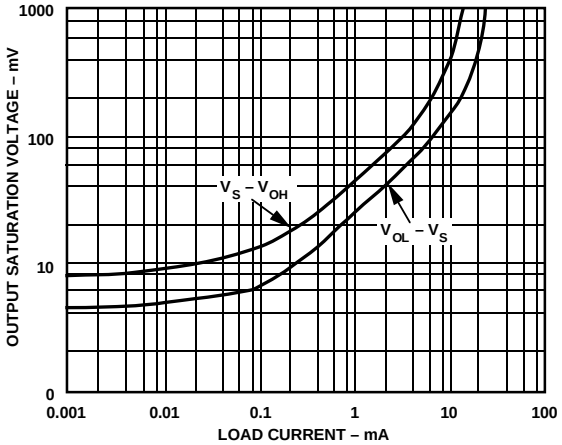

Figure 18. Output Saturation Voltage vs. Load Current

AD822–Typical Characteristics

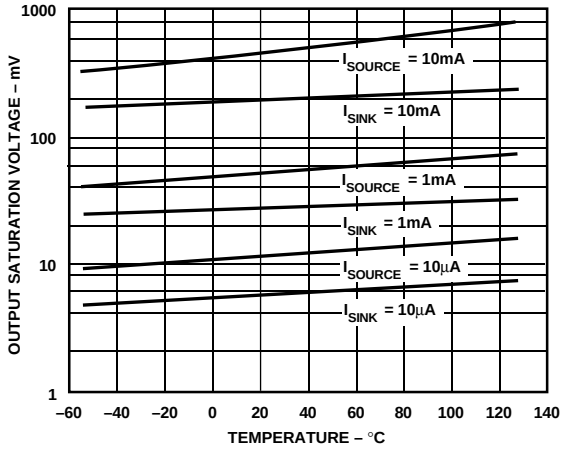

Figure 19. Output Saturation Voltage vs. Temperature

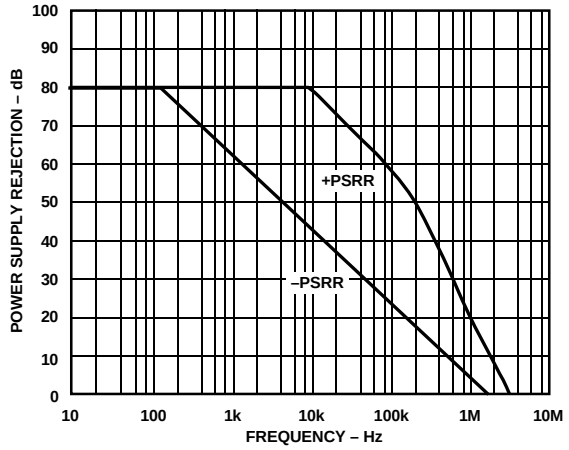

Figure 22. Power Supply Rejection vs. Frequency

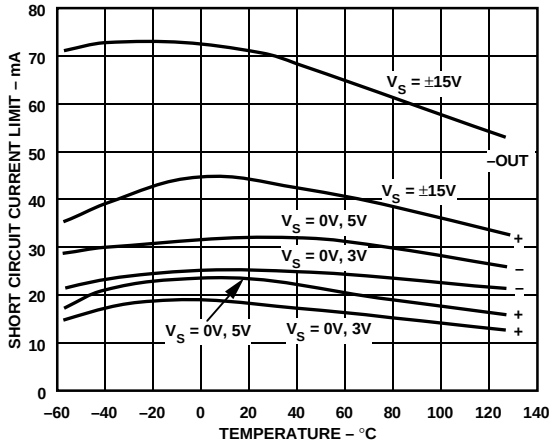

Figure 20. Short Circuit Current Limit vs. Temperature

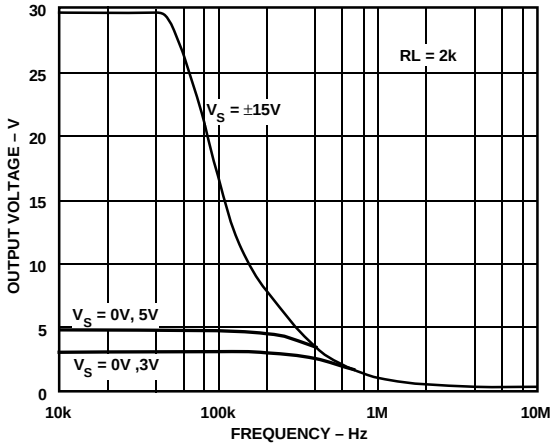

Figure 23. Large Signal Frequency Response

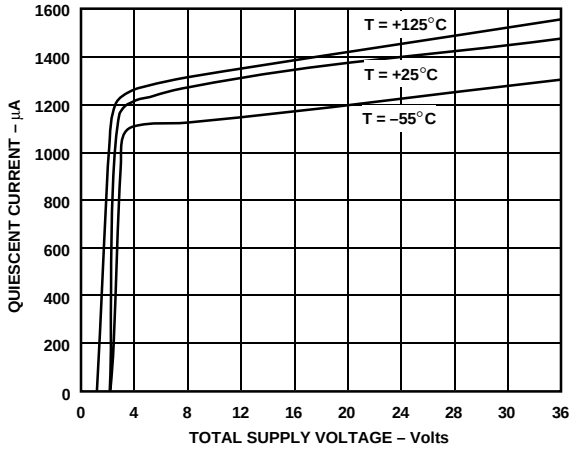

Figure 21. Quiescent Current vs. Supply Voltage vs. Temperature

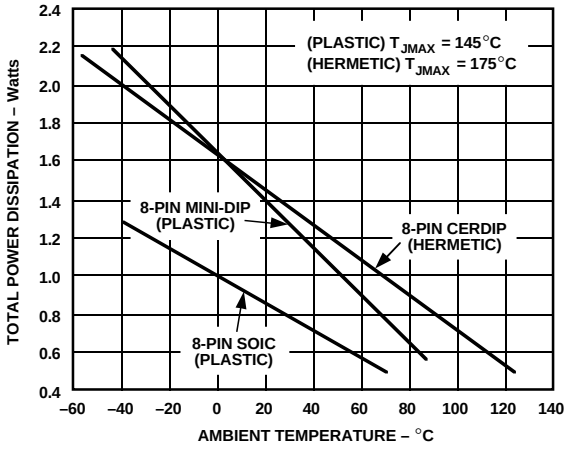

Figure 24. Maximum Power Dissipation vs. Temperature for Plastic and Hermetic Packages

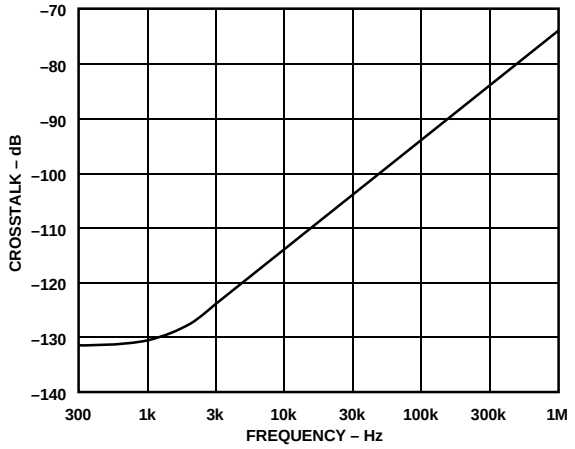

Figure 25. Crosstalk vs. Frequency

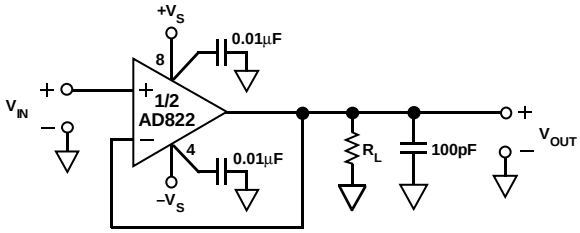

Figure 26. Unity-Gain Follower

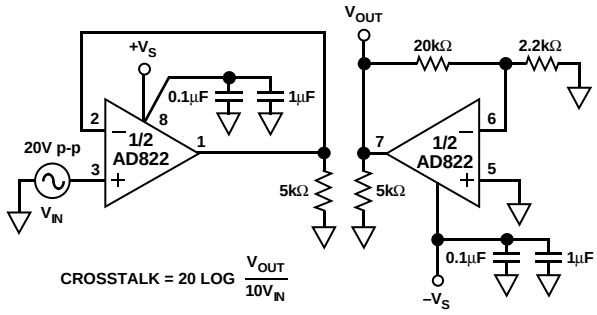

Figure 28. Crosstalk Test Circuit

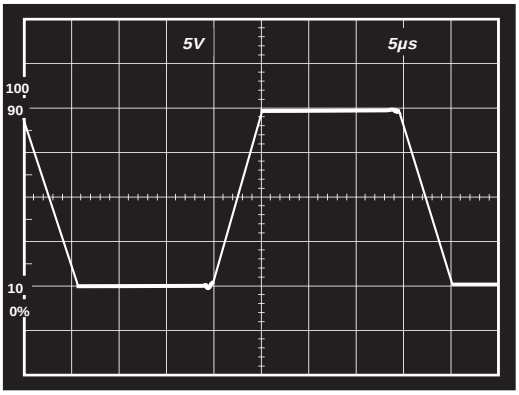

Figure 29. Large Signal Response Unity Gain Follower; $V_S = \pm 15$ V, $R_L = 10$ kΩ

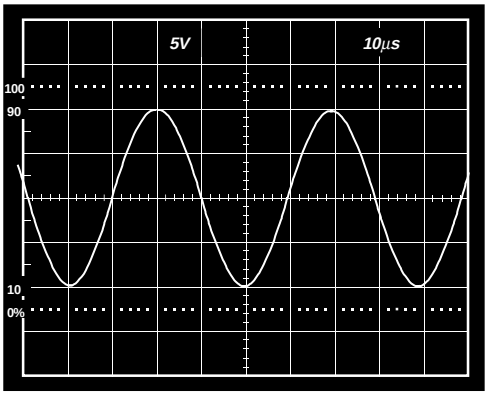

Figure 27. 20 V p-p, 25 kHz Sine Wave Input; Unity Gain Follower; $R_L = 600\ \Omega$, $V_S = \pm 15$ V

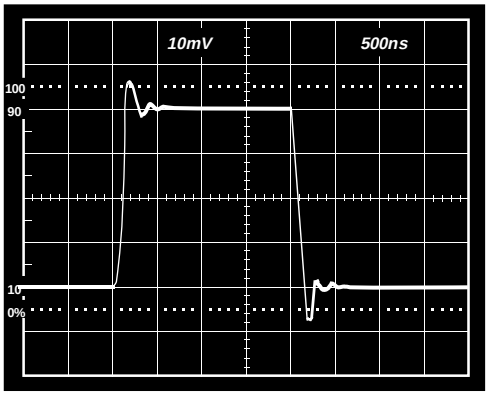

Figure 30. Small Signal Response Unity Gain Follower; $V_S = \pm 15$ V, $R_L = 10$ kΩ

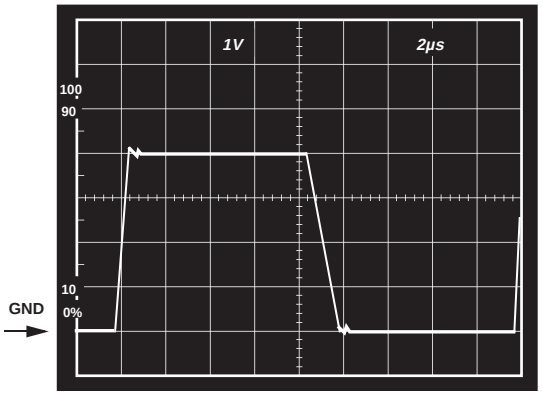

Figure 31. V_S = +5 V, 0 V; Unity Gain Follower Response to 0 V to 4 V Step

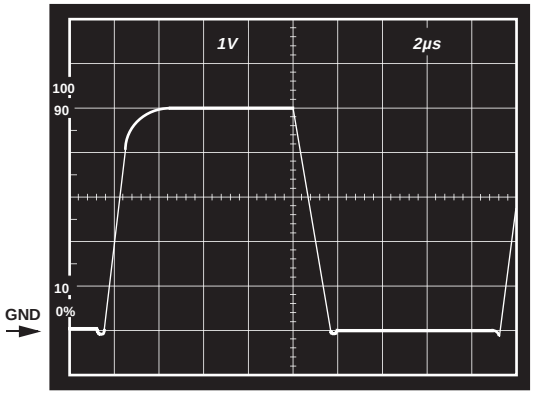

Figure 34. V_S = +5 V, 0 V; Unity Gain Follower Response to 0 V to 5 V Step

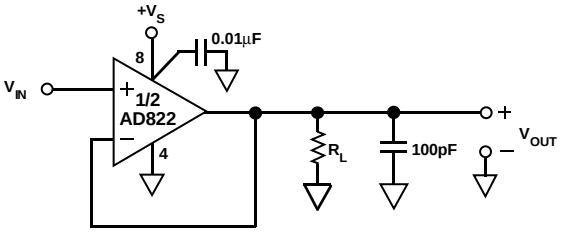

Figure 32. Unity Gain Follower

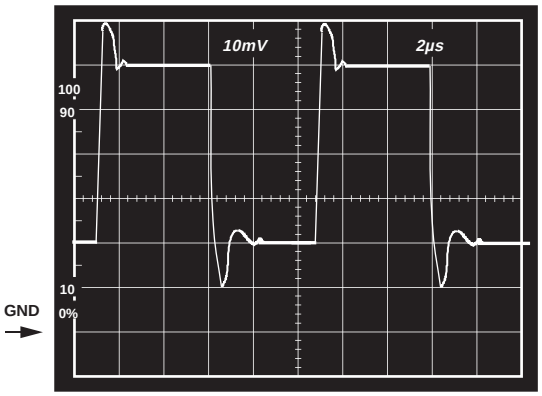

Figure 35. V_S = +5 V, 0 V; Unity Gain Follower Response, to 40 mV Step Centered 40 mV Above Ground, R_L = 10 kΩ

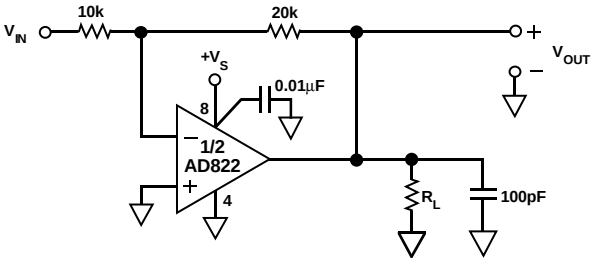

Figure 33. Gain of Two Inverter

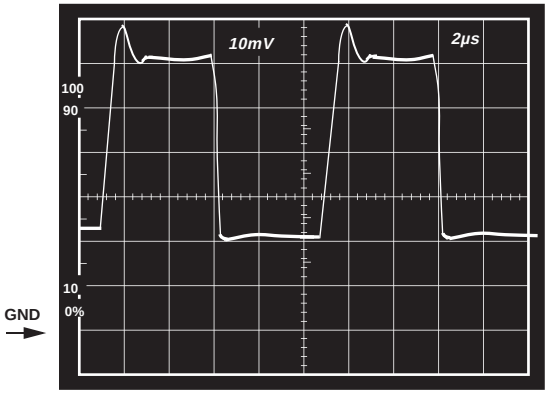

Figure 36. V_S = +5 V, 0 V; Gain of Two Inverter Response to 20 mV Step, Centered 20 mV Below Ground, R_L = 10 kΩ

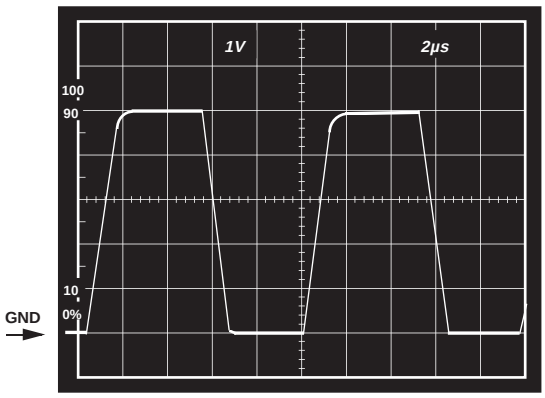

Figure 37. V_S = +5 V, 0 V; Gain of Two Inverter Response to 2.5 V Step Centered –1.25 V Below Ground, R_L = 10 kΩ

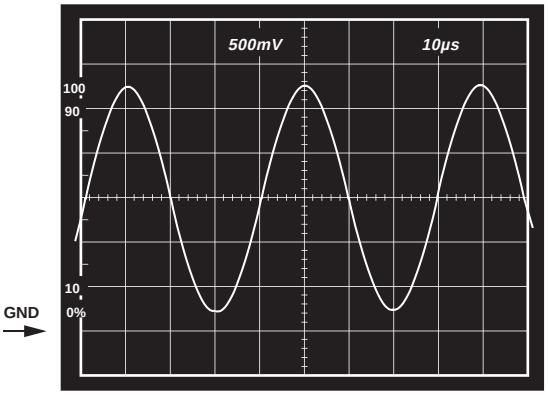

Figure 38. V_S = 3 V, 0 V; Gain of Two Inverter, V_{IN} = 1.25 V, 25 kHz, Sine Wave Centered at –0.75 V, R_L = 600 Ω

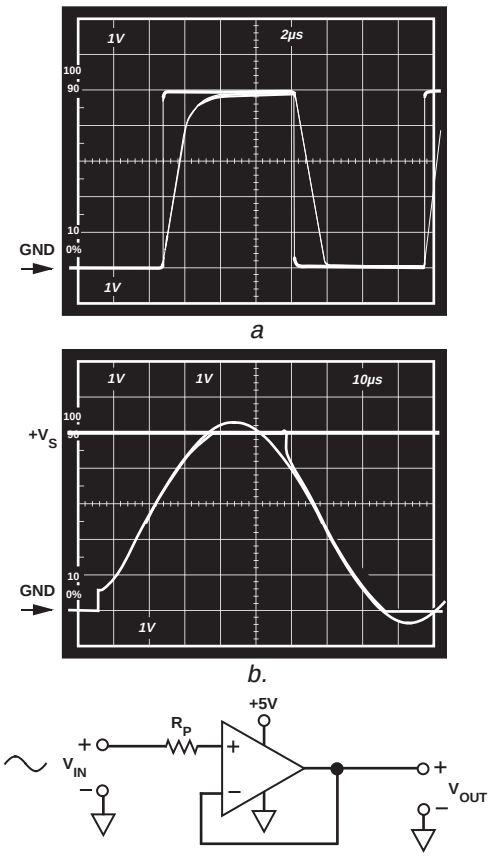

Figure 39. (a) Response with R_P = 0; V_{IN} from 0 to $+V_S$
(b) V_{IN} = 0 to $+V_S$ + 200 mV
V_{OUT} = 0 to $+V_S$
R_P = 49.9 kΩ

APPLICATION NOTES

INPUT CHARACTERISTICS

In the AD822, n-channel JFETs are used to provide a low offset, low noise, high impedance input stage. Minimum input common-mode voltage extends from 0.2 V below $-V_S$ to 1 V less than $+V_S$. Driving the input voltage closer to the positive rail will cause a loss of amplifier bandwidth (as can be seen by comparing the large signal responses shown in Figures 31 and 34) and increased common-mode voltage error as illustrated in Figure 17.

The AD822 does not exhibit phase reversal for input voltages up to and including $+V_S$. Figure 39a shows the response of an AD822 voltage follower to a 0 V to +5 V ($+V_S$) square wave input. The input and output arc superimposed. The output tracks the input up to $+V_S$ without phase reversal. The reduced bandwidth above a 4 V input causes the rounding of the output wave form. For input voltages greater than $+V_S$, a resistor in series with the AD822's noninverting input will prevent phase reversal, at the expense of greater input voltage noise. This is illustrated in Figure 39b.

Since the input stage uses n-channel JFETs, input current during normal operation is negative; the current flows out from the input terminals. If the input voltage is driven more positive than $+V_S$ – 0.4 V, the input current will reverse direction as internal device junctions become forward biased. This is illustrated in Figure 4.

A current limiting resistor should be used in series with the input of the AD822 if there is a possibility of the input voltage exceeding the positive supply by more than 300 mV, or if an input voltage will be applied to the AD822 when $\pm V_S$ = 0. The amplifier will be damaged if left in that condition for more than 10 seconds. A 1 kΩ resistor allows the amplifier to withstand up to 10 volts of continuous overvoltage, and increases the input voltage noise by a negligible amount.

Input voltages less than $-V_S$ are a completely different story. The amplifier can safely withstand input voltages 20 volts below the minus supply voltage as long as the total voltage from the positive supply to the input terminal is less than 36 volts. In addition, the input stage typically maintains picoamp level input currents across that input voltage range.

The AD822 is designed for 13 nV/√Hz wideband input voltage noise and maintains low noise performance to low frequencies (refer to Figure 11). This noise performance, along with the AD822's low input current and current noise means that the AD822 contributes negligible noise for applications with source resistances greater than 10 kΩ and signal bandwidths greater than 1 kHz. This is illustrated in Figure 40.

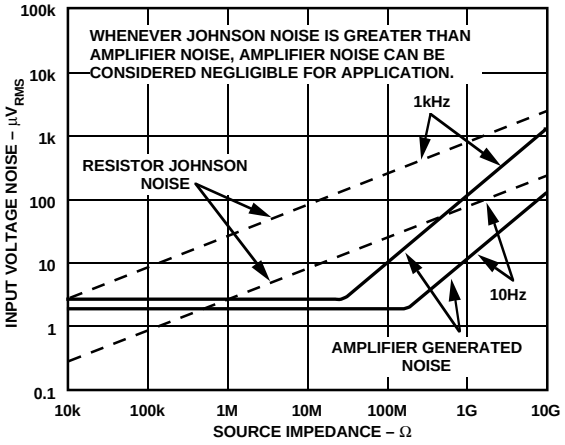

Figure 40. Total Noise vs. Source Impedance

OUTPUT CHARACTERISTICS

The AD822 s unique bipolar rail-to-rail output stage swings within 5 mV of the minus supply and 10 mV of the positive supply with no external resistive load. The AD822's approximate output saturation resistance is 40 Ω sourcing and 20 Ω sinking. This can be used to estimate output saturation voltage when driving heavier current loads. For instance, when sourcing 5 mA, the saturation voltage to the positive supply rail will be 200 mV, when sinking 5 mA, the saturation voltage to the minus rail will be 100 mV.

The amplifier's open-loop gain characteristic will change as a function of resistive load, as shown in Figures 7 through 10. For load resistances over 20 kΩ, the AD822's input error voltage is virtually unchanged until the output voltage is driven to 180 mV of either supply.

If the AD822's output is overdriven so as to saturate either of the output devices, the amplifier will recover within 2 μs of its input returning to the amplifier's linear operating region.

Direct capacitive loads will interact with the amplifier's effective output impedance to form an additional pole in the amplifier's feedback loop, which can cause excessive peaking on the pulse response or loss of stability. Worst case is when the amplifier is used as a unity gain follower. Figure 41 shows the AD822's pulse response as a unity gain follower driving 350 pF. This amount of overshoot indicates approximately 20 degrees of phase margin—the system is stable, but is nearing the edge. Configurations with less loop gain, and as a result less loop bandwidth, will be much less sensitive to capacitance load effects. Figure 42 is a plot of capacitive load that will result in a 20 degree phase margin versus noise gain for the AD822. Noise gain is the inverse of the feedback attenuation factor provided by the feedback network in use.

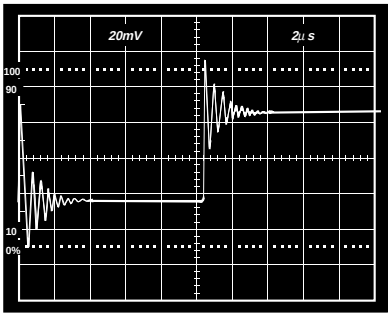

Figure 41. Small Signal Response of AD822 as Unity Gain Follower Driving 350 pF Capacitive Load

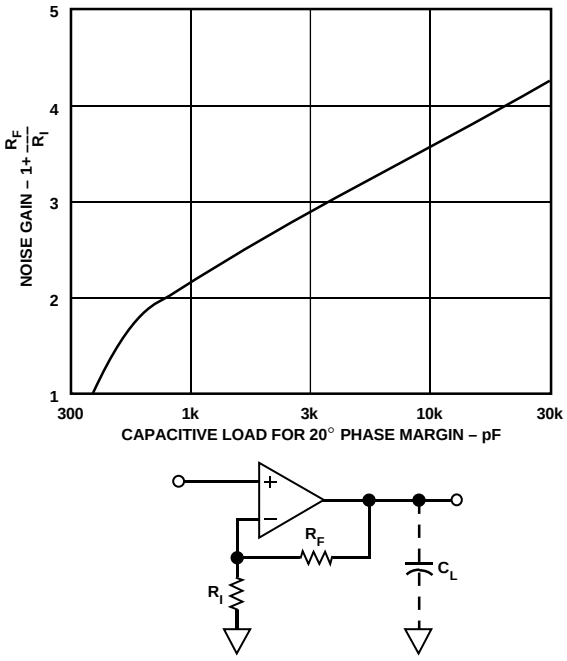

Figure 42. Capacitive Load Tolerance vs. Noise Gain

Figure 43 shows a method for extending capacitance load drive capability for a unity gain follower. With these component values, the circuit will drive 5,000 pF with a 10% overshoot.

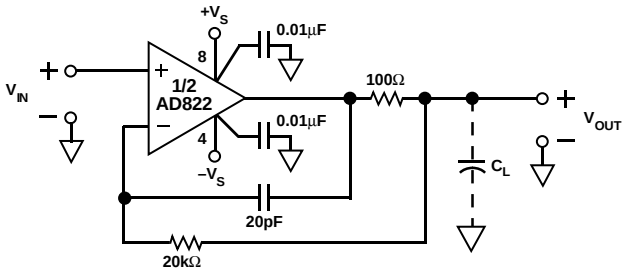

Figure 43. Extending Unity Gain Follower Capacitive Load Capability Beyond 350 pF

APPLICATIONS

Single Supply Voltage-to-Frequency Converter

The circuit shown in Figure 44 uses the AD822 to drive a low power timer, which produces a stable pulse of width t_1. The positive going output pulse is integrated by R1-C1 and used as one input to the AD822, which is connected as a differential integrator. The other input (nonloading) is the unknown voltage, V_{IN}. The AD822 output drives the timer trigger input, closing the overall feedback loop.

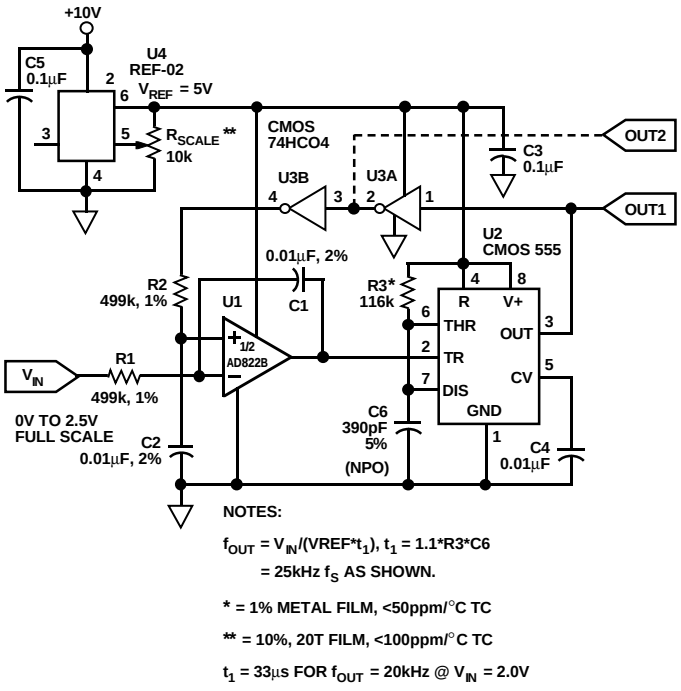

Figure 44. Single Supply Voltage-to-Frequency Converter

Typical AD822 bias currents of 2 pA allow megaohm-range source impedances with negligible dc errors. Linearity errors on the order of 0.01% full scale can be achieved with this circuit. This performance is obtained with a 5 volt single supply which delivers less than 1 mA to the entire circuit.

Single Supply Programmable Gain Instrumentation Amplifier

The AD822 can be configured as a single supply instrumentation amplifier that is able to operate from single supplies down to 3 V, or dual supplies up to ±15 V. Using only one AD822 rather than three separate op amps, this circuit is cost and power efficient. AD822 FET inputs' 2 pA bias currents minimize offset errors caused by high unbalanced source impedances.

An array of precision thin-film resistors sets the in amp gain to be either 10 or 100. These resistors are laser-trimmed to ratio match to 0.01%, and have a maximum differential TC of 5 ppm/°C.

Table I. AD822 In Amp Performance

Parameters	V_S = 3 V, 0 V	V_S = ±5 V
CMRR	74 dB	80 dB
Common-Mode		
Voltage Range	–0.2 V to +2 V	–5.2 V to +4 V
3 dB BW, G = 10	180 kHz	180 kHz
G = 100	18 kHz	18 kHz
$t_{SETTLING}$		
2 V Step (V_S = 0 V, 3 V)	2 µs	
5 V (V_S = ±5 V)		5 µs
Noise @ f = 1 kHz, G = 10	270 nV/√Hz	270 nV/√Hz
G = 100	2.2 µV/√Hz	2.2 µV/√Hz
I_{SUPPLY} (Total)	1.10 mA	1.15 mA

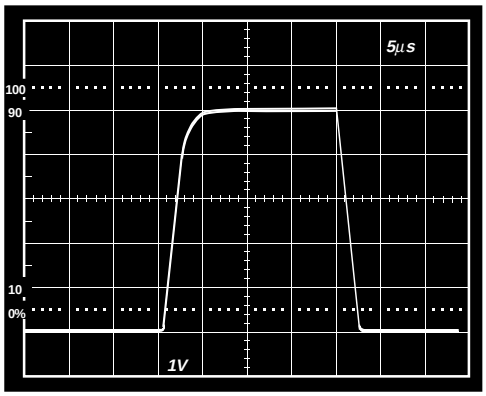

Figure 45a. Pulse Response of In Amp to a 500 mV p-p Input Signal; V_S = +5 V, 0 V; Gain = 10

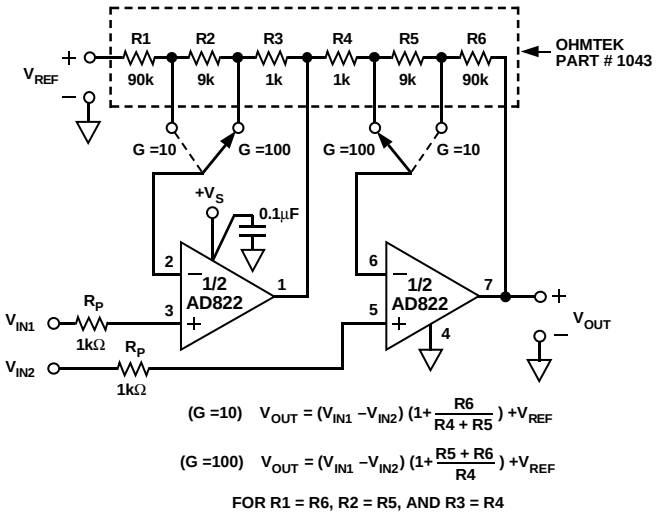

Figure 45b. A Single Supply Programmable Instrumentation Amplifier

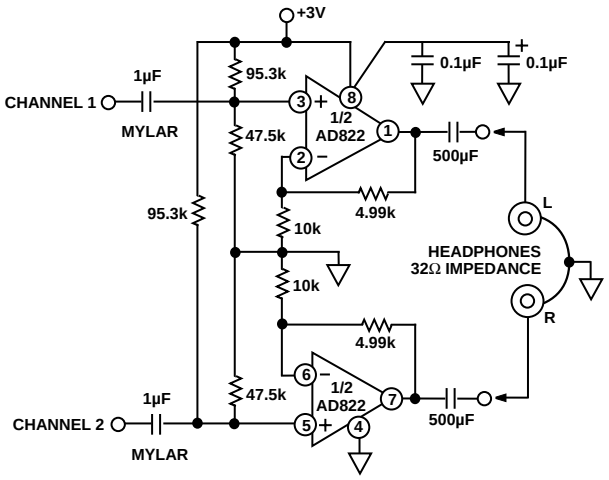

Figure 46. 3 Volt Single Supply Stereo Headphone Driver

3 Volt, Single Supply Stereo Headphone Driver

The AD822 exhibits good current drive and THD+N performance, even at 3 V single supplies. At 1 kHz, total harmonic distortion plus noise (THD+N) equals –62 dB (0.079%) for a 300 mV p-p output signal. This is comparable to other single supply op amps which consume more power and cannot run on 3 V power supplies.

In Figure 46, each channel s input signal is coupled via a 1 µF Mylar capacitor. Resistor dividers set the dc voltage at the noninverting inputs so that the output voltage is midway between the power supplies (+1.5 V). The gain is 1.5. Each half of the AD822 can then be used to drive a headphone channel. A 5 Hz high-pass filter is realized by the 500 µF capacitors and the headphones, which can be modeled as 32 ohm load resistors to ground. This ensures that all signals in the audio frequency range (20 Hz–20 kHz) are delivered to the headphones.

Low Dropout Bipolar Bridge Driver

The AD822 can be used for driving a 350 ohm Wheatstone bridge. Figure 47 shows one half of the AD822 being used to buffer the AD589—a 1.235 V low power reference. The output of +4.5 V can be used to drive an A/D converter front end. The other half of the AD822 is configured as a unity-gain inverter, and generates the other bridge input of –4.5 V. Resistors R1 and R2 provide a constant current for bridge excitation. The AD620 low power instrumentation amplifier is used to condition the differential output voltage of the bridge. The gain of the AD620 is programmed using an external resistor R_G, and determined by:

$$G = \frac{49.4\ k\Omega}{R_G} + 1$$

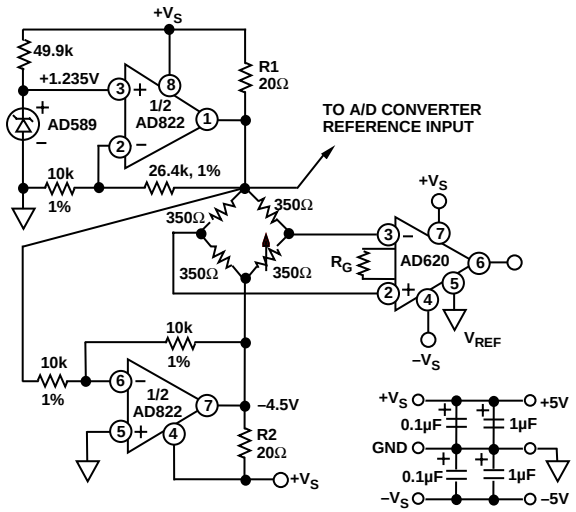

Figure 47. Low Dropout Bipolar Bridge Driver

C1821a–10–9/94

OUTLINE DIMENSIONS

Dimensions shown in inches and (mm).

Mini-DIP (N) Package

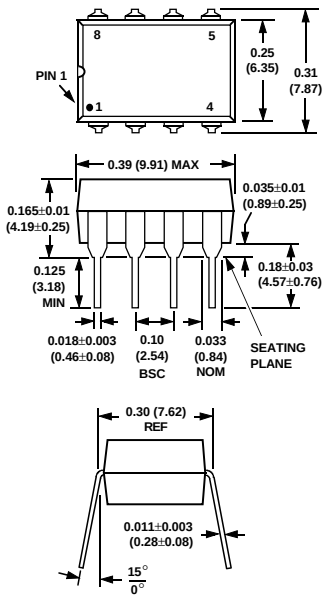

Cerdip (Q) Package

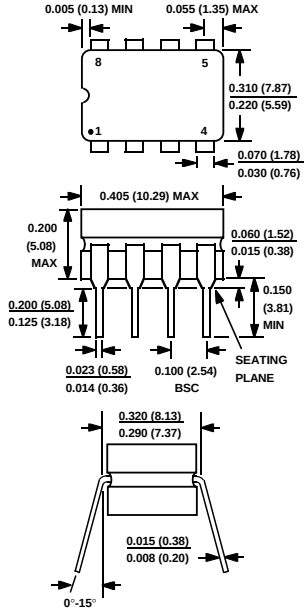

SOIC (R) Package

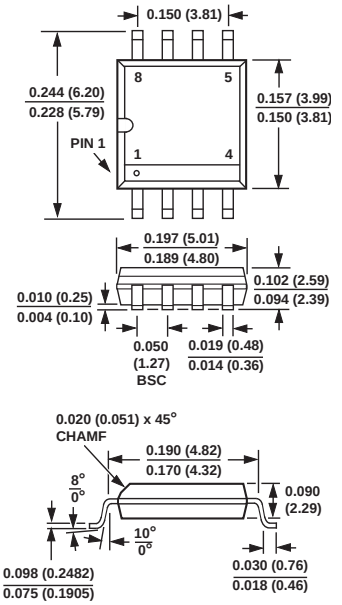

PRINTED IN U.S.A.

Low Cost Low Power Instrumentation Amplifier

AD620

FEATURES

Easy to use
- **Gain set with one external resistor (Gain range 1 to 10,000)**
- **Wide power supply range (±2.3 V to ±18 V)**
- **Higher performance than 3 op amp IA designs**
- **Available in 8-lead DIP and SOIC packaging**
- **Low power, 1.3 mA max supply current**

Excellent dc performance (B grade)
- **50 µV max, input offset voltage**
- **0.6 µV/°C max, input offset drift**
- **1.0 nA max, input bias current**
- **100 dB min common-mode rejection ratio (G = 10)**

Low noise
- **9 nV/√Hz @ 1 kHz, input voltage noise**
- **0.28 µV p-p noise (0.1 Hz to 10 Hz)**

Excellent ac specifications
- **120 kHz bandwidth (G = 100)**
- **15 µs settling time to 0.01%**

APPLICATIONS

Weigh scales
ECG and medical instrumentation
Transducer interface
Data acquisition systems
Industrial process controls
Battery-powered and portable equipment

CONNECTION DIAGRAM

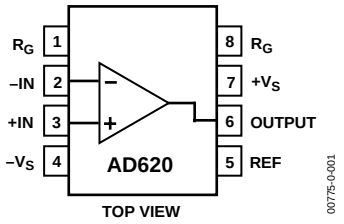

Figure 1. 8-Lead PDIP (N), CERDIP (Q), and SOIC (R) Packages

PRODUCT DESCRIPTION

The AD620 is a low cost, high accuracy instrumentation amplifier that requires only one external resistor to set gains of 1 to 10,000. Furthermore, the AD620 features 8-lead SOIC and DIP packaging that is smaller than discrete designs and offers lower power (only 1.3 mA max supply current), making it a good fit for battery-powered, portable (or remote) applications.

The AD620, with its high accuracy of 40 ppm maximum nonlinearity, low offset voltage of 50 µV max, and offset drift of 0.6 µV/°C max, is ideal for use in precision data acquisition systems, such as weigh scales and transducer interfaces. Furthermore, the low noise, low input bias current, and low power of the AD620 make it well suited for medical applications, such as ECG and noninvasive blood pressure monitors.

The low input bias current of 1.0 nA max is made possible with the use of Superβeta processing in the input stage. The AD620 works well as a preamplifier due to its low input voltage noise of 9 nV/√Hz at 1 kHz, 0.28 µV p-p in the 0.1 Hz to 10 Hz band, and 0.1 pA/√Hz input current noise. Also, the AD620 is well suited for multiplexed applications with its settling time of 15 µs to 0.01%, and its cost is low enough to enable designs with one in-amp per channel.

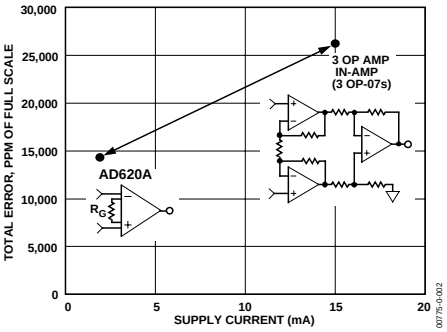

Figure 2. Three Op Amp IA Designs vs. AD620

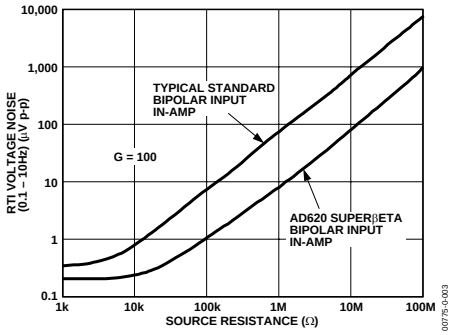

Figure 3. Total Voltage Noise vs. Source Resistance

Rev. G

One Technology Way, P.O. Box 9106, Norwood, MA 02062-9106, U.S.A.
Tel: 781.329.4700 **www.analog.com**
Fax: 781.326.8703

TABLE OF CONTENTS

REVISION HISTORY

12/04—Rev. F to Rev. G

Updated Format ..... Universal
Change to Features 1
Change to Product Description 1
Changes to Specifications 3
Added Metallization Photograph 4
Replaced Figure 4-Figure 6 6
Replaced Figure 15 7
Replaced Figure 33 10
Replaced Figure 34 and Figure 35 10
Replaced Figure 37 10
Changes to Table 3 13
Changes to Figure 41 and Figure 42 14
Changes to Figure 43 15
Change to Figure 44 17
Changes to Input Protection section 15
Deleted Figure 9 15
Changes to RF Interference section 15
Edit to Ground Returns for Input Bias Currents section 17
Added AD620CHIPS to Ordering Guide 19

7/03—Data Sheet changed from REV. E to REV. F

Edit to FEATURES 1
Changes to SPECIFICATIONS 2
Removed AD620CHIPS from ORDERING GUIDE 4
Removed METALLIZATION PHOTOGRAPH 4
Replaced TPCs 1–3 5
Replaced TPC 12 6
Replaced TPC 30 9
Replaced TPCs 31 and 32 10
Replaced Figure 4 10
Changes to Table I 11
Changes to Figures 6 and 7 12
Changes to Figure 8 13
Edited INPUT PROTECTION section 13
Added new Figure 9 13
Changes to RF INTERFACE section 14
Edit to GROUND RETURNS FOR INPUT BIAS CURRENTS section 15
Updated OUTLINE DIMENSIONS 16

SPECIFICATIONS

Typical @ 25°C, V_S = ±15 V, and R_L = 2 kΩ, unless otherwise noted.

Table 1.

Parameter	Conditions	AD620A			AD620B			AD620S[1]			Unit
		Min	Typ	Max	Min	Typ	Max	Min	Typ	Max	
GAIN	G = 1 + (49.4 kΩ/R_G)										
Gain Range		1		10,000	1		10,000	1		10,000	
Gain Error[2]	V_{OUT} = ±10 V										
G = 1			0.03	0.10		0.01	0.02		0.03	0.10	%
G = 10			0.15	0.30		0.10	0.15		0.15	0.30	%
G = 100			0.15	0.30		0.10	0.15		0.15	0.30	%
G = 1000			0.40	0.70		0.35	0.50		0.40	0.70	%
Nonlinearity	V_{OUT} = −10 V to +10 V										
G = 1–1000	R_L = 10 kΩ		10	40		10	40		10	40	ppm
G = 1–100	R_L = 2 kΩ		10	95		10	95		10	95	ppm
Gain vs. Temperature											
	G = 1			10			10			10	ppm/°C
	Gain >1[2]			−50			−50			−50	ppm/°C
VOLTAGE OFFSET	(Total RTI Error = V_{OSI} + V_{OSO}/G)										
Input Offset, V_{OSI}	V_S = ±5 V to ± 15 V		30	125		15	50		30	125	µV
Overtemperature	V_S = ±5 V to ± 15 V			185			85			225	µV
Average TC	V_S = ±5 V to ± 15 V		0.3	1.0		0.1	0.6		0.3	1.0	µV/°C
Output Offset, V_{OSO}	V_S = ±15 V		400	1000		200	500		400	1000	µV
	V_S = ± 5 V			1500			750			1500	µV
Overtemperature	V_S = ±5 V to ± 15 V			2000			1000			2000	µV
Average TC	V_S = ±5 V to ± 15 V		5.0	15		2.5	7.0		5.0	15	µV/°C
Offset Referred to the Input vs. Supply (PSR)	V_S = ±2.3 V to ±18 V										
G = 1		80	100		80	100		80	100		dB
G = 10		95	120		100	120		95	120		dB
G = 100		110	140		120	140		110	140		dB
G = 1000		110	140		120	140		110	140		dB
INPUT CURRENT											
Input Bias Current			0.5	2.0		0.5	1.0		0.5	2	nA
Overtemperature				2.5			1.5			4	nA
Average TC			3.0			3.0			8.0		pA/°C
Input Offset Current			0.3	1.0		0.3	0.5		0.3	1.0	nA
Overtemperature				1.5			0.75			2.0	nA
Average TC			1.5			1.5			8.0		pA/°C
INPUT											
Input Impedance											
Differential			10||2			10||2			10||2		GΩ_pF
Common-Mode			10||2			10||2			10||2		GΩ_pF
Input Voltage Range[3]	V_S = ±2.3 V to ±5 V	$-V_S$ + 1.9		$+V_S$ − 1.2	$-V_S$ + 1.9		$+V_S$ − 1.2	$-V_S$ + 1.9		$+V_S$ − 1.2	V
Overtemperature		$-V_S$ + 2.1		$+V_S$ − 1.3	$-V_S$ + 2.1		$+V_S$ − 1.3	$-V_S$ + 2.1		$+V_S$ − 1.3	V
	V_S = ± 5 V to ±18 V	$-V_S$ + 1.9		$+V_S$ − 1.4	$-V_S$ + 1.9		$+V_S$ − 1.4	$-V_S$ + 1.9		$+V_S$ − 1.4	V
Overtemperature		$-V_S$ + 2.1		$+V_S$ − 1.4	$-V_S$ + 2.1		$+V_S$ + 2.1	$-V_S$ + 2.3		$+V_S$ − 1.4	V

Parameter	Conditions	AD620A Min	AD620A Typ	AD620A Max	AD620B Min	AD620B Typ	AD620B Max	AD620S[1] Min	AD620S[1] Typ	AD620S[1] Max	Unit
Common-Mode Rejection											
Ratio DC to 60 Hz with											
1 kΩ Source Imbalance	V_{CM} = 0 V to ± 10 V										
G = 1		73	90		80	90		73	90		dB
G = 10		93	110		100	110		93	110		dB
G = 100		110	130		120	130		110	130		dB
G = 1000		110	130		120	130		110	130		dB
OUTPUT											
Output Swing	R_L = 10 kΩ										
	V_S = ±2.3 V to ± 5 V	$-V_S$ + 1.1		$+V_S$ – 1.2	$-V_S$ + 1.1		$+V_S$ – 1.2	$-V_S$ + 1.1		$+V_S$ – 1.2	V
Overtemperature		$-V_S$ + 1.4		$+V_S$ – 1.3	$-V_S$ + 1.4		$+V_S$ – 1.3	$-V_S$ + 1.6		$+V_S$ – 1.3	V
	V_S = ±5 V to ± 18 V	$-V_S$ + 1.2		$+V_S$ – 1.4	$-V_S$ + 1.2		$+V_S$ – 1.4	$-V_S$ + 1.2		$+V_S$ – 1.4	V
Overtemperature		$-V_S$ + 1.6		$+V_S$ – 1.5	$-V_S$ + 1.6		$+V_S$ – 1.5	$-V_S$ + 2.3		$+V_S$ – 1.5	V
Short Circuit Current			±18			±18			±18		mA
DYNAMIC RESPONSE											
Small Signal –3 dB Bandwidth											
G = 1			1000			1000			1000		kHz
G = 10			800			800			800		kHz
G = 100			120			120			120		kHz
G = 1000			12			12			12		kHz
Slew Rate		0.75	1.2		0.75	1.2		0.75	1.2		V/µs
Settling Time to 0.01%	10 V Step										
G = 1–100			15			15			15		µs
G = 1000			150			150			150		µs
NOISE											
Voltage Noise, 1 kHz	$Total\ RTI\ Noise = \sqrt{(e^2_{ni})} + (e_{no}/G)^2$										
Input, Voltage Noise, e_{ni}			9	13		9	13		9	13	nV/√Hz
Output, Voltage Noise, e_{no}			72	100		72	100		72	100	nV/√Hz
RTI, 0.1 Hz to 10 Hz											
G = 1			3.0			3.0	6.0		3.0	6.0	µV p-p
G = 10			0.55			0.55	0.8		0.55	0.8	µV p-p
G = 100–1000			0.28			0.28	0.4		0.28	0.4	µV p-p
Current Noise	f = 1 kHz		100			100			100		fA/√Hz
0.1 Hz to 10 Hz			10			10			10		pA p-p
REFERENCE INPUT											
R_{IN}			20			20			20		kΩ
I_{IN}	V_{IN+}, V_{REF} = 0		50	60		50	60		50	60	µA
Voltage Range		$-V_S$ + 1.6		$+V_S$ – 1.6	$-V_S$ + 1.6		$+V_S$ – 1.6	$-V_S$ + 1.6		$+V_S$ – 1.6	V
Gain to Output		1 ± 0.0001			1 ± 0.0001			1 ± 0.0001			
POWER SUPPLY											
Operating Range[4]		±2.3		±18	±2.3		±18	±2.3		±18	V
Quiescent Current	V_S = ±2.3 V to ±18 V		0.9	1.3		0.9	1.3		0.9	1.3	mA
Overtemperature			1.1	1.6		1.1	1.6		1.1	1.6	mA
TEMPERATURE RANGE											
For Specified Performance		–40 to +85			–40 to +85			–55 to +125			°C

[1] See Analog Devices military data sheet for 883B tested specifications.
[2] Does not include effects of external resistor R_G.
[3] One input grounded. G = 1.
[4] This is defined as the same supply range that is used to specify PSR.

ABSOLUTE MAXIMUM RATINGS

Table 2.

Parameter	Rating
Supply Voltage	±18 V
Internal Power Dissipation[1]	650 mW
Input Voltage (Common-Mode)	$\pm V_S$
Differential Input Voltage	25 V
Output Short-Circuit Duration	Indefinite
Storage Temperature Range (Q)	−65°C to +150°C
Storage Temperature Range (N, R)	−65°C to +125°C
Operating Temperature Range	
AD620 (A, B)	−40°C to +85°C
AD620 (S)	−55°C to +125°C
Lead Temperature Range	
(Soldering 10 seconds)	300°C

Stresses above those listed under Absolute Maximum Ratings may cause permanent damage to the device. This is a stress rating only; functional operation of the device at these or any other condition s above those indicated in the operational section of this specification is not implied. Exposure to absolute maximum rating conditions for extended periods may affect device reliability.

[1] Specification is for device in free air:
8-Lead Plastic Package: θ_{JA} = 95°C
8-Lead CERDIP Package: θ_{JA} = 110°C
8-Lead SOIC Package: θ_{JA} = 155°C

ESD CAUTION

ESD (electrostatic discharge) sensitive device. Electrostatic charges as high as 4000 V readily accumulate on the human body and test equipment and can discharge without detection. Although this product features proprietary ESD protection circuitry, permanent damage may occur on devices subjected to high energy electrostatic discharges. Therefore, proper ESD precautions are recommended to avoid performance degradation or loss of functionality.

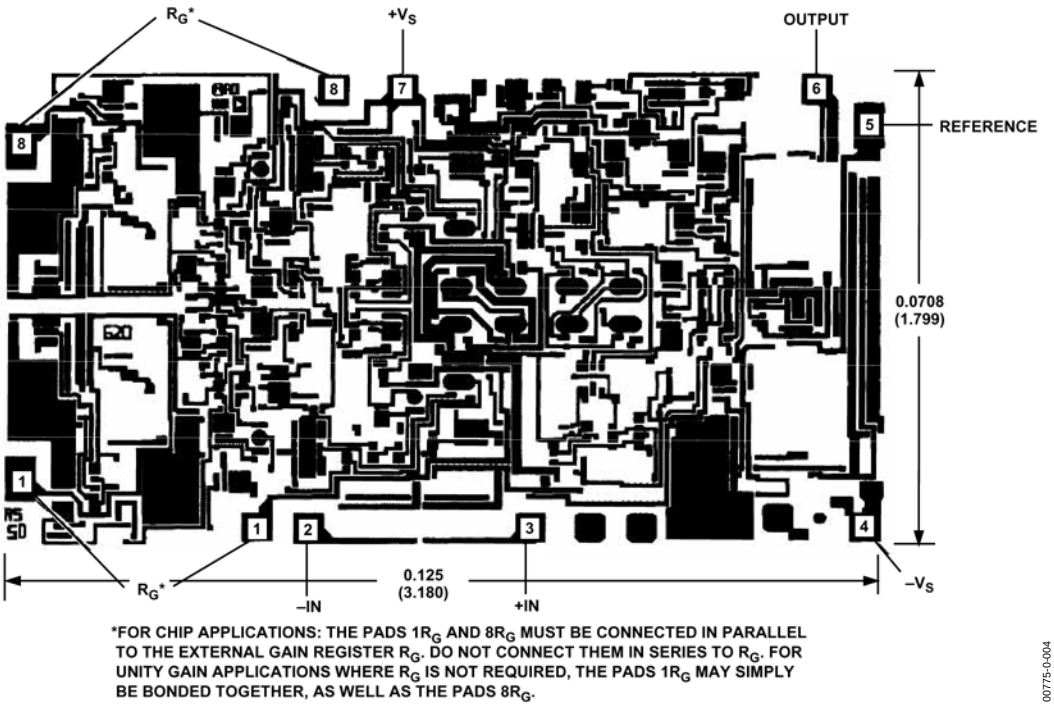

Figure 4. Metallization Photograph.
Dimensions shown in inches and (mm).

Contact sales for latest dimensions.

TYPICAL PERFORMANCE CHARACTERISTICS

(@ 25°C, V_S = ±15 V, R_L = 2 kΩ, unless otherwise noted.)

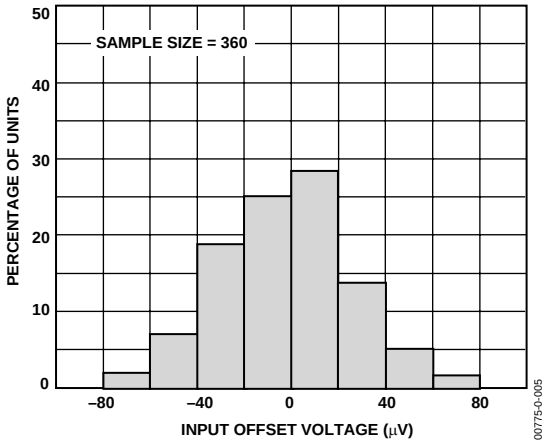

Figure 5. Typical Distribution of Input Offset Voltage

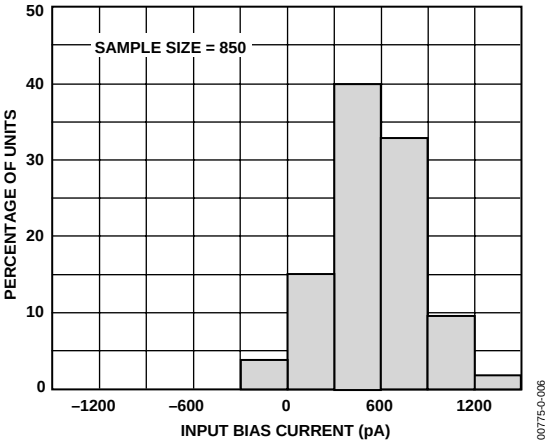

Figure 6. Typical Distribution of Input Bias Current

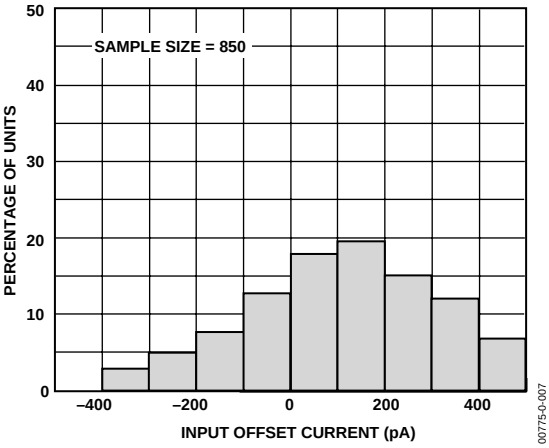

Figure 7. Typical Distribution of Input Offset Current

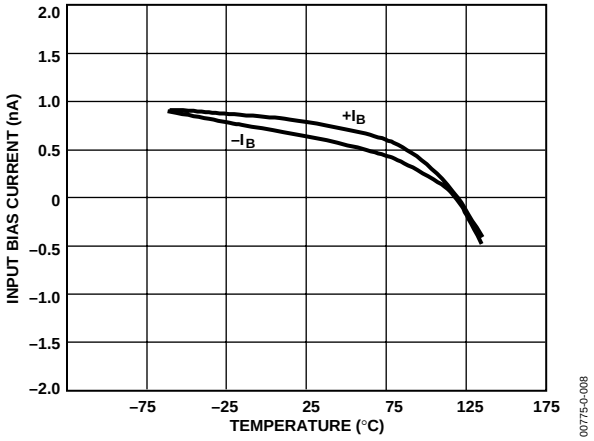

Figure 8. Input Bias Current vs. Temperature

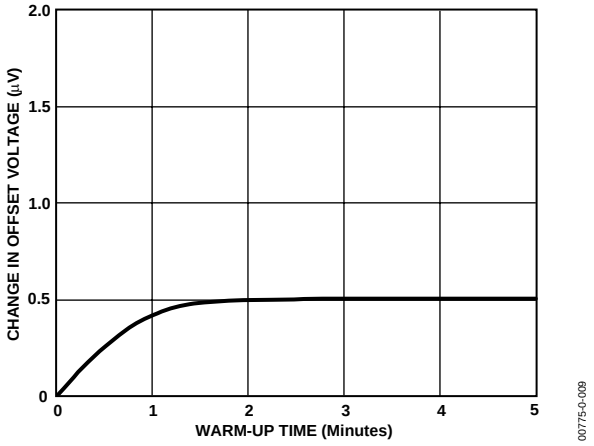

Figure 9. Change in Input Offset Voltage vs. Warm-Up Time

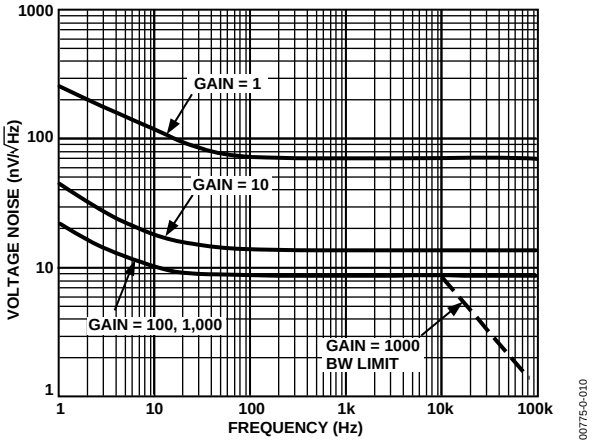

Figure 10. Voltage Noise Spectral Density vs. Frequency (G = 1–1000)

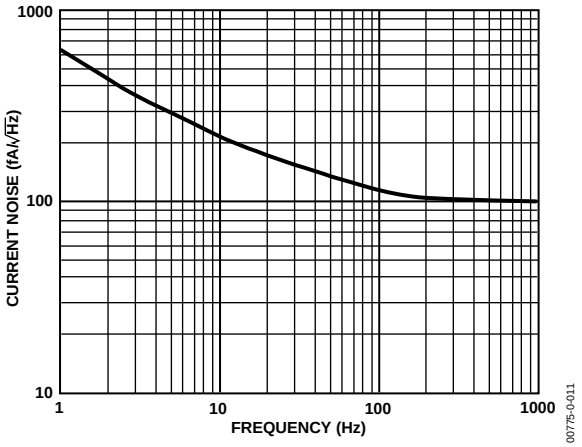

Figure 11. Current Noise Spectral Density vs. Frequency

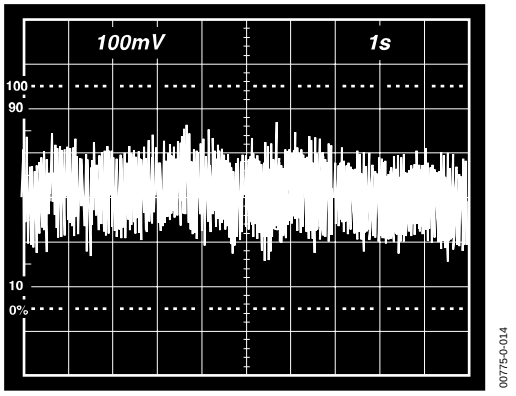

Figure 14. 0.1 Hz to 10 Hz Current Noise, 5 pA/Div

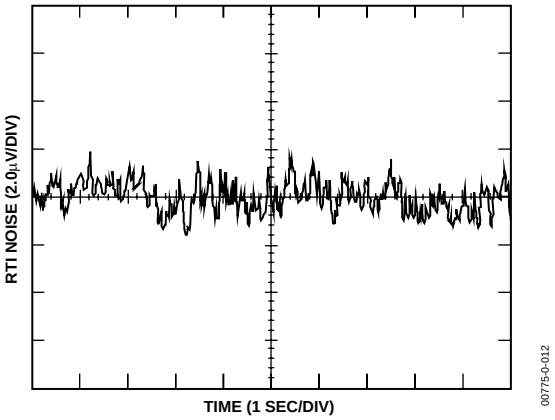

Figure 12. 0.1 Hz to 10 Hz RTI Voltage Noise (G = 1)

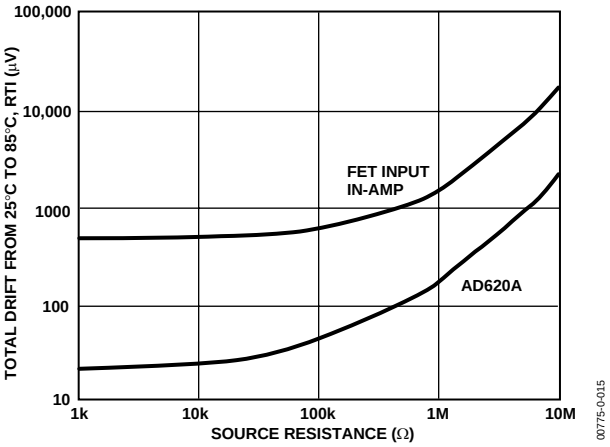

Figure 15. Total Drift vs. Source Resistance

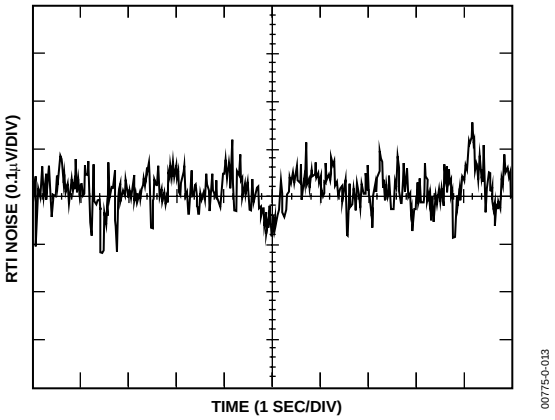

Figure 13. 0.1 Hz to 10 Hz RTI Voltage Noise (G = 1000)

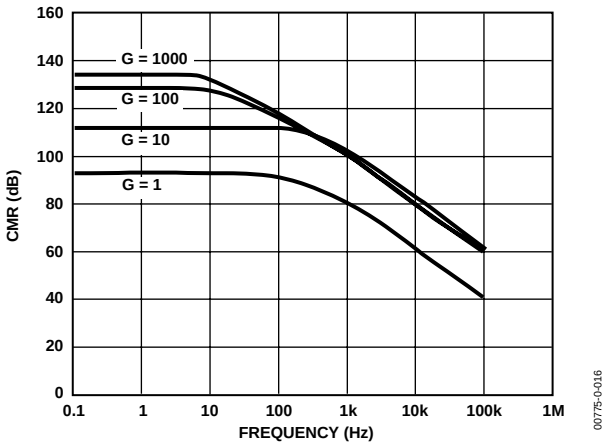

Figure 16. Typical CMR vs. Frequency, RTI, Zero to 1 kΩ Source Imbalance

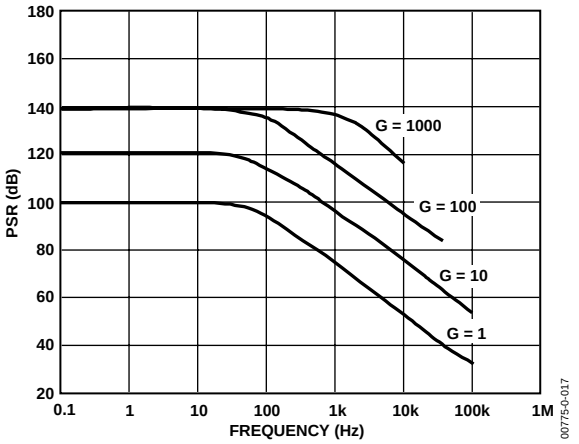

Figure 17. Positive PSR vs. Frequency, RTI (G = 1–1000)

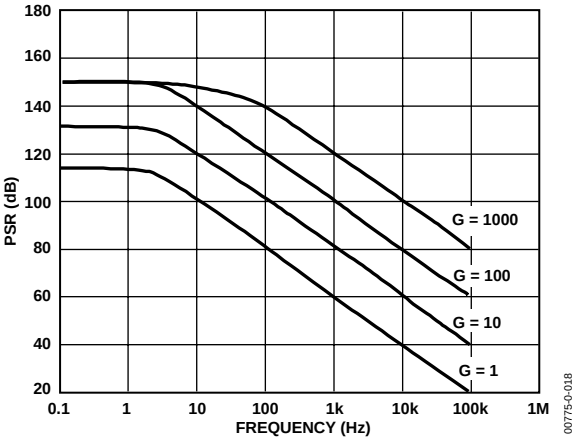

Figure 18. Negative PSR vs. Frequency, RTI (G = 1–1000)

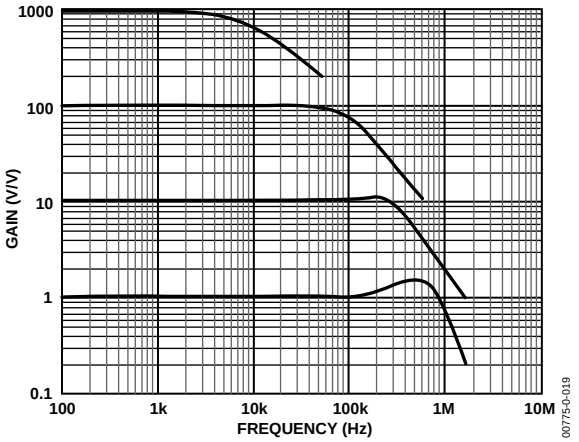

Figure 19. Gain vs. Frequency

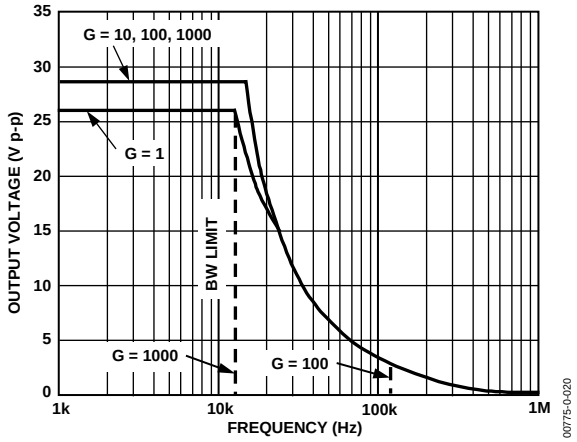

Figure 20. Large Signal Frequency Response

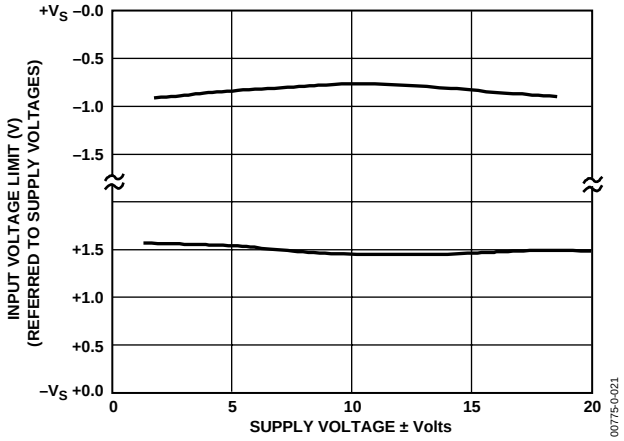

Figure 21. Input Voltage Range vs. Supply Voltage, G = 1

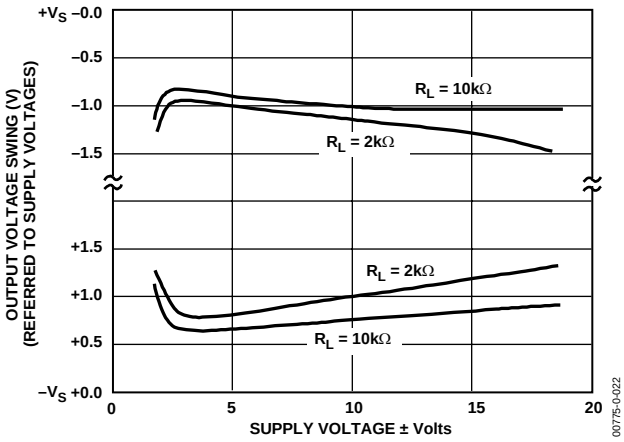

Figure 22. Output Voltage Swing vs. Supply Voltage, G = 10

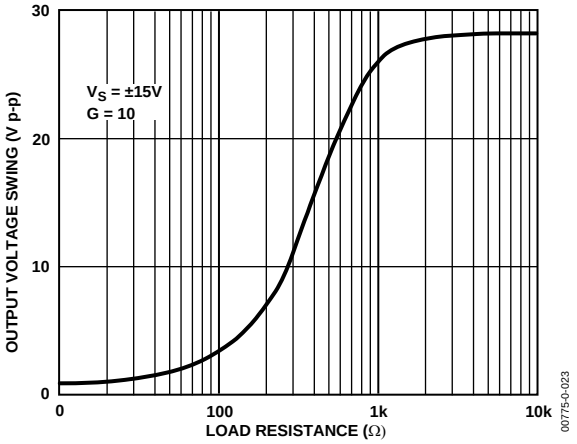

Figure 23. Output Voltage Swing vs. Load Resistance

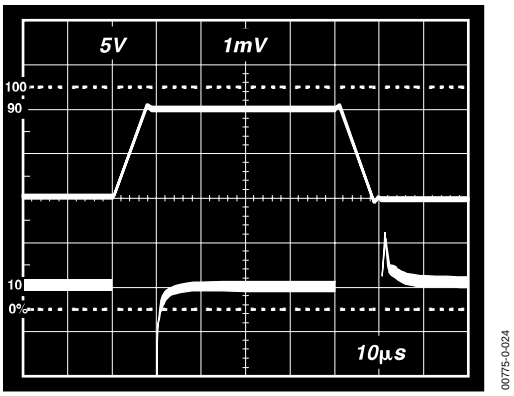

Figure 24. Large Signal Pulse Response and Settling Time G = 1 (0.5 mV = 0.01%)

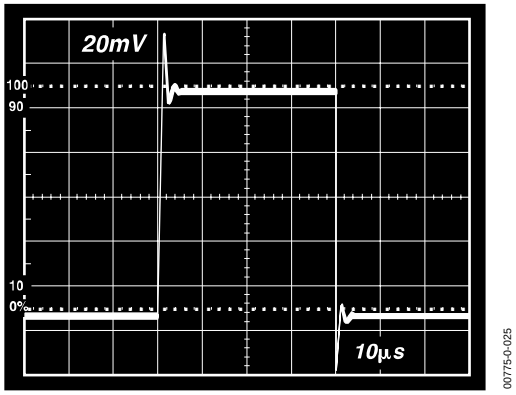

Figure 25. Small Signal Response, G = 1, R_L = 2 kΩ, C_L = 100 pF

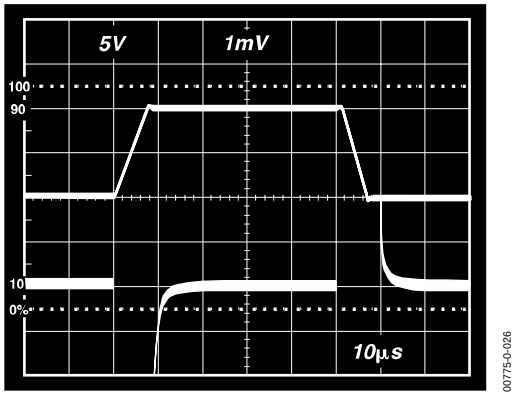

Figure 26. Large Signal Response and Settling Time, G = 10 (0.5 mV = 0.01%)

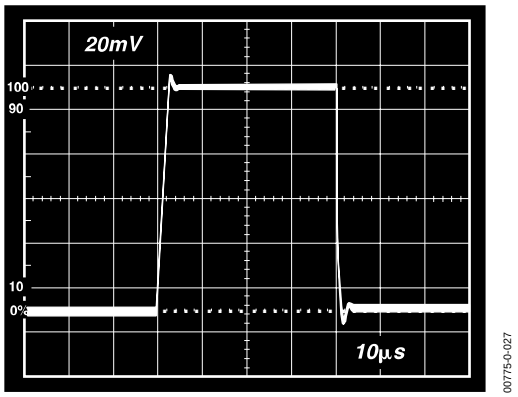

Figure 27. Small Signal Response, G = 10, R_L = 2 kΩ, C_L = 100 pF

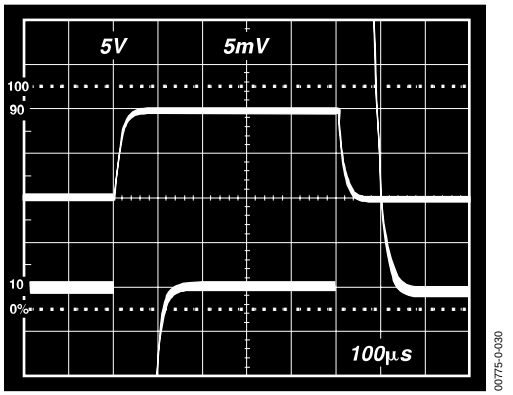

Figure 28. Large Signal Response and Settling Time, G = 100 (0.5 mV = 0.01%)

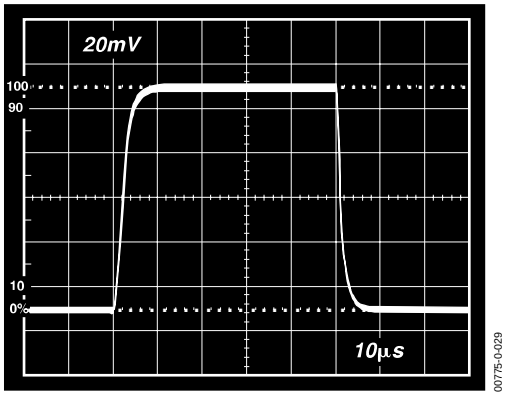

Figure 29. Small Signal Pulse Response, G = 100, R_L = 2 kΩ, C_L = 100 pF

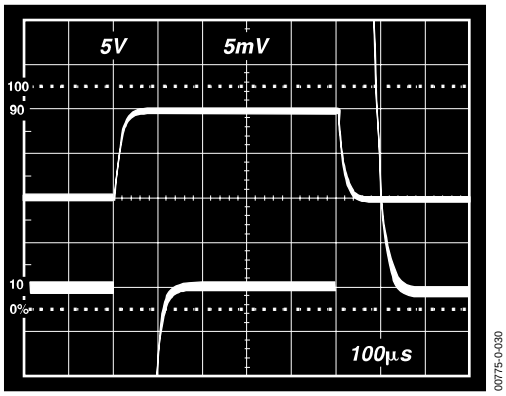

Figure 30. Large Signal Response and Settling Time, G = 1000 (0.5 mV = 0.01%)

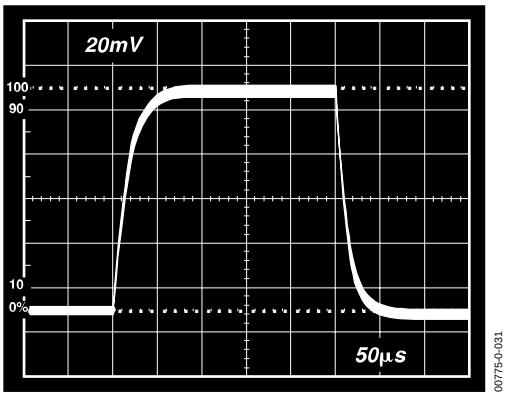

Figure 31. Small Signal Pulse Response, G = 1000, R_L = 2 kΩ, C_L = 100 pF

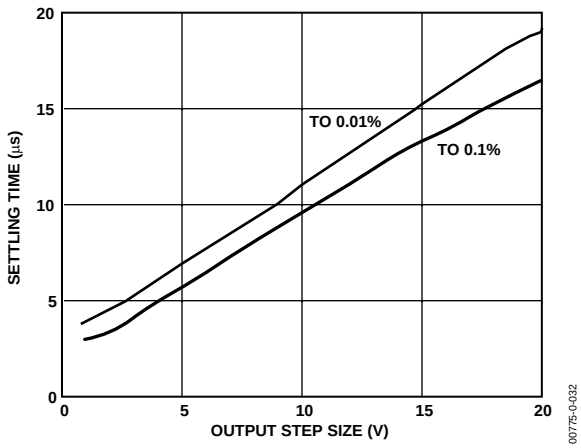

Figure 32. Settling Time vs. Step Size (G = 1)

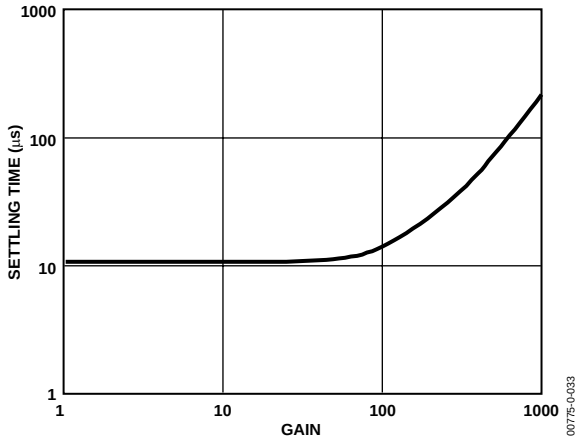

Figure 33. Settling Time to 0.01% vs. Gain, for a 10 V Step

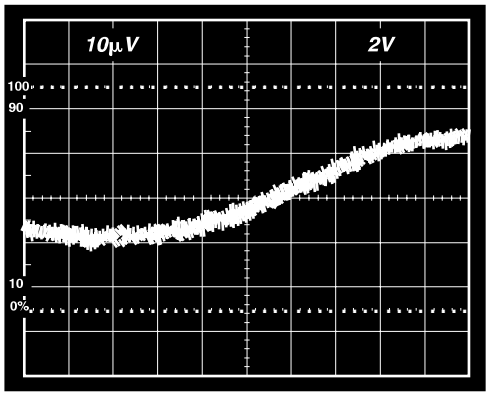

Figure 34. Gain Nonlinearity, G = 1, R_L = 10 kΩ (10 µV = 1 ppm)

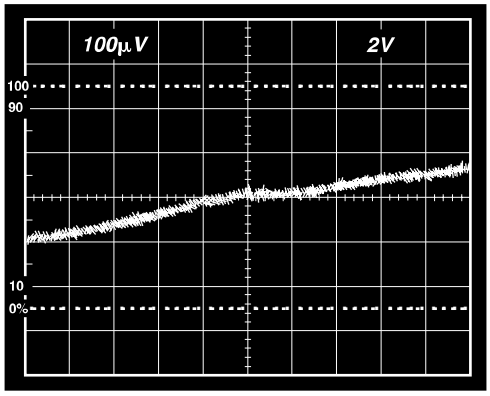

Figure 35. Gain Nonlinearity, G = 100, R_L = 10 kΩ (100 µV = 10 ppm)

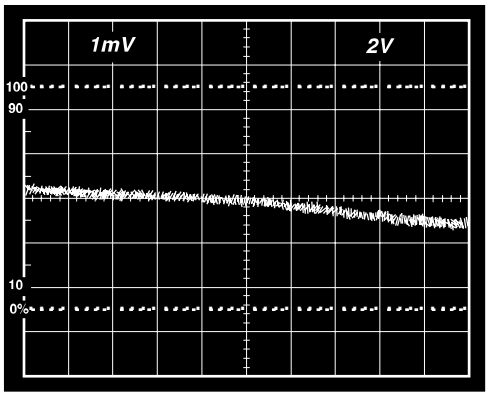

Figure 36. Gain Nonlinearity, G = 1000, R_L = 10 kΩ (1 mV = 100 ppm)

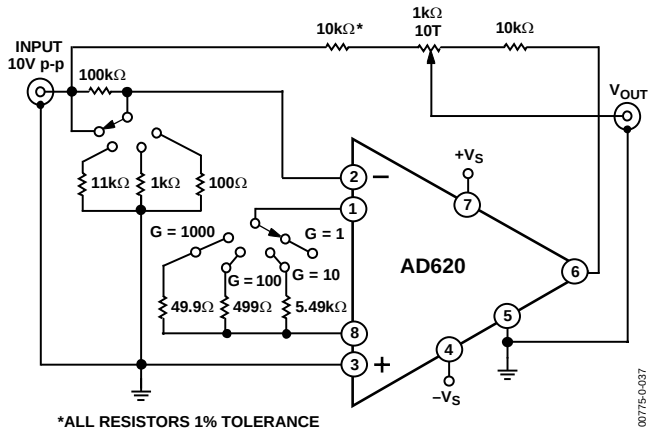

Figure 37. Settling Time Test Circuit

THEORY OF OPERATION

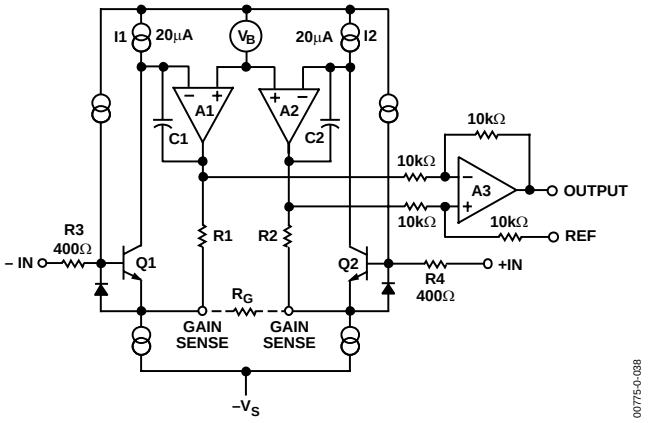

Figure 38. Simplified Schematic of AD620

The AD620 is a monolithic instrumentation amplifier based on a modification of the classic three op amp approach. Absolute value trimming allows the user to program gain *accurately* (to 0.15% at G = 100) with only one resistor. Monolithic construction and laser wafer trimming allow the tight matching and tracking of circuit components, thus ensuring the high level of performance inherent in this circuit.

The input transistors Q1 and Q2 provide a single differential-pair bipolar input for high precision (Figure 38), yet offer 10× lower input bias current thanks to Superβeta processing. Feedback through the Q1-A1-R1 loop and the Q2-A2-R2 loop maintains constant collector current of the input devices Q1 and Q2, thereby impressing the input voltage across the external gain setting resistor R_G. This creates a differential gain from the inputs to the A1/A2 outputs given by $G = (R1 + R2)/R_G + 1$. The unity-gain subtractor, A3, removes any common-mode signal, yielding a single-ended output referred to the REF pin potential.

The value of R_G also determines the transconductance of the preamp stage. As R_G is reduced for larger gains, the transconductance increases asymptotically to that of the input transistors. This has three important advantages: (a) Open-loop gain is boosted for increasing programmed gain, thus reducing gain related errors. (b) The gain-bandwidth product (determined by C1 and C2 and the preamp transconductance) increases with programmed gain, thus optimizing frequency response. (c) The input voltage noise is reduced to a value of 9 nV/√Hz, determined mainly by the collector current and base resistance of the input devices.

The internal gain resistors, R1 and R2, are trimmed to an absolute value of 24.7 kΩ, allowing the gain to be programmed accurately with a single external resistor.

The gain equation is then

$$G = \frac{49.4k\Omega}{R_G} + 1$$

$$R_G = \frac{49.4k\Omega}{G - 1}$$

Make vs. Buy: a Typical Bridge Application Error Budget

The AD620 offers improved performance over "homebrew" three op amp IA designs, along with smaller size, fewer components, and 10× lower supply current. In the typical application, shown in Figure 39, a gain of 100 is required to amplify a bridge output of 20 mV full-scale over the industrial temperature range of −40°C to +85°C. Table 3 shows how to calculate the effect various error sources have on circuit accuracy.

Regardless of the system in which it is being used, the AD620 provides greater accuracy at low power and price. In simple systems, absolute accuracy and drift errors are by far the most significant contributors to error. In more complex systems with an intelligent processor, an autogain/autozero cycle will remove all absolute accuracy and drift errors, leaving only the resolution errors of gain, nonlinearity, and noise, thus allowing full 14-bit accuracy.

Note that for the homebrew circuit, the OP07 specifications for input voltage offset and noise have been multiplied by √2. This is because a three op amp type in-amp has two op amps at its inputs, both contributing to the overall input error.

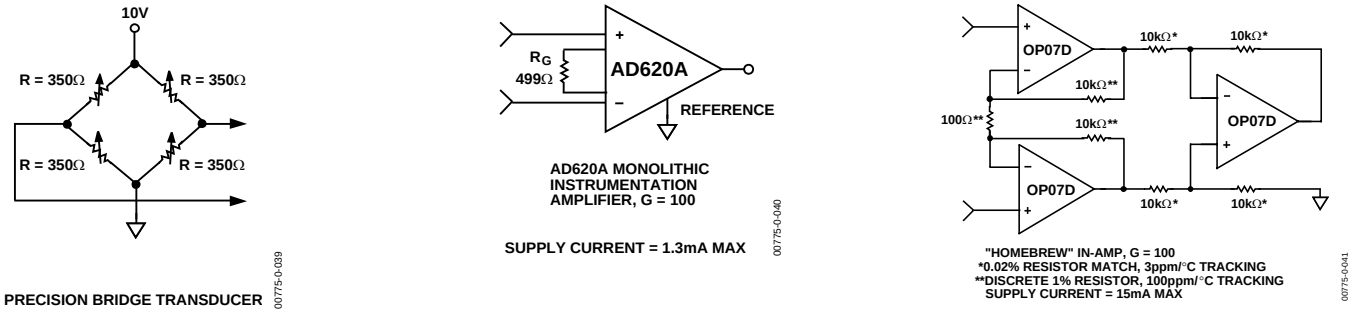

Figure 39. Make vs. Buy

Table 3. Make vs. Buy Error Budget

Error Source	AD620 Circuit Calculation	"Homebrew" Circuit Calculation	Error, ppm of Full Scale AD620	Homebrew
ABSOLUTE ACCURACY at T_A = 25°C				
Input Offset Voltage, µV	125 µV/20 mV	(150 µV × √2)/20 mV	6,250	10,607
Output Offset Voltage, µV	1000 µV/100 mV/20 mV	((150 µV × 2)/100)/20 mV	500	150
Input Offset Current, nA	2 nA ×350 Ω/20 mV	(6 nA ×350 Ω)/20 mV	18	53
CMR, dB	110 dB(3.16 ppm) ×5 V/20 mV	(0.02% Match × 5 V)/20 mV/100	791	500
		Total Absolute Error	7,559	11,310
DRIFT TO 85°C				
Gain Drift, ppm/°C	(50 ppm + 10 ppm) ×60°C	100 ppm/°C Track × 60°C	3,600	6,000
Input Offset Voltage Drift, µV/°C	1 µV/°C × 60°C/20 mV	(2.5 µV/°C × √2 × 60°C)/20 mV	3,000	10,607
Output Offset Voltage Drift, µV/°C	15 µV/°C × 60°C/100 mV/20 mV	(2.5 µV/°C × 2 × 60°C)/100 mV/20 mV	450	150
		Total Drift Error	7,050	16,757
RESOLUTION				
Gain Nonlinearity, ppm of Full Scale	40 ppm	40 ppm	40	40
Typ 0.1 Hz to 10 Hz Voltage Noise, µV p-p	0.28 µV p-p/20 mV	(0.38 µV p-p × √2)/20 mV	14	27
		Total Resolution Error	54	67
		Grand Total Error	14,663	28,134

G = 100, V_S = ±15 V.
(All errors are min/max and referred to input.)

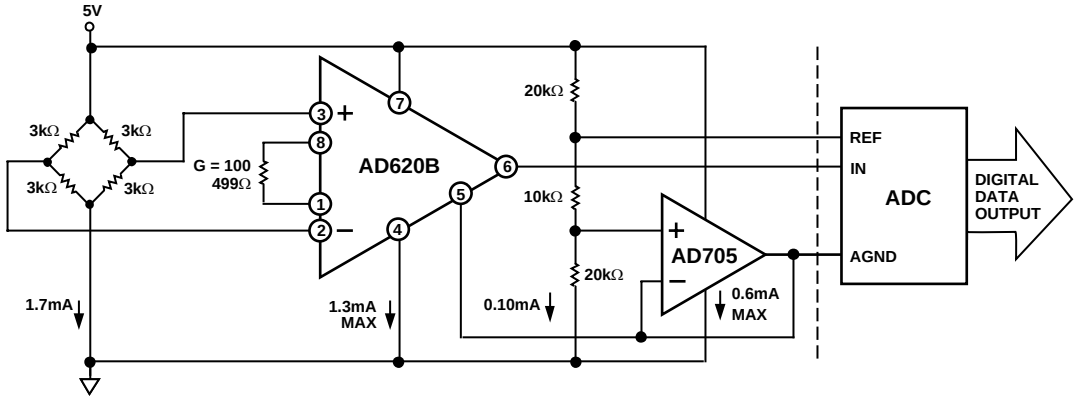

Figure 40. A Pressure Monitor Circuit that Operates on a 5 V Single Supply

Pressure Measurement

Although useful in many bridge applications, such as weigh scales, the AD620 is especially suitable for higher resistance pressure sensors powered at lower voltages where small size and low power become more significant.

Figure 40 shows a 3 kΩ pressure transducer bridge powered from 5 V. In such a circuit, the bridge consumes only 1.7 mA. Adding the AD620 and a buffered voltage divider allows the signal to be conditioned for only 3.8 mA of total supply current.

Small size and low cost make the AD620 especially attractive for voltage output pressure transducers. Since it delivers low noise and drift, it will also serve applications such as diagnostic noninvasive blood pressure measurement.

Medical ECG

The low current noise of the AD620 allows its use in ECG monitors (Figure 41) where high source resistances of 1 MΩ or higher are not uncommon. The AD620's low power, low supply voltage requirements, and space-saving 8-lead mini-DIP and SOIC package offerings make it an excellent choice for battery-powered data recorders.

Furthermore, the low bias currents and low current noise, coupled with the low voltage noise of the AD620, improve the dynamic range for better performance.

The value of capacitor C1 is chosen to maintain stability of the right leg drive loop. Proper safeguards, such as isolation, must be added to this circuit to protect the patient from possible harm.

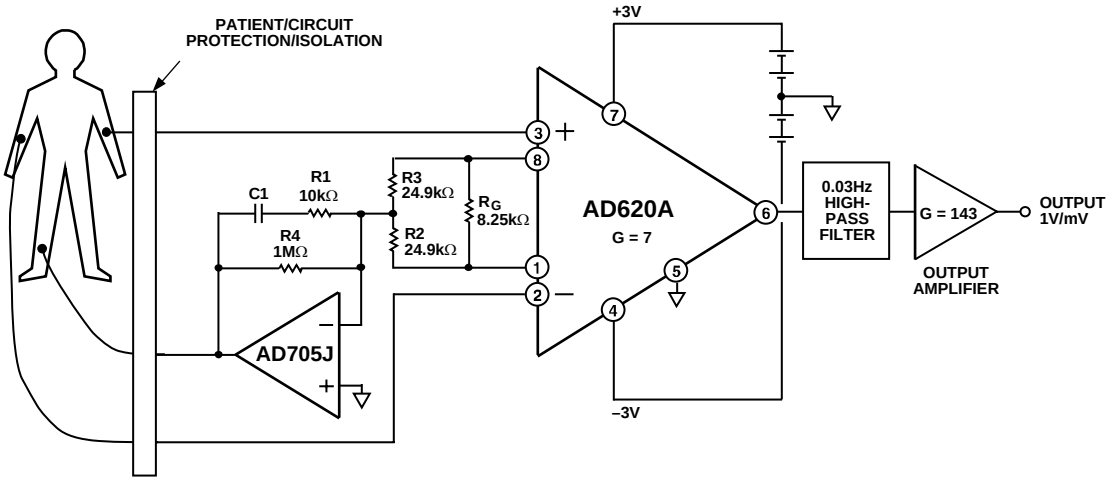

Figure 41. A Medical ECG Monitor Circuit

Precision V-I Converter

The AD620, along with another op amp and two resistors, makes a precision current source (Figure 42). The op amp buffers the reference terminal to maintain good CMR. The output voltage, V_X, of the AD620 appears across R1, which converts it to a current. This current, less only the input bias current of the op amp, then flows out to the load.

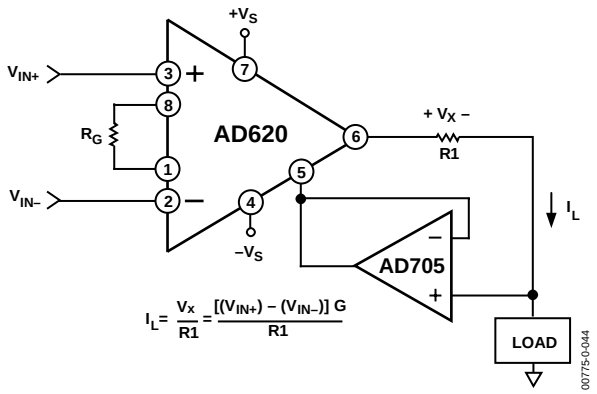

Figure 42. Precision Voltage-to-Current Converter (Operates on 1.8 mA, ±3 V)

GAIN SELECTION

The AD620's gain is resistor-programmed by R_G, or more precisely, by whatever impedance appears between Pins 1 and 8. The AD620 is designed to offer accurate gains using 0.1% to 1% resistors. Table 4 shows required values of R_G for various gains. Note that for G = 1, the R_G pins are unconnected ($R_G = \infty$). For any arbitrary gain, R_G can be calculated by using the formula:

$$R_G = \frac{49.4k\Omega}{G-1}$$

To minimize gain error, avoid high parasitic resistance in series with R_G; to minimize gain drift, R_G should have a low TC—less than 10 ppm/°C—for the best performance.

Table 4. Required Values of Gain Resistors

1% Std Table Value of R_G(Ω)	Calculated Gain	0.1% Std Table Value of R_G(Ω)	Calculated Gain
49.9 k	1.990	49.3 k	2.002
12.4 k	4.984	12.4 k	4.984
5.49 k	9.998	5.49 k	9.998
2.61 k	19.93	2.61 k	19.93
1.00 k	50.40	1.01 k	49.91
499	100.0	499	100.0
249	199.4	249	199.4
100	495.0	98.8	501.0
49.9	991.0	49.3	1,003.0

INPUT AND OUTPUT OFFSET VOLTAGE

The low errors of the AD620 are attributed to two sources, input and output errors. The output error is divided by *G* when referred to the input. In practice, the input errors dominate at high gains, and the output errors dominate at low gains. The total V_{OS} for a given gain is calculated as

Total Error RTI = input error + (output error/G)

Total Error RTO = (input error × G) + output error

REFERENCE TERMINAL

The reference terminal potential defines the zero output voltage and is especially useful when the load does not share a precise ground with the rest of the system. It provides a direct means of injecting a precise offset to the output, with an allowable range of 2 V within the supply voltages. Parasitic resistance should be kept to a minimum for optimum CMR.

INPUT PROTECTION

The AD620 features 400 Ω of series thin film resistance at its inputs and will safely withstand input overloads of up to ±15 V or ±60 mA for several hours. This is true for all gains and power on and off, which is particularly important since the signal source and amplifier may be powered separately. For longer time periods, the current should not exceed 6 mA ($I_{IN} \le V_{IN}/400\ \Omega$). For input overloads beyond the supplies, clamping the inputs to the supplies (using a low leakage diode such as an FD333) will reduce the required resistance, yielding lower noise.

RF INTERFERENCE

All instrumentation amplifiers rectify small out of band signals. The disturbance may appear as a small dc voltage offset. High frequency signals can be filtered with a low pass R-C network placed at the input of the instrumentation amplifier. Figure 43 demonstrates such a configuration. The filter limits the input signal according to the following relationship:

$$FilterFreq_{DIFF} = \frac{1}{2\pi R(2C_D + C_C)}$$

$$FilterFreq_{CM} = \frac{1}{2\pi RC_C}$$

where $C_D \ge 10C_C$.

C_D affects the difference signal. C_C affects the common-mode signal. Any mismatch in $R \times C_C$ will degrade the AD620's CMRR. To avoid inadvertently reducing CMRR-bandwidth performance, make sure that C_C is at least one magnitude smaller than C_D. The effect of mismatched C_Cs is reduced with a larger C_D:C_C ratio.

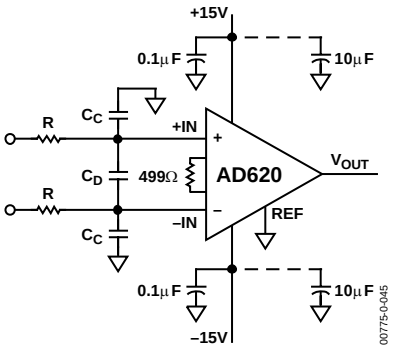

Figure 43. Circuit to Attenuate RF Interference

COMMON-MODE REJECTION

Instrumentation amplifiers, such as the AD620, offer high CMR, which is a measure of the change in output voltage when both inputs are changed by equal amounts. These specifications are usually given for a full-range input voltage change and a specified source imbalance.

For optimal CMR, the reference terminal should be tied to a low impedance point, and differences in capacitance and resistance should be kept to a minimum between the two inputs. In many applications, shielded cables are used to minimize noise; for best CMR over frequency, the shield should be properly driven. Figure 44 and Figure 45 show active data guards that are configured to improve ac common-mode rejections by "bootstrapping" the capacitances of input cable shields, thus minimizing the capacitance mismatch between the inputs.

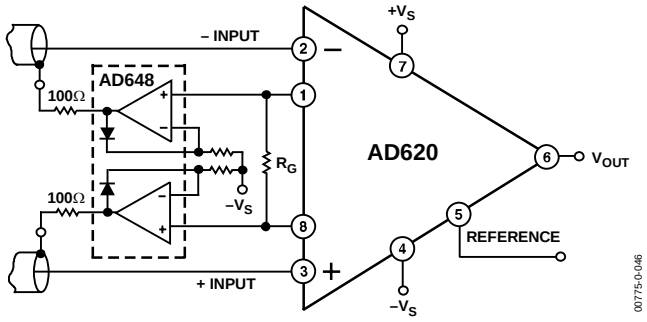

Figure 44. Differential Shield Driver

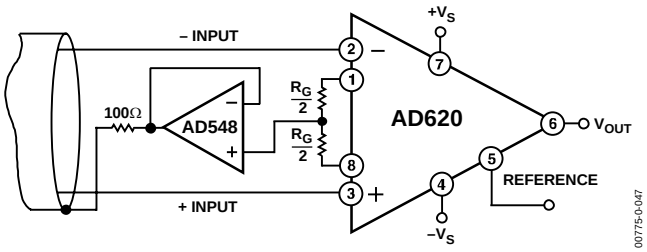

Figure 45. Common-Mode Shield Driver

GROUNDING

Since the AD620 output voltage is developed with respect to the potential on the reference terminal, it can solve many grounding problems by simply tying the REF pin to the appropriate "local ground."

To isolate low level analog signals from a noisy digital environment, many data-acquisition components have separate analog and digital ground pins (Figure 46). It would be convenient to use a single ground line; however, current through ground wires and PC runs of the circuit card can cause hundreds of millivolts of error. Therefore, separate ground returns should be provided to minimize the current flow from the sensitive points to the system ground. These ground returns must be tied together at some point, usually best at the ADC package shown in Figure 46.

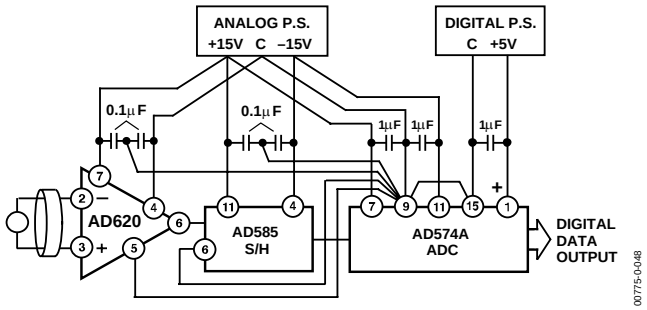

Figure 46. Basic Grounding Practice

GROUND RETURNS FOR INPUT BIAS CURRENTS

Input bias currents are those currents necessary to bias the input transistors of an amplifier. There must be a direct return path for these currents. Therefore, when amplifying "floating" input sources, such as transformers or ac-coupled sources, there must be a dc path from each input to ground, as shown in Figure 47, Figure 48, and Figure 49. Refer to *A Designer's Guide to Instrumentation Amplifiers* (free from Analog Devices) for more information regarding in-amp applications.

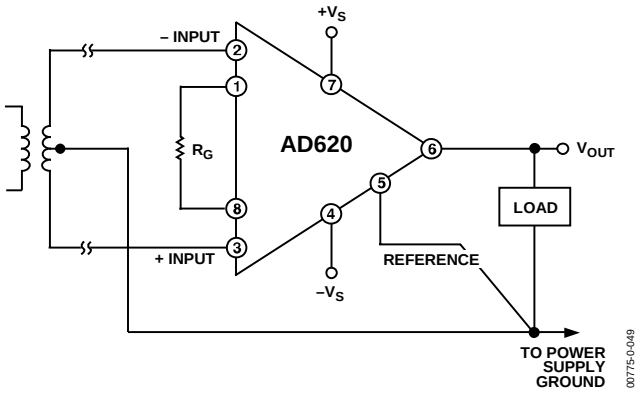

Figure 47. Ground Returns for Bias Currents with Transformer-Coupled Inputs

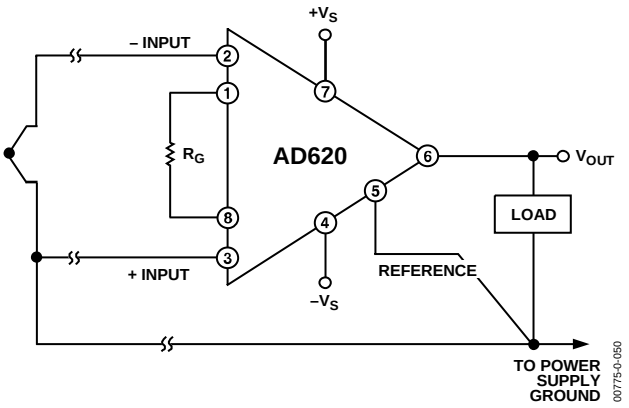

Figure 48. Ground Returns for Bias Currents with Thermocouple Inputs

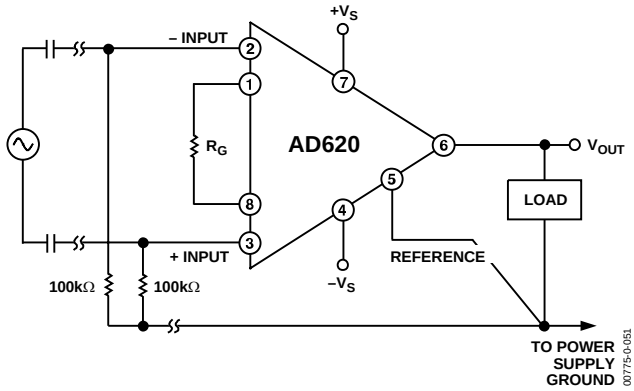

Figure 49. Ground Returns for Bias Currents with AC-Coupled Inputs

OUTLINE DIMENSIONS

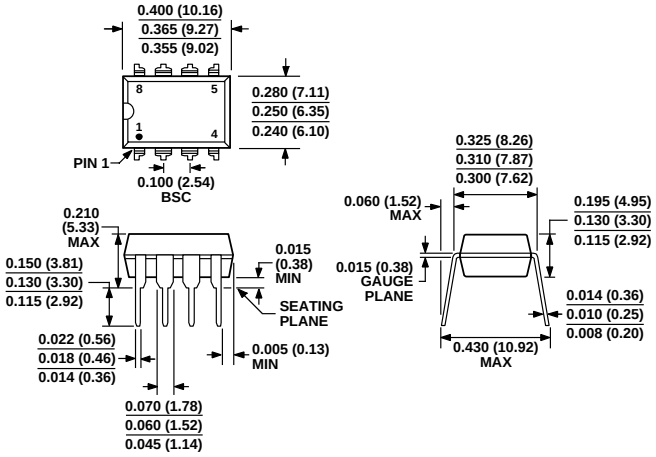

COMPLIANT TO JEDEC STANDARDS MS-001-BA
CONTROLLING DIMENSIONS ARE IN INCHES; MILLIMETER DIMENSIONS (IN PARENTHESES) ARE ROUNDED-OFF INCH EQUIVALENTS FOR REFERENCE ONLY AND ARE NOT APPROPRIATE FOR USE IN DESIGN. CORNER LEADS MAY BE CONFIGURED AS WHOLE OR HALF LEADS.

Figure 50. 8-Lead Plastic Dual In-Line Package [PDIP]

Narrow Body (N-8).
Dimensions shown in inches and (millimeters)

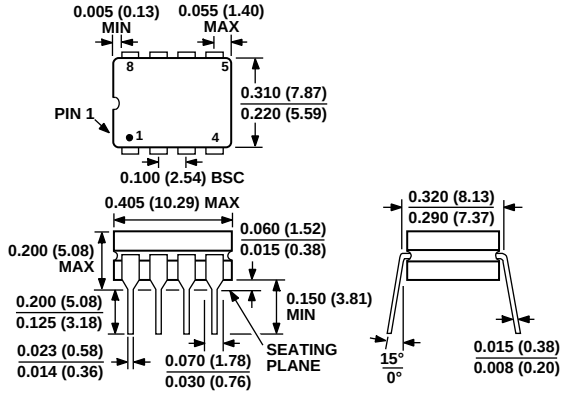

CONTROLLING DIMENSIONS ARE IN INCHES; MILLIMETER DIMENSIONS (IN PARENTHESES) ARE ROUNDED-OFF INCH EQUIVALENTS FOR REFERENCE ONLY AND ARE NOT APPROPRIATE FOR USE IN DESIGN

Figure 51. 8-Lead Ceramic Dual In-Line Package [CERDIP] (Q-8)
Dimensions shown in inches and (millimeters)

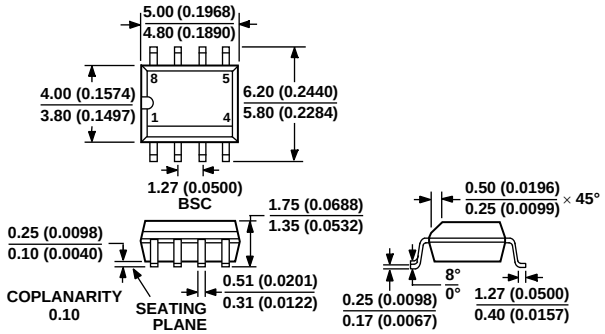

COMPLIANT TO JEDEC STANDARDS MS-012AA
CONTROLLING DIMENSIONS ARE IN MILLIMETERS; INCH DIMENSIONS (IN PARENTHESES) ARE ROUNDED-OFF MILLIMETER EQUIVALENTS FOR REFERENCE ONLY AND ARE NOT APPROPRIATE FOR USE IN DESIGN

Figure 52. 8-Lead Standard Small Outline Package [SOIC]

Narrow Body (R-8)
Dimensions shown in millimeters and (inches)

ORDERING GUIDE

Model	Temperature Range	Package Option[1]
AD620AN	−40°C to +85°C	N-8
AD620ANZ[2]	−40°C to +85°C	N-8
AD620BN	−40°C to +85°C	N-8
AD620BNZ[2]	−40°C to +85°C	N-8
AD620AR	−40°C to +85°C	R-8
AD620ARZ[2]	−40°C to +85°C	R-8
AD620AR-REEL	−40°C to +85°C	13" REEL
AD620ARZ-REEL[2]	−40°C to +85°C	13" REEL
AD620AR-REEL7	−40°C to +85°C	7" REEL
AD620ARZ-REEL7[2]	−40°C to +85°C	7" REEL
AD620BR	−40°C to +85°C	R-8
AD620BRZ[2]	−40°C to +85°C	R-8
AD620BR-REEL	−40°C to +85°C	13" REEL
AD620BRZ-RL[2]	−40°C to +85°C	13" REEL
AD620BR-REEL7	−40°C to +85°C	7" REEL
AD620BRZ-R7[2]	−40°C to +85°C	7" REEL
AD620ACHIPS	−40°C to +85°C	Die Form
AD620SQ/883B	−55°C to +125°C	Q-8

[1] N = Plastic DIP; Q = CERDIP; R = SOIC.
[2] Z = Pb-free part.

C00775–0–12/04(G)

Result of EMG:

From diabetic foot ulcer patient:

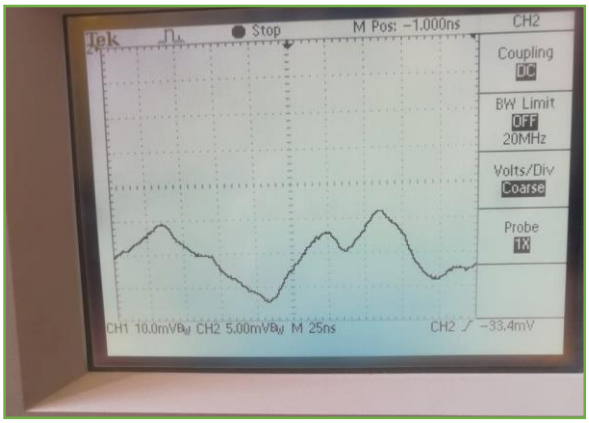

Figure 1

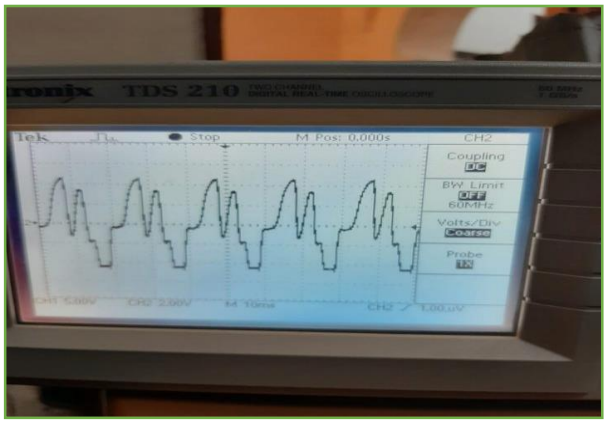

Figure 2

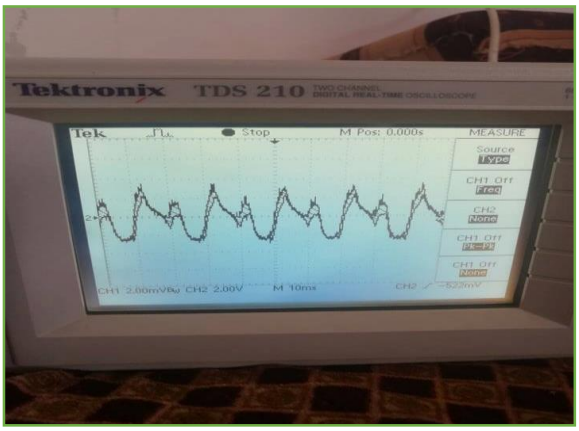

Figure 3

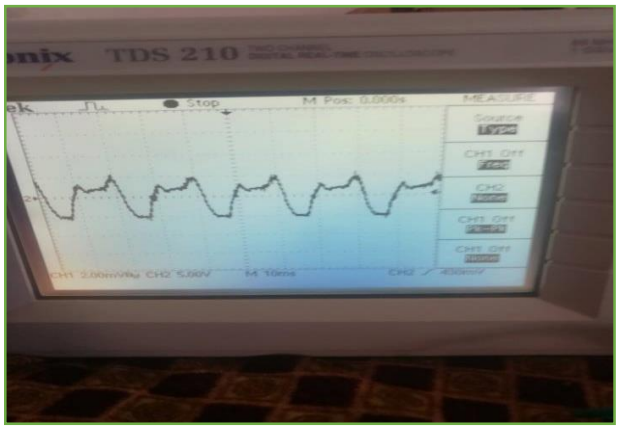

Figure 4

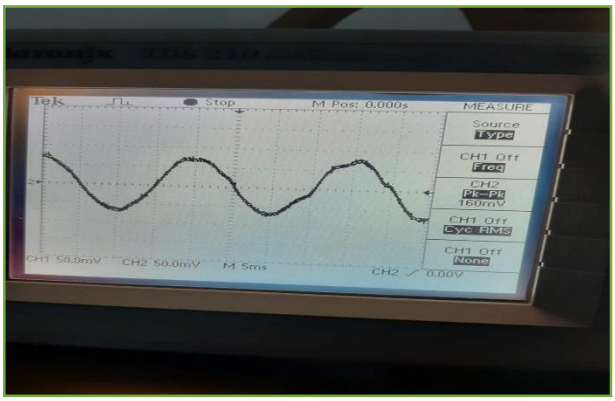

Figure 5

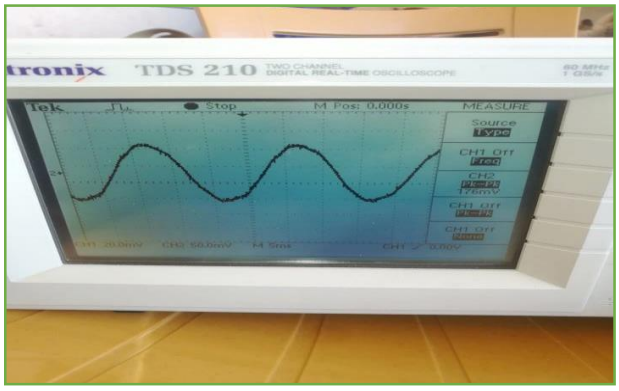

Figure 6

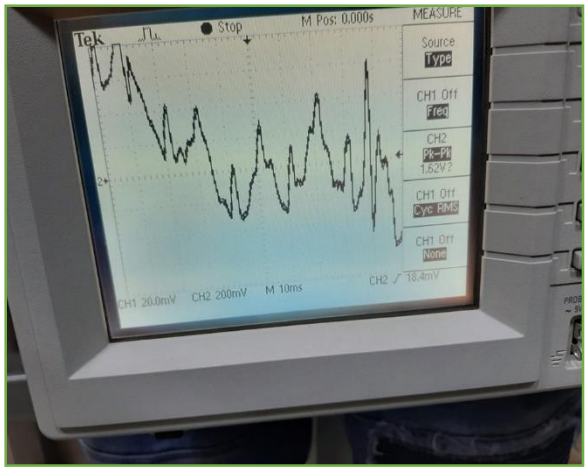

Figure 7

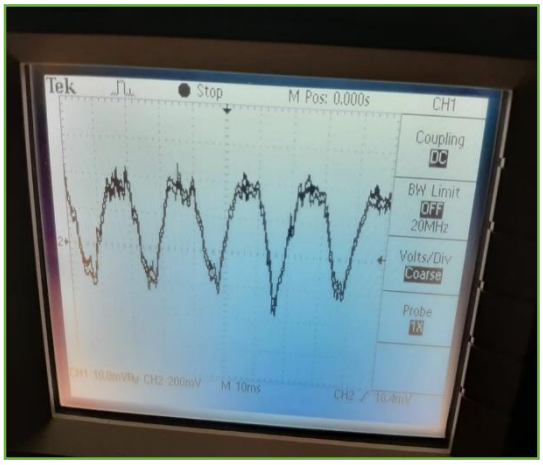

Figure 8

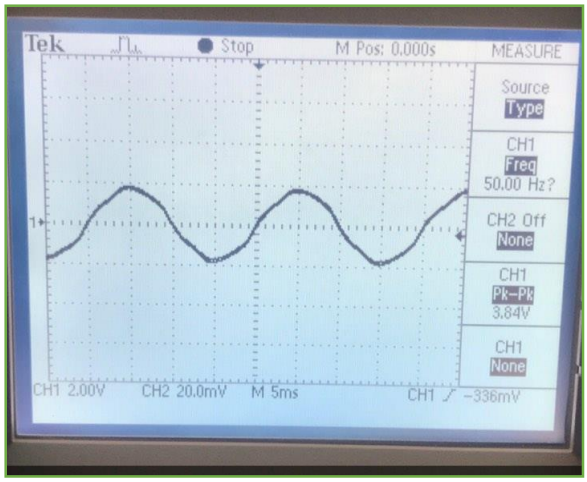

Figure 9

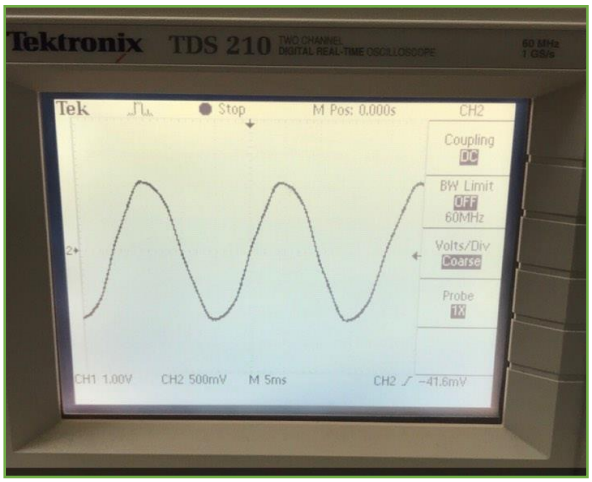

Figure 10

From diabetic patient:

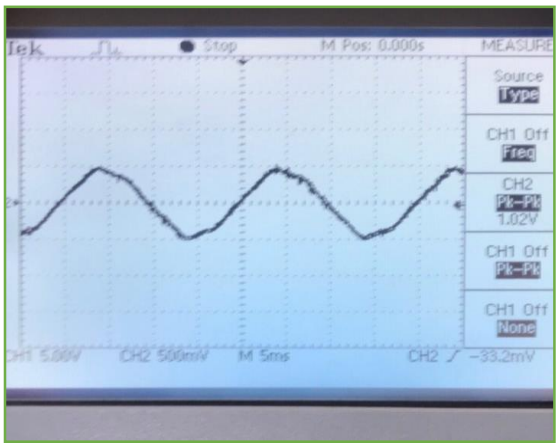

Figure 11

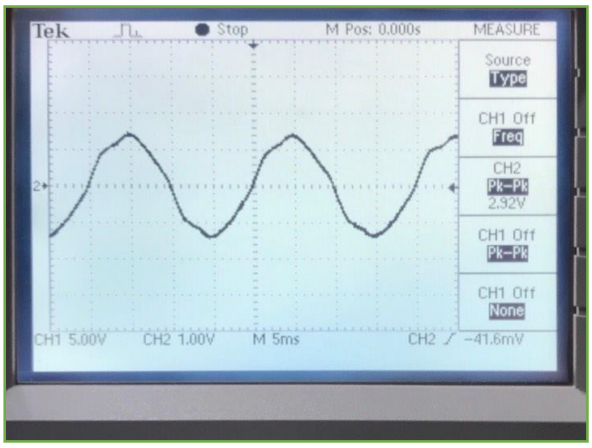

Figure 12

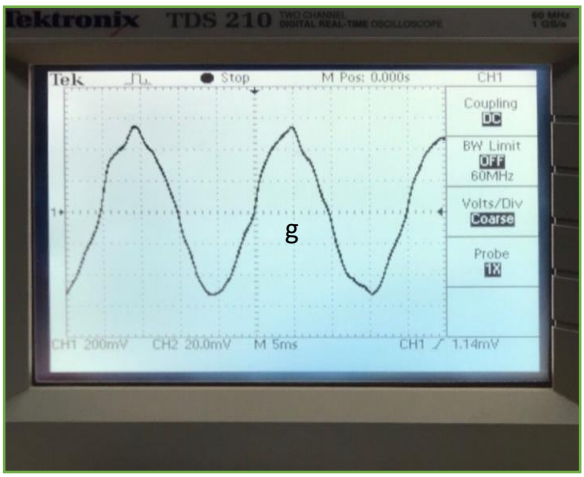

Figure 13

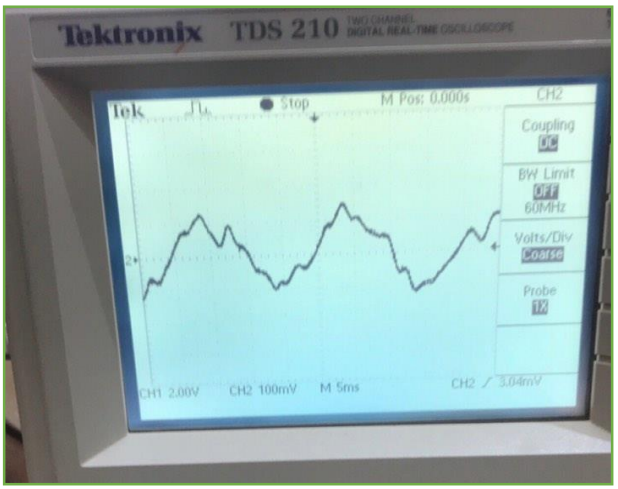

Figure 14

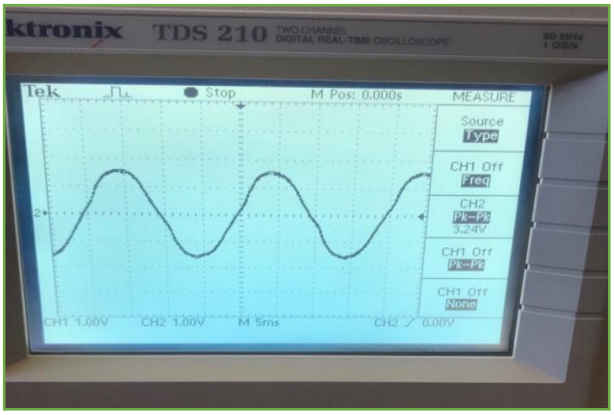

Figure 15

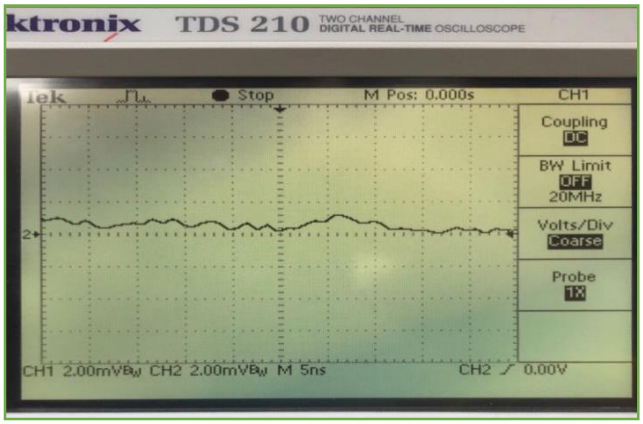

Figure 16

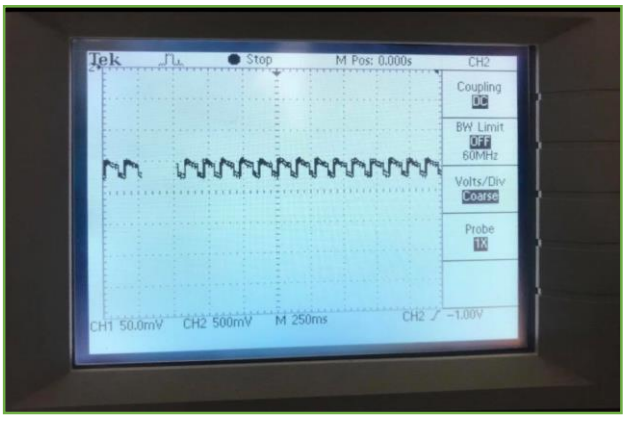

Figure 17

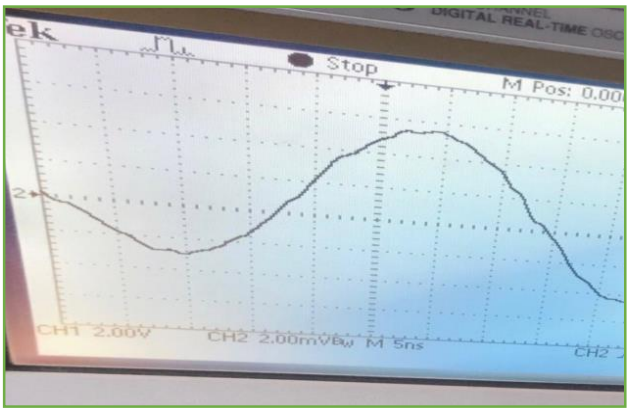

Figure 18

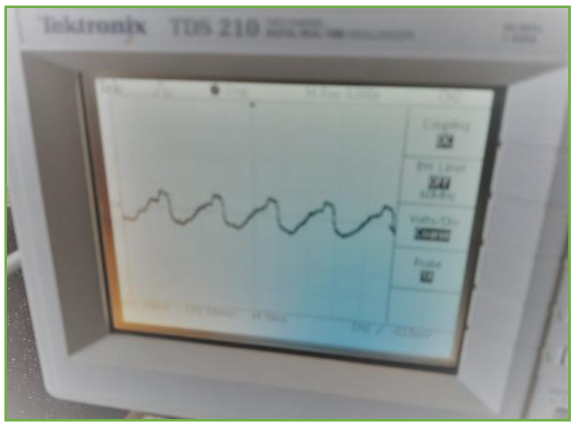

Figure 19

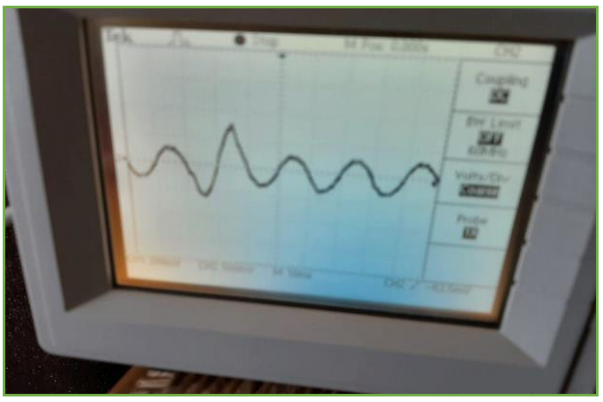

Figure 20

From normal patient:

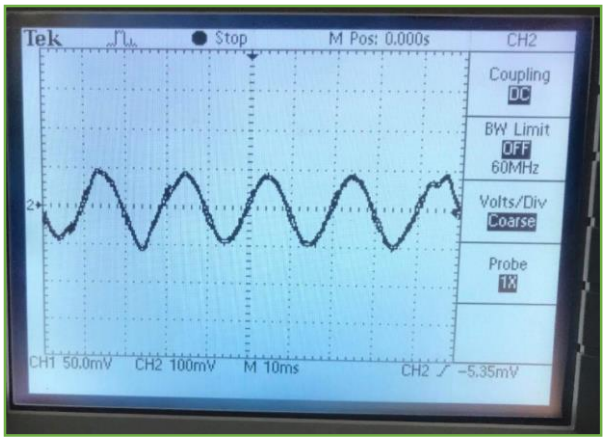

Figure 21

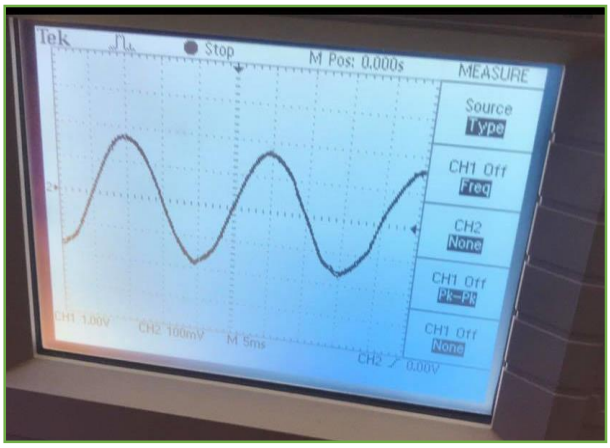

Figure 22

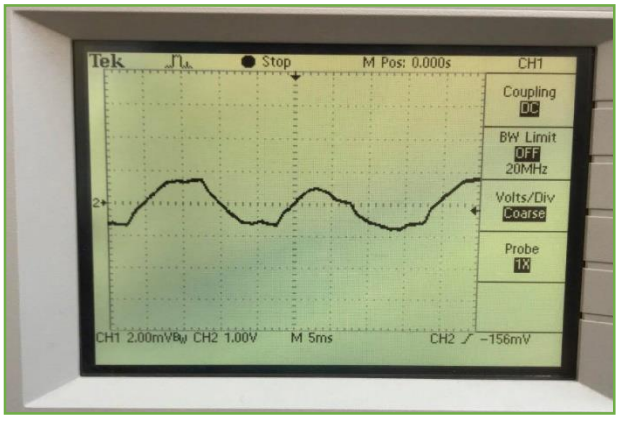

Figure 23

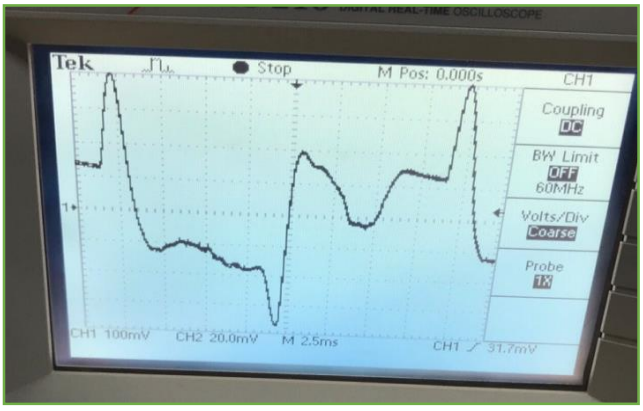

Figure 24

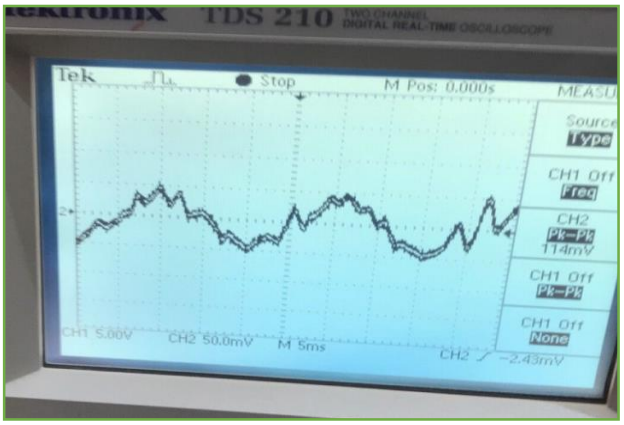

Figure 25

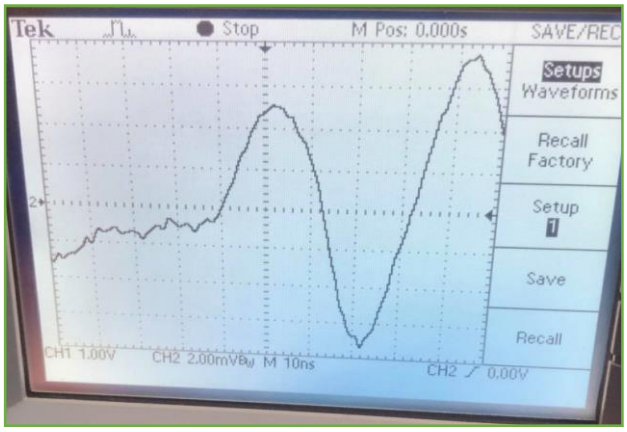

Figure 26

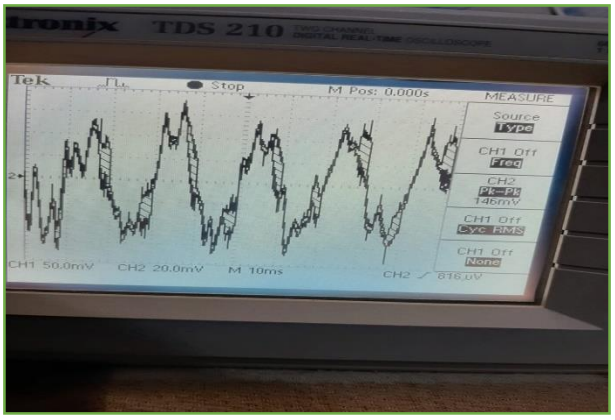

Figure 27

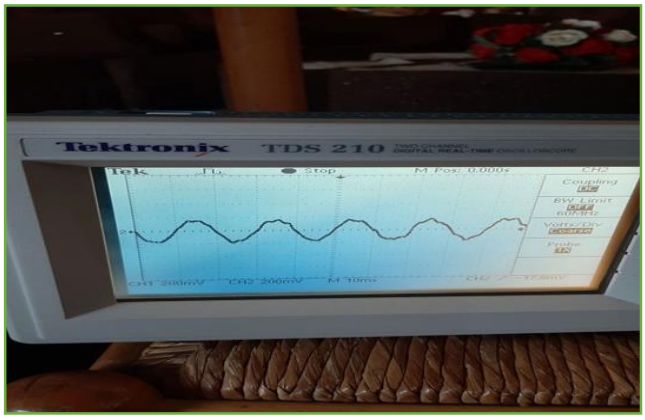

Figure 28

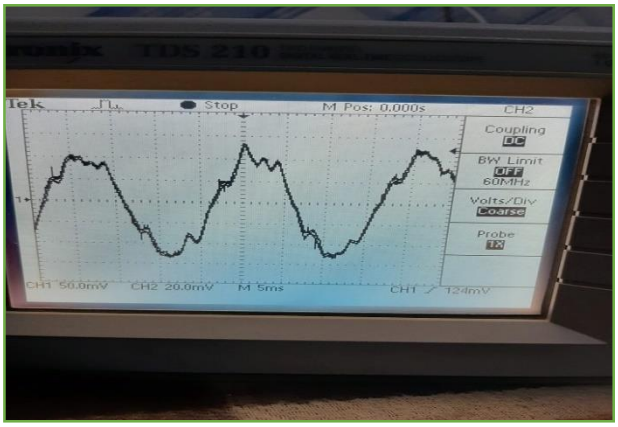

Figure 29

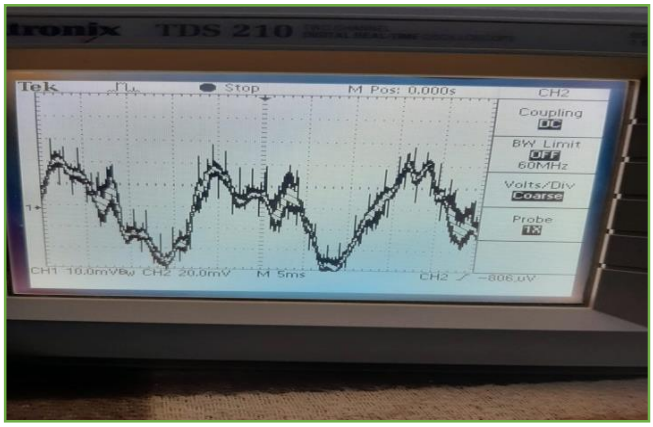

Figure 30

References:

[1] IRANI, ROSHEN N.; SHERMAN, MARY S;" The Pathological Anatomy of Club Foot"; JBJS: January 1963 - Volume 45 - Issue 1 - p 45-52.

[2] Palestinian Ministry of Health;" http://site.moh.ps/ ".

[3] Martha M. Funnel;" National Standards for Diabetes Self-M0anagement Education"; Diabetes Care 2009 Jan; 32(Supplement 1): S87-S94.

[4] N Kawakami, N Takatsuka, H Shimizu and H Ishibashi;" Depressive symptoms and occurrence of type 2 diabetes among Japanese men"; Diabetes Care 1999 Jul; 22(7): 1071-1076.

[5] N. Pound ,S. Chipchase ,K. Treece and F. Game;" Ulcer-free survival following management of foot ulcers in diabetes" ; 13 September 2005.

[6] Pendsey.S. P; "Understanding diabetic foot Int. J. Diabet. Dev. Ctries"; 30(2) 75-9.

[7] Alexiadou K and Doupis J;" Management of diabetic foot ulcers Diabetes Ther"; 3(4) 1-15.

[8] Pendsey.S; "Diabetic Foot: A Clinical Atlas. Jaypee Brothers Medical Publishers" ;.(US National Library of Medicine).

[9] Amit. J; "Amit Jain's system of practice for diabetic foot: the new religion in diabetic foot field"; 5(2); p (368-372).

[10] Hung, K.; Zhang, Y.T.; Tai, B. Wearable Medical Devices for Tele-Home Healthcare. In Proceeding of 26th Annual International Conference of the IEEE Engineering in Medicine and Biology Society (IEMBS '04), San Francisco, CA, USA, 1–5 September 2004; pp. 5384–5387.

[11] Bonato, P. Wearable sensors/systems and their impact on biomedical engineering. IEEE Eng. Med. Biol. Mag. 2003, 22, 18–20.

[12] Rodgers, M. Dynamic biomechanics of the normal foot and ankle during walking and running Phys. Ther. 1988, 68, 1822–1830.

[13] Margolis, D.J.; Knauss, J.; Bilker, W.; Baumgarten, M. Medical conditions as risk factors for pressure ulcers in an outpatient setting. Age Ageing 2003, 32, 259–264.

[14] Yong, F.; Yunjian, G.; Quanjun, S. A Human Identification Method Based on Dynamic Plantar Pressure Distribution. In Proceeding of 2011 IEEE International Conference on Information and Automation (ICIA), Shenzhen, China, 6–8 June 2011; pp. 329–332.

[15] Yamakawa, T.; Taniguchi, K.; Asari, K.; Kobashi, S.; Hata, Y. Biometric Personal Identification Based on Gait Pattern using Both Feet Pressure Change. In Proceeding of

2010 World Automation Congress (WAC), Kobe, Japan, 19–23 September 2010; pp. 1–6.

[16] Sazonov, E.S.; Fulk, G.; Hill, J.; Schutz, Y.; Browning, R. Monitoring of posture allocations and activities by a shoe-based wearable sensor. IEEE Trans. Biomed. Eng. 2011, 58, 983–990.

[17] Neaga, F.; Moga, D.; Petreus, D.; Munteanu, M.; Stroia, N. A Wireless System for Monitoring the Progressive Loading of Lower Limb in Post-Traumatic Rehabilitation. In Proceeding of International Conference on Advancements of Medicine and Health Care through Technology, Cluj-Napoca, Romania, 29 August–2 September 2011; pp. 54–59.

[18] Wada, C.; Sugimura, Y.; Ienaga, T.; Kimuro, Y.; Wada, F.; Hachisuka, K.; Tsuji, T. Development of a Rehabilitation Support System with a Shoe-Type Measurement Device for Walking.

[19] In Proceedings of SICE Annual Conference 2010, Taipei, Taiwan, 18–21 August 2010; pp. 2534–2537.

[20] Edgar, S.R.; Swyka, T.; Fulk, G.; Sazonov, E.S. Wearable Shoe-Based Device for Rehabilitation of Stroke Patients. In Proceeding of 2010 Annual International Conference of the IEEE Engineering in Medicine and Biology Society (EMBC), Buenos Aires, Argentina, 31 August–4 September 2010; pp. 3772–3775.

[21] Wild, S.; Roglic, G.; Green, A.; Sicree, R.; King, H. Global prevalence of diabetes: Estimates for the year 2000 and projections for 2030. Diabetes Care 2004, 27, 1047–1053.

[22] Gioftsidou, A.; Malliou, P.; Pafis, G.; Beneka, A.; Godolias, G.; Maganaris, C. The effects of soccer training and timing of balance training on balance ability. Eur. J. Appl. Phys. 2006, 96,659–664.

[23] Queen, R.; Haynes, B.; Hardaker, W.; Garrett, W. Forefoot loading during 3 athletic tasks. Am. J. Sports Med. 2007, 35, 630–636.

[24] MacWilliams, B.A.; Armstrong, P.F. Clinical Applications of Plantar Pressure Measurement in Pediatric Orthopedics. In Proceeding of Pediatric Gait, 2000. A New Millennium in Clinical Care and Motion Analysis Technology, Chicago, IL, USA, 22 July 2000; pp. 143–150.

[25] Novel Quality in Measurement. Available online: http://www.novel.de/ (accessed on 1 January 2012).

[26] Zebris Medical GmbH. Available online: http://www.zebris.de (accessed on 1 January 2012).

[27] Tekscan. Tactile Pressure Measurement, Pressure Mapping Systems, Force Sensors and Measurement Systems. Available online: http://www.tekscan.com/ (accessed on 1 January 2012).

[28] Bamberg, S.; Benbasat, A.Y.; Scarborough, D.M.; Krebs, D.E.; Paradiso, J.A. Gait analysis using a shoe-integrated wireless sensor system. IEEE Trans. Inf. Technol. Biomed. 2008, 12, 413–423.

[29] Tanwar, H.; Nguyen, L.; Stergiou, N. Force Sensitive Resistor (FSR)-Based Wireless Gait Analysis Device. In Proceeding of The Third IASTED International Conference on Telehealth, Montreal, QC, Canada, 31 May–1 June 2007.

[30] Lee, N.; Goonetilleke, R.; Cheung, Y.; So, G. A flexible encapsulated MEMS pressure sensor system for biomechanical applications. J. Microsyst. Technol. 2001, 7, 55–62.

[31] Shu, L.; Hua, T.; Wang, Y.; Li, Q.; Feng, D.; Tao, X. In-shoe plantar pressure measurement and analysis system based on fabric pressure sensing array. IEEE Trans. Inf. Technol. Biomed. 2009, 14, 767–775.

[32] Urry, S. Plantar pressure-measurement sensors. Meas. Sci. Technol. 1999, 10, doi: 10.1088/ 0957-0233/10/1/017.

[33] Luo, Z.; Berglund, L.; an, K. Validation of F-Scan pressure sensor system: A technical note.Development 1998, 35, 186–191.

[34] Madou, M. MEMS Fabrication. In The MEMS Handbook; CRC Press: Boca Raton, FL, USA, 2001.

[35] Windle, C.M.; Gregory, S.M.; Dixon, S.J. The shock attenuation characteristics of four different insoles when worn in a military boot during running and marching. Gait Posture 1999, 9, 31–37.

[36] Wahab, Y.; Zayegh, A.; Begg, R.K.; Veljanovski, R. Design of MEMS Biomedical Pressure Sensor for Gait Analysis. In Proceeding of IEEE International Conference on Semiconductor Electronics, 2008 (ICSE), Johor Bahru, Malaysia, 25–27 November 2008; pp. 166–169.

[37] Zhu, H.; Maalej, N.; Webster, J.G.; Tompkins, W.J.; Bach-Y-Rita, P.; Wertsch, J.J. An umbilical data-acquisition system for measuring pressures between the foot and shoe. IEEE Trans. Biomed.Eng. 1990, 37, 908–911.

[38] Zhu, H.; Wertsch, J.; Harris, G.; Loftsgaarden, J.; Price, M. Foot pressure distribution during walking and shuffling. Arch. Phys. Med. Rehabil. 1991, 72, 390–397.

[39] Hausdorff, J.M.; Ladin, Z.; Wei, J.Y. Footswitch system for measurement of the temporal parameters of gait. J. Biomech. 1995, 28, 347–351.

[40] Lawrence, T.L.; Schmidt, R.N. Wireless In-Shoe Force System (for Motor Prosthesis). In

[41] Proceedings of the 19th Annual International Conference of the IEEE Engineering in Medicine and Biology Society, Chicago, IL, USA, 30 October–2 November 1997; pp. 2238–2241.

[42] Yan, C.; Ming, Z. Measurement of In-Shoe Plantar Triaxial Stresses in High-Heeled Shoes. In Proceeding of 2010 3rd International Conference on Biomedical Engineering and Informatics (BMEI), Yantai, China, 16–18 October 2010; pp. 1760–1763.

[43] Healy, A.; Burgess-Walker, P.; Naemi, R.; Chockalingam, N. Repeatability of WalkinSense® in shoe pressure measurement system: A preliminary study. Foot 2012, 22, 35–39.

[44] Benocci, M.; Rocchi, L.; Farella, E.; Chiari, L.; Benini, L. A Wireless System for Gait and Posture Analysis based on Pressure Insoles and Inertial Measurement Units. In Proceeding of the third International Conference on Pervasive Computing Technologies for Healthcare, 2009. Pervasive Health 2009, London, UK, 1–3 April 2009; pp. 1–6.

[45] Crosbie, W.; Nicol, A. Reciprocal aided gait in paraplegia. Spinal Cord 1990, 28, 353–363.

[46] Salpavaara, T.; Verho, J.; Lekkala, J.; Halttunen, J. Wireless Insole Sensor System for Plantar Force Measurements during Sport Events. In Proceedings of IMEKO XIX World Congress on Fundamental and Applied Metrology, Lisbon, Portugal, 6–11 September 2009; pp. 2118–2123.

[47] Holleczek, T.; Ruegg, A.; Harms, H.; Troster, G. Textile Pressure Sensors for Sports Applications. In Proceeding of 2010 IEEE Sensors, Kona, HI, USA, 1–4 November 2010; pp. 732–737.

[48] Saito, M.; Nakajima, K.; Takano, C.; Ohta, Y.; Sugimoto, C.; Ezoe, R.; Sasaki, K.; Hosaka, H.; Ifukube, T.; Ino, S.; Yamashita, K. An in-shoe device to measure plantar pressure during daily human activity. Med. Eng. Phys. 2011, 33, 638–645.

[49] De Rossi, S.M.M.; Lenzi, T.; Vitiello, N.; Donati, M.; Persichetti, A.; Giovacchini, F.; Vecchi, F.; Carrozza, M.C. Development of an In-Shoe Pressure-Sensitive Device for Gait Analysis. In Proceeding of 2011 Annual International Conference of the IEEE Engineering in Medicine and Biology Society, Boston, MA, USA, 30 August–3 September 2011; pp. 5637–5640.

[50] Hills, A.; Hennig, E.; McDonald, M.; Bar-Or, O. Plantar pressure differences between obese and non-obese adults: A biomechanical analysis. Int. J. Obes. 2001, 25, 1674–1679.

[51] Perttunen, J.; Kyrolainen, H.; Komi, P.V.; Heinonen, A. Biomechanical loading in the triple jump.J. Sports Sci. 2000, 18, 363–370.

[52] Dimas Adiputraa, Ubaidillahb, Saiful Amri Mazlana, Hairi Zamzuria, Mohd Azizi Abdul Rahmana," FUZZY LOGIC CONTROL FOR ANKLE FOOT ORTHOSES

EQUIPPED WITH MAGNETORHEOLOGICAL BRAKE", Teknologi Malaysia (UTM), 54100, Kuala Lumpur, Malaysia.

[53] T. M. Owings, J. Apelqvist*, A. Stenstro ¨m†, M. Becker‡, S. A. Bus§, A. Kalpen–, J. S. Ulbrecht‡ and P. R. Cavanagh," Original Article: Complications Plantar pressures in diabetic patients with foot ulcers which have remained healed", Accepted 8 August 2009.